# MAPPING AND CHARACTERISATION OF RESISTANCE TO SEPTORIA TRITICI BLOTCH IN WINTER WHEAT

Patrick Michael Seed

Thesis submitted to the University of Nottingham

for the degree of Doctor of Philosophy

The University of Nottingham

School of Bioscience

Division of Plant and Crop Science

Sutton Bonington Campus

Loughborough, LE12 5RD, UK

March 2022 (Re-submitted June 2023)

Acknowledgements

I would like to thank my supervisors Dr Rumiana Ray, Dr Sean Mayes & Dr Ruth Bryant (RAGT) for all their support and guidance throughout the course of my PhD. Their feedback was extremely useful in the submission of this thesis. I would also like to thank Dr Dimitra Angelopoulou for her generous help throughout the PhD.

I would also want to acknowledge the efforts of the glasshouse and field teams who were essential in the day-to-day running of my experiments (Sue flint, Mark Meacham). I also acknowledge the contribution of Xiaoran Li for her role in field data collection in 2019.

Lastly, I would like to thank BBSRC and RAGT for the opportunity to do this PhD.

## Contents:


## Abstract (6-7)

## 1. Chapter 1: Introduction and literature review (8-41)

1. Global food security and wheat (*Triticum aestivum*) (9)
2. *Zymoseptoria tritici (Mycosphaerella graminicola)* (10)
3. Epidemiology - Life cycle of *Z.tritici* (11-16)
    - 3.1 Inoculum source and dispersal (11)
    - 3.2 Germination and infection (11)
    - 3.3 Asymptomatic phase of infection (13)
    - 3.4 Necrotrophic phase of infection (14)
    - 3.5 Pycnidia and pseudothecia production (14-16)
4. Septoria tritici blotch (STB) management (17-20)
    - 4.1 Chemical control (17-19)
    - 4.2 Cultural control (19-20
5. Wheat resistance to *Z.tritici* (20-28)
    - 5.1 Historical significance of *Z.tritici* (20)
    - 5.2 Qualitative source of resistance (21)
    - 5.3 Identified sources of resistance (22-24)
    - 5.4 Incorporation of qualitative source of resistance (24-26)
    - 5.5 Quantitative resistance (26-28)
6. Disease escape (27)
7. Major source of resistance in Cougar (27-29)
8. Mechanisms of resistance to *Z.tritici* (29-36)
    - 8.1 Pathogen recognition and gene-for-gene resistance (29-31)
    - 8.2 Preformed defence (31-32)
    - 8.3 Chloroplast defence mechanisms (32-34)
    - 8.4 Transcriptomic analysis of defence mechanisms (34-36)
9. High-throughput phenotyping for plant breeders
    - 9.1 Visual range image analysis (37)
    - 9.2 Hyperspectral reflectance measurements (37-38)
    - 9.3 Chlorophyl fluorescence measurements (38-40)
10. PhD Aims and objectives (40-41)

**2. Chapter 2: QTL analysis of a novel source of resistance in Cougar using Chlorophyll fluorescence and hyperspectral phenotyping tools (42-74)**

1. Introduction (43-47)
2. Methods (48-53)
    - 2.1. Plant material (48)
    - 2.2. Genetic map construction and QTL analysis (48)
    - 2.3. Instruments for phenotyping (49)
    - 2.4. STB resistance screening in the field (49)
    - 2.5. Cougar resistance phenotyping under controlled environmental conditions (52)
    - 2.6. Statistical analysis (53)
3. Results (54-68)
    - 3.1. Phenotypic characterisation of STB disease response (54-55)
    - 3.2. Stepwise linear regression and correlation analysis (56-58)
    - 3.3. QTL analysis of resistance to STB caused by *Z.tritici*, & coinciding spectral indices and chlorophyll fluorescence measurements (60-64)
    - 3.4. Phenotypic evaluation of 4D resistance to *Z.tritici* (IPO323) under controlled environmental conditions (65-68)
4. Discussion (69-74)

**3. Chapter 3: Chlorophyll fluorescence phenotyping and transcriptomic analysis of a novel source of resistance to *Z.tritici* in the winter wheat cultivar Cougar (75-119)**

1. Introduction (76-80)
2. Methods (81-85)
    - 2.1. Plant material and controlled environmental conditions (81)
    - 2.2. *Z.tritici* inoculations (81)
    - 2.3. STB disease and Pycnidia assessments (81-82)
    - 2.4. Chlorophyll fluorescence and gas exchange measurements (82)
    - 2.5. RNA-seq analysis (82-83)
    - 2.6. Hormone quantification (83)
    - 2.7. qRT-PCR of xanthophylls and candidate genes (84)
    - 2.8. Candidate resistance gene mapping (84-85)
    - 2.9. Statistical analysis (85)

3. Results (86-114)
3.1. Disease and chlorophyll fluorescence phenotype of 4D-R resistance (86-89)
3.2. Xanthophyll enzyme and hormone quantification (90-91)
3.3. Transcriptomic analysis of the conserved incompatible 4D-R interaction (92-96)
3.4. Transcriptomic analysis of the differential response of 4D-R to HT-22 and IPO323 (97-104)
3.5. Transcriptomic analysis of *Z.tritici* isolates HT-22 & IPO323 (105-107)
3.6. *Z.tritici* candidate effector identification (108)
3.7. Candidate resistance gene(s) identification (109-122)
3.8. Candidate resistance gene(s) SNP 4D-R/S comparison (113-114)
4. Discussion (115-119)

**4. Chapter 4: Chlorophyll fluorescence phenotyping and transcriptomic analysis of a novel source of resistance to *Z.tritici* in the winter wheat cultivar Cougar (120-)**

1. Introduction (121-123)
2. Methods (124-128)
2.1. Plant material and controlled environmental conditions (124)
2.2. *Z.tritici* inoculations (124)
2.3. STB disease assessments (124-125)
2.4. Chlorophyll fluorescence and gas exchange measurements (125)
2.5. ROS staining (125-126)
2.6. Stomatal and fungal staining (126)
2.7.1. RT-qPCR of xanthophylls cycle enzyme conversion genes (126-127)
2.7.2. Xanthophyll quantification (127)
2.8. Hormone quantification (127-128)
2.9. Statistical analysis (128)
3. Results (129-141)
3.7. Visual assessment of *Z.tritici* isolates HT-22 & 508 symptoms on 4D-R & 4D-S NILs (129-130)
3.8. Chlorophyll fluorescence measurements (131-135)
3.9. Fungal and stomatal staining assay (131-137)
3.10. Superoxide and hydrogen peroxide ROS assay (138-139)
3.11. Carotenoid & xanthophyll enzyme quantification (139-140)

3.12. Hormone quantification (141)

4. Discussion (142-146)

**5. Chapter 5: General discussion and conclusions (147-152)**

**6. Bibliography and supplementary materials (152-263)**

1. Supplementary table S1 (154-156)
2. Supplementary table S2 a & b (157-158)
3. Supplementary table S3 (159)
4. Supplementary table S4 (160)
5. Supplementary table S5 (161-164)
6. Supplementary table S6 a & b (165-172)
7. Supplementary table S7 a & b (173)
8. Supplementary table S8 a & b (174-181)
9. Supplementary table S9 a & b (182-183)
10. Supplementary table S10 (184)
11. Supplementary table S11 (185-187)
12. Supplementary figure S1 (188)
13. Supplementary figure S2 (189)
14. Supplementary figure S3 (190)
15. Supplementary figure S4 (191)
16. Supplementary table S12 (192-193)
17. Supplementary table S13 (194-196)
18. Supplementary table S14 (197-199)
19. Supplementary table S15 (200-206)
20. Supplementary table S16 (207)
21. Supplementary table S17 (208-209)
22. Supplementary table S18 (210)
23. Supplementary table S19 (211-215)
24. Supplementary table S20 (216-217)
25. Supplementary table S21 (218-225)
26. References (226-263)

## Abstract

The resistance of cv. Cougar to *Zymoseptoria tritici* has been investigated in detail, involving Quantitative trait loci (QTL) analyses to map the resistance, various physiological measurements to investigate the mechanism of resistance and transcriptomic analyses to identify candidate resistance genes. To map the resistance in cv. Cougar, QTL analyses utilised visual septoria tritici blotch (STB) assessments, chlorophyll fluorescence measurements & hyperspectral reflectance measurements. Additionally, these physiological measurements were used to map other sources of resistance from both cv. Cougar and cv. Scout and to predict future STB disease within a growing season. Utilising a set of near isogenic lines (NILs) for the source of resistance in Cougar, and two incompatible *Z.tritici* isolates (HT-22/IPO323), transcriptomic analysis characterised the conserved incompatible wheat-*Z.tritici* transcriptome and identified candidate resistance gene(s) at the location identified on chromosome 4D. The Cougar resistance mechanism was investigated using a range of techniques including chlorophyll fluorescence measurements, hormone, carotenoid and xanthophyll enzyme quantification, superoxide and hydrogen peroxide accumulation, stomatal behaviour, stomatal morphology and *Z.tritici* spore germination rates. These techniques were used to investigate the effect of compatibility by utilising a *Z.tritici* isolate which has overcome the Cougar resistance (508, compatible) and an avirulent isolate (HT-22, incompatible). STB assessments and hyperspectral reflectance measurements mapped the cv. Cougar resistance to chromosome 4D in 2018, with a breakdown of this resistance in 2019, likely due to the evolution of pathogen genotypes with virulence to cv Cougar. NPQI (Pheophitinization of chlorophyll a to phaeophytin) was the best index at mapping the resistance to chromosome 4D and was unique to this QTL. This study also demonstrated the broader application of chlorophyll fluorescence and hyperspectral reflectance measurements in identifying novel sources of resistance, with indices such as D2 (chlorophyll fluorescence), ND705 (chlorophyll content) and ARI (anthocyanin content) tightly correlating with septoria tritici blotch (STB) disease in a manner consistent with previous studies. Transcriptomic analysis identified 3 candidate resistance genes at the location identified on chromosome 4D, with upregulation of protein kinases, F-box proteins and cytochrome P450 proteins amongst the main transcripts associated with incompatibility. Resistance was associated with a photoinhibitory and photoprotective mechanism involving both the qI and qE components of NPQ and a change in carotenoid composition reflected by changes in xanthophyll enzyme expression and a decrease in superoxide accumulation. Additionally, changes in SA, JA and

ABA content was associated with the Cougar defence response. Preformed defence traits such as stomatal morphology, behaviour and spore germination rates were not associated with compatibility. These results demonstrate that the major source of resistance in cv. Cougar resides on chromosome 4D and likely involves a form of effector triggered immunity which induces a photoinhibitory and photoprotective resistance mechanism involving altered carotenoid and hormone metabolism.

# Chapter 1.

## Introduction and literature review

# 1. Global food security and wheat (*Triticum aestivum*)

Throughout this century global food yields need to increase to account for population growth (Van Dijk *et al* 2021), decreased land availability (Winkler *et al* 2021), climate change (IPCC 2021) and the evolution of fungicide/pesticide resistant pathogens (Savary *et al* 2019). Global population estimates predict the global population to reach 8.5 billion in 2030, 9.7 billion in 2050 and 10.4 billion in 2100 (UNDESA 2022). Furthermore, desertification induced by climate change and land competition with cash crops (Ryschawy *et al* 2017), biofuels (Krasuska *et al* 2010) and urbanisation (Barthel *et al* 2019) puts increased pressure on global food yield requirements. Climate change will also impact global food yields by increasing the frequency of extreme weather events (Zandalinas *et al* 2021), influence the geographical locations where specific crops can be productively grown (Sloat *et al* 2020) and increase insect pest geographical ranges (Skendžić *et al* 2021). Wheat is one of the most important cereal crops with an estimated global yield of 770.8 million tonnes in 2022, accounting for 27.6% of global cereal production (GIEWS FAO 2022). Between 2001-2003 weeds, animal pests, pathogens and viruses accounted for 11-59% of total yield losses globally, with crop protection strategies reducing bread wheat (*Triticum aestivum* L) yield losses from 50% to 29% (Oerke 2006). Yield loss in wheat from pathogens ranged from 16% to 10%, indicating the importance of pathogen management strategies, whilst also highlighting the prevalence of pathogen induced yield losses in wheat even in the presence of crop protection strategies (Oerke 2006).

Modern hexaploid wheat was domesticated in south-eastern Turkey & north Syria (Lev-Yadun 2000) approximately 8,000 years ago (Vergauwen & Smet 2017) and has since undergone extensive breeding during the green revolution in the 1960s to become the high yielding varieties grown today. The most notable breeding breakthrough involved the incorporation of semi-dwarfing genes, which increased grain yields by reducing straw and leaf production, as well as improving nutrient uptake (Smale 1997). Due to the importance of wheat, and the prevalence of a variety of socio-economic, biotic and abiotic pressures influencing global wheat yields, concerted efforts must be made to ensure high yields are maintained to preserve global food security.

## 2. *Zymoseptoria tritici* (*Mycosphaerella graminicola*)

*Zymoseptoria tritici*, also known as *Mycosphaerella graminicola* or by the anamorph name *Septoria tritici*, is a fungal pathogen which evolved in synchrony with the domestication of wheat in the Middle East in the fertile crescent at around 8-9000 BC (Stukenbrock *et al* 2007, 2012). *Z.tritici* (*Zymoseptoria tritici*) causes septoria tritici blotch (STB) and is widely considered one of the most damaging diseases of wheat alongside leaf rust (*Puccinia triticina*) and fusarium headblight (*Fusarium graminearum*) (Savary *et al* 2019). Yield losses from *Z.tritici* are variable and highly dependent on the cultivar's resistance, *Z.tritici* isolate population composition, geographical location, fungicide treatment regime, environmental conditions, and other STB management strategies. For example, Yitagesu *et al* (2020) utilised a range of different fungicide regimes and demonstrated up to 39.4% yield loss across three cultivars over two sites in Ethiopia. Furthermore, under different nitrogen treatments and *Z.tritici* isolate inoculations, yield reduction varied between 16.6 – 44.9% in a study by Simón *et al* (2002). Because *Z.tritici* is amongst the most damaging pathogens for wheat (Savary *et al* 2019), an estimated €1.3/1.8bn annual fungicide expenditure is spent on wheat with €1/1.3bn primarily targeted towards managing *Z.tritici* (Torriani *et al* 2015). Consequently, yield losses from STB in France, Germany and the UK in 2014 was estimated to range from €720 – 1440 million (Torriani *et al* 2015), demonstrating the huge economic impact of *Z.tritici*. Due to the significant impact of STB on global wheat yields, a concerted effort is required to develop and maintain effective and sustainable STB management practices to promote global food security and minimise economic impacts.

# 3. Epidemiology - Life cycle of *Z.tritici*

## 3.1 Inoculum source and dispersal

*Z.tritici* pseudothecia from the previous year's wheat debris/stubble initiates the infection cycle by releasing ascospores (Bathgate & Loughman 2001). Ascospore release is triggered by environmental conditions favourable for *Z.tritici* spore germination and infection rates. This includes low radiation levels (Cordo *et al* 2017) and temperatures exceeding 2-7$^{O}$C (Gladders *et al* 2000; Pietravalle *et al* 2003), whilst high humidity levels caused by recent rainfall or dew is the most influential factor involved in ascospore release (Bathgate & Loughman 2001; Garcia & Marshall 1992; Leath *et al* 1993). Ascospores are wind dispersed (Hunter *et al* 1999), and hence large proportions of *Z.tritci* infections result from immigrant isolates (Zhan *et al* 1998; Zhan *et al* 2001), with large distances (Kabbage *et al* 2009) or temperate and physical barriers required to prevent migration of foreign isolates (Abrinbana *et al* 2010). Removal of wheat debris, and hence ascospores, delays the epidemic (Suffert & Sache 2011). Whilst ascospores initiates the infection cycle, ascospore concentration doesn't contribute to disease severity (Morais *et al* 2016) and is unimportant in the progression of the epidemic (Eriksen *et al* 2001). Therefore, whilst ascospores are important in initiating the epidemic, with 30% of the pathogen population resulting from sexual reproduction (Eriksen *et al* 2001), asexually produced pycnidiospores are primarily responsible for disease progression (Zhan *et al* 1998; Suffert & Sache 2011).

## 3.2 Germination and infection

Optimum temperatures for spore germination range between 16 - 25$^{O}$C (Magboul *et al* 1992), with Chungu *et al* (2001) demonstrating a range of 15$^{O}$C during the night and 18-22$^{O}$C during the day. *Z.tritici* spores germinate on the leaf surface and initiate filamentous growth which is essential for pathogenicity (Mehrabi *et al* 2006; Steinberg 2015). The mechanism for leaf penetration involves germ tube stomatal penetration (Rohel *et al* 2001; Duncan & Howard 2000; Kema *et al* 1996a; Stergiopoulos *et al* 2003; Goodwin *et al* 2011; Cousin *et al* 2006). There is conflicting evidence whether hyphae grow directionally towards stomata (Duncan & Howard 2000; Cousin *et al* 2006), randomly (Kema *et al* 1996a) or grow directionally away from stomata (Shetty *et al* 2003). More recently Fones *et al* (2017) modelled hyphal growth and demonstrated a random growth pattern, although it is likely that different *Z.tritici* isolates might vary in their behaviour due to different thigmotropic or chemotropic detection abilities that might be isolate specific.

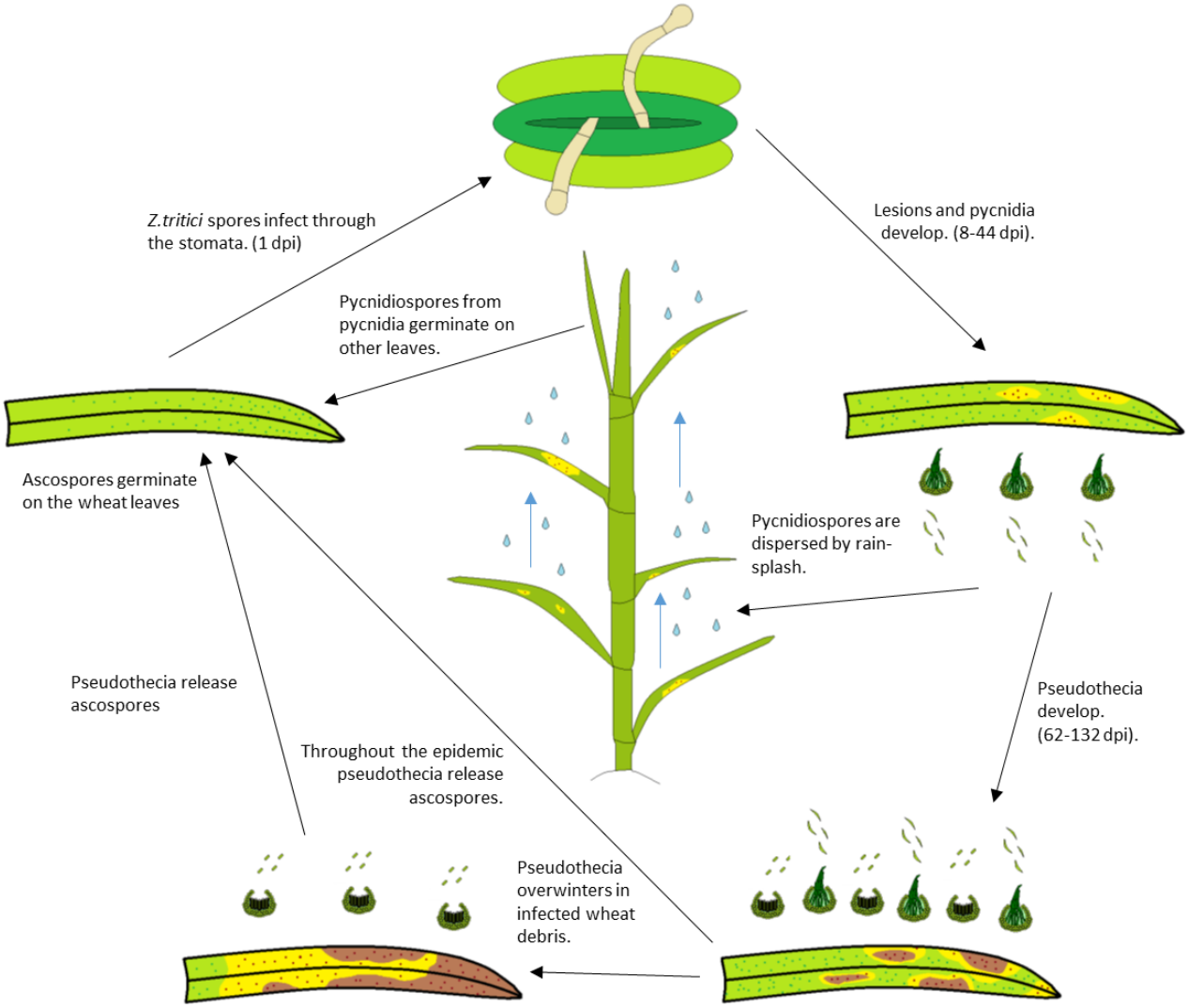



Figure 1: Diagrammatic representation of the lifecycle of *Z.tritici*.

## 3.3 Asymptomatic phase of infection

Once *Z.tritici* has infected the leaf it undergoes an asymptomatic phase where is colonises the mesophyll and sub-stomatal openings (Fig 2) (Shetty *et al* 2003; Steinberg 2015). This asymptomatic phase typically lasts for 8 - 13 days under laboratory conditions (Shetty *et al* 2007) (Kema *et al* 1996a) and 5 - 35 days under field conditions (Shipton *et al* 1971) (Armour *et al* 2004), although this depends on the wheat/*Z.tritici* genotypes present (Steinberg 2015). During this phase *Z.tritici* gains little mass (Keon *et al* 2007) and is purely constrained to the apoplast, whereby it colonises the sub-stomatal cavities and forms pre-pycnidia (Shetty *et al* 2003). During this asymptomatic phase there is no parasitism of host cells (Keon *et al* 2007) (Sanchez-Vallet *et al* 2015) or formation of specialist feeding structures such as haustoria (Kema *et al* 1996a) (Shipton *et al* 1971). *Z.tritici* primarily relies on carbon stores during its asymptomatic phase (Keon *et al* 2007) and hence lacks specialist feeding structures typical of biotrophs (Kema *et al* 1996a; Fones *et al* 2017), and instead behaves as an endophyte by colonising the apoplast before its necrotic phase, in a similar manner to other necrotrophic pathogens (Atkins *et al* 2010; ). Because of these lifecycle traits *Z.tritici* could be classified as a latent necrotroph instead of as a hemi-biotroph (Sanchez-Vallet *et al* 2015).

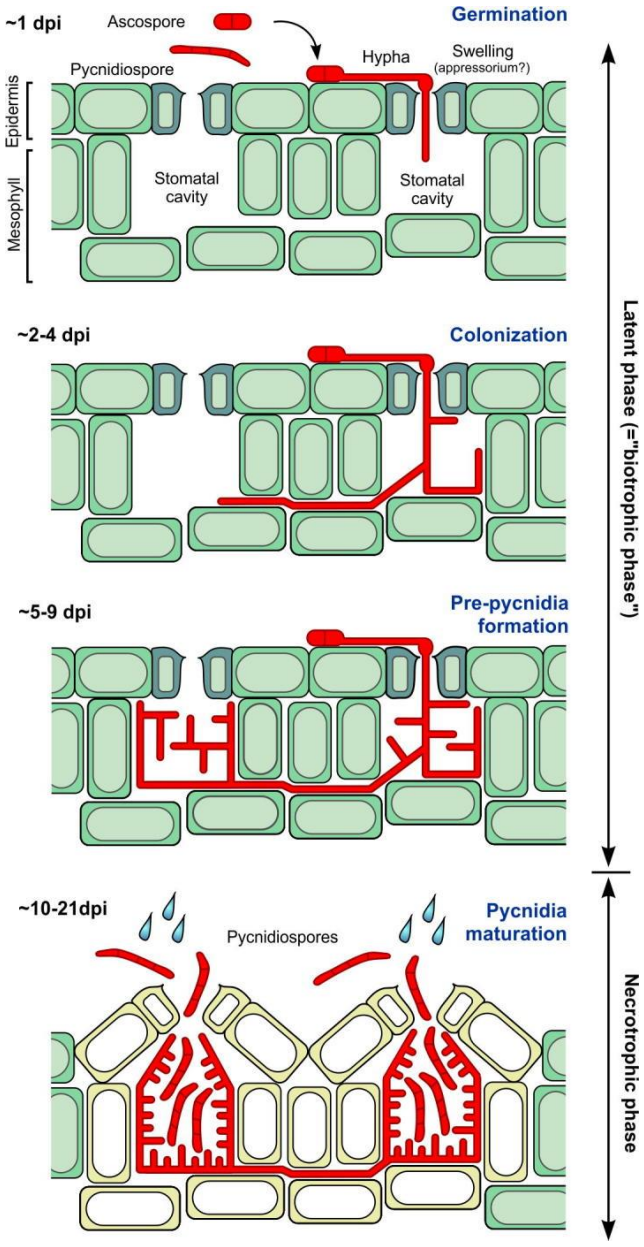



Figure 2: Diagrammatic representation of the progression of STB in Wheat leaves post-infection. (Taken from Steinberg 2015)

## 3.4 Necrotrophic phase of infection

Approximately 9-14 days after stomatal penetration (6-36 days under field conditions (Shipton *et al* 1971; Armour *et al* 2004)) *Z.tritici* switches to a nectrotrophic (symptomatic) phase of infection whereby rapid cell death is initiated which releases nutrients and carbon into the apoplast to fuel growth for further hyphal colonisation (Keon *et al* 2007), pycnidia (asexual fruiting bodies) and pseudothecia formation (sexual fruiting bodies), leading to an exponential increase in fungal biomass. This switch to necrotrophy is accompanied by differential regulation of wheat mitogen-activated protein kinase cascades (Keon *et al* 2007; Rudd *et al* 2008) and increased expression of cell-wall degrading enzymes (Kema *et al* 2008; Siah *et al* 2010) amongst other responses captured by transcriptomic studies (Keon *et al* 2005; Yang *et al* 2013; Rudd *et al* 2015; Palma-Guerrero *et al* 2016). Examples of genes involved in the transition to necrotrophy involve ZtNIP1 and ZtNIP2, which are temperature and light dependent proteins upregulated at 8-12 dpi (Ben M'Barek *et al* 2015) and TaR1 which supresses plant cell death and is required to delay the necrotrophic phase (Lee *et al* 2015).

## 3.5 Pycnidia and pseudothecia production

Pre-pycnidia form 5-9 days post inoculation in the sub-stomatal cavities (Kema *et al* 1996a; Duncan & Howard 2000) with full pycnidia formation commencing from the start of the necrotrophic stage of infection (Kema *et al* 1996a). Pycnidia are asexual fruitifications which, in the field, form 8 – 44 days after inoculation (Kema *et al* 1996a; Hunter *et al* 1999), are subglobose and commonly resign alone in each sub-stomatal cavity (Kema *et al* 1996a). Pycnidia produce and release asexual spores (pycnidospores) which are clear and threadlike, measuring 2.6 x 62.5µm (Ponomarenko *et al* 2012; Gough 1978). Pycnidiospores are released from the pycnidia on infected leaf tissue in response to high moisture, with 100% relative humidity (RH) releasing twice as many pycnidiospores than 98% RH and 11 to 23 times as many than 86% RH (Gough & Lee 1985). Pycnidiospores are dispersed through a rain-splash mechanism (Shaw & Royle 1993; Sanderson *et al* 1985; Bannon & Cooke 1998) (Fig 3). This mechanism involves the rain drops transferring pycnidiospores from the lower infected leaves to higher leaves and the leaves of neighbouring plants by splashing the spores up the leaf canopy. Because of the importance of rain in facilitating the spread of *Z.tritici* the severity of outbreaks is highly dependent on a high frequency of rainfall events (Gough & Lee 1985).

Sexual recombination assists *Z.tritici* to overcome novel wheat resistance genes and evolve resistance to fungicides (Goodwin *et al* 2011). *Z.tritici* reproduces sexually through the meeting

of MAT1-1 and MAT1-2 idiomorphs in a bipolar heterothallic mating system (Kema *et al* 1996b). These idiomorphs are commonly found in roughly equal ratios amongst *Z.tritici* populations (Zhan *et al* 2002; Waalwijk *et al* 2002), although there are a few studies indicating that there are slightly fewer MAT1-1 isolates (44-48%) instead of an exact 50:50 ratio (Elbekali *et al* 2012; Allioui *et al* 2014). These idomorphs form pseudothecia, which are globose, dark brown structures 68-130 µm in diameter and form underneath the epidermis (Sanderson 1972; Ponomarenko *et al* 2012; Hoorne *et al* 2002). These fruiting bodies contain numerous asci, which are 11-14 x 30-42µm and encapsulate eight two celled ascospores sized 2-4 x 8-16 µm (Ponomarenko *et al* 2012) (Hoorne *et al* 2002). Pseudothecia formation in the field takes roughly 62 – 132 days, compared to 14 – 44 for pycnidia formation (Hunter *et al* 1999). Ascospores also had a longer latent period of approximately 3-4 days compared to pycnidiospores (Morais *et al* 2015). Ascospores and pycnidiospores are functionally similar, however, they provide different distinct roles in the *Z.tritici* lifecycle, providing both the benefits of rapid asexual reproduction (pycnidia) and the genomic recombination of sexual reproduction (pseudothecia).

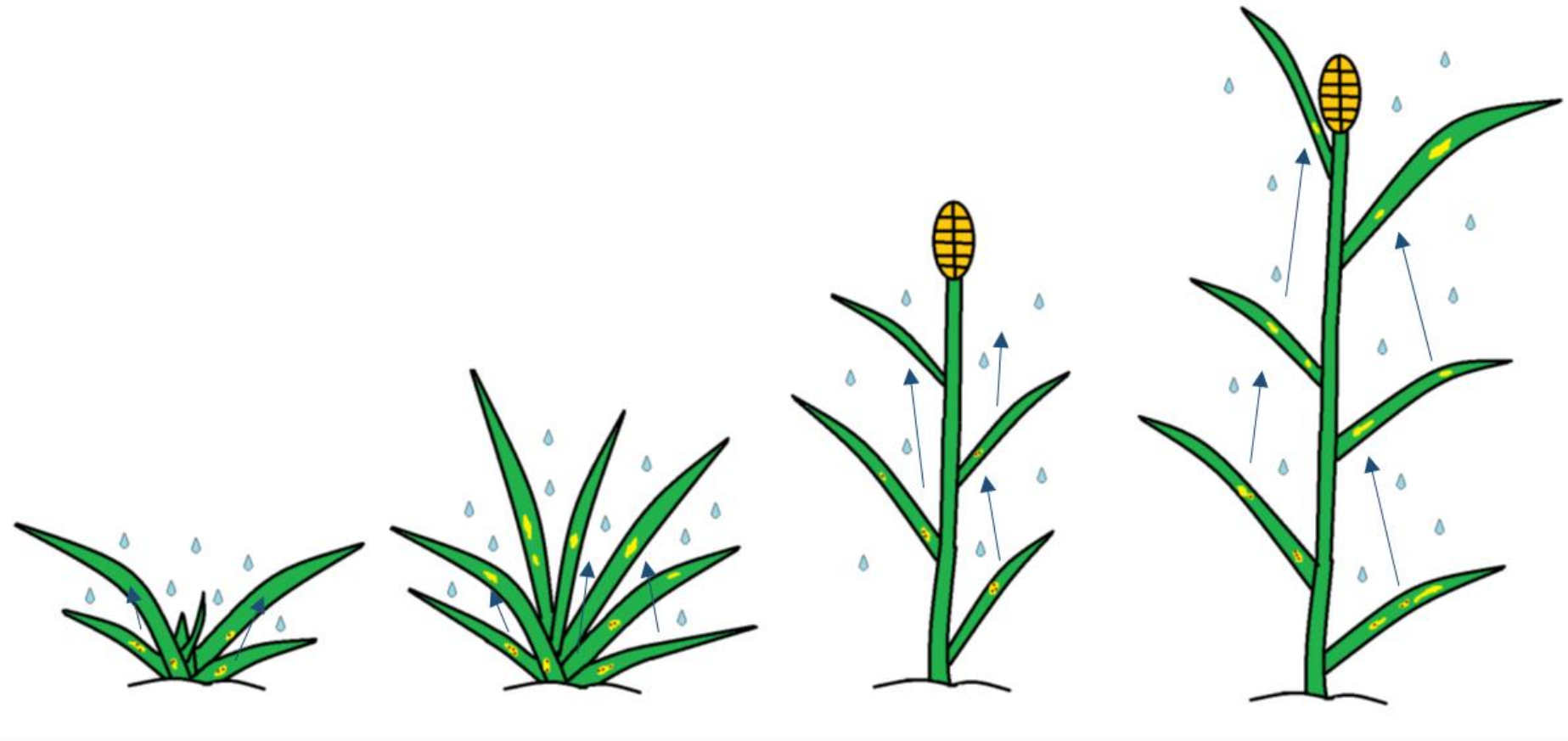


Figure 3: Diagrammatic representation of the rain splash mechanism which enables infection of the whole plant throughout its growth cycle.

# 4. STB Management

## 4.1 Chemical control

Fungicide treatment constitutes the main method to manage STB, with 1.3 billion euros spent on their use to control for *Z.tritici* (Torriani *et al* 2015). Fungicides used to manage *Z.tritici* include azoles (demethylation inhibitors; DMI), Strobilurins (quinone-outside inhibitors; QoI) and Carboxamides (succinate dehydrogenase inhbitors; SDHI). Azoles are the largest group of fungicides and have been extensively used since their discovery in the 1960-70s to combat *Z.tritici* (Morton & Staub 2008). Azole fungicides bind to the cytochrome P450 enzyme (CYP51) of *Z.tritici*, which mediates the essential sterol 14α-demthylation step in the ergosterol pathway (Nes & McKean 1977). Azole fungicides thus inhibit the production of ergosterol, a fundamental component of the fungal cell membranes, and hence reduce hyphal growth following sporulation (Sundin *et al* 1999) acting at the asymptomatic stage of infection (Thies Marten Heick *et al* 2015). Whilst azole fungicides have been and still are extensively used to control *Z.tritici*, many *Z.tritici* populations have accumulated mutations which increase their resistance to azoles (Stammler *et al* 2007) (Beyer *et al* 2011). Resistance to DMIs has been documented in European countries such as the UK, Germany, Ireland & France (Jorgensen *et al* 2021; Stammler *et al* 2011; Kildea *et al* 2017; Strobel *et al* 2017; Blake *et al* 2018). This resistance to azoles can be attributed to numerous mutations at amino acid positions 50, 136, 137, 188, 379, 381, 459-462 & 513 in the CYP51 gene (Stammler *et al* 2007; Cools & Fraaije 2006; Brunner *et al* 2008; Fraaije *et al* 2007).

Strobilurins have also been extensively used to control *Z.tritici* since their introduction in 1996 (Gisi *et al* 2002) with QoI spray use reaching 80% in 2002 (Beyer *et al* 2011). Strobilurins inhibit mitochondrial respiration by binding to the cytochrome bc1 enzyme complex (cytb), preventing the transfer of electrons to produce ATP (Gisi *et al* 2002). However, fungicide resistance has rapidly evolved in the case of strobilurins, involving over 11 point mutations in the cytb gene known to confer partial resistance (Gisi *et al* 2002), as well as the G143A mutation known to confer strong levels of resistance, leading to a mere 4% use in 2008 (Beyer *et al* 2011). However, QoI's were used in countries such as Poland since 2008 due to their beneficial effects on the development of plants and potential increase in yield (Pieczul & Wasomska 2017), although there are reports of QoI resistance (Pieczul *et al* 2015). More recently, 50-70% isolates tested from Estonia, Finland, Latvia, and Lithuania had the cytb G143A mutation conferring strobilurin resistance (Mae *et al* 2020), demonstrating widespread

resistance to strobilurins. Because large proportions of *Z.tritici* populations are highly resistant to strobilurins (Pieczul & Wasowska 2013; Mae *et al* 2020; Hagerty *et al* 2017), combined with a lack of fitness costs associated with these point mutations such as G143A (Gisi *et al* 2002), strobilurins are relatively ineffective compared to alternative fungicide treatments such as azoles and carboxamides.

Succinate dehydrogenase inhibitors (SDHI's) of the class of carboxamides inhibit the tricarboxylic acid enzyme cycle, which is essential in the oxidation of succinate to fumarate during respiration (Skinner *et al* 1998). The first carboximide used as a fungicide was discovered in the 1960s (Carboxin) (Schmeling & Kulka 1966), with boscalid being the first used to manage *Z.tritici* from 2003 (Stammler *et al* 2007). With evidence of resistance against Boscalid involving mutations in the SDH gene (Stammler *et al* 2010) there is an increasing use of secondary generation SDHIs including fluopyram (Scalliet *et al* 2012), bixafen (Omrane *et al* 2015), and isopyrazam, which was effective against large proportions of *Z.tritici* populations (Dubos *et al* 2012). There is also evidence of a west to east gradient across Europe of SDHI resistance mutations T79N and N86S, being highest in Ireland and England, which has gradually increased over the past decade (Hellin *et al* 2021).

To combat the evolution of *Z. tritici* fungicide resistance, fungicide treatment strategies need to be optimised to slow the accumulation of resistance mutations whilst maintaining high levels of protection to maximise yields. There is significant evidence that a mixture of SDHI's, DMI's and multisite inhibitors such as Folpet have additive effects in controlling *Z.tritici* infection (Thies Marten Heick *et al* 2017). The use of multiple fungicides with different modes of actions also reduces the selection of mutations leading to fungicide resistance, with the more diverse use of fungicides leading to a decreased selection of CYP51 mutations associated with SDHI resistance (Thies Marten Heick *et al* 2017). *Z.tritici* resistance to fungicides is commonly associated with a growth cost for the fungus (Van den Bosch *et al* 2018; Thies Marten Heick *et al* 2017). Hence, using fungicides with different modes of action provides an additive growth cost to the pathogen. However, only specific combinations of fungicides might be effective together, hence the properties of fungicide mixtures need to be experimentally demonstrated (Mavroeidi & Shaw 2006). The use of multiple fungicides may not be sustainable however, since some *Z.tritici* isolates have evolved multi-drug resistance genes such as MgAtr1,2,3,4&5 and MgMfs1 (Zwiers & Waard 2000; Stergiopoulos *et al* 2002; Roohparvar *et al* 2007; Zwiers *et al* 2003; Omrane *et al* 2015) and/or accumulated mutations in multiple genes encoding

enzymes which are fungicide targets such as CYP51 (Stammler *et al* 2007), SDH-B (Rehfus *et al* 2017), beta-tubilin (Hawkins *et al* 2016) and Cyt b (Allioui *et al* 2013).

The discovery of novel fungicides with different mode of actions is highly desirable to help combat *Z.tritici* and reduce our reliance on existing fungicides with large levels of resistance built-up in *Z.tritici* populations. The discovery of novel fungicides is rare and time consuming, although a new fungicide (Fenpicoxamid) has recently been approved in 2019 (Kildea *et al* 2022). Fenpicoxamid is a quinone inside-inhibitor (QiI) which binds to the quinone site reduction complex and is the first QiI to demonstrate activity against ascomycete fungi (Kildea *et al* 2022). Fenpicoxamid sensitivity was also only generally associated with multi-drug resistance genes and not specific QoI mutations such as C143A, suggesting a lack of specific resistance mutations in European *Z.tritici* populations. Therefore, Fenpicoxamid could be an important novel fungicide to manage *Z.tritici* in combination with other previously used fungicides and fungicide SDHI – DMI mixtures.

## 4.2 Cultural control

Chemical control alone is not sufficient to control and manage STB on a global scale. *Z.tritici* populations have rapidly revolved resistance to fungicides over the past couple of decades, with few novel fungicides replacing obsolete ones. Fungicide application is also costly (Torriani *et al* 2015) and there is an increasing incentive from organizations such as the European Union to minimise inputs and adopt more integrated pest management strategies. Farmers can take steps to reduce the severity of *Z.tritici* outbreaks by modifying the growing environment (cultural control). For example, delayed sowing can reduce initial *Z.tritici* infections, as well as provide benefits against other pathogens such as eyespot and some rusts (McDonald & Mundt 2016), although planting cannot be excessively delayed or seedlings fail to establish in time due to wet soils, leading to yield losses in excess of that caused by *Z.tritici*. The two main methods to control for *Z.tritici* is through tillage and crop rotation. Tilling can break up wheat debris which unearths pseudothecia buried from the previous season leading to increased ascospore dispersal (Bankina *et al* 2015; Bankina *et al* 2018). Hence no tillage or reduce tillage regimes would help reduce the severity of *Z.tritici* outbreaks. Crop rotation can also be employed to reduce *Z.tritici* infection. By planting wheat every other year the presence of the previous year's stubble containing pseudothecia to reinfect the subsequent year's wheat crop is removed. This helps break the cycle of infection since pseudothecia rarely survive for more than year because under high moisture conditions they release ascospores irrespective of

the presence of the host plant. Thus, crop rotations of more than a year reduce the severity of *Z.tritici* because the wheat debris no longer contains viable pseduothecia (Fernandez *et al* 1998; Bailey *et al* 2001; Katamadze & Paura 2015). However, as many primary infections are also initiated by immigrant ascospores, local removal and management of wheat debris alone cannot prevent primary infections (Schuh 1990). Stubble management therefore requires conserved and widespread regional implementation to be effective (McDonald & Mundt 2016).

# *5.* Wheat resistance to *Z.tritici*

## 5.1 Historical significance of resistance

Fungicide application and cultural control methods aren't fully effective at controlling *Z.tritici*, especially since *Z.tritici* populations have accumulated mutations to combat fungicides (Simón *et al* 2002; Yitagesu *et al* 2020; McDonald & Mundt 2016) and cultural control methods can be difficult to implement effectively (McDonald & Mundt 2016; Katamadze & Paura 2015). Phylogeographic studies indicate that *Z.tritici* has evolved with *Triticum aestivum* from the Middle East during the spread of wheat cultivation (Stukenbrock *et al* 2007; McDonald *et al* 1999; Banke *et al* 2004). Therefore, since the domestication of wheat approximately 8,000 years ago (Lev-Yadun 2000; Vergauwen & Smet 2017), there has been evolutionary pressure for wheat to evolve resistance to *Z.tritici*. In addition, primitive selective breeding practices have knowingly or unknowingly been selecting for resistance to *Z.tritici*. Since the green revolution in the 1960-70s and the introduction of semi-dwarfing (Rht) genes there have been concerted efforts to breed selectively resistant wheat cultivars to minimise yield losses from *Z.tritici*. The introduction of semi-dwarf cultivars, which were more susceptible to *Z.tritici* (Eyal 1981), combined with a decrease in cultivar diversity, increased the prominence of *Z.tritici* worldwide in the 1960's. The increased threat *Z.tritici* was posing to global food security was demonstrated by the severe outbreak in North Africa in 1968-1969 (Saari and Wilcoxson 1974), such that STB was considered a major problem by the late 1970s (Hardwick *et al* 2001; Shaw *et al* 2008). Therefore, since the 1960-70's breeders have been highly incentivised to select cultivars with resistance to *Z.tritici* in order to maintain high yields (Brown *et al* 2015).

## 5.2 Qualitative sources of resistance

Over twenty genes have been identified which provide qualitative resistance to STB (Brown *et al* 2015). Qualitative sources of resistance typically provide strong levels of resistance, although this resistance is commonly race-specific and quickly broken down (Arraiano & Brown 2017). Therefore, whilst these sources of resistance might initially seem appealing to breeders due to the strong levels of resistance they provide, they commonly don't provide durable resistance. Relying on qualitative sources of resistance is likely an unsustainable approach to consistently supply growers with cultivars that are highly resistance to *Z.tritici* (Brown 2021). A case study to demonstrate this point is the over-reliance of major sources of resistance in mildew (*Blumeria graminis*) between 1950 and 1980, whereby alleles of the Mla gene were introduced from other sources outside Europe (Jørgensen, 1994), which *Blumeria graminis* subsequently overcame in a matter of years (Wolfe 1984; Brown 1994). Pyramiding qualitative resistance genes can be a more durable strategy to increase the effective gene lifespan (Grimmer *et al* 2015), however this is typically only effective against pathogens with low sexual reproduction rates and relies on good survey data to assess the presence of corresponding pathogen virulence genes (Bayles *et al* 1997; Brown 2021). For example, pyramiding strategies were used with *Mla* genes for mildew resistance, however they were ineffective at delaying their rapid resistance breakdown (Wolfe 1984; Brown 1994; Brown 2021). Despite qualitative sources of resistance having only temporary value for breeders due to their rapid breakdown, the scientific literature has focused almost extensively on these sources of resistance to *Z.tritici*. The focus on qualitative resistance likely stems from these genes inducing substantial resistant phenotypes making them easy to study, whereas more durable sources of resistance are typically polygenic and provide small effects, making them extremely difficult to investigate (Brown 2021).

Qualitative resistance typically follows a gene-for-gene relationship (Flor 1956). This form of immunity is also coined effector triggered immunity (ETI), whereby the host has a resistance gene which recognises a specific avirulence effector produced by the pathogen (Yuan *et al* 2021). This form of immunity typically arises from the 'zig-zag model' whereby the pathogen evolves a virulence effector which facilitates infection, however the host consequently co-evolves a gene which can detect this virulence effector. This leads to a boom-bust cycle of co-evolution, with strong levels of resistance followed by strong levels of susceptibility and vice versa (Yuan *et al* 2021). However, it is worth noting that ETI doesn't always provide strong levels of resistance, which is widely purported in the literature (Brown & Cowger 2019).

## 5.3 Identified sources of resistance

Stb1, 2, 3 & 4 were the first named STB genes (Wilson 1985). These genes were mapped to the chromosome 5BL (Adhikari *et al* 2004a), 1B (Liu *et al* 2013) and 7AS (Goodwin *et al* 2011). Whilst qualitative sources of resistance are typically overcome rapidly, Stb1 is arguably relatively durable since its introduction from Bulgaria 88 in 1966 (Rillo and Caldwell 1966) until 1989 (Johnson 1984; Shaner and Buechley 1989), with reports of its durability as recent as 2004 (Adhikari *et al* 2004a), although this could have been conflated with stb6 (Brown *et al* 2015). Stb2, 3 and 4 have contributed significant levels of resistance since their discovery, however there is evidence that many *Z.tritici* populations have overcome these sources of resistance for Stb2 and Stb3 (Ponomarenko *et al* 2011; Makhdoomi *et al* 2014) and Stb4 (Somasco *et al* 1996; Jackson *et al* 2000; Goodwin *et al* 2007).

Stb7 and Stb12 are examples of gene clustering, which commonly occurs with plant defence genes (Bharadwaj *et al* 2021). Stb7 was mapped to chromosome 4AL(Xwmc313) in ST6, conferring resistance to Canadian isolate MG2 (McCartney *et al* 2003), whilst Stb12 was mapped to a similar location in Kavkaz-K4500 L.6.A.4 (KK), conferring resistance to Isr398 but not IPO87019 (Chartrain *et al* 2005a). Stb12 was mapped closer to Xgwm219 than to Xwmc313, indicating the presence of two closely positioned genes. Additionally, four lines from the single-seed descent progeny of KK were resistant to ISR398 but susceptible to IPO97019, confirming the presence of two resistance genes (Chartrain *et al* 2005a; Brown *et al* 2015). More recently, an avirulence effector (Avr3D1) was identified which was postulated to be recognised by Stb7 or Stb12, suggesting the presence of a gene-for-gene relationship (Meile *et al.* (2018). Dalvand *et al.* (2018) and Mahboubi *et al.* (2020) investigated the Stb12 resistance, although both studies didn't investigate Stb12 without the presence of other Stb genes, so Stb12's effectiveness against current isolates is unknown. However, there is evidence that Stb7 has broken down in response to Iranian isolates (Dalvand *et al* 2018), with a wide variety of isolates from geographically distinct countries also overcoming the Stb7 resistance (Czembor *et al* 2010). Therefore, Stb7 is likely ineffective against the majority of *Z.tritici* populations, whilst there is insufficient evidence to evaluate the durability of Stb12.

Stb9 was mapped to chromosome 2BL (Chartrain *et al* 2009), whilst Stb10 was mapped to chromosome 1D in the same variety (KK) where Stb12 was discovered (Chartrain *et al* 2005a). Stb9 was ineffective against 10 isolates tested by Mahboubi *et al* (2020), whilst KK containing both Stb10 and Stb12 and was resistant to all 10 isolates. Stb9 is therefore unlikely to provide

durable resistance whilst Stb10 could provide more durable resistance, although this could be attributed to Stb12. Stb10 effectiveness might also be sensitive to unknown environmental factors due to a lack of expression in previous studies (Arraiano & Brown 2006). More research into the presence and effectiveness of Stb9/10 is needed to understand their contribution to resistance to *Z.tritici* in modern day cultivars.

Stb11 was mapped to chromosome 1BS (Chartrain *et al* 2005b), however, Stb2 and StbWW have also subsequently been mapped at or near to Stb11 (Liu *et al* 2013; Raman *et al* 2009) suggesting that these could be the same resistant gene (Piaskowska *et al* 2021) or are part of a gene cluster like with Stb7 and Stb12 (Chartrain *et al* 2005a; Brown *et al* 2015). However, Stb11 and Stb2 were mapped using different cultivars/*Z.tritici* isolates so further research is needed to understand the overlap between Stb11 and Stb2. Stb11 could still be effective due to its apparent incorporation into elite CIMMYT breeding lines (Brown *et al* 2015), however there is currently no information reporting to its presence or functionality in the literature.

Stb13 and Stb14 were mapped to 7BL and 3BS respectively (McCartney *et al* 2002; Cowling 2006). Stb13 and Stb14 are reported to be present in 96.1% & 58.3% of 180 cultivars tested in Ethiopia respectively (Mekonnen *et al* 2019), however studies by Dalvand *et al* (2018) and Mekonnen *et al* (2020) demonstrated widespread breakdown of both resistance genes.

Stb15 was mapped to 6AS (Arraiano *et al* 2007) and was present in 60% of UK cultivars (Arraiano & Brown 2006). Czemor *et al* (2010), Mehrabi *et al* (2015), Makhdoomi *et al* (2015) and Mahboubi *et al* (2020) demonstrated that Stb15 provided good levels of resistance in Iran, suggesting that this resistance gene is still effective in modern day cultivars, although further research in other geographical regions is needed to fully understand it's current effectiveness.

Stb18 was mapped to 6DS (Tabib Ghaffary *et al* 2011), however, it was inconsistently expressed in adult plants. No other study has investigated Stb18, making its durability and presence in current breeding programs unknown.

Stb6 has been extensively researched since its discovery on chromosome 3AS by Brading *et al* (2002). Stb6 is involved in a gene-for-gene relationship with the corresponding AvrStb6 effector found in IPO323 (Kema *et al* 2000; Brading *et al* 2002). Stb6 has been introduced at least six times into European germplasm (Brown *et al* 2015) and hence is the second most commonly reported STB gene at 15% in the UK (Arraiano & Brown 2006). Resistance from Stb6 has since broken down (Dalvand *et al* 2018; Kosellek *et al* 2013) with a strong selection against susceptible AvrStb6 protein isoforms in European *Z.tritici* populations (Stephens *et al*

2021). There is also evidence from quantitative trait loci (QTL) analyses that Stb6 is associated with other closely linked sources of resistance (Eriksen *et al* 2003; Zwart *et al* 2010; Tabib Ghaffary *et al* 2011; Kelm *et al* 2012; Goudemand *et al* 2013) which might have contributed to its independent widespread incorporation into many European cultivars (Brown *et al* 2015).

Synthetic hexploids are artificially created varieties which contain additional genetic variation from tetraploid and diploid relatives of bread wheat (Li *et al* 2018). Therefore, these cultivars can be valuable sources of resistance which could be introduced into modern elite cultivars (Brown *et al* 2015). Four STB genes originate from these sources; Stb5, 8, 16q and 17. Stb5 was mapped to 7DS (Arrianao *et al* 2001), Stb8 to 7BL (Adhikari *et al* 2003), Stb16q to 3DL and Stb17 to 5AL (Tabib Ghaffary *et al* 2012). Stb5 was effective at providing resistance as reported by Czembor *et al* (2011) and Simon *et al* (2007), although more recent studies by Dalvand *et al* (2018) and Mahboubi *et al* (2020) suggest breakdown of this resistance. Stb8 was also reported to be ineffective by Mahoubi *et al* (2020), although more information is needed to ascertain its durability. Stb16q and Stb17 have been investigated in the M3 cultivar, whereby Makhdoomi *et al* (2015), Mehrabi *et al* (2015) and Mahboubi *et al* (2020) demonstrated effective levels of resistance in M3, with Dalvand *et al* (2018) showing susceptible reactions. Stb16, purported to be Stb16q due to its location (Xinyao *et al* 2021), also demonstrated good levels of broad-spectrum resistance (Xinyao *et al* 2021; Mekonnen *et al* 2020). However, there are recent reports of rapid breakdown of resistance in cv. Cellule in Ireland, likely due to the presence of *Z.tritici* isolates with specific virulence to Stb16q.

The latest STB genes to be identified; Stb19 and Stb20q have been mapped to 1DS and 5D respectively (Yang *et al* 2018; Langlands-Perry *et al* 2021). However, both genes are from modern cultivars Lorikeet & Renan respectively, and hence they are probably already incorporated into breeding programs and aren't novel sources of resistance.

## 5.4 Incorporation of qualitative sources of resistance

Despite the identification and mapping of over twenty STB resistance genes, the vast majority have significant evidence purporting to their widespread breakdown. Few STB genes lack evidence of their breakdown, with fewer still demonstrating current effective levels of resistance against global *Z.tritici* populations. Many studies researching these qualitative sources of resistance postulate their use in breeding programs. For example, Czembor *et al* (2011) suggested incorporation of Stb2, Stb5, Stb15 and Stb16, whilst more recently Stb19 and Stb20q have been identified as genes to introgress into other cultivars (Yang *et al* 2018;

Langlands-Perry *et al* 2021). However, there are limitations associated with utilising studies to incorporate qualitative STB genes into breeding programs. Firstly, studies in the literature rarely account for the population diversity of *Z.tritici* isolates, unless naturally infected field trials are conducted over a variety of sites, which is rarely the case. Environmental conditions and isolate populations also vary considerably, hence a STB gene identified by researchers might not provide resistance the following year, or might only provide resistance at specific field sites, making it undesirable for breeders. Also, many studies such as Czembor *et al.* (2011) demonstrate the virulence of isolates on cultivars with a specific STB gene. Separating major gene effects from background resistance in these studies is difficult, with some STB genes appearing more durable due to high levels of background quantitative resistance, which could mislead breeders. Therefore, many scientific studies investigating specific STB genes might not provide transferable information for breeders.

Furthermore, many STB genes which have been identified from QTL analyses have already been available to breeders. If the identified resistance gene provided widespread durable resistance it would have likely already been incorporated into modern cultivars. For example, Stb15 was mapped in 2007 (Arraiano *et al* 2007) yet was already present in 60% of European cultivars (Arraiano & Brown 2006). Therefore, genes such as Stb19 and Stb20q which have been identified in modern cultivars might already be widespread amongst elite germplasm (Yang *et al* 2018; Langlands-Perry *et al* 2021). Tracking STB genes can also be challenging, since breeding companies commonly build upon competitor's varieties, whereby information pertaining to their specific resistance profile is not available, although high-throughput marker systems can reconstruct pedigrees to some degree (Fradgley *et al* 2019). Because of the unknown presence of STB genes in modern cultivars, efforts to incorporate old STB genes might not be effective (Goodwin *et al* 2007; 2011). STB genes already present in plant breeding programs are also likely to be ineffective against current *Z.tritici* populations. Incorporating these qualitative sources of resistance could also introduce susceptible genes for other pathogens. For example, genes introduced between the 1950s and 1980s to increase yield, rust resistance and eyespot resistance could have also introduced susceptibility genes to *Z.tritici* (Arraiano & Brown 2017). High selection pressures can also exclude desirable traits which could reduce yields despite an increase in resistance to *Z.tritici* (Brown & Rant 2013). Overreliance on these sources of resistance is also a high-risk strategy and could create boom-and-bust cycles as demonstrated by powdery mildew of spring barley in the 1980's (Wolfe

1984; Brown 1994). Therefore, incorporating or pyramiding these qualitative genes into modern cultivars might not be a sustainable solution to improve resistance to *Z.tritici*.

However, novel qualitative sources of resistance identified in the scientific literature can bolster resistance to *Z.tritici*. For example, synthetic hexaploids have generated four STB genes which were otherwise unavailable to breeders (Arrianao *et al* 2001; Adhikari *et al* 2003; Tabib Ghaffary *et al* 2012). Provided good levels of quantitative background resistance are present, introgression of qualitative sources of resistance can briefly bolster the resistance to *Z.tritici*. Researching qualitative sources of resistance can also help breeders understand how likely sources of resistance are to break down. For example, cultivars with numerous STB genes could prove to be more 'high-risk' compared to cultivars less reliant on qualitative sources of resistance. Additionally, information on geographical population structures of corresponding AvrStb genes and specific virulence studies could help identify 'vulnerable' STB genes, which breeders might want to avoid using.

## 5.5 Quantitative resistance

Durable resistance to *Z.tritici* is highly desirable for breeders and growers alike, since breeders can collect royalties from a specific cultivar for a longer period of time and risk is reduced for growers. However, achieving durable resistance to *Z.tritici* can be highly challenging. Durable resistance commonly consists of quantitative sources of resistance typically involving polygenic genes with small additive effects which aren't race-specific (Brown 2021). Quantitative resistance encompasses preformed defences triggered by pathogen associated molecular patterns (PAMP) and damage associated molecular patterns (DAMP), although it can also debatably involve weak forms of ETI (Cowger & Brown 2019; Iakovidis *et al* 2016). Quantitative resistance has been demonstrated to be relatively durable due to high levels of resistance being maintained in many cultivars despite over-representation of reported breakdowns in the scientific literature, likely a result of publication bias (Cowger & Brown 2019). Serial passage experiments can be utilised to investigate the durability of quantitative sources of resistance (Cowger & Brown 2019; Gilbert & Parker 2010), however, *Z.tritici* literature lacks such experiments in favour of investigation into major sources of qualitative resistance. Understanding the gradual breakdown of quantitative resistance could aid breeders since, whilst qualitative and quantitative resistance are commonly referred to in a black or white manner, there is a grey area for some sources of resistance which might be deemed quantitative (Cowger & Brown 2019). Identifying sources of quantitative resistance can be challenging

since association genetics techniques which associate the plant phenotype with genetic markers might not detect these sources of resistance because of their small additive effects (Arraiano & Brown 2016). Sources of durable resistance could accidently be removed from breeding programs if background sources of resistance are side-lined over genetic markers associated with strong levels of qualitative resistance. Hence, it is more important for breeders to remove susceptible genotypes and markers instead of strongly selecting for resistance markers which are more likely to be associated with a form of non-durable qualitative resistance (Brown 2021). Quantitative resistance is the backbone of plant breeding, preventing the collapse of *Z.tritici* resistance when qualitative sources of resistance are inevitably broken down. The value of quantitative resistance has been demonstrated recently with the breakdown of a major source of resistance from Cougar (Kildea *et al* 2021), whereby disease resistance ratings decreased by 0.6 – 1.8. Although this is a significant decrease in resistance to *Z.tritici*, the majority of these cultivars still display an acceptable level of resistance, with quantitative resistance likely playing a significant role in preventing a complete collapse of resistance.

## 6. Disease escape

In addition to qualitative and quantitative sources of resistance, disease escape traits can be utilised to reduce the severity of *Z.tritici* epidemics. Disease escape traits typically include morphological traits that reduce infection rates to *Z.tritici* through mechanistic barriers or changes in developmental timings. For example, delayed heading date can be associated with reduced *Z.tritici* severity (Arraiano *et al* 2009; Simon *et al* 2005; Eyal *et al* 1987; Van Beuningen & Kohli 1990; Camacho Casas *et al* 1995; Gerard *et al* 2017). Other morphological traits which can influence *Z.tritici* disease in the field include plant height and inter-leaf distance. These two traits are interlinked, with taller plants generally having larger inter-leaf distances. Taller plants tend to display reduced *Z.tritici* disease (Robert *et al* 2008; Arraiano *et al* 2009; Simon *et al* 2004; Eyal *et al* 1981; Bannon and Cooke 1998; Baltazar *et al* 1990), which could be attributed to greater inter-leaf distances reducing the spread of pycnidiospores through rain splash (Robert *et al* 2008). However, these disease escape traits, whilst beneficial in controlling for *Z.tritici,* can be associated with yield penalties (Judge 2015) and logistical challenges making them undesirable as a whole for crop improvement.

## 7. Major source of resistance in Cougar

The UK recommended list (RL) published by AHDB is a useful tool for growers to select winter wheat varieties with high yields. Cougar was added to the RL in 2013 in part due to its

*Z.tritici* resistance score of 7, as well as high levels of yellow rust (*Puccinia striiformis*) resistance. However, Cougar was swiftly removed by 2015 due to a rapid decrease in resistance to *Z.tritici*. Understanding this decrease in resistance to *Z.tritici* is important since Cougar has been used as a parental line to develop novel cultivars. (KWS firefly, LG Illuminate, RGT Saki, Merit, LG Prince, LG Astronomer, Swallow) The removal of Cougar from the RL sparked a project by AHDB aiming to 1) Phenotype identified Cougar virulent isolates on Cougar and other RL varieties 2) Sequence the isolates 3) Test isolates for resistance to fungicides (Caiazzo *et al* 2019). This project concluded that isolates virulent on Cougar weren't more virulent on other cultivars and that no unexpected fungicide mutations were present. These results, whilst described as "positive result for growers", demonstrated that Cougar contains a major source of resistance, likely a form of gene-for-gene qualitative resistance. Despite a breakdown in resistance to *Z.tritici* in 2015, because of Cougar's resistance to *Z.tritici* and yellow rust (*Puccinia striiformis*) it has been incorporated into the pedigrees of 8 out of 22 of UK winter wheat cultivars on the 2021/2022 RL. Since reports by Caiazzo *et al* (2019) demonstrated Cougar specific resistance breakdown, Kildea *et al* (2021) investigated resistance breakdown in winter wheat cultivars with Cougar parentage in Ireland. Despite Cougar never been grown commercially in Ireland, *Z.tritici* Cougar virulent isolates were generally virulent on cultivars grown in Ireland with Cougar parentage. However, some Cougar virulent isolates were incompatible with Cougar-derived cultivars, such as KWS Firefly and LG Astronomer which both had cv Alchemy in their pedigree, which were postulated to include Stb8 (Adhikari *et al* 2003), Stb13 and Stb14 (Cowling 2006) (Kildea *et al* (2021). This highlights how pyramiding genes can aid in maintaining resistant levels. Interestingly, KWS firefly demonstrated the most severe breakdown in resistance in 2021/2022, likely suggesting the presence of different *Z.tritici* isolates compared to those studied in Kildea *et al* (2021) and/or breakdown of other source(s) of resistance in KWS firefly. Incorporation of Cougars *Z.tritici* resistance could be deemed short-sighted in hindsight, since breeders were aware of *Z.tritici* resistance breakdown in Cougar as early as 2015. However, Cougar's major source of resistance has remained relatively effective up until 2020/2022, demonstrating ~7 years of effective use (AHDB; Kildea *et al* 2021). Cougar's major source of resistance was also likely already being incorporated into breeding programs before 2015, hence removing this resistance, which was still functional, would have been impractical for breeders. Additionally, cultivars with Cougar parentage weren't solely reliant on this major source of resistance, with a decrease in ~0.6 – 1.9 resistance score in 2021/2022. Therefore, whilst breakdown of this resistance is undesirable, it wasn't

completely disastrous. In addition to Caiazzo *et al* (2019) and Kildea *et al* (2021) this PhD project aims to contribute to our understanding of the major source of resistance in Cougar.

# 8. The mechanisms of resistance to *Z.tritici*

## 8.1 Pathogen recognition & gene-for-gene resistance

Relatively little is known about mechanisms of resistance to *Z.tritici* (O'Driscoll *et al* 2014; Brown 2021). This is likely in part due to breeders being able to successfully incorporate durable resistance into modern cultivars without knowledge of mechanisms of resistance or genetics (Brown 2021). For example, quantitative resistance can be steadily incorporated into novel cultivars through genomic selection by removing susceptible genotypes (Brown 2021). Whilst improving mechanistic knowledge of resistance to *Z.tritici* might not directly benefit breeders, as is the case with many scientific advancements the downstream applications of such research, whether directly relatable to *Z.tritici* resistance breeding or to more general fungal or plant research, isn't always forthcoming but can be substantial. However, understanding the mechanisms of resistance can provide some useful information to breeders, in addition to furthering our understanding of *Z.tritici* and resistance genes.

Research into the mechanisms of quantitative resistance is extremely difficult since the effects are typically small, polygenic and difficult to decipher from qualitative sources of resistance. For example, Ajigboye *et al* (2021) characterised the resistance of cv. Cougar relative to cv. Sacramento, whereby differences in resistance to *Z.tritici* could be attributed to the major source of resistance in Cougar and/or background quantitative sources of resistance. Near isogenic lines (NILs) could be used to exclude known sources of qualitative resistance to better characterise quantitative resistance, although the "background resistance" would likely still include a multitude of genetic effects which could be qualitative. Therefore, the majority of research into understanding the mechanisms of resistance to *Z.tritici* has been performed on qualitative sources of resistance since they typically display strong phenotypic differences, are controlled by a single gene, and can be investigated using near isogenic lines (NILs) with the same genetic background.

Four STB genes (Stb7, Stb12, Stb6, Stb16q) have evidence purporting to the presence of a gene-for-gene relationship, indicating specific recognition of an avirulence protein to initiate strong levels of resistance (Meile *et al* 2018; Brading 2002; Saintenac *et al* 2021). Meile *et al* (2018) used a quantitative trait loci analysis (QTL) combined with transcriptomic analysis on

two rural Swiss strains 3D1/3D7 to identify a 75 kb candidate region housing six candidate genes. Subsequent ATMT transformations created knockout lines to identify an avirulent effector (Avr3D1) which was recognised by three cultivars containing Stb7, and possibly Stb12, to provide intermediate levels of resistance. Whereas Meile *et al* (2018) investigated the avirulent effector in the pathogen, Saintenac *et al* (2021) utilised similar techniques to identify and characterise Stb16q in wheat. Use of a biparental mapping population utilising the Stb16q donor accession M3 identified two candidate genes in the 272kb interval. Subsequent sequencing and cloning identified candidate gene Crk6 to be Stb16q, which provided broad-spectrum resistance when introduced into susceptible cv. Courtot (Saintenac *et al* 2021). Whilst Stb16q provided resistance to all 11 isolates tested, the dramatic differences in symptoms between Stb16q+ve and Stb16q-ve lines is indicative of a gene-for-gene relationship. Further evidence for a gene-for-gene relationship was demonstrated by Kildea *et al* (2021) whereby two isolates obtained from cv. Cellule and cv. Costello were virulent on Cellule containing Stb16q. A greater diversity of isolates and subsequent investigation of avirulence effectors (Meile *et al* 2018) would help validate the presence of a gene-for-gene relationship for Stb16q.

Stb6 has been one of the most extensively researched STB genes since its discovery (Brading *et al* 2002). A corresponding AvrStb6 effector was mapped to chromosome 5 utilising QTL analysis on expression data, combined with subsequent functional validation with mutant strains (Mirzadi Gohari 2015). Zhong *et al* (2017) confirmed the presence of a gene-for-gene relationship by combining both QTL and GWAS analyses on over 100 strains to create a narrow candidate window, composed of nine candidate AvrStb effector genes. By combing both QTL and GWAS analysis this clearly identified 1A5.g5534 as the most promising AvrStb6 candidate. Functional validation involved cloning 1A5.g5534 by transformation into both parental strains, with visual phenotyping confirming 1A5.g5534 to be AvrStb6 (Zhong *et al* 2017). Identification of AvrStb effectors can help inform plant breeders of geographical *Z.tritici* population compositions for specific AvrStb effectors. This information could be used to inform breeders where specific STB genes might be most/least effective as well as to predict resistance breakdown (Stephens *et al* 2021). Stb6 was subsequently cloned using a map-based cloning approach to identify two candidate genes; TaWAKL3 and TaWAKL4 (Saintenac *et al* 2018). Five sources of evidence demonstrated TaWAKL4 to be Stb6. 1) Gene analysis demonstrated greater expression of TaWAKL4. 2) TaWAKL4 contained a missense mutation causing a p.Ile447Asp amino acid change, whereas there were no SNPs identified in TaWAKL3. 3) Virus induced gene silencing (VIGS) of TaWAKL4 compromised Stb6

mediated resistance. 4) Tilling lines with predicted nonsense and missense mutations in TaWAKL4 compromised Stb6 mediated resistance. 5) Cloning of TaWAKL4 into IPO323 susceptible cultivars cv. Courtot and cv. Bobwhite demonstrated Stb6 mediated resistance (Saintenac *et al* 2018). Identification of Stb6 highlights many techniques and tools available to identify qualitative sources of resistance (Saintenac *et al* 2018). This PhD aims to begin to incorporate some of these techniques to identify the major source of qualitative resistance in Cougar, although additional work would be required to validate candidate genes utilising VIGS, tilling populations and cloning techniques.

## 8.2 Preformed defence

Whilst this research provides significant insight into gene-for-gene resistance and pathogen detection, the characterisation of resistance is also important. Resistance phenotypes could be highly conserved, or involve significantly different resistance strategies. Characterising the mechanisms of resistance to *Z.tritici* in wheat could highlight additional phenotypic parameters associated with resistance, which could aid breeders in identifying novel sources of resistance. Understanding mechanisms of resistance could also highlight targets for candidate fungicides, as well as furthering our knowledge of *Z.tritici* infection. To my knowledge, seven studies have investigated the resistance response to *Z.tritici* in wheat (Lee *et al* 2015; Saintenac *et al* 2021; Battache *et al* 2022; Ajigboye *et al* 2021; Orton *et al* 2017; Palma-Guerrero *et al* 2016; Benbow *et al* 2020). Stb16q resistance involves preformed defence, whereby confocal microscopy demonstrated a lack of progression of germ tubes into the stomata (Saintenac *et al* 2021). Further characterisation of Stb16q by Battache *et al* (2022) confirmed this phenotype, with a 5% success rate for penetration attempts in the incompatible interaction. Additionally, hyphae that were successful in penetrating the stomata swiftly stopped in the sub-stomatal cavity (Battache *et al* 2022). This preformed resistant phenotype, combined with Stb16q providing resistance to all 11 isolates tested, explains why it was characterised as a quantitative source of resistance (q) (Saintenac *et al* 2021; Battache *et al* 2022). However, evidence of resistance breakdown in specific isolates (Kildea *et al* 2021) suggests that Stb16q is a form of qualitative resistance, whereby this preformed defence response is only effective on specific isolates with a corresponding AvrStb effector. Further investigation utilising isolates which have fully or partially evolved resistance to Stb16q (Kildea *et al* 2021) is necessary to confirm the qualitative/quantitative nature of Stb16q. The role of preformed defence traits in resistance has also been demonstrated in the resistant cv. Cougar, compared to the susceptible cv. Sacramento (Ajigboye *et al* 2021). Cougar had a lower density of stomata, which were narrower and longer,

with an increase in the expression of a wax biosynthesis gene TaFAR3. *Z.tritici* spores on Cougar didn't directionally grow towards the stomata and exhibited longer unbranched hyphae compared to Sacramento, which formed compact hyphal networks that directionally grew towards the stomata (Ajigboye *et al* 2021). Whilst research on Stb16q was investigated using NILs, preformed defence traits demonstrated by Ajigboye *et al* (2021) cannot be solely associated with the major source of resistance in Cougar. These preformed resistance traits are a combination of both the background quantitative resistance and the major source of qualitative resistance. The characterisation of resistance in Cougar by Ajigboye *et al* (2021) is arguably more useful to breeders than specific characterisation of a gene such as Stb16q since the background quantitative resistance phenotype is also characterised. This PhD aims to utilise NILs to characterise the qualitative source of resistance in Cougar, with results from this project highlighting what resistance traits are part of the major source of resistance. Therefore, Cougar resistance traits identified by Ajigboye *et al* (2021), but which are not characterised using Cougar NILs in this PhD, are likely a form of background quantitative resistance.

## 8.3 Chloroplast defence mechanisms

The chloroplast plays a significant role in plant defence, being the site for the synthesis of defence molecules such as Jasmonic acid (JA), Salicylic acid (SA) and Abscisic acid (ABA) (de Torres Zabala *et al* 2015). The chloroplast is also a major source of reactive oxygen species (ROS), which can initiate a hypersensitive response (HR) involving programmed cell death (PCD) (Serrano *et al* 2016) through chloroplast-to-nucleus retrograde signalling (Lee *et al* 2015; Galvez-Valdivieso *et al* 2010). ROS signalling is also known to be influential in plant-pathogen interactions (Bharath *et al* 2021; Fichman *et al* 2020), with ROS accumulation being key in facilitating compatible *Z.tritici*-wheat interactions during the switch to necrotrophy (Foyer & Noctor 2005; Choi *et al* 2016). Therefore, the chloroplast is a likely battleground for Wheat-*Z.tritici* interactions and resistant strategies. Currently, two studies have primarily investigated the role of the chloroplast in the wheat resistant response to *Z.tritici* (Lee *et al* 2015; Ajigboye *et al* 2021). In lines harbouring Stb6, two key chloroplast genes involved in chlorophyll and carotenoid biosynthesis (TaChlH & TaPDS) were silenced (Lee *et al* 2015). Chlorophyll deficient TaChlH and TaPDS lines exhibited rapid accumulation of $H_2O_2$, which was associated with rapid tissue collapse and hyphal penetration followed by accelerated PCD, demonstrating the importance of the chloroplast in Stb6-mediated defence against *Z.tritici* (Lee *et al* 2015). Whereas Lee *et al* (2015) investigated two influential chloroplastic genes, Ajigboye *et al* (2021) utilised chlorophyll fluorescence measurements, ROS assays, RT-qPCRs of

relevant genes and metabolomic analysis of the xanthophyll cycle to investigate the role of the chloroplast in greater depth.

Chlorophyll fluorescence measurements provide a useful tool to decipher chloroplast functionality in a non-destructive manner (Murchie & Ruban 2020). Photoprotective mechanisms have evolved to prevent the accumulation of damaging ROS, hence it is possible that *Z.tritici* could manipulate these processes to induce PCD. Excess energy absorbed by the light harvesting complexes can be dispersed in an uncontrolled manner, which leads to ROS accumulation and PCD, or in a controlled manner (non-photochemical quenching, NPQ). NPQ primarily comprises of a fast-acting qE component Ruban *et al* (2012). The qE component of NPQ is triggered by protonation of PsbS, which binds to the light harvesting complex, forming a tightly associated quenching state which slightly dissociates from the PSII core (Li *et al* 2004). In addition to PsbS protonation, violaxanthin is reversibly converted into zeaxanthin which replaces violaxanthin in the peripheral light harvesting complexes. Whilst zeaxanthin is typical of the qE quenching state, it is not essential, and instead contributes towards a more tightly associated light harvesting complex (Ruban *et al* 1997; Ruban *et al* 2012). NPQ also consists of a slow-relaxing qI component that is indicative of photoinhibition of PSII via phosphorylation of D1, leading to targeted lateral migration of phosphorylated PSII cores to the lateral stromal thylakoid membranes (Rintamäki *et al* 1995). In addition to the qE and qI components of NPQ, other characterised components involve the qT component which accounts for the effect of state transitions whereby light harvesting complexes migrate from PSII to PSI (Quick and Stitt, 1989; Nawrocki *et al* 2016); the qH component which involves sustained photoprotective antenna quenching (Malnoe 2018); and the qM component involving phototropin induced chloroplast movement (Dall'Osto *et al* 2014). NPQ measurements have been extensively used to investigate plant-pathogen interactions (Prokopova *et al* 2010; Chávez-Arias *et al* 2019; Passari *et al* 2019), herbicide mode of action and potency (Frankart *et al* 2003; Moustaka *et al* 2015), abiotic stress responses (Zhou *et al* 2017; Hazrati *et al* 2017), and crop improvement strategies (Kaiser *et al* 2016).

In addition to chlorophyll fluorescence measurement being a valuable tool to investigate photoprotective and photoinhibatory NPQ defence responses, these techniques can also be used to calculate OJIP derived measurements (Strasser *et al* 2000). The OJIP fluorescence transient quantifies the energy flux through PSII and hence provides information on the function and structure of the photosynthetic apparatus (Strasser *et al* 2000). OJIP fluorescence transients have been demonstrated to be effective in phenotyping plant responses to diseases such as

powdery mildew (*Blumeria graminis*) (Ajigboye *et al* 2016), eyespot (*Oculimacula yallundae/acuformis*) (Ajigboye *et al* 2016), fusarium head blight (*Fusarium culmorum*) (Ajigboye *et al* 2016; Katanic *et al* 2021; Warzecha *et al* 2019) and tobacco mosaic virus (Tseliou *et al* 2021). Whereas NPQ provides information on photoprotection and photoinhibition through timely light induction curves, OJIP measurements take ~1 second which eliminates the effect of NPQ. These OJIP measurements gives information on the absorption of energy from the light harvesting complexes (ABS_RC), the trapping rate of electrons in PSII (TRo_RC), the dissipated energy as heat/fluorescence (Dlo_RC), and electron transport from Qa to Qb (ETo_RC) (Strasser *et al* 2000). Therefore, these measurements can provide additional information which could supplement information gained from NPQ measurements.

Chlorophyll fluorescence measurements could be a valuable phenotyping tool to investigate the major source of resistance in Cougar. Previous research by Ajigboye *et al* (2021) demonstrated that Cougar upregulated the slow-relaxing NPQ component (qI), as well as downregulating photosynthesis, demonstrating both a photoinhibatory and a photoprotective defence response (Ajigboye *et al* 2021). Because carotenoids play an integral role in the light harvesting complex's (Lokstein & Götze 2021), as well as being potent anti-oxidants Ajigboye *et al* (2021) investigated the role of the xanthophyll cycle in the Cougar defence response, demonstrating increased synthesis of neoxanthin leading into ABA accumulation. The Cougar defence response was also characterised by JA biosynthesis, increased expression of chloroplast-specific ROS scavenging enzymes, and decreased $H_2O_2$/ROS accumulation. Therefore, this PhD will aim to build on the study of Ajigboye *et al* (2021) by characterising the photoprotective resistant response in Cougar NILs to decipher the major qualitative source of resistance from the background quantitative resistance.

## 8.4 Transcriptomic analysis of defence mechanisms

To date, around 10 transcriptomic studies have been published regarding the wheat-*Z.tritici* interaction, however only recently has the wheat resistance response been investigated (Benbow *et al* 2020). Previous research has focused on quantification of specific defence-related genes to gain insight into the wheat-*Z.tritici* resistant response (Ray *et al* 2003; Adhikari *et al* 2007; Shetty *et al* 2009). These studies demonstrated the importance of specific genes in the wheat-*Z.tritici* defence response such as R-1 and lipoxygenase (Ray *et al* 2003), phenylalanine ammonia lyase (Adhikari *et al* 2007) and β-1,3-glucanase (Shetty *et al* 2009).

However, these studies only investigated one *Z.tritici* isolate, making the conservation of these defence related processes in response to other isolates uncertain, although Shetty *et al* (2009) did functionally validate β-1,3-glucanase. For example, Orton *et al* (2017) investigated these genes alongside 8 other defence related genes known to encompass different aspects of defence-related process in host-pathogen interactions. However, no differential expression was detected for the incompatible interactions for all 11 genes, despite Orton *et al* (2017) using the same isolate (IPO323) as Shetty *et al* (2009). These results demonstrate that investigation into specific defence-related genes might be unrepeatable and/or be highly specific to the cultivar-isolate interaction. Utilising a diverse range of cultivars and isolates to identify conserved defence-related gene expression could help characterise quantitative sources of resistance, as well as highlighting conserved defence responses from qualitative sources of resistance from major STB genes. Whereas studies like Orton *et al* (2017) investigated a specific set of genes, transcriptomic analyses can quantify over 10,000 genes, providing a more holistic approach to characterise the wheat-*Z.tritici* resistant response. This approach can identify pathways and processes which are differentially expressed instead of relying on specific "key" genes to quantify the resistant response. Transcriptomic analyses can also be combined with QTL analyses to investigate specific genes associated with specific sources of resistance (Odilbekov *et al* 2019; Saini *et al* 2022). Using this approach, Odilbekov *et al* (2019) identified F-box proteins to be the most represented gene expressed in all three identified QTL regions, followed by nucleotide-binding site (NBS) leucine rich repeat (LRR) disease resistance proteins and receptor-like kinases (RLK). F-box proteins are involved in the JA and SA hormonal pathways (Yu *et al* 2007), whilst NBS-LRRs typically confer resistance to various pathogens and RLKs are involved in the detected of pathogen-virulence effectors, such as AvrStb6 for example (Saintenac *et al* 2018; Zhong *et al* 2017). Saini *et al* (2022) also demonstrated the value of combining QTL analyses with transcriptomic analyses to identify genes underlying the defence response, although this focused on genes associated with multiple disease resistance (MDR), and hence wasn't specific to *Z.tritici*. To my knowledge, Benbow *et al* (2020) is the only study which primarily investigated the different transcriptomic profiles in wheat-*Z.tritici* compatible and incompatible interactions. Benbow *et al* (2020) demonstrated large differences in the resistant response in a time-dependent manner of over 500 genes. Cv. Longbow (compatible) initiated a PAMP defence response at 24 hpi, whereas cv. Stigg suppressed defence related genes. These results suggests that *Z.tritici* manipulates Longbows defence response to facilitate infection, whilst Stigg staves off disease progression by downregulating many biological processes to extend the latent phase of disease (Benbow *et al* 2020). However, it is worth noting

that Benbow *et al* (2020) only used one *Z.tritici* isolate, and hence this defence response might be either unique to these cultivars and/or unique to this isolate. Therefore, it's unknown if the resistant response in Stigg is a conserved or unique resistant strategy. This PhD used QTL analyses to locate a candidate region for the major source of resistance in Cougar, with subsequent transcriptomic analysis to identify the candidate gene(s). In addition, this study utilised transcriptomic analyses to quantify the qualitative source of resistance in Cougar NILs. Whilst Bendow *et al* (2020) compared two cultivars with differing susceptibility to *Z.tritici,* it's unknown what sources of resistance in Stigg are primarily responsible for the resistance response. By comparing NILs with and without the Cougar resistance, this PhD can better characterise the major source of resistance in Cougar whilst reducing the presence of confounding background resistance. Additionally, two isolates with incompatible interactions with the Cougar resistance was used to reduce isolate specific effects and identify the common transcriptomic defence responses. This study also briefly investigates the *Z.tritici* transcriptome to identify potential avirulence effectors, as well as general processes associated with corresponding compatible and incompatible interactions. Although this PhD focuses on characterising a qualitative source of resistance, transcriptomic studies could also be utilised to identify minor genes and processes associated with quantitative sources of resistance which would otherwise be undetectable. Overall, transcriptomic studies provide a wealth of information which can be used to investigate the wheat-*Z.tritici* resistant response in a holistic approach.

## 9. High-throughput phenotyping for plant breeders

*Z.tritici* and wheat research should primarily serve plant breeders to help develop wheat cultivars, with high levels of resistance to *Z.tritici,* in a durable and sustainable manner. A significant bottleneck for breeders is efficient and reliable phenotyping of field trails used to develop novel cultivars. Breeders need to phenotype numerous field trials involving thousands of plots for a multitude of traits over a limited timeframe. *Z.tritici* disease is currently assessed on a 1-9 scale on the RL, although some breeders assess *Z.tritici* in even less depth due to time constraints. Breeders commonly utilise QTL studies to identify markers associated with sources of resistance to *Z.tritici* to incorporate them into breeding programs, as well as to track them in other cultivars. Quantitative trait loci (QTL) studies rely on genomic recombination between two parents, combined with a phenotype of the subsequent population lines to link genomic regions with phenotypic traits, such as resistance to *Z.tritici* (Carbonell *et al* 1992). QTL studies are the main technique used to identify qualitative sources of resistance in the

scientific literature (Brown *et al* 2015) but are also instrumental for plant breeders to identify desirable and non-desirable markers to include or omit in breeding programs. High-throughput phenotyping techniques could help breeders identify more sources of resistance to *Z.tritici* by increasing the number and size of field trials. Proximal phenotyping tools can also provide accurate, repeatable and quantitative data (Gryzbowski *et al* 2021) which could replace manual visual *Z.tritici* assessments. Phenotyping tools could therefore provide more precise confidence intervals on specific sources of resistance, whilst also providing breeders with additional information not available with traditional visual *Z.tritici* assessments. Proximal phenotyping tools include RGB-imaging combined with manual or automatic image analysis (Karisto *et al* 2018), multi and hyperspectral reflectance (Yu *et al* 2018), thermal sensors, chlorophyll fluorescence imaging (Odilbekov *et al* 2018), and 3D imaging (Mahlein 2016).

## 9.1 Visual range image analysis

Automatic image analysis of *Z.tritici* symptoms can provide quantitative and repeatable measurements of disease severity. Stewart *et al* (2016) developed an ImageJ macro which can quantify *Z.tritici* symptoms on detached individual leaves, however whilst this is likely effective on a leaf level, this cannot be used to quantify *Z.tritici* disease on a canopy scale. Photos of individual field trial plots could enable subsequent quantification by image analysis, however, currently no such programs exist in the literature. Whilst image analysis of field trial plots could provide more repeatable and precise data, this is likely more time consuming than visual assessments. To utilise image analysis in a high-throughput manner requires the use of UAVs (Wei *et al* 2021; White *et al* 2012) or other remote vehicles to collect the data, which pose their own technical and practical challenges.

## 9.2 Hyperspectral reflectance measurements

One of the more promising phenotyping tools to phenotype *Z.tritici* symptoms in a high-throughput manner at a canopy level is the use of spectroradiometers to calculate hyperspectral reflectance indices (Mahlein 2016). Hyperspectral indices are calculated from formulas utilising the reflectance of specific wavelengths, with specific indies demonstrated to be associated with specific molecular components such as carotenoids (Chappelle *et al* 1992), chlorophylls (Blackburn 1998), anthocyanins (Gitelson *et al* 2001) and water content (Penuelas *et al* 1993), or even a specific disease such as leaf rust (Ashourloo *et al* 2014). Because hyperspectral indices can provide information on molecular components, this information can also be used to inform on the potential mechanisms of resistance since molecules such as

carotenoids and chlorophylls play key roles in host defence (Lee *et al* 2015; Ajigboye *et al* 2021). Hyperspectral reflectance measurements have also been demonstrated to be a valuable tool to phenotype various wheat diseases such as leaf rust (Ashourloo *et al* 2014) and fusarium head blight (Mustafa *et al* 2022). Three studies have investigated the use of hyperspectral indices in characterising *Z.tritici* symptoms (Yu *et al* 2018; Odilbekov *et al* 2018; Anderegg *et al* 2019). Yu *et al* (2018) investigated the role and order of importance of indices in predicting and explaining STB disease at specific growth stages, whereas Odilbekov *et al* (2018) investigated a more extensive range of indices over a time series. Anderegg *et al* (2019) investigated the use of spectral-temporal features based on hyperspectral time-series measurements to reduce the effect of confounding factors such as canopy architecture, morphology and environmental conditions, using a combination of indices with STB sensitive and insensitive traits. These three studies provide significant insight into the best indices to quantify STB, as well as the effect of canopy architecture between different genotypes (Anderegg *et al* 2019), and the effect of time and growth stage on the effectiveness and reliability of indices. Therefore, hyperspectral reflectance measurements could be an effective tool for breeders and researchers alike to phenotype STB resistance in a high-throughput, non-invasive, quantitative and precise manner (Grzybowski *et al* 2021; Mahlein 2016).

## 9.3 Chlorophyll fluorescence measurements

Chlorophyll fluorescence measurements (CFMs) have been demonstrated to be effective in quantifying *Z.tritici* resistance in cv. Cougar (Ajigboye *et al* 2021). Whilst precise instruments such as the LI-COR-6400 used in Ajigboye *et al* (2021) provide a wealth of information, measurements are highly time-consuming with protocols reaching ~45 minutes whilst requiring a period of dark adaptation in excess of ~30 minutes (Murchie & Lawson 2013). However, a range of CFM phenotypic tools are available which are designed to phenotype quickly in the field such as FluorPen FP 110 (Photon Systems Instruments, Czech Republic) and MultispeQ (PhotosynQ; Kuhlgert *et al* 2016). Instruments such as the FluorPen measure the OJIP transient, which quantifies the energy flux through PSII and hence provides information on the function and structure of the photosynthetic apparatus (Strasser *et al* 2000). The transients O-J-I-P represent the amplitude of fluorescence during specific phases of induction from $F_O$ (O) to Fm (P) with two intermediate inflection points, J (at about 2 ms) and I (at about 20 ms), appearing between Fo and Fm (Ajigboye *et al* 2018). OJIP transients have been used to phenotype a variety of plants in response to abiotic stress (Hazem *et al* 2014; Zushi *et al* 2017; Rapacze *et al* 2019) and biotic stress (Campos *et al* 2021; Ajigboye *et al*

2021). To my knowledge, two studies have utilised OJIP measurements to phenotype the *Z.tritici*-wheat interaction (Spyroglou *et al* 2022; Odilbekov *et al* 2018). Odilbekov *et al* (2018) utilised OJIP transients to calculate the quantum yield of PSII (QY), demonstrating QY as one of the best predictors of STB chlorotic and necrotic lesions. Spyroglou *et al* (2022) utilised in-depth chlorophyll fluorescence parameters calculated from OJIP measurements, combined with deep learning networks, to demonstrate that differences in OJIP CFMs at 8 dpi could reliably estimate subsequent disease resistance. The extensive use of OJIP parameters in the literature, combined with two specific case studies demonstrating OJIP use in phenotyping STB disease, suggests that OJIP measurements (FluorPen) could be an effective phenotyping tool for breeders. Another more recently developed instrument which can measure chlorophyll fluorescence is the MultispeQ (PhotosynQ) (Kuhlgert *et al* 2016). The MultispeQ uses PAM fluorometry to calculate a suite of chlorophyll fluorescence parameters such as non-photochemical quenching (PhiNPQ), non-regulatory energy dissipation (PhiNO) and redox state of $Q_A$ (Phi2). These measurements require a short period of dark adaptation (~2 minutes), which does reduce the potential for this instrument to be used as a high-throughput method, however, this is significantly shorter than using a LI-COR to calculate equivalent parameters. The MultispeQ can also calculate NPQ(t) without the need for a $F_o$ value, removing the dark adaption requirement and decreasing protocol duration to a few seconds (Tietz *et al* 2017). The MultispeQ has been previously used to phenotype plant populations, primarily investigating photosynthetic responses in response to abiotic stress (Fernandez-Calleja *et al* 2020; Liaqat ali *et al* 2022), although some biotic stresses have also been quantified, such as lesion mimic mutants with resistance to stripe rust and powdery mildew (Li *et al* 2022). To my knowledge, no studies have used the MultispeQ to phenotyping *Z.tritici*-wheat interactions. However, the MultispeQ could be useful in obtaining specific chlorophyll fluorescence measurements which were previously only be available using a more time-intensive instrument such as a LI-COR gas-exchange analyser. Because of the time constraints required for each measurement using a FluorPen and/or MultispeQ compared to visual assessments, combined with the lack of canopy level measurements, these might not be effective high-throughput tools. However, the information they provide is unique and could point to the putative mechanisms behind resistance. Other chlorophyll fluorescence tools such as chlorophyll fluorescence imaging using a FluorCam can also be a useful high-throughput method to phenotype populations, however, these instruments aren't designed to phenotype field populations since the plants need to be put into a FluorCam chamber. Overall, these phenotypic instruments could be promising

candidates for breeders to use to phenotype plant populations in a high-throughput, precise, quantitative and repeatable manner, which could help accelerate breeding programs.

This PhD aims at using a range of phenotyping tools such as hyperspectral measurements and chlorophyll fluorescence measurements (FluorPen, MultispeQ) to identify the major source of resistance in Cougar using QTL analysis. I will also evaluate how effective these instruments are at identifying other sources of resistance to *Z.tritici* and predicting subsequent disease. These measurements might also help characterise the source of resistance in Cougar, as well as to characterise *Z.tritici* resistance in general. The results generated from this PhD will hopefully help inform breeders of the value of these phenotypic instruments in STB gene discovery to accelerate the breeding process.

## 10. PhD aims objectives and hypotheses

This PhD commenced in 2017, before the more recent reports of widespread breakdown of the major source of resistance in Cougar (Caiazzo *et al* 2019; Kildea *et al* 2021). This PhD stemmed from the evidence of a breakdown in resistance in Cougar in 2015, and followed a previous collaboration between the University of Nottingham and RAGT (Ajigboye *et al* 2021) characterising the resistance in cv. Cougar compared to cv. Sacramento. This project builds on the work by Ajigboye *et al* (2021) by characterising the major source of resistance, using a set of near isogenic lines (NILs) to remove background genetic effects. The main objective of this project was to identify the candidate gene(s) responsible for the major source of resistance and to understand the mechanism behind this source of resistance. Therefore, this PhD starts by aiming to identify the location of the major source of resistance using a cv. Cougar x cv. Scout DH population over two years (2018/2019). A range of phenotyping tools were used to determine their value for breeders to phenotype *Z.tritici* symptoms in field populations, as well as to characterise the major source of resistance in Cougar. The candidate region was narrowed down further using a higher density of markers on a cv. Cougar population created from backcrossing cv. Cougar with cv. Cashel until BC3, with subsequent transcriptomic analysis used to identify candidate genes within that region. Virus induced gene silencing (VIGs), work with tilling lines and cloning techniques were also on the table to validate the major source of resistance in Cougar in a similar manner as Stb6 (Zhong *et al* 2017) and Stb16q (Saintenac *et al* 2021). However, due to time constraints associated with obtaining a set of NILs, as well as the impact of the Covid pandemic, there was not enough time to carry out these techniques. A range of instruments and methods was used to investigate the Cougar resistance mechanism

utilising near isogenic lines obtained from the cv. Cougar cv. Cashel BC3 population. These included; Automated image analysis (ImageJ), Chlorophyll fluorescence, ROS assays, stomatal and spore behaviour characteristics, Xanthophyll quantification and hormonal quantification. The findings from this PhD provides significant insight into the major source of resistance in Cougar by identifying candidate STB genes, whilst also contributing to our understanding of the mechanisms of resistance to *Z.tritici*, and the value of phenotypic instruments in characterising *Z.tritici* disease.

Based on the review of the current literature, this PhD therefore aims to test the following hypotheses:

Chapter 2:

1) The major source of resistance in Cougar involves leaf defence traits against *Z.tritici*.
2) Visual STB assessments, hyperspectral reflectance indices and chlorophyll fluorescence measurements can identify and characterise the major source of resistance in Cougar.
3) Visual STB assessments, hyperspectral reflectance indices and chlorophyll fluorescence measurements can identify and characterise other sources of resistance.
4) Hyperspectral reflectance and chlorophyll fluorescence indices obtained in asymptomatic plants or early in plant development can be used to detect resistance or predict *Z.tritici* disease later in the season.

Chapter 3:

1) The major source of resistance in Cougar involves a photo-protective defence response.
2) Transcriptomic analysis can identify and characterise candidate genes responsible for the major source of resistance in Cougar.
3) The holistic resistance mechanism in Cougar can be investigated through hormonal and transcriptomic analysis of near isogenic lines.

Chapter 4:

1) A range of pre-formed and inducible (structural/physiological/biochemical) factors are associated with incompatibility between cv. Cougar and an avr *Z.tritici* isolate.
2) A range of pre-formed and inducible (structural/physiological/biochemical) factors contribute to isolate-non-specific resistance.

# Chapter 2.

## QTL analysis of a novel source of resistance in Cougar using Chlorophyll fluorescence and hyperspectral phenotyping tools

# 1 Introduction

Septoria tritici blotch (STB), caused by *Zymoseptoria tritici*, is considered one of the most damaging diseases of wheat (Savary *et al* 2019), with yield losses of up to 50% (Yitagesu *et al* 2020; Simón *et al* 2002). *Z.tritici* infects wheat through germination of ascospores or pycnidiospores on the leaf surface and subsequent penetration of the stomata (Kema *et al*., 1996), whereby the pathogen undergoes a period of asymptomatic growth, followed by a necrotrophic phase involving cell death and pycnidia formation (Shetty *et al* 2003).

The two main methods for managing the disease, fungicide application (Torriani *et al* 2015) or major gene resistance, have proved to be short-term solutions against the disease. Fungicide control is inconsistent since most *Z.tritici* strains have evolved resistance to many fungicides including quinone outside inhibitors and methyl benzimidazole carbamates, with a selection towards resistance to demethylation inhibitions and succinate dehydrogenase inhibitors currently taking place across Europe (Hellin *et al* 2021). *Z.tritici* undergoes numerous sexual reproduction cycles each season, making it adept at evolving to overcome host resistant genes (Hunter *et al* 1999). Thus, the reliance on major sources of resistance can be unsustainable as the majority of known resistance genes have been rapidly overcome and no longer provide widespread control of *Z.tritici* (Arraiano & Brown 2006; Mehrabi *et al* 2015; Makhdoomi *et al* 2014; Arraiano *et al* 2009). Modern breeding practices have made significant progress in developing a high level of background resistance to *Z.tritici* by selecting for partial resistance (Brown *et al* 2015). These successes demonstrate that a slow and steady approach involving the selection of partial resistance can be more sustainable in the longer term than the boom-and-bust approach of selecting for major sources of resistance.

Novel or previously unidentified resistance genes can be identified via quantitative trait loci (QTL) studies (Brown *et al* 2015). Identifying markers associated with a resistance gene can help breeders select for numerous sources of resistance. Having multiple QTL field trials across different geographical regions enables detection of resistance genes to provide more durable, non-isolate-specific resistance. In addition to identifying markers associated with resistance, QTL studies are commonly used to identify QTLs associated with susceptibility. This is important since the main aim of resistance breeding is to remove susceptible varieties, with this approach indirectly selecting for more durable forms of resistance. Efficient and reliable phenotyping of wheat populations can be a significant bottleneck for breeders to collect the data needed to detect QTLs to incorporate into breeding programs (Mahlein 2016). STB

phenotyping data is commonly obtained in the form of field visual disease scoring, ranging from characterising plots using a few categories, to more in-depth scales representing percentage lesion coverage. Breeders must constantly assess the inherent trade-off between phenotyping quickly, or to spend more time getting more information on each plot to improve the accuracy of the scoring. Proximal phenotyping involves the use of non-invasive tools to phenotype and characterise plant populations, and is quickly becoming a promising method to phenotype in a high-throughput manner instead of more traditional visual phenotyping methods. Proximal phenotyping can be utilised to characterize STB responses in a non-invasive, quantitative and precise manner, although there may be trade-offs in how quickly phenotyping sensors can be practically used compared to traditional visual assessments (Mahlein 2016). Such sensors include RGB-imaging combined with manual or automatic image analysis (Karisto *et al* 2018), multi and hyperspectral reflectance measurements (Yu *et al* 2018), thermal sensors, chlorophyll fluorescence imaging (Odilbekov *et al* 2018), and 3D imaging (Mahlein 2016). Whilst RGB-imaging and 3D imaging only obtain information already visible and present to the individual, phenotyping using multi and hyperspectral reflectance, thermal or fluorescence imaging sensors provides additional information on genetic responses not available through visual assessments alone, which can characterise STB QTLs (O'Driscoll *et al* 2014).

Hyperspectral reflectance measurements are amongst the most common form of proximal phenotyping and have been used to quantify leaf foliar diseases in wheat such as leaf rust (Ashourloo *et al* 2014), fusarium head blight (Mustafa *et al* 2022), powdery mildew (Feng *et al* 2017) and septoria tritici blotch (Yu *et al* 2018; Odilbekov *et al* 2018; Anderegg *et al* 2019). Other crops for which hyperspectral imaging has been utilised to detect foliar pathogens include barley (Thomas *et al* 2017), sugar beet (Mahlein *et al* 2012), tomato (Xie *et al* 2016), strawberries (Yeh *et al* 2016) and cotton (Jin *et al* 2013). Spectroradiometers can simultaneously detect a broad range of wavelengths, which are termed hyperspectral reflectance measurements. The reflectance at selected wavelengths has been used to calculate spectral reflectance indices that can be used as a proxy for various leaf components and molecules such as chlorophyll, anthocyanin, carotenoid and water content (Wu *et al* 2008; Gitelson *et al* 2001; Gitelson *et al* 2002; Penuelas *et al* 1993). Since molecules such as carotenoids and chlorophylls play key roles in host defence (Lee *et al* 2015; Ajigboye *et al* 2021) spectral reflectance indices could provide information on the potential mechanism of resistance. Additionally, these measurements can detect responses to foliar diseases prior to

visual symptoms, which would increase the phenotyping window for STB resistance genes (Thomas *et al* 2017; Odilbekov *et al* 2018; Anderegg *et al* 2019) and/or provide information on specific resistance traits such as pycnidia formation by *Z.tritici* (Bohenenkamp *et al* 2021).

Other tools for phenotyping disease responses in the field include handheld chlorophyll fluorescence sensors that can quantify and dissect the efficiency of the photosynthetic apparatus using a range of measurements (Strasser *et al* 2001). These tools include; pulse-amplitude modulated fluorometry (PAM) (Murchie & Lawson 2013), and fast induction fluorescence rises (OJIP) (Strasser *et al* 2000). The chloroplast is essential in mediating wheat-*Z.tritici* interactions (Lee *et al* 2015) and enhanced resistance has been associated with photoprotective mechanisms through processes such as non-photochemical quenching (NPQ) (Ajigboye *et al* 2021; Murchie & Ruban 2020). Chlorophyll fluorescence sensors can thus be useful to detect regions of interest associated with the functionality of photosystem II that is not captured by hyperspectral reflectance measurements.

The OJIP fluorescence transient quantifies the energy flux through PSII and hence provides information on the function and structure of the photosynthetic apparatus (Strasser *et al* 2000). Whilst OJIP fluorescence transients typically rely on a period of dark-adaptation (Ajiboye *et al* 2018; Strasser *et al* 2000) light-adapted samples also exhibit a fluorescence transient which levels off at a new steady state and can be detected using a plant efficiency analyser (PEA) with an appropriate time resolution (~10µs) (Strasser *et al* 1985; Srivastava *et al* 1995). By omitting the dark-adapting period, which can be upwards of ~30 minutes, PEA fluorescence tools can be utilised to quickly phenotype large populations of plants in a high-throughput manner (Ajigboye *et al* 2016; Ajigboye *et al* 2018). OJIP fluorescence transients have also been demonstrated to be effective in phenotyping plant responses to diseases such as powdery mildew (*Blumeria graminis*) (Ajigboye *et al* 2016), eyespot (*Oculimacula yallundae* and *acuformis*) (Ajigboye *et al* 2016), fusarium head blight (*Fusarium culmorum*) (Ajigboye *et al* 2016; Katanic *et al* 2021; Warzecha *et al* 2019) and tobacco mosaic virus (Tseliou *et al* 2021). Therefore, measurements derived from OJIP parameters could prove to be a promising tool to characterise novel sources of resistance to *Z.tritici* in a high-throughput manner.

PAM fluorometry using a MultispeQ can be used to calculate a suite of chlorophyll fluorescence parameters such as non-photochemical quenching (PhiNPQ), non-regulatory energy dissipation (PhiNO) and redox state of $Q_A$ (Phi2) by estimating $F_0$ by applying pulses of actinic light after a short period of dark adaptation (~2 minutes) (Genty et al 1989; Kuhlgert

*et al* 2017). Additionally, the MultispeQ can calculate NPQ (NPQt) in the absence of dark adaptation (without $F_0$ value) thus decreasing protocol duration to a few seconds (Tietz *et al* 2017). NPQt can also better compensate for chloroplast movements and does not require full relaxation of the quenching process (Tietz *et al* 2017). The MultispeQ has since been extensively used to phenotype plant populations, primarily investigating photosynthetic responses in response to abiotic stress (Fernandez-Calleja et al 2020; Liaqat ali *et al* 2022), although biotic stresses have also been quantified, such as lesion mimic mutants with resistance to stripe rust and powdery mildew (Li *et al* 2022). Whilst PAM fluorometry is more time consuming than OJIP derived measurements, the ability of the MultispeQ to account for changes in actinic light and to calculate NPQt, which can be quickly measured, makes it a promising instrument to characterise novel sources of resistance to *Z.tritici*. Overall, chlorophyll fluorescence measurements (CFMs) are more time consuming than hyperspectral reflectance measurements and are typically performed at an individual leaf rather than at a canopy level. However, the information obtained is unique and can point to the putative mechanisms behind resistance, proving to be a useful tool to characterize resistant QTLs in greater depth further down the breeding pipeline.

The cultivar Cougar was added to the recommended list (RL) in 2013 but was swiftly removed by 2015 due to a decline in resistance rating for STB. Because of the high levels of yellow rust (*Puccinia striiformis*), Cougar has been incorporated into 8/22 of the RL varieties in 2021/2022. Unfortunately, breakdown of STB resistance was apparent in 2021/2022 with a decrease of 0.6 – 1.9 points in cultivars with Cougar parentage (AHDB 2022). Isolates virulent to Cougar and Cougar progeny were also detected in 2020 in Ireland (Kildea *et al* 2021). Therefore, Cougar likely contains a major source of resistance, which has been swiftly broken down, likely in a similar manner to the major genes introduced into Spring Barley in the 1950-80s to combat powdery Mildew (Jørgensen *et al* 1994). Understanding and characterising this source of resistance could further our understanding of major sources of resistance and prevent the introduction or reliance of non-durable major genes into commercial varieties. Ajigboye *et al* (2021) demonstrated that the resistance in Cougar was associated with increased capacity for non-photochemical quenching (NPQ), leading to downregulation of PSII quantum yield, decreased chlorophyll a:b and increased carotenoid:chlorophyll ratio. Additionally, elevated ABA in Cougar correlated with preformed leaf defence traits such as low stomatal density, increased wax biosynthesis and lignification gene expression. QTL studies to confirm the presence and contribution of a major gene from Cougar to STB resistance have not yet been

performed. Therefore, it is important to understand the extent to which Cougar's *Z.tritici* resistance is reliant on a putative major gene or background genetic resistance, as this could help to inform the incorporation of background genetic resistance of this variety into breeding programs.

The aim of this study was to identify the QTL responsible for the major source of resistance in cv. Cougar using visual assessments and a range of proximal phenotyping methods such as hyperspectral reflectance measured by the FieldSpec HandHeld 2 spectroradiometer and CFMs using the FluorPen FP 110 and MultispeQ instruments. These proximal phenotyping tools were compared to traditional visual phenotyping methods to evaluate their usefulness and accuracy in detecting QTLs, particularly prior to full symptom expression, in addition to predicting future STB disease. Lastly, the major source of resistance in Cougar was characterised under growth room conditions using visual assessments, automated image analysis and CFMs. This study set out to test the following hypotheses:

5) The major source of resistance in Cougar involves leaf defence traits against *Z.tritici*.
6) Visual STB assessments, spectral reflectance indices and chlorophyll fluorescence measurements can identify and characterise the major source of resistance in Cougar.
7) Visual STB assessments, spectral reflectance indices and chlorophyll fluorescence measurements can identify and characterise other sources of resistance.
8) Spectral reflectance and chlorophyll fluorescence indices obtained in asymptomatic plants or early in plant development can be used to detect resistance or predict *Z.tritici* disease later in the season.

# 2 Methods

## 2.1 Plant material

A wheat mapping population consisting of 88 doubled-haploid (DH) lines was developed from a F5 cross between Cougar and Scout (CxS) by RAGT Seeds. Scout was used as a parent due to the presence of minor sources of resistance to *Z.tritici*. Lines were drilled at 300 seeds $m^{-2}$ on 10/10/2017 and 3/10/2018 in 2 blocks and 3 blocks respectively at the University of Nottingham Sutton Bonington campus. Plots were 1 $m^2$ with 4 rows. Fungicides applied in the growing season aimed to control foliar (yellow rust and mildew) and stem-base diseases (eyespot, brown foot rot, sharp eyespot) having low or no efficacy against STB. The following applications were made: 180 g $ha^{-1}$ pyraclostrobin at Growth Stage (GS) 29 (Zadoks *et al* 1974), 75 kg $ha^{-1}$ cyprodinil and 125 g $ha^{-1}$ tebuconazole GS37, 250 g $ha^{-1}$ azoxystrobin and 562 g $ha^{-1}$ fenpropimorph GS41. Four lines with and without the major source of resistance in Cougar, identified by RAGT Seeds and this study on chromosome 4D (AX94733088), were selected for controlled environmental phenotyping using KASP markers developed by RAGT (Dr Ruth Bryant).

## 2.2 Genetic map construction and QTL analysis

A genetic map was constructed using markers from the Bristol 35K Axiom array (Allen *et al* 2017) and KASP markers from RAGT (JoinMap 5.0 (Van Ooijen & Voorrips., 2001). Kosambi correction was used to account for double crossovers (Kosambi, 1944). 1712 markers were selected from 2202 based on high levels of heterozygosity between lines as well as physical location to ensure an even spread of markers which cover each chromosome. 32 linkage groups covered 21 chromosomes. Chromosomes 1A, 1D, 2A, 3B, 3D, 4B, 4D, 5B, 5D, 6B, 6D, 7B, 7D comprised of 1 linkage group for the whole chromosome whereas 1B, 2B, 2D, 3A, 4A, 5A, 6A, 7A had linkage groups for both the short and long arm of the chromosome. MapQTL6 was used to perform Interval Mapping followed by MQM mapping analysis for selected traits and non-normalized data were angular transformed. Cofactors were selected based on preliminary interval mapping analysis with additional cofactors added until the model stabilised, such that no new significant changes were introduced. Cofactors selected were unique to each STB assessment and are displayed in table 5. HH2 & CFM measurements were analysed using the corresponding assessment cofactor. The approximate Log likelihood of the odds (LOD) threshold of 3.0 was calculated based on a genome-wide 1000 permutation test in MapQTL6.

## 2.3 Instruments for phenotyping

The FieldSpec HandHeld 2 spectroradiometer (HH2) was used to measure reflectance from 325 nm to 1075 nm. Five measurements were taken per plot (centre, bottom left, bottom right, top left, top right) at ~0.5 meter height above the crop. The HH2 was calibrated after every block in addition to calibration due to changes in ambient light intensity. Spectral reflectance indices were calculated based on previously published experiments as shown in table 1. Thirty-one indices were calculated including indices related to green biomass, chlorophyll, carotenoids, anthocyanins, plant water content, senescence and fungal diseases (Table. 1).

The FluorPen FP 110 (Photon Systems Instruments, Czech Republic) was used to measure the transient kinetics with minimal fluorescence (Fo) determined as fluorescence intensity at 50 μs to maximal fluorescence (Fm) intensity with fluorescence intensity at the J step (Fj) at 2 ms, fluorescence intensity at the I step (Fi) at 30ms, and fluorescence intensity at 300 μs (OJIP) reviewed in detail by Strasser *et al*. (2000). Fast fluorescence transients were induced by saturating light of 3000 μmol $m^{-2}$ $s^{-1}$. Fluorescence signals were recorded with a data acquisition rate of 100,000 points $s^{-1}$ within a timespan of 10 μs to 1s. OJIP based biophysical parameters were automatically computed according to Strasser *et al* (2000, 2004); The MultispeQ calculated non-photochemical quenching (NPQt) as per Tietz *et al* (2017), as well as the quantum yield of PSII (Phi2), the fraction of light dedicated to non-photochemical quenching (PhiNPQ) and the fraction of light lost via non-regulated photosynthesis inhibitor processes (PhiNO) (Kuhlgert *et al* 2016). Fluorpen and MultispeQ instruments were used on the latest fully emerged leaf at early growth stages, and the flag leaf once fully emerged of two random plants in each plot. Calculated parameters from fluorescence measurements are shown in Table 2.

## 2.4 Septoria tritici blotch (STB) resistance screening in the field

Visual STB assessments were made at GS 23, 39, 55, 61 in 2018 and at GS 26, 33, 39, 55, 69, 71 in 2019. At GS 23 and 26 four rows of plants per plot were assessed as percentage chlorotic and necrotic lesions STB lesion coverage of total green area and averaged. At GS33 and subsequent assessments the canopy was parted between each row of plants and the percentage STB chlorotic and necrotic lesions lesion of total green area was visually assessed on the $4^{th}$ leaf layer. STB lesion coverage between each row of plants was averaged per plot. Symptoms from other pathogens such as yellow rust were absent from these field trials and only STB disease was assessed.

**Table 1.** Spectral indices calculated from hyperspectral reflectance measurements (FieldSpec HandHeld 2 spectroradiometer) in field experiments 2018, 2019.

| Measurement function | Spectral index | Equation | Reference |
|---|---|---|---|
| **Carotenoids** | **Ratio analysis of reflectance spectra (RARSc)[9]** | **R760/R500** | **(Chappelle *et al* 1992)** |
| Carotenoids | Pigment specific simple ratio C (PSSRc)[12] | R800/R470 | (Blackburn 1998) |
| Carotenoids | Pigment specific normalized difference (PSNDc)[13] | (R800-R470)/(R800+R470) | (Blackburn 1998) |
| Carotenoids | Carotenoid reflectance index (CRI1)[14] | $(R510)^{-1}$-$(R550)^{-1}$ | (Gitelson *et al* 2002) |
| Carotenoids | Carotenoid reflectance index (CRI2)[15] | $(R510)^{-1}$-$(R700)^{-1}$ | (Gitelson *et al* 2002) |
| Carotenoids | Red edge carotenoid index (CAR(R))[16] | $[(R510)^{-1}$-$(R700)^{-1}]$×R770 | (Gitelson *et al* 2006) |
| Carotenoids | Red edge carotenoid index (CAR(G))[17] | $[(R510)^{-1}$-$(R550)^{-1}]$×R770 | (Gitelson *et al* 2006) |
| Carotenoids | Carotenoid index (CARI)[31] | $R720/R521^{-1}$ | (Zhou *et al* 2017) |
| **Chlorophyll fluorescence** | **Derivative index (D2)[28]** | **705/722** | **(Zarco-Tejada *et al* 2002)** |
| **Chlorophyll** | **Modified normalized difference at 705nm(ND705)[27]** | **(R750 – R705)/(R750 + R705)** | **(Sims & Gamon 2002)** |
| Chlorophyll | Merris Terrestrial Chlorophyll Index (MTCI)[29] | (750-710)/(710-680) | (Dash & Curran 2004) |
| Chlorophyll | modified chlorophyll absorption ratio index (MACRI)[30] | ((701-671)-0.2x(701-549))/(701/671) | (Wu *et al* 2008) |
| **Chlorophyll a** | **Pigment specific simple ratio A (PSSRa)[10]** | **R800/R675** | **(Blackburn 1998)** |
| Chlorophyll a | Ratio analysis of reflectance spectra (RARSa)[7] | R675/R700 | (Chappelle *et al* 1992) |
| **Chlorophyll b** | **Pigment specific simple ratio B (PSSRb)[11]** | **R800/R650** | **(Blackburn 1998)** |
| Chlorophyll b | Ratio analysis of reflectance spectra (RARSb)[8] | R675/(R650xR700) | (Chappelle *et al* 1992) |
| **Anthocyanin** | **Anthocyanin reflectance index 1 (ARI1)[18]** | **1/R550-1/R700** | **(Gitelson *et al* 2001)** |
| Anthocyanin | Anthocyanin reflectance index 2 (ARI2)[19] | R800x(1/R550-1/R700) | (Gitelson *et al* 2001) |
| **Leaf Rust** | **leaf rust disease severity index 2 (LRDSI2)[5]** | **4.2x(695/455)-0.38** | **(Ashourloo *et al* 2014)** |
| Leaf Rust | leaf rust disease severity index 1 (LRDSI1)[4] | 6.9x(605/455)-1.2 | (Ashourloo *et al* 2014) |
| **chlorophyll degragation** | **Normalized Pheophytinization Index (NPQI)[23]** | **(R415-R435)/(R415+R435)** | **(Penuelas *et al* 1995a)** |
| **Water** | **Plant water index (PWI)[6]** | **R970/R900** | **(Penuelas *et al* 1993)** |
| Misc | Plant senescence reflectance index (PSRI)[20] | (R678-R500)/R750 | (Merzlyak *et al* 1999) |
| Misc | Modified photochemical reflectance index (PRIm1)[21] | (R512-R531)/(R512+R531) | (Hernández-Clemente *et al* 2011) |
| Misc | Simple Ratio (Sr(car))[22] | R515/R570 | (Hernández-Clemente *et al* 2011) |
| Misc | The structure-insensitive pigment index (SIPI)[24] | (R800-R435)/(R415+R435) | (Penuelas *et al* 1995a) |
| Misc | Photochemical reflectance index (PRI)[25] | (R570-R531)/(R570+R531) | (Gamon *et al* 1992) |
| Misc | Reflectance band ratio index (RBRI)[26] | R672/(R550×R708) | (Datt 1998) |
| Misc | Normalised difference vegetation index (NDVI)[1] | (R900-R680)/(R900+R680) | (Tucker 1979) |
| Misc | Red normalised difference vegetation index (NDVI)[2] | (R780-R670)/(R780+R670) | (Tucker 1979), Gitelson *et al* (1996) |
| Misc | Green normalised difference vegetation index (NDVI)[3] | (R780-R550)/(R780+R550) | (Tucker 1979), Gitelson *et al* (1996) |

Indices in **BOLD** were taken forward for QTL analysis

**Table 2.** Common derivations and definitions of OJIP parameters obtained from the recorded OJIP fluorescence transients & MultispeQ parameters.

| Instrument | **Technical fluorescence parameters** (Ajigboye OO *et al.*, 2016)(Strasser *et al.*, 2000) | **Definition** |
|---|---|---|
| **Fluorpen** | $F_0$ | Minimal fluorescence at 50 µs, used as initial value of fluorescence |
| | $F_{300\ \mu s}$ | Fluorescence value at 300 µs |
| | $F_J \equiv F_{2\ ms}$ | Fluorescence value at 2 ms (J level) |
| | $F_I \equiv F_{60\ ms}$ | Fluorescence value at 60 ms (I level) |
| | $F_M = F_P$ | Maximal fluorescence under saturating light |
| | $F_V = F_M - F_0$ | Maximum variable Chl fluorescence |
| | $V_J = (F_{2\ ms} - F_0)/(F_M - F_0)$ | Relative variable fluorescence at 2 ms |
| | $V_I = (F_{60\ ms} - F_0)/(F_M - F_0)$ | Relative variable fluorescence at 60 ms |
| | $M_0 = (TR_0/RC) - (ET_0/RC)$ $= 4\ ms^{-1}\ (F_{300\ \mu s} - F_0)/(F_M - F_0)$ | Initial slope of relative variable Chl fluorescence curve (approximate value) |
| | **Energy fluxes** | **Definition** |
| | ABS | Total photon flux absorbed by the PSII antenna pigments |
| | $TR_0$ | Trapped exciton flux by PSII reaction centers |
| | $DI_0$ | Dissipated energy flux in PSII, e.g., as heat and fluorescence |
| | $ET_0$ | Electron transport flux from $Q_A$ to $Q_B$ |
| | **Quantum yield** | **Definition** |
| | $F_V/F_M = \varphi_{Po} = TR_0/ABS = (F_M - F_0)/F_M$ | Maximum quantum yield of primary PSII photochemistry at time 0 |
| | **Specific energy fluxes (per active PSII reaction centers)** | **Definition** |
| | $ABS/RC = (M_0/V_J) \cdot (1/\varphi_{Po})$ | Average absorbed photon flux per PSII reaction center (apparent antenna size of an active PSII) |
| | $TR_0/RC = M_0/V_J$ | Maximum trapped exciton flux per PSII reaction center |
| | $DI_0/RC = (ABS/RC) - (TR_0/RC)$ | Dissipated energy flux per PSII reaction center |
| | $ET_0/RC = (M_0/V_J) \cdot (1 - V_J)$ | Electron transport flux from $Q_A$ to $Q_B$ per PSII reaction center |
| **MultispeQ** | (Tietz *et al.*, 2017)(Kuhlgert *et al.*, 2016) | |
| | NPQt | Non-photochemical quenching of chlorophyll fluorescence |
| | PhiNPQ | Ratio of non-photochemical quenching of chlorophyll fluorescence compared to PhiNO & Phi2 |
| | PhiNO | Ratio of PSII quantum yield of non-regulated NPQ process compared to PhiNPQ & Phi2 |
| | Phi2 | Ratio of PSII quantum yield compared to PhiNO & PhiNPQ |

## 2.5 Cougar resistance phenotyping under controlled environmental conditions

Four DH lines with 4D resistance (4D-R) from Cougar and four lines lacking this resistance (4D-S) were selected based on visual phenotype and resistant marker solution. Genotypes were grown in John Innes No.2 soil medium in 9cm tall pots for 5 weeks with weekly Hortifeed (15(N):7(P2O5):30(K2O)). Environmental conditions included 16 hour 22$^{o}$C-16$^{o}$C day-night cycle with 273µmols $m^{-2}s^{-1}$ Photosynthetic Photon Flux Density (PPFD), light intensity (80-110 millimoles of light energy per square meter (PAR)). Plants were inoculated with $1x10^{6}$ spore suspension of *Z.tritici*, isolate IPO323 obtained from Dr Kostya Kanyuka (NIAB, UK), prepared by dislodging spores in sterile water from previously grown cultures for 4 days post inoculation (dpi) on Potato Dextrose Agar (PDA). Spray inoculated plants were sprayed until runoff with spore suspension of *Z.tritici* with 1 drop of tween added per 100ml. Plants with a fully emerged 3$^{rd}$ leaf were infiltrated with 1ml of IPO323 spore suspension in the centre of the leaf. Inoculated plants were kept in separate humidity tents at ~100% relative humidity for 4 dpi. Fluorpen and MultispeQ were used to take measurements at 4 hpi, 18 hpi, 1 dpi, 2 dpi, 4 dpi, 7 dpi, 10 dpi, 13 dpi and 16 dpi. The fully emerged leaf at inoculation was measured using the MultispeQ and Fluorpen for both treatments. Infiltrated leaves were sampled by measuring above the infiltration spot. Visual assessments were taken at 4 dpi, 7 dpi, 10 dpi, 13 dpi, 16 dpi for the infiltration treatment and 7 dpi, 10 dpi, 13 dpi, 16 dpi, 19 dpi, 22 dpi for the spray treatment. Percentage chlorotic and necrotic lesions of the total leaf area for three marked leaves were assessed and were averaged to give one value per biological replicate. Pycnidia incidence was quantified as 0 or 1 for the three marked leaves. The experiment was repeated twice with additional images taken using a Canon scan LIDE 220 flatbed scanner for ImageJ analysis from the second experiment. Visually assessed leaves were scanned in a non-destructive manner and immediately after visual assessments were made. Images were later analysed using the macro from Stewart *et al* (2016). Macro settings used for chlorotic lesion quantification detected were: Min0 0 Max0 255 Min1 97 Max1 124 Min2 147 Max2 164 colmode 2 Pass_Stop_H 1 Pass_Stop_S 1 Pass_Stop_B 1 maximaNoise 18 leafAreaUpper 210 leafAreaLower 0. For necrotic lesion and pycnidia quantification macro settings were: Min0 0 Max0 255 Min1 118 Max1 255 Min2 0 Max2 255 colmode 2 Pass_Stop_H 1 Pass_Stop_S 1 Pass_Stop_B 1 maximaNoise 18 leafAreaUpper 210 leafAreaLower 0 pycnidiaLesionSize 5 lesionSize 5 red_weight_pycn 0.75

green_weight_pycn 0.25 blue_weight_pycn 0 sigmaGauss 0.25 pycnidiaSize 0.001-0.022 pycnidiaCircularity 0.8-1.0 pycnidiaPerLesion Yes.

## 2.6 Statistical analysis

Statistical analyses were performed used GenStat version 16 for Windows. Summary statistics of the STB assessment data included the mean and range of the Cougar Scout population with values for both parents and ANOVA analysis to test for visual STB assessment differences between lines at each growth stage and year (Table 3, Supp table S1). Stepwise linear regression analysis was used to identify indices which best explained STB disease severity over both years. Indices were compared to subsequent visual STB assessments with year as a block factor. Multiple indices were not included in the models due to high levels of autocorrelation. The most consistent indices over both years and across growth stages for each measurement function (Table 1) are shown in Table 4. Correlation coefficients were obtained using Pearson product-moment correlation coefficient analysis, with hyperspectral reflectance and CFMs analysed against STB disease data across all growth stages (Supp tables S2&3).

Visual and ImageJ STB assessments under growth room conditions were analysed using area under the disease progress curve (AUDPC) calculations with Student's t-tests to compare 4D-R and 4D-S lines within each treatment (one experiment was analysed). Percentage chlorotic and necrotic lesion coverage and pycnidia incidence/number was also analysed using ANOVA analysis. OJIP Chlorophyll fluorescence data under growth room conditions was analysed using Student's t-test for time dependent comparisons between 4D-R and 4D-S lines as per the experimental design using two experiments. Repeated measurement analysis was also carried out to identify trends over the time for chlorophyll fluorescence for 4D-R & 4D-S lines (Time*Gene, Block = Experiment). Experiments were analysed as replicates when there were no significant interactions between experiment used as a treatment factor, genotype and inoculation for the measured physiological variables.

# 3 Results

## 3.1 Phenotypic characterisation of STB disease response

Parental and CxS population lines means, and ranges for STB disease severity are shown in Table 3. ANOVA results indicated that there were significant differences in STB severity between Cougar and Scout (CxS) lines at all growth stages ($P<0.05$, Table 3) with greater disease severity in 2019. The frequency distribution of Cougar and Scout relative to the population used in this study is shown in figure 1, with significantly decreased STB lesions in Cougar relative to Scout at GS 39 and 55 in 2018 (Table 3, Fig. 1). Scout had 21.7% lower STB severity compared to Cougar at GS 71 in 2019 (Table 3, Fig. 1).

**Table 3.** Means, ranges, least significant differences (LSD) and P-value (ANOVA) of visual STB disease assessments of CxS lines. ANOVA table included in supplementary table S1.

| Year | STB assessment[(a)](%) | Parent | | CxS population (N=100) | | | |
|---|---|---|---|---|---|---|---|
| | | Cougar | Scout | Mean | Range | *P* value | LSD |
| 2018 | GS23 | 15.0 | 17.5 | 15.4 | 3.6-30.0 | 0.025 | 8.0 |
| | GS39 | 16.7 | 34.2 | 23.1 | 5.0-50.0 | <0.001 | 11.6 |
| | GS55 | 9.2 | 21.7 | 20.5 | 6.7-43.3 | <0.001 | 7.9 |
| | GS61 | 15.8 | 13.3 | 15.6 | 1.7-43.3 | <0.001 | 9.0 |
| | Flag leaf GS61 | 10.0 | 10.0 | 9.0 | 0.0-23.8 | <0.001 | 4.0 |
| 2019 | GS26 | 11.1 | 10.6 | 11.1 | 3.3-21.7 | <0.001 | 5.3 |
| | GS33 | 33.3 | 38.3 | 32.4 | 11.7-48.3 | <0.001 | 6.2 |
| | GS39 | 25.6 | 29.4 | 29.2 | 11.7-45 | <0.001 | 7.8 |
| | GS55 | 26.7 | 28.3 | 29.3 | 8.3-50.0 | <0.001 | 8.7 |
| | GS69 | 36.1 | 32.8 | 35.2 | 10-53.3 | <0.001 | 8.9 |
| | GS71 | 55.0 | 40.6 | 49.0 | 20.0-86.7 | <0.001 | 12.7 |
| | Flag leaf GS71 | 40.0 | 18.3 | 34.3 | 5.0-80.0 | <0.001 | 15.8 |

[(a)] % Septoria tritici blotch (STB) symptom area of total green area per plot

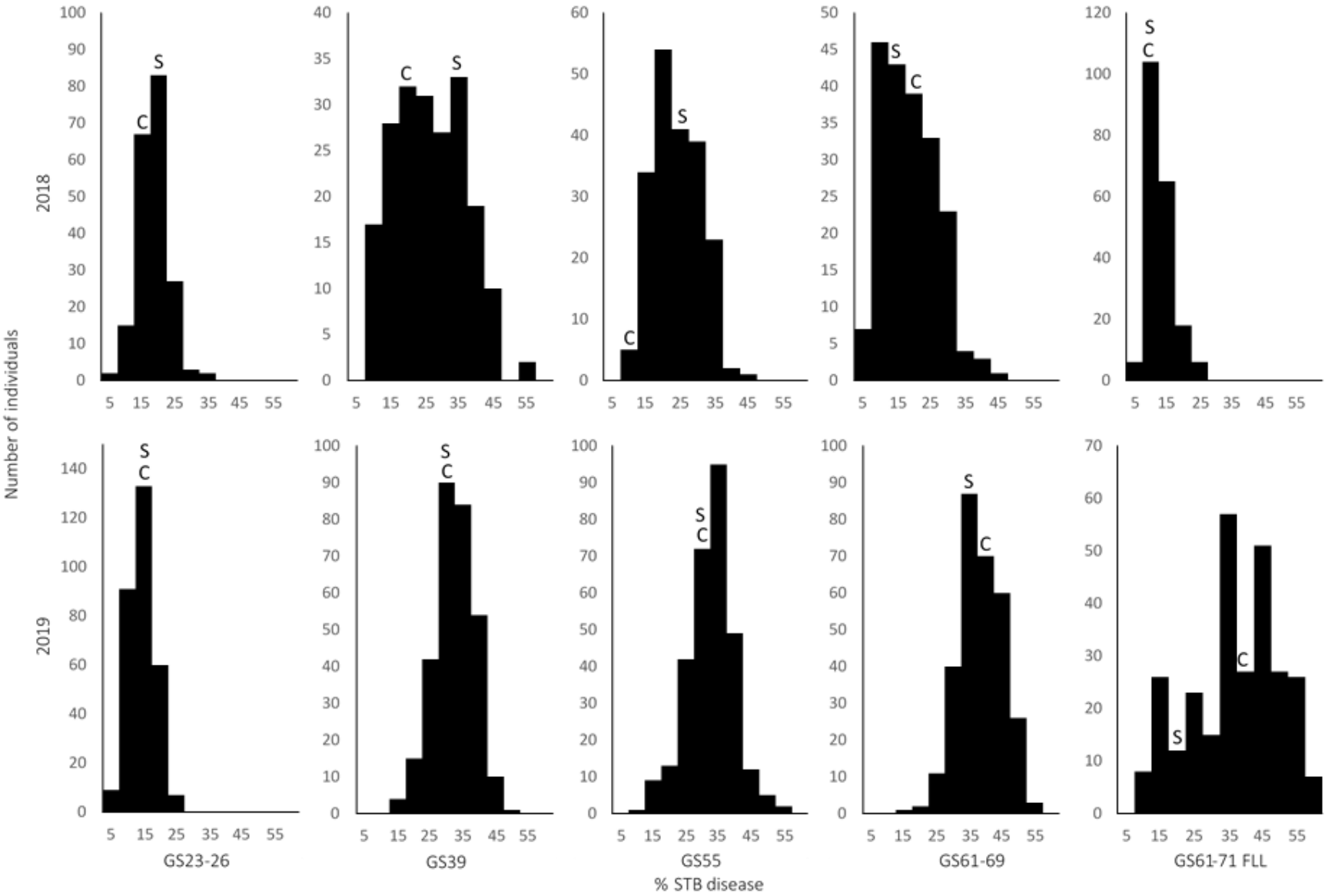



**Figure 1.** Distributions of Cougar(C) x Scout(S) population for Septoria tritici blotch (STB) assessment (%). Disease severity was assessed as % STB of total green area per plot.

## 3.2 Stepwise linear regression and correlation analysis

The indices which best predicted STB disease were identified using stepwise linear regression and correlation analysis. Indices were classified by function, with the most consistent indices at predicting subsequent STB disease over both years selected for QTL analysis. Derivative 2 (D2) (Chlorophyll fluorescence) measured at GS33 was the most consistent index at explaining 48% of disease variation at GS 39 and 55 for both years of experimentation (Table 4). Anthocyanin reflectance index 1 (ARI1) explained 40-45% of the variation of subsequent disease at GS 39-55. Leaf rust disease susceptibility index 1 & 2 (LRDSI1 & LRDSI2) explained accounted for 44-45% of disease variation, although correlation analysis demonstrated LRDSI2 correlating marginally better with STB disease than LRDSI1 (Supp Table 2a, b). Pigment specific simple ratio A & B (PSSRa/b) indices associated with chlorophyll content were more effective than the ratio analysis of reflectance spectra of chlorophyll a/b (RARSa/b) at predicting subsequent STB variation at GS55. PSSRa/b rather than RARSa/b correlated more with STB disease across multiple growth stages for both years (Supp Table 2a, b). Additional indices associated with chlorophyll content included: Modified normalized difference at 705nm (ND705), Merris terrestrial chlorophyll index (MTCI) and modified chlorophyll absorption ratio index (MCARI). Out of these indices, ND705 at GS55 was the only index to predict STB disease at GS61-69 explaining 78% of STB variation. Correlation analysis also demonstrated ND705 correlated strongly with disease relative to MTCI & MCARI, although MTCI was also effective at predicting future disease as demonstrated by the correlation analysis (Supp Table 2a, b). Out of the 9 indices associated with carotenoid content reflectance spectra of carotenoids (RARSc) was the most reliable index to account for subsequent disease variation, although this was influenced by the year and growth stage (Supp Table 2a, b). The best indices at quantifying subsequent STB disease for each biological function, and the indices taken forward for QTL analysis included: LRDSI2 (Leaf rust), ARI1 (Anthocyanins), PSSRa (Chlorophyll a), PSSRb (Chlorophyll b), ND705 (Total chlorophyll content), RARSc (Carotenoids), and D2 (Chlorophyll fluorescence). Additionally, NPQI and PWI were investigated further in the QTL analysis due to previous research by Yu *et al* (2018) and Odilbekov *et al* (2018), and the unique information these indices provide relating to plant water content (PWI) and phaeophytization of chlorophyll a (NPQI)

Other indices analysed by stepwise linear regression, (Data not shown) included NDVI, NDVI (R/G) (Normalised vegetative index), SIPI (Chlorophyll:Carotenoid ratio), PRI/PRI(M1) (de-

poxidation of xanthophyll's), PSRI (plant senescence) & RBRI (chlorophyll+carotenoid content). These indices were not incorporated into the QTL analysis since they provide little additional information not already captured by LRDSI2, ARI1, PSSRa, PSSRb, ND705, RARSc and D2. However, correlation analysis demonstrated that many of these indices were also effective at quantifying future STB disease. Most notably, PSRI measured at GS33 was the best index at explaining STB disease variation at GS39, alongside D2, and was tightly correlated with disease (Supp Table S2a, b). Using multiple linear regression, incorporating number of significant indices did not improve the variation explained by individual indices in the model (Table 4b).

Fluorescence measurements weakly correlated with STB disease in 2018, with NPQt, DIo/RC and ETo/RC correlating with STB disease at GS55 and 61-69 (Supp Table S3). However, there were discrepancies between correlations from fluorescence measurements taken at GS39 or 55 for $F_v'/F_m'$ and PhiNPQ. In 2019, fluorescence measurements failed to correlate with STB disease at GS55, 71 and 71 (FLL), with only $F_v'/F_m'$, Dlo/RC and ABS/RC measured at GS33 correlating with STB disease at GS69 (Supp Table S3). However, $F_v'/F_m'$ and Phi2 measured at GS33, positively correlated with STB disease at GS39, whilst Dlo/RC, TRo/RC, ABS/RC, NPQt and PhiNPQ were negatively correlated (Supp Table S3). There were no consistent chlorophyll fluorescence measurement correlations between both years. Stepwise linear regression analysis demonstrated that only Dlo/RC, TRo/RC, ABS/RC, ETo/RC, $F_v'/F_m'$ and PhiNO accounted between 10.3 and 10.7% of STB variation at GS39. Overall, hyperspectral reflectance indices had stronger correlations with subsequent STB disease compared to chlorophyll fluorescence measurements.

**Table 4a.** Linear regression analysis of hyperspectral reflectance indices with subsequent STB assessment values at GS 39, 55 & 61-69 as dependent variables. Multiple indices couldn't be used in models due to high levels of correlation between indices. The most consistent indices explaining the most variation over both years for each function are displayed.

| Growth stage of STB assessment % | Growth stage (GS) of Measurement | Hyperspectral reflectance Index | Year | Equation | $R^2$ | *P*-value |
|---|---|---|---|---|---|---|
| 39 | 33 | D2 | 2018<br>2019 | y = 190x-75.7<br>y = 226.5x-60.5 | 0.483 | < 0.001 |
| | | ND705 | 2018<br>2019 | y = -165.5x-115.95<br>y = -185.5x+168.25 | 0.469 | < 0.001 |
| | | LRDSI2 | 2018<br>2019 | y = 18.27x-133.8<br>y = 3.9x-0.6 | 0.440 | < 0.001 |
| | | PSSRb | 2018<br>2019 | y = -3.125x+51.87<br>y = -0.452x+43.85 | 0.430 | < 0.001 |
| | | PSSRa | 2018<br>2019 | y = -2.714x-+50.13<br>y = -0.328x+ 41.74 | 0.427 | < 0.001 |
| | | RARSc | 2018<br>2019 | y = -3.278x+62.26<br>y = -0.441x+42.46 | 0.409 | < 0.001 |
| | | ARI1 | 2018<br>2019 | y = 13.53x-16.76<br>y = 1.4x+24.76 | 0.408 | < 0.001 |
| 55 | 33 | D2 | 2018<br>2019 | y = -48.5x-45.46<br>y = 227.9x-60.74 | 0.491 | < 0.001 |
| | | ND705 | 2018<br>2019 | y = 44.8x-4.85<br>y = -169.65x-169.65 | 0.487 | < 0.001 |
| | | PSSRb | 2018<br>2019 | y = 0.933x+11.75<br>y = -0.551x+47.57 | 0.482 | < 0.001 |
| | | PSSRa | 2018<br>2019 | y = 0.799x+12.38<br>y = -0.429x+46.14 | 0.481 | < 0.001 |
| | | RARSc | 2018<br>2019 | y = 0.96x+8.86<br>y = -0.603x+47.86 | 0.462 | < 0.001 |
| | | ARI1 | 2018<br>2019 | y = -2.96x+29.01<br>y = 1.97x+23.49 | 0.459 | < 0.001 |
| | | LRDSI2 | 2018<br>2019 | y = -5.55x+68<br>y = 3.04x+6.4 | 0.452 | < 0.001 |
| | 39 | | - | | | |
| 61-69 | 33 | | - | | | |
| | 39 | | - | | | |
| | 55 | ND705 | 2018<br>2019 | y = -5.55x+68<br>y = 3.04x+6.4 | 0.782 | < 0.003 |

**Table 4b.** Stepwise multiple linear regression analysis with STB assessment values at GS 39, 55 & 61-69 as dependent variables for 9 hyperspectral indices. Independent variables selected in the analyses contributed significantly to the models. The models explaining the most levels of variation are displayed.

| Growth stage of STB assessment % | Growth stage (GS) of measurement | Year | Equation | $R^2$ | *P*-value |
|---|---|---|---|---|---|
| 39 | 33 | 2018 | y = 6.60a - 107.5b + 63.9 | 0.50 | < 0.001 |
| | | 2019 | y = 0.851a - 167.2b + 151.9 | | |
| 55 | 33 | 2018 | y = 1.9a + 1.297c + 2.8 | 0.51 | < 0.001 |
| | | 2019 | y = 1.705a - 0.489c + 40.31 | | |
| | 39 | 2018 | - | - | - |
| | | 2019 | - | - | - |
| 61-69 | 55 | 2018 | y = -85.2b + 80.2 | 0.78 | < 0.001 |
| | | 2019 | y = -284.6b + 263.1 | | |

STB disease score; y, ARI1; a, ND705; b, PSSRa; c.

## 3.2 Quantitative trait loci (QTL) analysis of resistance to STB caused by *Z. tritici*, and coinciding spectral indices and chlorophyll fluorescence measurements

Sixteen QTLs for resistance to STB with LOD(L)>3.0 were identified during experimentation over both years. QTLs for STB were found on 2B, 4D and 6B in 2018, and 1B, 2A, 2B, 2D, 3B and 5A in 2019 (Fig. 2). Resistance QTLs originated from both parents (Cougar and Scout) with Scout STB resistance constrained to 2A, 2B, 2D and 3B in 2019, whilst Cougar STB resistance was constrained to 2B, 4D and 6B in 2018 and 1B, 2B, 3B and 5A in 2019 (Fig. 2). The most significant QTL was on 4D at GS39 in 2018 (Cougar, L=10.9, Fig. 3). The peak marker on 4D was AX94733088 with an interval between 15.8 – 17.5 cm. All other STB resistant QTLs had LOD scores ranging from 3.02 – 5.71. The high LOD score of the 4D STB resistant QTL, combined with the peak marker matching previous QTL analyses, provides strong evidence in support that this is the main source of resistance from Cougar responsible for the differences in STB disease in the parents at GS 33 and 39 in 2018 (Table 3, Fig. 1).

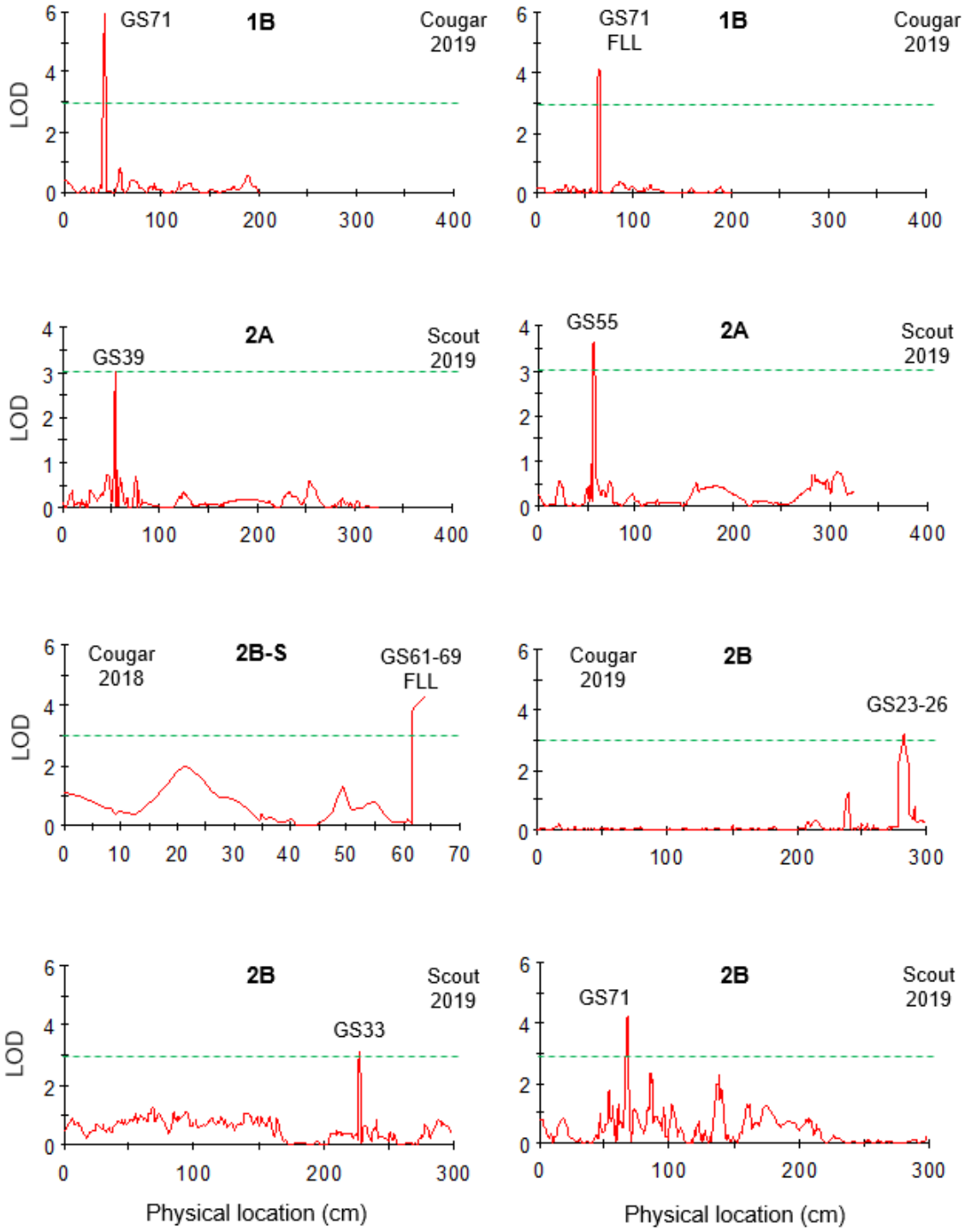



**Figure 2a.** STB assessment QTL support intervals. Source of resistance (Cougar/Scout), year, growth stage & chromosome displayed. Dotted green line indicates significance threshold (LOD > 3.0, P < 0.005)

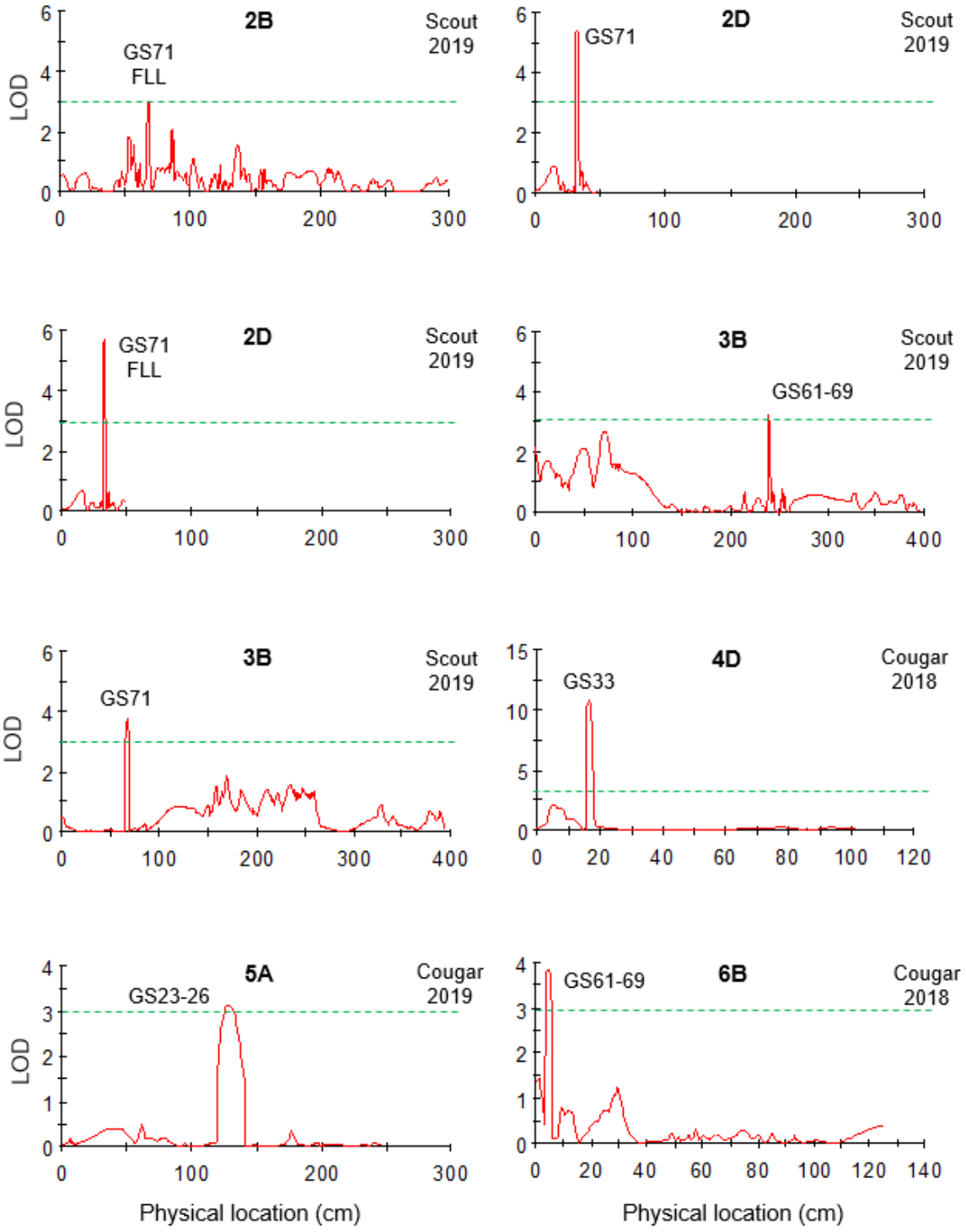



**Figure 2b.** STB assessment QTL support intervals. Source of resistance (Cougar/Scout), year, growth stage & chromosome displayed. Dotted green line indicates significance threshold (LOD > 3.0, P < 0.005)

Nine hyperspectral reflectance indices at GS33 were effective at quantifying the major source of resistance in Cougar in 2018, with NPQI having a similar LOD value of 10.7 as STB assessments at GS39 with a LOD of 10.86 (Table 5). RARSc was the best index to quantify resistance at GS39 (L = 6.89), however only LRSDI2 was associated with the 4D QTL at both GS33 and 39. Cougar resistance was associated with increased indices for Chlorophyll a and b content (ND705, PSSRa, PSSRb), but decreased phaeophytization of chlorophyll a (NPQI), decreased chlorophyll fluorescence (D2), increased carotenoid content (RARSc), and decreased anthocyanin content (ARI1). In 2019 the major QTL of resistance on 4D was not detectable using visual STB assessments, hyperspectral reflectance measurements or CFMs. However, there were common indices for both years that were associated with different QTLs for resistance. NPQI and LRSDI2 were not significant for any other QTL, being unique for the major 4D QTL from Cougar.

Apart from the major source of resistance in Cougar in 2018, no hyperspectral indices detected any STB resistance QTLs at growth stages prior to the STB assessments. All 9 spectral reflectance indices which detected STB resistance QTLs, independent of year or resistance source, were consistently associated with disease as per the correlation analysis (Supp Table 2a, b). Resistance from Scout was detectable on 2A and 2B at GS 55 and 33 respectively in 2019, with D2 being the best predictor followed by PSSRb and PSSRa. RARSc was unique to 2A whilst ND705 was unique to 2B (Table 5). PWI, LRDSI2 and NPQI did not detect any Scout QTLs, being unique to Cougar. ARI1 detected the resistance from Scout on 2B at GS55 and 71 despite the STB assessment only detecting the STB resistance QTL at GS33. Another STB resistance QTL from Scout on 2B was only detectable using the chlorophyll fluorescence measurement PhiNO, which increased in lines containing the resistance and measured at GS33, whilst the STB assessments detected the STB resistance QTL at GS71. Indices detecting Scout STB resistance QTLs were more effective at quantifying the resistance than visual STB assessments. All indices detecting the 2A STB resistance QTL had higher LOD values (4.21 – 4.03) compared to the STB assessment (3.60), whilst D2, ND705 and PSSRb (5.98, 4.51, 3.47) also had higher LOD values than the STB assessment (3.12) on 2B (Table 5). Hyperpectral reflectance indices also detected resistance from Cougar in 2019 on 1B and 3B at GS71 and 61-69 respectively (Table 5). ARI1 was the only index to detect the resistance on 3B whilst PSSRa, PWI, PSSRb, D2, ND705 and ARI1 detected the resistance on 1B.

**Table 5.** STB assessment QTLs & corresponding spectral indices and fluorescence measurements. Physical locations, marker, support interval and LOD values displayed.

| Year | Chromosome | Growth stage | Trait | QTL interval | Physical location | Cofactor peak axiom marker | Peak LOD value | mu_Cougar(a) | mu_Scout(b) | % VarExpl |
|---|---|---|---|---|---|---|---|---|---|---|
| | | 39 | STB assessment | 15.8 - 17.5 | 16.5 | AX-94733088 | 10.86 | 17.5 | 31 | 44.1 |
| | | 33 | NPQI | 15.8 - 17.5 | | | 10.7 | -0.0555 | -0.449 | 43.6 |
| | | 33 | PWI | 15.8 - 17.5 | | | 8.97 | 0.938 | 0.953 | 38.1 |
| | | 33 | LRDSI2 | 15.8 - 17.5 | | | 8.55 | 8.42 | 8.87 | 36.7 |
| | | 33 | D2 | 15.8 - 17.5 | | | 8.28 | 0.5 | 0.545 | 35.8 |
| | | 33 | ND705 | 15.8 - 17.5 | | | 7.89 | 0.58 | 0.532 | 34.5 |
| | | 33 | RARSc | 15.8 - 17.5 | | | 6.92 | 12.8 | 10.6 | 31 |
| | | 33 | PSSRb | 15.8 - 17.5 | | | 6.81 | 10.1 | 7.77 | 30.6 |
| 2018 | 4D | 33 | PSSRa | 15.8 - 17.5 | | | 6.7 | 11 | 8.32 | 30.1 |
| | | 33 | ARI1 | 15.8 - 17.5 | | | 5.59 | 2.77 | 3.25 | 25.9 |
| | | 39 | RARSc | 15.8 - 17.5 | | | 6.89 | 24 | 18.5 | 26.1 |
| | | 39 | PSSRa | 15.8 - 17.5 | | | 4.65 | 27 | 23.2 | 22 |
| | | 39 | PWI | 15.8 - 17.5 | | | 4.54 | 0.874 | 0.886 | 21.6 |
| | | 39 | ND705 | 15.8 - 17.5 | | | 4.52 | 0.719 | 0.7 | 21.5 |
| | | 39 | PSSRb | 15.8 - 17.5 | | | 4.38 | 23.9 | 20.8 | 20.9 |
| | | 39 | D2 | 15.8 - 17.5 | | | 3.74 | 0.423 | 0.436 | 15.4 |
| | | 39 | LRSDI2 | 15.8 - 17.5 | | | 3.11 | 7.03 | 7.43 | 15.3 |
| | | 71 | STB assessment | 39.6 - 42.6 | 42.6 | AX-95652713 | 5.93 | 45.6 | 56.1 | 16 |
| | | 71 | PSSRa | 41.6 - 42.6 | | | 3.91 | 15.1 | 13.2 | 15.6 |
| | | 71 | PWI | 39.6 - 42.6 | | | 3.91 | 0.813 | 0.83 | 18.9 |
| 2019 | 1B | 71 | PSSRb | 41.6 - 42.6 | | | 3.64 | 13 | 11.5 | 16.6 |
| | | 71 | D2 | 39.6 - 42.6 | | | 3.55 | 0.516 | 0.534 | 13.6 |
| | | 71 | ND705 | 39.6 - 42.6 | | | 3.46 | 0.622 | 0.595 | 13.9 |
| | | 71 | ARI1 | 42.6 | | | 3.14 | 3.55 | 4.27 | 12.8 |
| | | 55 | STB assessment | 56.3 - 58.4 | 57.4 | AX-95171275 | 3.6 | 32.1 | 27.2 | 17.6 |
| | | 55 | D2 | 56.3 - 59.4 | | | 4.21 | 0.388 | 0.378 | 20.2 |
| 2019 | 2A | 55 | PSSRb | 56.3 - 59.4 | | | 4.18 | 35.6 | 40 | 20 |
| | | 55 | RARSc | 56.3 - 59.4 | | | 4.17 | 31.2 | 34.4 | 20 |
| | | 55 | PSSRa | 56.3 - 59.4 | | | 4.03 | 40.2 | 44.9 | 19.4 |
| | | 71 | STB assessment | 66.3 - 68.5 | 67.5 | AX-95230317 | 4.22 | 55.1 | 46.6 | 10.9 |
| | | 71 | STB FLL assessment | 66.3 - 68.5 | | | 3.01 | 41.7 | 33.2 | 9.6 |
| 2019 | 2B | 39 | PhiNO | 67.3 - 68.5 | | | 3.37 | 0.4 | 0.463 | 15.9 |
| | | 33 | STB assessment | 228.2-228.5 | 228.5 | AX-94814715 | 3.12 | 35 | 30.4 | 15.4 |
| | | 33 | D2 | 227.2-228.5 | | | 5.98 | 0.403 | 0.391 | 23.9 |
| | | 33 | ND705 | 227.2-228.5 | | | 4.51 | 0.743 | 0.756 | 18.1 |
| | | 33 | PSSRb | 228.2-228.5 | | | 3.47 | 30.6 | 34.2 | 14.6 |
| 2019 | 2B | 33 | PSSRa | 228.2-228.5 | | | 3.01 | 35.8 | 40.6 | 14.9 |
| | | 55 | ARI1 | 228.2-228.5 | | | 3.14 | 1.07 | 0.548 | 15.5 |
| | | 71 | ARI1 | 227.2-228.5 | | | 3.52 | 4.36 | 3.58 | 14.6 |
| | | 61 - 69 | STB assessment | 240.1 | 240.1 | AX-94701598 | 3.22 | 33.2 | 37.5 | 15.8 |
| 2019 | 3B | 61 - 69 | ARI1 | 239.7 - 240.1 | | | 3.53 | 2.33 | 2.93 | 17.2 |

### 3.3 Phenotypic evaluation of 4D resistance to *Z.tritici* (IPO323) under controlled environmental conditions

CxS lines with the 4D resistance from Cougar were phenotyped under controlled environmental conditions to confirm that the resistance is functional at the seedling to ~GS27 stage. 4D-R lines developed fewer symptoms (AUDPC) compared to 4D-S lines for both spray and infiltration treatments, although ImageJ analysis did not detect significant differences in the spray treatment (Fig 3). Visual and ImageJ analysis assessments were significantly different for the infiltration treatment, with decreased lesions detected using ImageJ analysis (Supp Table S4). Breakdown of the AUDPC into chlorotic and necrotic symptoms (Fig 4) demonstrated reduced chlorotic and necrotic symptoms in the spray treatment for 4D-R lines with visual assessments, whilst the ImageJ analysis failed to detect differences in chlorotic symptoms, with an interaction between time and 4D-R/S for necrosis (Supp Table S5). Pycnidia incidence was lower for 4D-R lines compared to 4D-S lines, with no detectable differences using ImageJ analysis. In the infiltration treatment 4D-R lines had reduced chlorotic lesions for both assessment types, with only ImageJ assessment detecting reduced necrotic symptoms for 4D-R lines (Fig 5). Visual assessments detected a reduction in pycnidia incidence in the infiltration treatment whilst the ImageJ assessment detected an interaction between 4D-R/S and time (Supp Table S5).

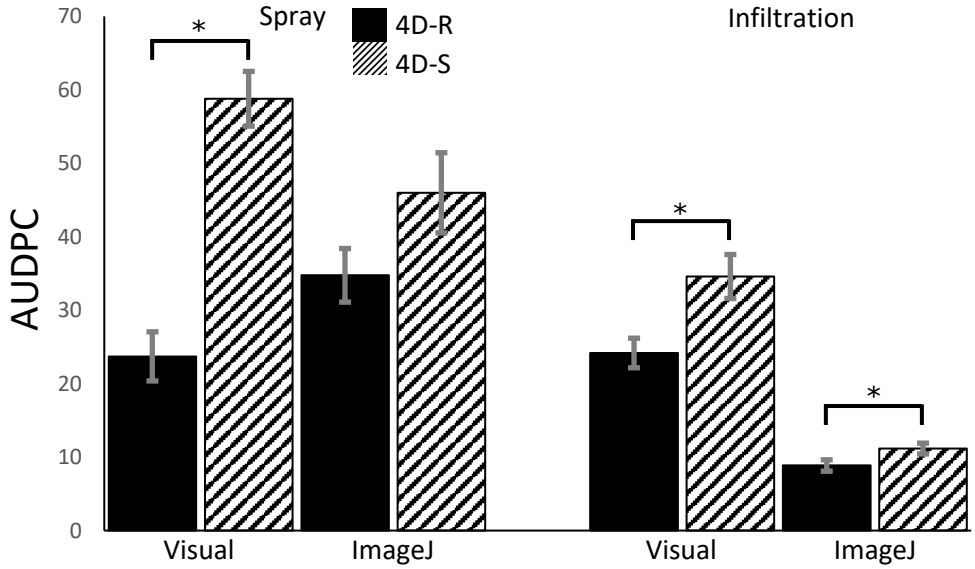



**Figure 3.** Area under the disease progress curve (AUDPC) visual and ImageJ assessment of four 4D-R and four 4D-S CxS lines under Spray or infiltration treatments of *Z.tritici* (IPO323). Students T-test indicate significant comparisons between 4D-R & 4D-S lines within treatments, Spray visual ($P < 0.001$), Spray ImageJ ($P = 0.095$), Infiltration visual ($P = 0.006$), Infiltration ImageJ ($P = 0.037$). Interactions between Visual and ImageJ treatments was tested for using ANOVA analysis displayed in Supp Table S4.

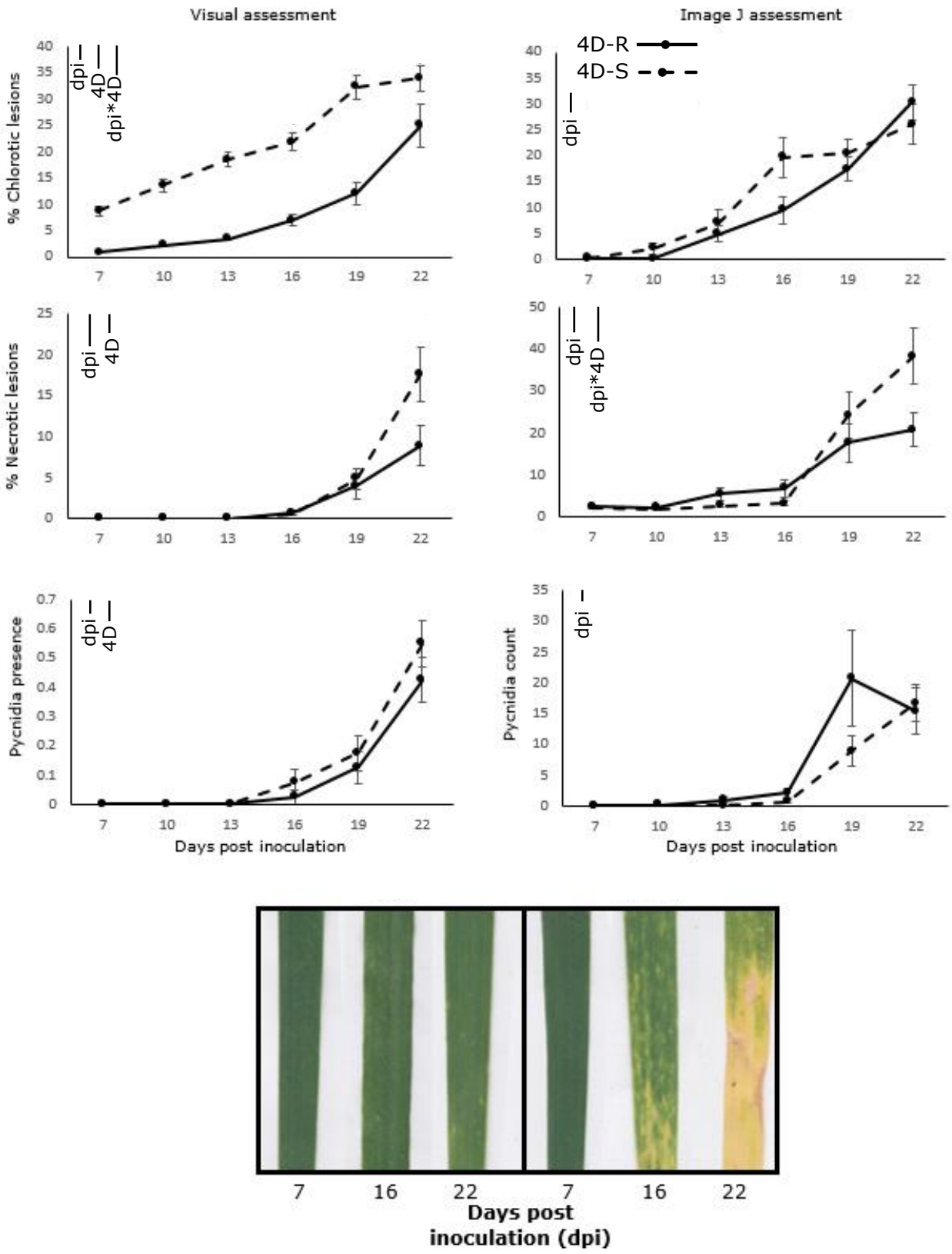



**Figure 4.** Spray inoculated STB assessments (Visual analysed left, ImageJ macro analysed right). Pycnidia presence indicates presence or absence of pycnidia on leaf. Pycnidia count is number of pycnida detected on necrotic lesions. Analysed by ANOVA, LsD values of significant interactions are displayed, SE bars displayed. (ANOVA table sup table 5)

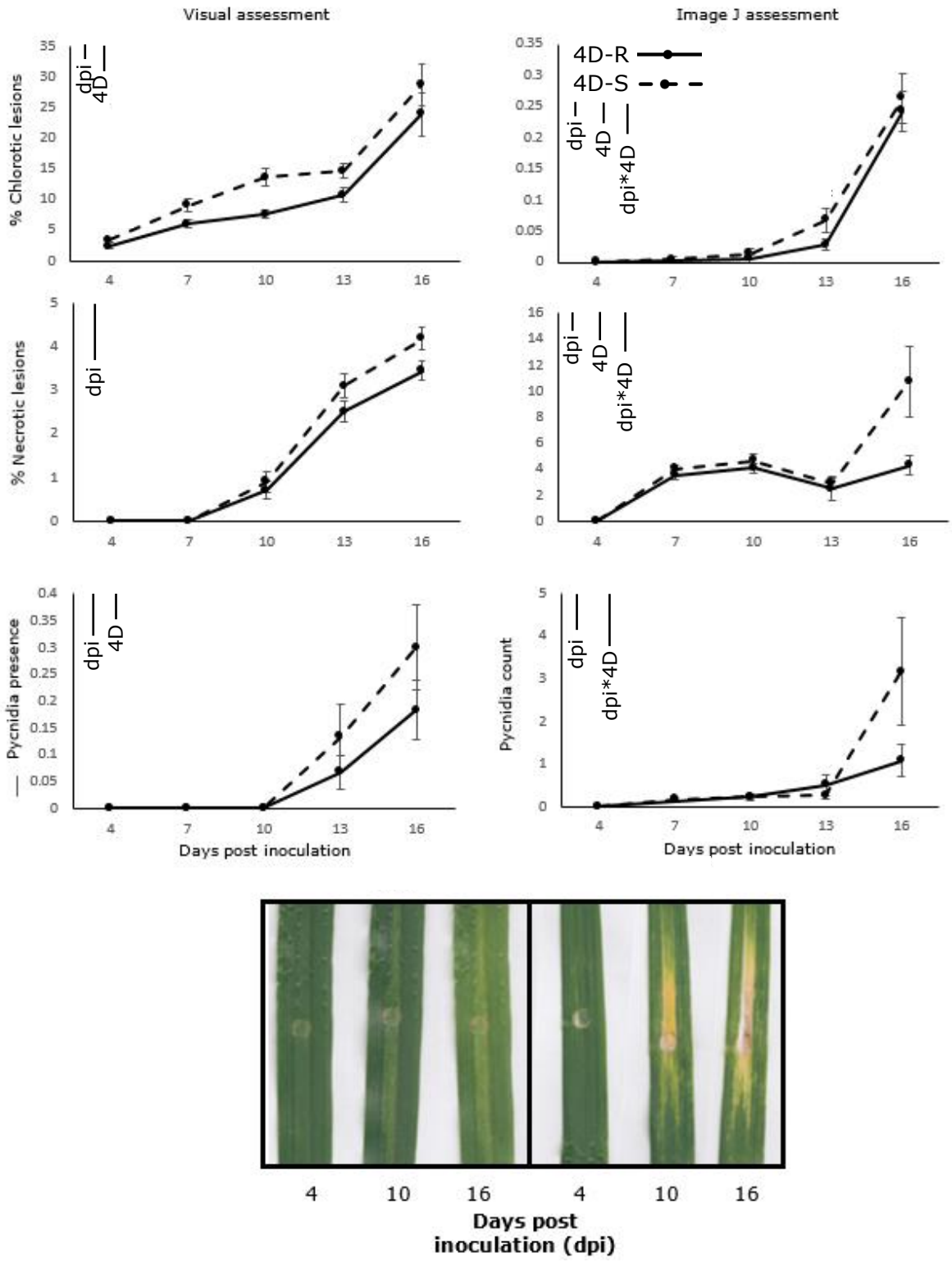



**Figure 5.** Infiltration inoculated STB assessments (Visual analysed left, ImageJ macro analysed right). Pycnidia presence indicates presence or absence of pycnidia on leaf. Pycnidia count is number of pycnida detected on necrotic lesions. Analysed by ANOVA, LsD values are displayed for significant interactions ($P < 0.05$), SE bars displayed. (ANOVA table sup table 6)

CFMs were taken to investigate the functionality of photochemistry in the 4D resistant response. Both spray and infiltration treatments showed significant differences between 4D-R or S lines for $F_v$'/$F_m$', trapping rate (TRo/RC), electron transport (ETo/RC) per reaction centre and Phi2 (Table 6). For both treatments 4D-R lines had lower TRo/RC and ETo/RC at 16 dpi ($P<0.05$). In the spray treatment the MultispeQ detected differences in Phi2 and PhiNO as early as 18 hpi with decreased PhiNO and increased Phi2 in 4D-R lines. In the infiltration treatment an increase in Phi2 wasn't observed until 16 dpi. In both spray and infiltration treatments 4D-R increased $F_v$'/$F_m$' at 4 dpi (Spray) and 7/10 dpi (Infiltration). For the infiltration treatment 4D-R was characterised by decreased ABS/RC and Dlo/RC at 10dpi and NPQt and PhiNPQ at 13 dpi. Repeated measurement analysis showed significant interaction between time and 4D-R/S for ETo/RC (Supp Table 6 a & b), demonstrating increased ETo/RC for 4D-R compared to 4D-S at ~1 dpi, and a decrease at 16 dpi.

**Table 6.** Pairwise comparison of 4D and No4D lines chlorophyll fluorescence measurements in spray & infiltration treatments (Fluorpen, MultispeQ). Students t-test, ($P<0.05$). Standard errors displayed of 4 lines involving 5 biological replicates (SE). Repeated measurement analysis in Supp Table S6 a&b.

| Inoculation | Instrument | Measurement | DPI | 4D (SE) | No 4D (SE) | *P* value |
|---|---|---|---|---|---|---|
| Spray | Fluorpen | FvFm' | 4 | 0.748 (0.002) | 0.740 (0.002) | 0.001 |
| | | TRo/RC | 16 | 2.406 (0.048) | 2.543 (0.059) | 0.039 |
| | | ETo/RC | 16 | 0.851 (0.016) | 0.888 (0.019 | 0.031 |
| | MultispeQ | Phi2 | 0.625 | 0.555 (0.011) | 0.525 (0.010) | 0.027 |
| | | PhiNO | 0.625 | 0.347 (0.010) | 0.373 (0.009) | 0.031 |
| Infiltration | Fluorpen | Fv/Fm' | 7 | 0.730 (0.002) | 0.715 (0.008) | 0.037 |
| | | Fv/Fm' | 10 | 0.721 (0.003) | 0.702 (0.008) | 0.017 |
| | | ABS/RC | 10 | 3.436 (0.059) | 3.672 (0.085) | 0.015 |
| | | TRo/RC | 10 | 2.474 (0.034) | 2.551 (0.031) | 0.048 |
| | | DIo/RC | 10 | 0.963 (0.027) | 1.121 (0.063) | 0.014 |
| | | ETo/RC | 10 | 0.851 (0.012) | 0.878 (0.011) | 0.049 |
| | | TRo/RC | 16 | 2.833 (0.063) | 2.943 (0.044) | 0.08* |
| | | ETo/RC | 16 | 0.8549 (0.023) | 0.924 (0.015) | 0.007 |
| | MultispeQ | NPQt | 13 | 0.567 (0.03) | 0.728 (0.077) | 0.031 |
| | | PhiNPQ | 13 | 0.206 (0.010) | 0.244 (0.018) | 0.037 |
| | | Phi2 | 16 | 0.330 (0.017) | 0.291 (0.016) | 0.049 |

## 4. Discussion

The major source of resistance in Cougar was identified on chromosome 4D using a visual STB assessment at GS39 and hyperspectral indices of NPQI and LRSDI2 being unique to the QTL in 2018. This study confirmed that the Cougar resistance at this field location was effective in 2018, whilst in 2019 there was a breakdown of resistance which predates the widespread resistance breakdown reported in 2022 (AHDB 2022). The *Z.tritici* population likely included more isolates which were virulent to Cougar (Kildea *et al* 2021), although dramatic differences in environmental factors between years could have also had an effect. Quantification of STB disease under controlled environmental conditions confirmed the effect of the major source of resistance in Cougar. The major source of resistance in Cougar is likely to also involve some leaf defence traits against *Z.tritici* because differences between 4D-R and S lines were greater in spray than in infiltration treatments.

Spectral reflectance indices were most effective at quantifying Cougars major source of resistance. NPQI (Pheophitinization of chlorophyll a to phaeophytin) coincided with the 4D QTL and was unique to the Cougar resistance correlating positively with disease. Yu *et al* (2018) also showed that NPQI was associated with heavily diseased canopies. An increase in RARSc, PSSRa,/b, ND705 (chlorophyll & carotenoid content) and a decrease in NPQI (chlorophyll a degradation) (NPQI) suggests that the resistant lines are likely to possess elevated chlorophyll and carotenoid content. Carotenoids are a key component of the light harvesting complexes in PSII (Lokstein, Renger, & Götze, 2021) and play major roles in regulating chloroplast redox state via reactive oxygens species production or detoxification associated in response to *Z.tritici* (Ajigboye *et al* 2021). The resistance on 4D in Cougar was associated with decreased D2 (Chlorophyll fluorescence), which could be indicative of PSII downregulation as demonstrated by Ajigboye *et al* (2021). This is consistent with a reduction in electron transport (ETo/RC) and trapping rate (TRo/RC) in both 4D-R spray and infiltration treatments detected by OJIP analysis suggesting that in 4D-R lines reaction centres are trapping fewer excitons, preventing the reduction of $Q_A$ to $Q_A^-$ and thus reducing the transfer of electrons to PSI (Strasser *et al* 2004). Whilst reduced electron transport decreased as demonstrated previously in Cougar (Ajigboye *et al* 2021), Fv'Fm' increased in 4D-R lines at earlier time-points indicating increased maximum quantum yield of PSII consistent with the MultispeQ measurements demonstrating increased maximum quantum yield of PSII (Phi2). Phi2 dynamic differences detected between spray and infiltration treatments are most likely related to pathogen-triggered immunity (PTI) or effector-triggered immunity (ETI) resistance responses

at different phases of pathogen infection respectively. These results also likely reflect the presence of other sources of resistance in these eight 4D-R/S lines, such as those identified in the QTL analysis, which might be masking 4D associated chlorophyll fluorescence OJIP phenotypes.

This study demonstrated that many hyperspectral reflectance indices are associated with the major source of resistance in Cougar, however some were not specific to Cougar, and were associated generally with STB disease and previously shown to relate to other diseases. ND705 (Yu *et al* 2018; Odilbekov *et al* 2018), D2, PSSRa/b & ARI (Odilbekov *et al* 2018) correlated with STB disease in the same manner as in this study. Additionally, other STB resistance QTLs detected using these spectral reflectance indices in this study correlated in the same manner as with the Cougar QTL. Widening the scope to other diseases, LRDSI1/2 for leaf rust (Ashourloo *et al* 2014), SIPI, PSSRa/b, RARSc and LRDSI1/2 for Fusarium Head Blight (Ghulum *et al* 2022) and PWI/ARI for Powdery Mildew (Feng *et al* 2017) had the same correlations as with this study, whilst NPQI and PWI for Fusarium Head Blight (Mustafa *et al* 2022) were reversed. Due to many indices tested in this study sharing similar correlations with other studies and with other pathogens, the QTL LOD score of specific indices are likely to be more important than a correlative analysis in identifying traits which are closely associated with sources of resistance to STB. Overall, this study demonstrated that visual STB assessments and hyperspectral reflectance indices can identify the major source of resistance in Cougar. Further work with near isogenic lines (NILs) is needed to reduce background genetic effects which are likely influencing the characterisation of this major source of resistance using CFMs and visual assessments.

This study identified other sources of minor resistance from both Cougar and Scout, which could be viable targets for breeders to include in breeding programs. Hyperspectral reflectance indices were effective at detecting these resistant QTLs, and in some cases were more effective than the visual assessments. For example, the sources of resistance from Scout on 2A and 2B, were detectable at the same growth stage with a higher LOD score by D2 (chlorophyll fluorescence) and PSSRb (chlorophyll b). Overall, D2, PSSRa and PSSRb were consistently effective at detecting resistant QTLs from both Cougar and Scout at different growth stages. This suggests that decreased chlorophyll fluorescence and increased chlorophyll a and b content are associated with STB resistance. A decrease in chlorophyll fluorescence (D2) could be a consequence of photoinhibition or photoprotection reducing PSII activity (Ajigboye *et al* 2021), whilst an increase in chlorophyll content could be a consequence of decreased

chlorophyll degradation from decreased *Z.tritici* induced necrosis. However, care should be taken using spectral indices to infer these assumptions about plant physiology since the evidence linking hyperspectral indices to specific molecule content is limited and correlative. LRDSI2 & NPQI was not associated with any other STB resistance QTLs, whereas RARSc and PWI only detected one STB resistance QTL apart from the major source of resistance, suggesting that these indices can best quantify specific STB resistance QTLs. Lastly, ARI1 and ND705 was associated with two STB resistance QTLs, although ARI1 also identified a Scout STB resistance QTL after its detection by visual assessments at GS33. Interestingly, the STB resistance QTL from Scout on 2B was only detectable using PhiNO, whereby the resistance was associated with an increase in non-regulated quenching. This is contrary to previous work by Ajigboye *et al* (2021) on Cougar, suggesting that different sources of resistance could induce different resistant mechanisms associated with varying chlorophyll fluorescence phenotypes. Therefore, this study demonstrated that visual STB assessments, hyperspectral reflectance indices and CFMs can identify other sources of resistance. Additionally, specific indices or CFMs could be characterising specific STB resistance QTLs whilst some like D2, PSSRa and PSSRb are likely more universal indicators of STB resistance.

Hyperspectral measurements taken early in plant development were shown to be effective in predicting future STB disease later in the season. Of the 9 selected indices, D2 (chlorophyll fluorescence) followed by ND705 (Chlorophyll content) were the most consistent indices over both years at predicting future disease at GS39 and 59. Additionally, ND705 was the only index to predict disease at GS61-69. Due to high levels of correlation between indices, use of multiple indices in the stepwise linear regression model added little to the percentage of variation explained. Therefore, a singular index such as D2 of ND705 might be more reliable and consistent. In addition to the indices analysed as part of the stepwise linear regression analysis, correlation analysis of all 31 indices demonstrates widespread correlation of the majority of indices with future STB disease over both years (Table S2). Most notably PSRI was highly correlated with future disease, which is supported by findings from Yu *et al* (2018) which showed PSRI to also be one of the best indices at early growth stages. Additionally, Odilbekov *et al* (2018) demonstrated that D2, LRDSI1, and LRDSI2 were the best chlorotic predictive indices whilst ARI1 was amongst the best necrotic predictive indices. Results from this study confirm that D2, LRDSI1, LRDSI2 and ARI1 correlated strongly with disease, as well as being strong predictors for future STB disease.

Compared to hyperspectral reflectance measurements, CFMs were relatively inconsistent at predicting future STB disease. CFMs stepwise linear regression analysis demonstrated that no measurements significantly accounted for future STB disease, although correlation analysis highlighted some CFMs measured at GS23-26 and GS55 which loosely predicted future disease, although this wasn't consistent between years. CFMs measured at GS26 in 2019, which correlated with STB disease at GS33, did demonstrate that the STB disease was associated with an increase in PSII yield (Phi2, Fv'/Fm'), which is congruent with the spectral reflectance index D2 (Chlorophyll fluorescence) positively correlating with disease. STB disease was also correlated with decreasing photon flux absorbed by the antenna (ABS/RC), reduced dissipation (DIo/RC) (Strasser *et al* 2004) and a decrease in regulated quenching processes (PhiNPQ), suggesting that susceptible lines were unable to dissipate excess excitation energy in a regulated manner, which might lead to ROS accumulation and cell death (Ajigboye *et al* 2021; Murchie & Ruban 2020; Lee *et al* 2015). It is also worth noting that PhiNO measured at GS39 was the only proximal phenotyping measurement which predicted a subsequent STB resistance QTL at GS71. Overall, this study demonstrated that hyperspectral reflectance and chlorophyll fluorescence indices obtained in asymptomatic plants or early in plant development can be used to detect resistance or predict *Z.tritici* disease later in the season. However, CFMs were less consistent at predicting future STB disease. This could be due in part to how CFMs are measured on individual leaves instead of at a canopy level so environmental factors specific to individual leaves could be confounding the results. CFM differences are also highly time dependent, as demonstrated in this study by their time dependent differences between 4D-R/S lines under growth room conditions. Hence, naturally infected field plots where individual leaves are constantly infected by different *Z.tritici* isolates throughout the growing season could likely create significant noise preventing effective STB resistance QTL and subsequent disease detection. Furthermore, the lack of a dark adaptation period is likely having a significant impact on CFM outputs.

STB resistance QTLs detected by both visual assessments and proximal phenotyping methods were time and year dependent. This demonstrates the need for breeders to test multiple sites over many growth stages with sufficient replicates to detect the majority of a cultivar's genetic resistance. Hyperspectral measurements also detected numerous QTLs which lacked visual STB confirmation. Therefore, hyperspectral measurements may be detecting far more STB resistance QTLs than traditional visual assessments, although this cannot be confirmed without more data. These indices might also be detecting many traits associated with abiotic defence

and resistance to other pests and pathogens. Indices consistently correlate with other diseases (Ashourloo *et al* 2014; Mustafa *et al* 2022; Feng *et al* 2017), as well as other desirable traits such as yield (Xavier *et al* 2006) and nitrogen use (Frels *et al* 2018) in a similar manner. Therefore, breeders could utilise the same measurements highlighted in this study to detect QTLs for a multitude of desirable traits, replacing the need to assess for specific diseases such as STB. Efficient, reliable and precise phenotyping is necessary for breeders to identify desirable traits, such as resistance to *Z.tritici*. Compared to visual phenotyping, high-throughput proximal phenotyping methods can be significantly quicker, whilst providing more quantitative and repeatable data (Reynolds *et al* 2019). To our knowledge, four studies have now demonstrated the value of spectral reflectance indices in predicting/correlating STB disease (This study; Yu *et al* 2018; Odilbekov *et al* 2018; Anderegg *et al* 2019). Whilst previous studies have extensively demonstrated the effectiveness of hyperspectral reflectance indices to quantify STB disease, this is the first study to demonstrate their use in QTL analyses to identify specific STB resistance QTLs, which could then be incorporated into breeding programs. Plant breeders could utilise UAVs (Wei *et al* 2021; White *et al* 2012) or other remote vehicles, combined with portable spectroradiometers to collect remotely extensive data sets which could be used for GWAS and/or QTL analyses (Reynolds *et al* 2019). Indices identified in this and previous studies could help identify specific novel STB resistance QTLs. Additionally, the data could also be used to identify other resistance QTLs for other diseases such as leaf rusts (Ashourloo *et al* 2014) as well as other desirable abiotic traits. However, this form of high throughput phenotyping might not be appealing to breeders due to the lack of index specificity to a disease or trait. Synonymous use of hyperspectral reflectance measurements and RGB-imaging could help solve this issue by confirming the visual phenotype and providing a reference for manual review. This study also demonstrated the value of automated image analysis in quantifying STB in a repeatable quantitative manner, which could be combined with the reflectance data as discussed.

In summary, this study located the major source of resistance in Cougar on 4D and demonstrated a breakdown of this resistance in 2019. We confirmed that this major source of resistance can be identified using a range of visual STB assessments and spectral reflectance indices, whilst characterising this resistance in controlled environmental conditions using CFMs. Characterisation using spray and infiltration inoculation techniques also suggested that this major source of resistance involves limited preformed leaf defence traits against *Z.tritici*. Visual STB assessments and spectral reflectance measurements were also effective in

identifying other sources of resistance in 2019. This study also demonstrated that hyperspectral reflectance and chlorophyll fluorescence indices, such as D2 and ND705, obtained in asymptomatic plants or early in plant development can be used to detect resistance QTLs or predict *Z.tritici* disease later in the season. These findings build on previous work by Yu *et al* (2018), Odilbekov *et al* (2018) and Anderegg *et al* (2019) by highlighting and confirming the best indices to quantify STB. This study also demonstrates the potential for hyperspectral reflectance indices to be incorporated into QTL analyses to detect novel STB resistance QTLs, as well as the challenges associated with utilising CFMs. Spectroradiometers and automated image analysis prove to be promising tools for plant breeders to phenotype populations in a more quantitative, repeatable, time efficient and precise manner. High-throughput phenotyping could replace or supplement traditional visual phenotyping methods to help optimise gene discovery and facilitate the incorporation of sources of resistance to *Z.tritici* into high yielding commercial wheat cultivars in a more sustainable manner.

# Chapter 3.

## Chlorophyll fluorescence phenotyping and transcriptomic analysis of a novel source of resistance to *Zymoseptoria tritici* in the winter wheat cultivar Cougar

# 1. Introduction

*Zymoseptoria tritici* is a latent necrotrophic fungal pathogen causing septoria tritici blotch (STB) on *Triticum aestivum* (wheat) (Sanchez-Vallet *et al* 2015). STB is widely considered as one of the main pathogens leading to wheat yield losses (Savary *et al* 2019), with research into *Z.tritici* aimed at improving global food security (Fones & Gurr 2015). Organizations such as the European Commission are promoting integrated disease management principles to reduce fungicide inputs (EC, 2019), hastening the need for breeding companies to develop wheat cultivars with high levels of resistance to pathogens such as *Z.tritici*. Currently, over 20 *Stb* resistance genes have been identified, although the presence or absence of these resistance genes in commercial cultivars is uncertain. The wheat defence response involves pathogen associated molecular pattern (PAMPs) triggered immunity (PTI), and effector triggered immunity (ETI). PTI is typically non-isolate specific and involves a variety of pre-formed and basal defence mechanisms to provide quantitative resistance. ETI involves the recognition of specific *Z.tritici* avirulence effectors that are recognised by the host to induce a stronger defence response than PTI and is typically coined qualitative resistance. For example, Stb6 is a well characterised qualitative resistant gene encoding a wall associate kinase (WAK), shown to be involved in ETI by binding with the *Z.tritici* AvrStb6 effector (Zhong *et al* 2017) to induce a defence response. Therefore, *Z.tritici* typically rapidly evolves resistance to qualitative STB resistance genes through sexual recombination by obtaining isoforms of the AvrStb gene which are not recognised by the corresponding STB gene (Erikson & Munk 2003). For example, in the case of Stb6, rapid spread of virulent AvrStb6 isoforms in European populations (Stephens *et al* 2021) has contributed to the breakdown of Stb6 resistance (Dalvand *et al* 2018; Kosellek *et al* 2013). However, qualitative sources of resistance typically exhibit strong resistant responses, providing cultivars with strong levels of resistance until the resistance is overcome (Brown *et al* 2021). Provided qualitative sources of resistance are combined with strong levels of background quantitative resistance in a responsible manner, these sources of resistance can help improve the *Z.tritici* resistance profile in modern cultivars.

Whilst the gene-for-gene relationship in wheat-*Z.tritici* interactions has been investigated for Stb6 (Zhong *et al* 2017) and Stb16q (Meile *et al* 2018; Saintenac *et al* 2021), there is relatively little research into the downstream defence responses of these and other STB resistance genes. Understanding the wheat-*Z.tritici* resistant response can help further our understanding of the *Z.tritici* lifecycle, gene-for-gene resistance, downstream resistance genes and defence pathways. Additionally, characterisation of the resistant response could help identify targets

for candidate fungicides, as well as to contribute to our wider knowledge of wheat defence which could have far-reaching applications for other pathosystems. Qualitative sources of resistance are ideal candidates for investigating the *Z.tritici* resistance response in wheat due to the strong resistant effect which is typically controlled by a single gene. Chapter 2 of this PhD located a qualitative source of resistance in cv. Cougar on chromosome 4D, demonstrating that either a single gene or a small cluster of genes are responsible for this resistance. Utilising near isogenic lines (NILs) of this source of resistance will enable us to thoroughly investigate the mechanisms of resistance associated with this resistance, whilst minimising the confounding effects of background sources of resistance. Despite the major source of resistance in cv. Cougar breaking down in the field as early as 2015, with more recent reports on Cougar (Caiazzo *et al* 2019) and Cougar derived cultivars (Kildea *et al* 2021) resistance breaking down by 2021/2022 (AHDB 2021/2022, RL), this resistance can still be useful to investigate the wheat-*Z.tritici* resistance response for isolates avirulent to the Cougar resistance.

Transcriptomic studies can be an important tool to understand the resistance response between wheat and *Z.tritici*. Whereas many previous studies have focused on specific defence related genes (Ray *et al* 2003; Adhikari *et al* 2007; Shetty *et al* 2009) transcriptomic analyses enables quantification of the entire transcriptome, providing a more holistic approach to understand the processes involved in the downstream defence response. To date, around 10 transcriptomic studies have been published regarding the *Z.tritici*-wheat interaction. The first transcriptomic studies on *Z.tritici* involved a single isolate compatible genotype comparison regarding cv. Riband and cv. Sevin at various timepoints (Keon *et al* 2005; Yang *et al* 2013; Rudd *et al* 2015) and the first isolate comparison was published by Palma-Guerrero *et al* (2016) comparing the transcriptome of Drifter and Riband (Rudd *et al* 2015). It is worth noting that these first transcriptomic studies focused on the transcriptome in *Z.tritici* compatible interactions and didn't investigate the wheat defence response. One of the first studies which investigated the defence response of wheat to *Z.tritici* was by Orton *et al* (2017), although this was not a full transcriptomic analysis and instead focused on the expression of 14 defence related genes in different compatible and incompatible *Z.tritici*-wheat interactions. Palma-Guerrero *et al* (2017) investigated the transcriptomes of four *Z.tritici* isolates with differing levels of virulence to cv. Drifter, although again this focused on *Z.tritici* and didn't investigate the differing wheat defence responses in Drifter. Haueisen *et al* (2019) also investigated the transcriptome of multiple *Z.tritici* isolates which were used to inoculate cv. Obelisk, although these had similar virulence. One of the first studies which utilised transcriptomics to quantify resistance to

*Z.tritici* was by Odilbekov *et al* (2019) which was used in combination with QTL analyses. A more recent study (Benbow *et al* 2020) compared the transcriptome of the synthetically derived cultivar Stigg with "exceptional STB resistance" to a susceptible wheat cultivar. Odilbekov *et al* (2019) identified F-box proteins followed by nucleotide-binding site (NBS) leucine rich repeat (LRR) disease resistance proteins and receptor-like kinases (RLK) to be the most important genes associated with resistance. However, Benbow *et al* (2020) demonstrated that a downregulation of biological processes and a lack of expression of disease related proteins was associated with the resistant response in cv. Stigg. Therefore, whilst Benbow *et al* (2020) was the first study to fully characterise the transcriptome of a compatible and incompatible interaction, additional work is needed to confirm if these downstream resistant responses are consistent with other sources of resistance or if this is unique to cv. Stigg. The main limitation of Benbow *et al* (2020) as well as other studies investigating incompatible wheat-*Z.tritici* interactions is that even though the two cultivars used share two distinct phenotypes (compatible, incompatible), differences in the genetic backgrounds could be responsible for the transcriptome expression which may be independent of STB resistance. To minimise the genetic background effect, near isogenic lines (NILs) are needed so differences in the transcriptomic profile can be more accurately attributed to the source of resistance. Therefore, this study aims at utilising Cougar NILs with and without the source of resistance to characterise the transcriptome of the major source of resistance.

Wheat defence responses typically include the synthesis and signalling of phytohormones such as Jasmonic acid, Salicylic acid, Ethylene, Abscisic acid, Auxins, Cytokinins, Brassinosteroids and Gibberellic acid (Alazem & Lin 2015). Whilst transcriptomic analyses can inform resistance mechanisms involving specific hormones and/or hormonal and resistance pathways, quantification of hormones is required to validate hypotheses brought about from transcriptomics. Therefore, this study aims to link transcriptomic gene expression with hormonal data to characterise the role of specific hormones and genes in the Cougar defence response. In addition to characterising the resistant wheat-*Z.tritici* incompatible interaction, transcriptomic analyses can also be utilised to identify candidate genes on 4D which might be responsible for the major source of resistance. Gene expression analysis has previously been used to help identify TaWAKL4 to be Stb6 (Saintenac *et al* 2018) and hence a similar technique could be used to identify the gene(s) responsible for the major source of resistance in Cougar. Whilst the corresponding *Z.tritici* transcriptome has not been mapped to identify a candidate

region which might contain a AvrStb gene specific to the Cougar resistance, *Z.tritici* candidate effectors can still be identified, although these may be numerous.

Previous research by Ajigboye *et al* (2021) has demonstrated the role of photoprotective mechanisms in the Cougar resistance, with Lee *et al* (2015) demonstrating the importance of the chloroplast in wheat-*Z.tritici* defence. Reactive oxygen species (ROS) serve as molecular messengers to initiate a defence response or cause programmed cell death to stop pathogen progression. The accumulation of ROS is key in facilitating compatible wheat-*Z.tritici* interactions (Choi *et al* (2016) during the switch to necrotrophy. The main source of ROS in plants originates from the photosynthetic apparatus involved in the capture of energy required for photosynthesis and dissipation of energy for redox homeostasis (Foyer & Noctor 2005). To prevent irreversible damage to photosystems from the excessive accumulation of ROS during environmental stress, photoprotective mechanisms function in plants. A major mechanism regulating photoprotection is non-photochemical quenching (NPQ) controlling thermal dissipation of energy away from photosystems (Murchie & Ruban 2020). The main component of NPQ is the fast-relaxing qE component, although other components such as the state transitions qZ & qT and the slow-relaxing component qI contribute to NPQ. qE involves the xanthopyll zeaxanthin, the PSII external protein PsbS, and acidification of the lumen which initiates energy dissipation by limiting the transfer of electrons from the PS2-LHCII to the electron transport chain to PSI. The mechanism of slow-relaxing form of NPQ qI is not fully understood, although it is believed that also involves zeaxanthin and is associated with reorganisation of LHCII (Ajigboye *et al* 2021). Ajigboye *et al* (2021) demonstrated that the Cougar-*Z.tritici* defence response involved a reduction of ROS ($H_2O_2$/superoxide), which is likely a product of an increase in the qI component of NPQ and a downregulation of PSII activity. Zeaxanthin and other carotenoids such as lutein, antheraxanthin, violaxanthin and neoxanthin are involved in binding in the LHCII (Lokstein, H., Renger, G., & Götze, J. P. 2021) and are part of the xanthophyl cycle involved in ABA synthesis from neoxanthin and the enzyme NCED. The resistance in Cougar was associated with an accumulation of neoxanthin and ABA, demonstrating the role of the xanthophyll cycle in the Cougar defence response (Ajigboye *et al* 2021). The significant role ROS has in mediating infection in compatible *Z.tritici* interactions (Foyer & Noctor 2005; Choi *et al* 2016), combined with Ajigboye *et al* (2021) characterising the Cougar photoprotective defence response, demonstrates that the chloroplast is a likely battleground for plant-pathogen interactions. Whilst chlorophyll fluorescence measurements were relatively ineffective at characterising resistance under field

conditions compared to other phenotyping methods (Chapter 2), under controlled environmental conditions chlorophyll fluorescence proves to be a promising tool to characterise the wheat-*Z.tritici* resistance response (Ajigboye *et al* 2021). Additionally, whereas in Chapter 2 high-throughput chlorophyll fluorescence tools such as the MultispeQ (PhotosynQ) and Fluorpen (Photon Systems Instruments, Czech Republic) were used to try and characterise a Cougar x Scout population, use of more precise phenotyping tools (Ajigboye *et al* 2021) could provide a more accurate and reliable characterisation of the major source of resistance in Cougar. Whilst Ajigboye *et al* (2021) characterised the resistance in cv. Cougar compared to the susceptible cv. Sacramento, access to NILs in this study enables characterisation of the photoprotective resistance mechanism in Cougar whilst minimising the presence of confounding background resistance from Sacramento or Cougar. Additionally, quantification of xanthophyll related genes will help us investigate the role of the xanthophyll cycle in the major source of resistance in Cougar, as well as the role of the hormone ABA.

Therefore, this study aims to characterise the major source of resistance in Cougar using a set of NILs to minimise background genetic effects and two incompatible isolates to identify effects shared by more than one avirulent isolate and therefore may be related to avirulence to Cougar rather than isolate-specific reactions. Hormonal analysis, chlorophyll fluorescence measurements and xanthophyll cycle gene expression will be used in conjunction with the transcriptomic analysis to provide a holistic characterisation of the major source of resistance in Cougar. Further mapping of the major source of resistance on 4D will help narrow down the candidate region using a Cougar x Cashel population, with transcriptomic analysis of gene expression used to identify candidate genes, as well as other genes associated with the resistance. Candidate genes will also be investigated further, by confirming expression using qRT-PCRs, and using sequencing data to identify missense and nonsense mutations which could influence gene functionality between the NILs. Transcriptomic analysis of both *Z.tritici* transcriptomes will be used to identify candidate Avr effectors, as well as genes associated with compatible and incompatible interactions. This study therefore set out to test these main hypotheses:

1) The major source of resistance in Cougar involves a photo-protective defence response.
2) Transcriptomic analysis can identify and characterise candidate genes responsible for the major source of resistance in Cougar.
3) The holistic resistance mechanism in Cougar can be investigated through hormonal and transcriptomic analysis of near isogenic lines.

## 2. Materials and Methods

### 2.1 Plant material and controlled environmental conditions

Near isogenic lines (NILs) were developed by RAGT and constituted the 4D Cougar resistance region and a background of Cashel (susceptible). Cougar was backcrossed with Cashel up till BC3 with marker and phenotyping data used to confirm the presence of the major source of resistance on 4D. Both NILs did not contain Stb6 based on marker data from RAGT. Seeds were grown in modular trays using John Innes No.2 compost and transferred to 8cm deep pots after 10 days. Plants were kept in a tray of water with a bi-weekly application of 15:7:30 Hortifeed and had transparent sleeves fitted to minimize leaf damage. Conditions were 16-22 $^{O}$C for a 16-hour day night cycle with a ~270 μmols $m^{-2}$ $s^{-1}$ Photosynthetic Photon Flux Density (PPFD). Physiological measurements were performed on 3 biological replicates and an additional 4 biological replicates (separate plants) for the visual phenotype. 5 technical replicates were pooled into 3 biological replicates for the RNA-seq destructive collection.

### 2.2 *Z.tritici* inoculations

Two isolates with avirulence to the 4D resistance was used (IPO323, HT-22). IPO323 is a commonly used isolate when it comes researching *Z.tritici*, hence its inclusion could aid in comparing the results from this study to other papers, HT-22 has virulence to Stb6 but is used in this study due to the 4D Cougar resistance providing strong levels of resistance to it. Both were sourced from Dr Kostya Kanyuka (NIAB). Isolates were chosen to help identify common transcripts in the resistant interaction to identify potential 4D candidate genes. Isolates were stored in 50% glycerol at -80$^{O}$C and grown for 5 days at room temperature on potato dextrose agar (PDA). Spore concentration was diluted to $1x10^{6}$ concentration using a haemocytometer with ~1 drop of Tween 20 per 100ml added to assist with spore adhesion to the leaf. Plants were sprayed till runoff at 4 weeks and kept under a humidity tent with trays of water to ensure ~100% humidity before being taken off after 4 days. Plants were taken out of the tent for measurement purposes with effort taken to maintain high levels of humidity.

### 2.3 STB disease and Pycnidia assessments

Plants were assessed for percentage chlorotic lesion area, percentage necrotic lesions area and Pycnidia presence at 7, 10, 13 & 16 dpi. The same plants and leaves, which were analysed for the chlorophyll fluorescence measurements, were also assessed for disease in addition to 2

other leaves. The 3 most expanded leaves at the time of inoculation were tagged and later assessed.

### 2.4 Chlorophyll fluorescence and gas exchange measurements

The infrared gas analyser (IRGA), LI-6400 (LI-COR Biosciences, Nebraska, USA) was used to measure chlorophyll fluorescence and gas exchange. The IRGA had a flow rate of 500 mL $min^{-1}$ and a curvet temperature of 20 °C, $CO_2$ concentration of 400 ppm, and relative humidity of ~60%. Leaves were dark adapted for ~1 h using aluminium foil to ensure maximum oxidation of the reaction centres to get a true measurement for Fm. The protocol involved applying a low measuring light insufficient to induce significant variable fluorescence ($F_o$), followed by a saturating pulse to get maximum fluorescence ($F_m$). Actinic light (1500 µmol $m^{-2}$ $s^{-1}$) was turned on at 2 min, a saturating pulse of 7000µmol $m^{-2}$ $s^{-1}$ (for 0.8 s) was applied to determine maximum fluorescence ($F_m$'). Actinic light was switched off for 2s with far-red light applied to determine $F_o$'. Application of a series of saturating pulses every 2 min over a period of 16 min under actinic light and for another 16 min under darkness (actinic light turned off), allowed calculation of $F_o'$ and $F_m'$. Chlorophyll fluorescence parameters were calculated directly from LICOR 6400XT software. Measurements obtained included including non-photochemical quenching (NPQ), maximum quantum efficiency of PSII photochemistry ($F_v/F_m$), photochemical quenching (qP), electron transport (ETR) and efficiency of PSII (PhiPS2). The fast relaxing component (qE) was calculated as ($F_m/F_m'$) - ($F_m/F_m''$), while the slowly relaxing component (qI) was calculated as ($F_m - F_m''$)/$F_m''$, where $F_m''$ is the maximal yield of fluorescence after 16 min of dark relaxation. We assumed that after 16 min of dark treatment the NPQ consists only of qI.

### 2.5 RNA-seq analysis

Leaves were collected from 4-week-old plants a day prior to inoculation (0 hpi) and at 6 hpi and 11 dpi. 5 plants were pooled to make up each of 3 biological replicates for each treatment and timepoint (HT-22 +4D, HT-22 -4D, IPO323 +4D, IPO323 -4D). Samples were flash frozen in liquid nitrogen with the tips of the leaves omitted from sampling due to expected changes in the transcriptome from damage during sampling and stored at -80$^{O}$C. Samples were manually ground using a pestle and mortar under liquid nitrogen prior to RNA extractions. RNA was extracted utilising a modified protocol from RNAeasy kit (Qiagen). Modified protocol included using Triazole followed by chloroform to extract the RNA. Samples were eluted in 50µl of RNase free water and quantified using Nanodrop ND-1000 Spectrophotometer and gel

electrophoresis, which also confirmed suitable integrity and minimal degradation of RNA. RNA-seq was carried out by Novogene (Cambridge, UK) on its Illumina NovaSeq platform. Sequence reads were mapped to the reference genome of wheat (Chinese Spring) and IPO323 using HISAT2 algorithm. Transcript expression was calculated using the Fragments Per Kilobase of transcript sequence per Millions base pairs sequenced (FPKM) method. DESeq2 R package was used to perform pairwise comparisons analysis at each time point with P-values adjusted using the Benjamini & Hochberg (1995) method for controlling the false discovery rate (Padj). Enrichment analysis of the DEGs was performed using the clusterProfiler software, including GO Enrichment, GSEA & KEGG analysis. KEGG analysis not shown due to lack of significant pathways at 6hpi and results at 11 dpi encompassed by the GO and GSEA analysis. Knetminer, Uniprot & ensemble were used to investigate transcript functionality for investigated transcripts, especially where GO-term and other annotations were lacking. *Z.tritici* effector prediction was performed using:

TargetP-20 (https://services.healthtech.dtu.dk/service.php?TargetP-2.0)
EffectorP3 (https://effectorp.csiro.au/)
Localizer (http://localizer.csiro.au/)

**2.6 Hormone quantification**

The same samples obtained for the transcriptomic analysis were used for hormonal quantification (see section 2.5). The endogenous contents of hormones, including ABA; Abscisic acid, SA; Salicylic acid, JA; Jasmonic acid, OPDA; oxo-Phytodienoic acid, Ja-Ile; jasmonoyl-L-isoleucine, IAA; Indole-3-acetic acid, GA1, 3, 7; Gibberellin, ACC; 1-Aminocyclopropane 1-carboxylic acid, IPA; Indole-3-propionic acid, 2iP; 6-(γ,γ-Dimethylallylamino)purine, Z; Zeatin, ZR; zeatin riboside were determined by liquid chromatography coupled to electrospray ionization tandem mass spectrometry (LC/ESI-MS/MS) as described by Müller and Munné-Bosch (2011). 100mg freeze dried leaf sample was extracted using a mixture of methanol:isopropanol:acetic acid, 50:49:1 (v/v/v) using ultra-sonication (Branson 2510 ultrasonic cleaner, Bransonic, Danbury, CT, USA). Deuterium-labeled plant hormones were added to the initial extract to estimate recovery rates. Extract was vortex and centrifuged at 4°C for 10 min at 1300 rpm. Supernatant was collected, pooled and filtered using 0.22-μm hydrophobic PTFE Syringe Filters (Phenomenex, Torrance, CA, USA). This was then injected into the UHPLC/ESI-MS/MS system. All hormones analysed using negative ion mode, except cytokinins (measured using positive ion mode).

## 2.7 qRT-PCR of xanthophylls and candidate genes

RNA was converted into cDNA using the iScript cDNA synthesis kit (Biorad) and quantified using nanodrop to ensure consistent DNA concentrations of 20ngul$^{-1}$. Primers at 50 μM concentration were used along with SYBR mix. Ubiquitin (Ubi) & ADP-ribosylation factor (ADP) housekeeping genes were used to control for error between samples. qRT-PCRs consistent of 2 technical replicates. The protocol used was consistent for all primers; 95$^{O}$C for 30s, 40 cycles of 95 $^{O}$C for 15s and 60 $^{O}$C for 30s followed by a melt curve between 65 and 95$^{O}$C. Candidate gene expression primers were based on the reference Chinese Spring sequence. Zeaxanthin epoxidase (ZEP), 9-cis-epoxycarotenoid dioxygenase (NCED) & Violaxanthin depoxidase (VDE) primers were used from Ajigboye *et al* (2021). Relative expression was calculated as 2^(Sample CQ – Housekeeping CQ) to compare the target gene relative to the housekeeping gene. qRT-PCRs were performed on the RNA used in the RNA-seq. In addition, qRT-PCRs were performed on cDNA from a future experiment (Chapter 4) to investigate candidate gene expression when the resistant NIL is inoculated with an isolate that has overcome its resistance (508). This utilised a set of NILs from a different pipeline, although they were developed in the same manner as the set of NILs used in this study.

Primers used:

6300 – F (TGTTCCAGAGGAAATTGGCAG) R (CCAGCACACAACTCAGGTGG)
7300 – F (GGTGGTGTTCTGCACCATGT) R (TGCATCGTCATGGGTCTTCT)
7600 – F (AGCAGGATTGACAAGCAGCC) R (AATCAGCGGCGAAAGATCAA)
VDE – F (CCCGAGCTAGAAAGGGCTAC) R (ACCACAGGTGTTGTCTGTCC)
ZEP – F (GGACTTCAACGACCCCTTGT) R (TACCCTATTGTACACCCTCGGT)
NCED – F (TAAGTGCTACAAGAGTGACTACC) R (CCTGTAGCGAAGCAGTAGG)

## 2.8 Candidate resistance gene mapping on 4D

The MQM mapping from Chapter 2 identified the major source of resistance in Cougar to be located on 4D at AX-94733088. The interval was 15.8 – 17.5, with markers flanking the peak AX-94733088 marker (3609069) (AX-95167116_K - AX-94456463) falling outside this interval. A greater density of markers between these flanking markers was used to try and narrow down the candidate gene region. These included markers: AX-94516693 (Physical location (PL): 1710372), AX-94724450 (PL: 3253201), AX-94980093 (PL: 3253219), AX-95200287_k (PL: 3253229), AX-94904565 (PL: 3404600), BS00022283 (PL: 3436415), AX-

94410073 (PL: 3436468), AX-94891432_k (PL: 3721148), AX-95148209_K (PL: 3839045), AX-95185840_k (PL: 3840295), AX-94706201_k (PL: 3840416), AX-94719284_k (PL: 4353431), AX-94797660_k (PL: 4353459), AX-94929205_k (PL: 4353761), AX-95201027_k (PL: 4358153), AX-94954877_k (PL: 4358180), AX-94627860_k (PL: 4361772), AX-94913996_k (PL: 5362467), AX-89639967_K (PL: 6758600). Mapping was carried out by RAGT (Dr Ruth Bryant).

### 2.9 Statistical analysis

Experiments were designed using a random block structure including a random distribution of 4D-R/S NILs to account for environmental variability. Different isolate inoculations were kept in separate humidity tents and benches to prevent cross contamination. RT-qPCRs, hormone quantification, chlorophyll fluorescence measurements & disease assessments were analysed using Genstat 19$^{th}$ edition (VSN international). Students T-tests were performed to compare differences between treatments in all comparisons ($P<0.05$). The effect of compatibility was assessed for xanthophyll RT-qPCRs and hormonal quantification using the following statistical model using ANOVA: Isolate + Compatibility.

# 3. Results

## 3.1 Disease and chlorophyll fluorescence (CF) phenotype of 4D-R resistance

NILs with (4D-R) or without 4D (4D-S) resistance were inoculated with IPO323 and HT-22 to assess disease and CF phenotype. Both HT-22 & IPO323 inoculated 4D-R NILs had reduced necrotic lesions at 16 dpi, and reduced pycnidia incidence at 13dpi & 16dpi, compared to 4D-S NILs (Fig. 1b, c). However, HT-22 inoculated 4D-R NILs displayed less chlorosis at 13 & 16dpi compared to IPO323, which had greater chlorotic lesions compared to the 4D-S NILs (Fig. 1a). The visual assessment demonstrates that the major source of resistance in Cougar in the 4D-R NILs provides resistance to both isolates (HT-22 & IPO323), although there were isolate differences in the chlorotic phenotype (Fig. 1a, d).

In HT-22 inoculated NILs there was a sustained decrease of $F_v/F_m$ in 4D-R NILs at 6 & 12 hours post inoculation (hpi) compared to 4D-S NILs (Fig. 2a). The induction and relaxation curves of NPQ showed significant increases in the slow relaxing component of NPQ (qI) in 4D-R NILs at the same time points, 6 & 12 hpi (Fig 2b, c), accompanied by decreased NPQ (qE) induction in the light at 12 hpi (Fig 2c). There were no differences in NPQ induction and relaxation at 24 and 48 hpi (Fig 2d, e). 4D-R NILs also increased stomatal responsiveness to light stimulus at 12 & 24 hpi (Fig. 2k, l).

In IPO323 inoculated NILs there was no differences in Fv/Fm (Fig. 3a). At 6 hpi, NPQ in the light (qE) was induced in the 4D-R NILs, compared to the 4D-S NILs, whilst NPQ in the dark (qI) relaxed (Fig. 3b). This trend reversed at 48 hpi with 4D-R NILs inducing NPQ (qI) and relaxing NPQ (qE). 4D-R NILs also increased stomatal responsiveness to dark stimulus at 12 hpi (Fig. 3k) and increased PhiPS2 at 48 hpi (Fig. 3m).

Both 4D-R NILs inoculated with HT-22 or IPO323 exhibited a decrease in PhiPS2 compared to 4D-S NILs (Fig. 2f, 3f), indicating downregulation of PSII quantum yield which was associated with decreased necrotic lesions and pycnidia incidence (Fig. 1b, c). A summary of other CF parameters not displayed in Figure 2/3 are displayed in supplementary table S7a, b.

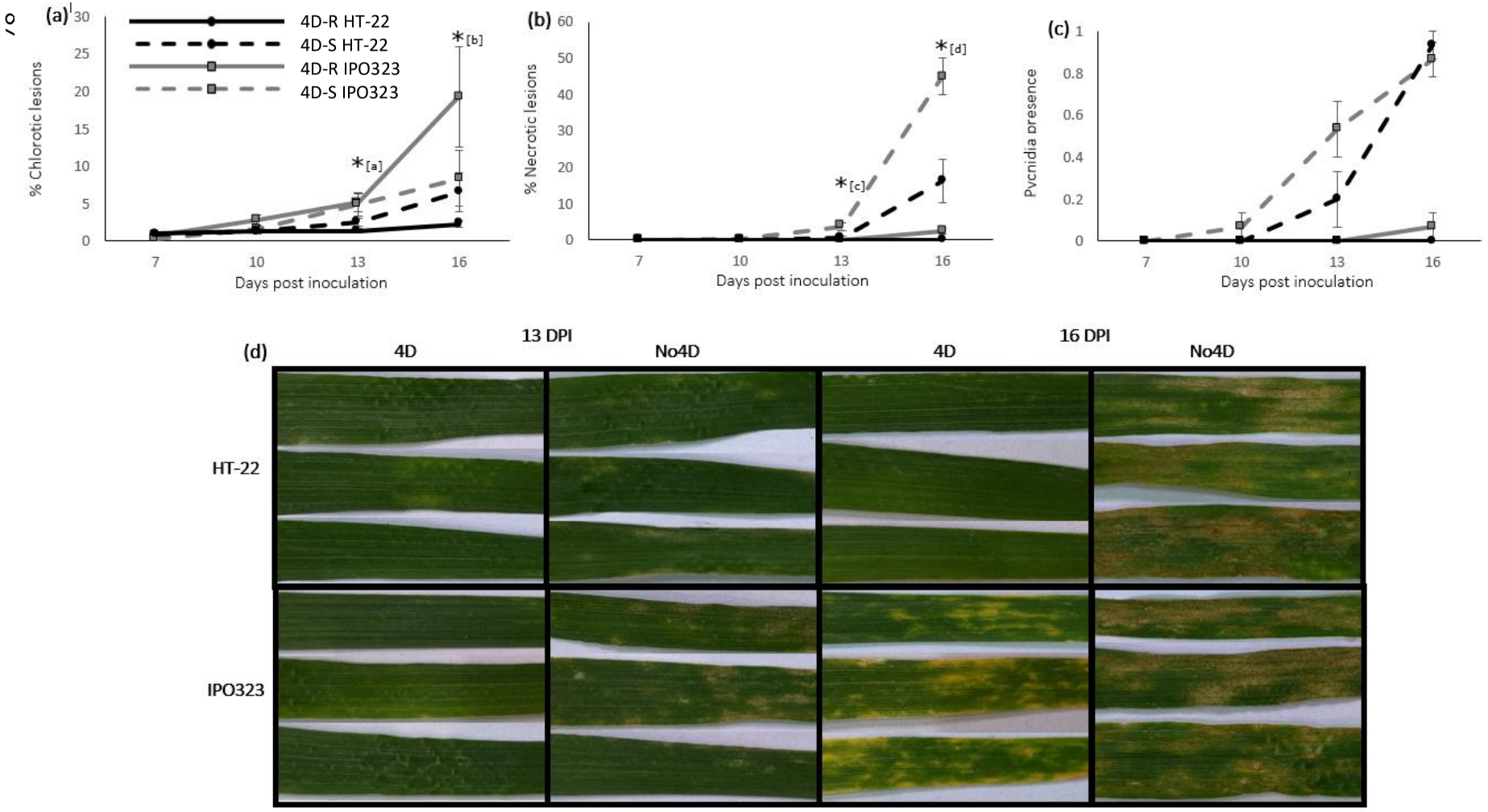



**Figure 1.** *Z.tritici* visual assessment of 4D-R & 4D-S NILs inoculated with HT-22 or IPO323. (a) % Chlorotic lesion area coverage, (b) % Necrotic lesion area coverage, (c) Pycnidia incidence, (d) Disease symptoms comparison. Data displayed are means of 4 biological replicates and analysed at each time point using Students T-test ($P < 0.05$). SE bars are shown

*[a] P=0.047, 4D-R<4D-S, HT-22
*[a] P=0.021, HT-22<IPO323, 4D-R
*[b] P=0.031, HT-22<IPO323, 4D-R
*[c] P=0.019 HT-22<IPO323, 4D-S
*[d] P<0.005 4D-R, P=0.003 4D-S (HT-22<IPO323)
*[d] P<0.001 4D-R<4D-S (HT-22 & IPO323)

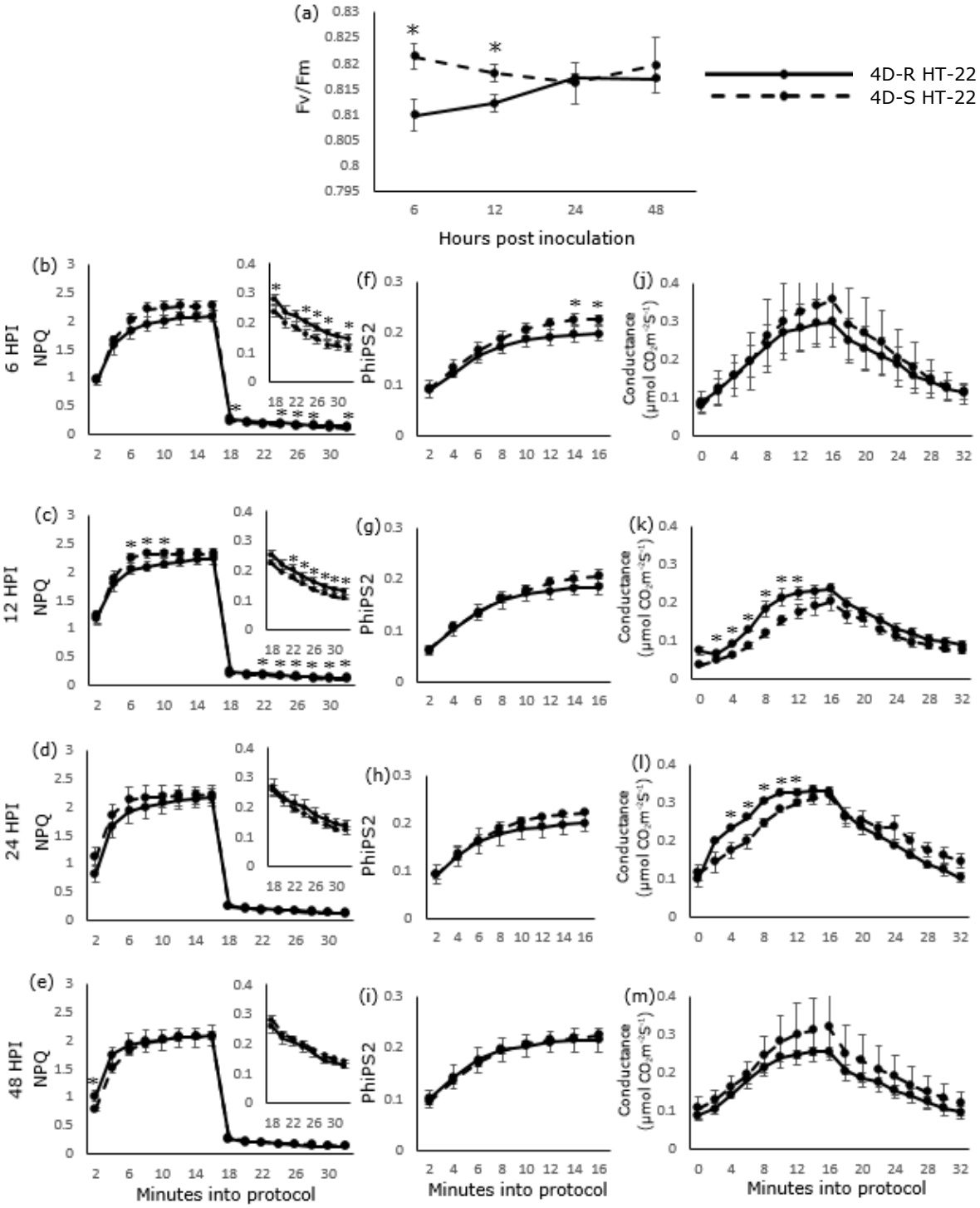



**Figure 2.** Chlorophyll fluorescence measurements for 4D-R and 4D-S NILs when inoculated by *Z.tritici* isolate HT-22. Measurements include Fv/Fm (a), NPQ (b-e), PhiPS2 (f-i) & Conductance (µmol $CO_2m^{-2}S^{-1}$)(J-m). Data displayed are means of 3 biological replicates. 4D v No4D comparison analysed at each timepoint using Students T-test ($P<0.05$). SE bars are shown.

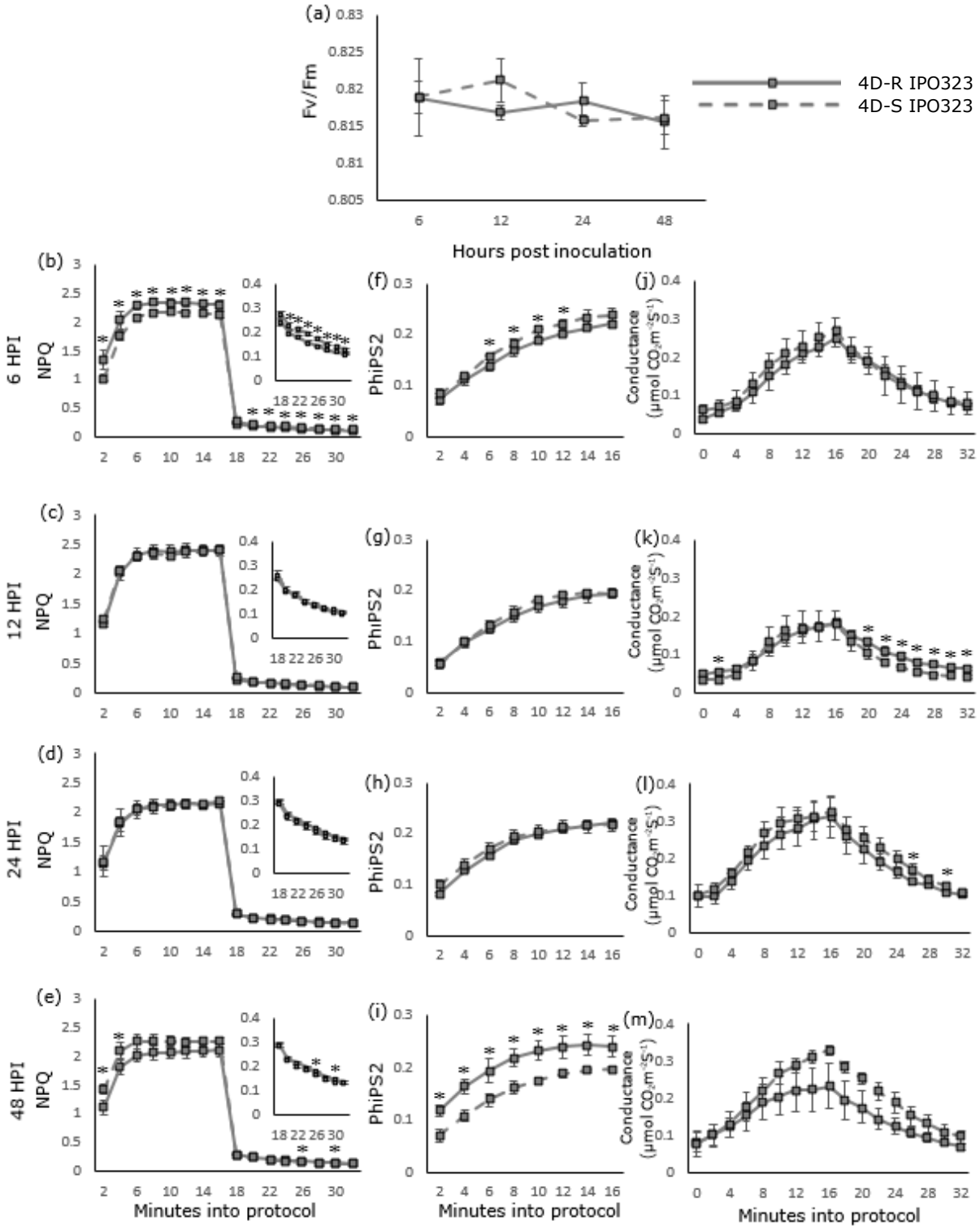



**Figure 3.** Chlorophyll fluorescence measurements for 4D-R and 4D-S NILs when inoculated by *Z.tritici* isolate IPO323. Measurements include Fv/Fm (a), NPQ (b-e), PhiPS2 (f-i) & Conductance (µmol $CO_2m^{-2}S^{-1}$)($J^{-m}$). Data displayed are means of 3 biological replicates. 4D v No4D comparison analysed at each timepoint using Students T-test ($P<0.05$). SE bars are shown.

### 3.2 Xanthophyll enzyme and hormone quantification

To determine the role of zeaxanthin and the xanthophyll cycle in the phenotypic differences displayed between *Z.tritici* isolates and 4D-R/S NILs, three major enzymes VDE (violaxanthin de-epoxidase), ZEP (zeaxanthin epoxidase) & NCED (9-cis-epoxycarotenoid dioxygenase) were quantified using qRT-PCRs on RNA used for the transcriptomic analysis (Fig. 4). VDE, which catalyses the conversion of violaxanthin to zeaxanthin, decreased in relative expression from 6 hpi to 11 dpi, however there were no differences between 4D-R/S NILs. ZEP, which catalyses the reverse reaction of violaxanthin to zeaxanthin, was downregulated after *Z.tritici* infection. ZEP expression increased in 4D-R compared to 4D-S when inoculated with HT-22 at 11 dpi. NCED expression increased between 6 and 11dpi in 4D-R NILs in response to both isolates and was significantly upregulated in 4D-R compared to 4D-S at 11 dpi when inoculated with HT-22. There was no significant effect of compatibility on VDE, ZEP or NCED expression.

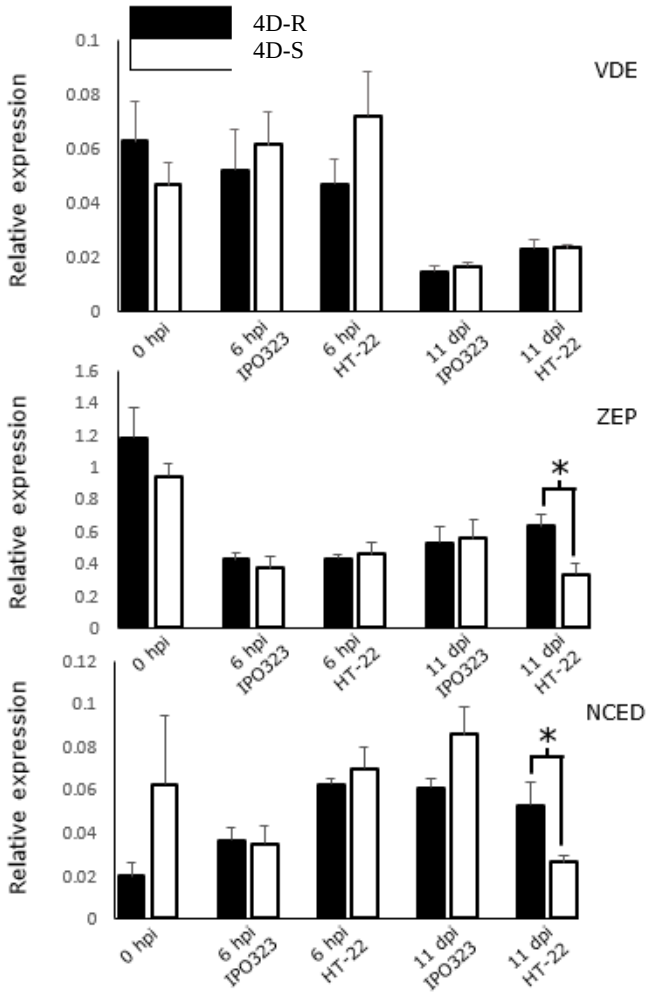



**Figure 4.** Relative expression qRT-PCRs for VDE (violaxanthin de-epoxidase), ZEP (zeaxanthin epoxidase) & NCED (9-cis-epoxycarotenoid dioxygenase) between 4D-R & 4D-S NILs at 0 hpi and infected with HT-22 or IPO323 at 6 hpi & 11 dpi. Data from 3 biological replicates and analysed by students T-test. Asterix indicates significance ($P<0.05$).

Hormone quantification demonstrated a decrease in GA4, ZR and ACC before *Z.tritici* infection in 4D-R NILs. In response to HT-22, SA increased at 6 hpi and in response to IPO323 SA decreased at 11 dpi (Table. 1). There was a significant impact of isolate for GA3, IPA and SA at 6 hpi, with decreased hormone levels in response to IPO323 compared to HT-22 independent of NIL. The only effect of compatibility was at 11 dpi whereby the 4D-R NIL had significantly lower SA content than 4D-S. (ANOVA tables displayed in supplementary Table 8a, b.)

**Table 1.** Hormone content of 4D-R & 4D-S NILs inoculated with HT-22 or IPO323. 4D-R & 4D-S lines infected by HT-22 or IPO323 are analysed using student T-tests. (Asterix indicates $P < 0.05$ between 4D-R/S) Effect of compatibility analysed using an ANOVA. Data are means of 3 biological replicates.

| Hormone | 0 hpi | | 6hpi | | | | 11 dpi | | | |
|---|---|---|---|---|---|---|---|---|---|---|
| (ng/g DW) | Water | | HT-22 | | IPO323 | | HT-22 | | IPO323 | |
| | 4D-R | 4D-S | 4D-R | 4D-S | 4D-R | 4D-S | 4D-R | 4D-S | 4D-R | 4D-S |
| ABA | 32.3 | 33.9 | 36.7 | 26.7 | 27.4 | 27.0 | 37.8 | 19.7 | 21.7* | 14.4* |
| SA | 1217.0 | 860.1 | 586.9* | 357.6* | 305.9 | 279.7 | 337.0 | 468.3 | 334.6* | 444.8* |
| JA | 1.7 | 2.2 | 4.7 | 3.5 | 2.2 | 4.3 | 4.6 | 65.0 | 63.7 | 73.3 |
| OPDA | 2.4 | 2.2 | 2.6 | 2.5 | 1.4 | 2.1 | 1.5 | 1.4 | 1.8 | 2.9 |
| Ja-Ile | 0.0 | 0.1 | 0.2 | 0.1 | 0.0 | 0.1 | 0.1 | 0.3 | 0.1 | 0.1 |
| IAA | 586.3 | 648.7 | 779.8 | 820.8 | 882.3 | 612.3 | 433.7 | 449.3 | 352.6 | 360.5 |
| GA1 | 187.7 | 126.2 | 198.3 | 126.9 | 164.4 | 206.8 | 478.9 | 69.6 | 98.1 | 346.2 |
| GA3 | 172.0 | 245.7 | 206.3 | 213.1 | 133.5 | 61.7 | 127.7 | 83.3 | 60.7 | 77.3 |
| GA4 | 521.0* | 900.3* | 954.8 | 919.3 | 833.7 | 1226.4 | 933.1 | 1209.1 | 1011.3 | 1166.6 |
| GA7 | 114.2 | 174.7 | 147.5 | 120.3 | 122.2 | 189.8 | 147.7 | 91.1 | 81.6 | 106.8 |
| ACC | 94.2* | 229.6* | 262.0 | 200.2 | 196.9 | 217.2 | 123.7 | 219.3 | 138.5 | 161.5 |
| Mel | 4.5 | 12.4 | 10.7 | 10.6 | 8.5 | 17.6 | 29.0 | 21.1 | 22.6 | 27.6 |
| IPA | 31.4 | 34.4 | 69.9 | 78.6 | 37.9 | 65.9 | 22.9 | 46.9 | 36.3 | 28.7 |
| 2iP | 3.0 | 3.5 | 3.9 | 4.8 | 4.1 | 6.1 | 4.8 | 10.5 | 8.7 | 6.8 |
| Z | 3.9 | 3.2 | 5.7 | 4.4 | 3.6 | 7.8 | 6.4 | 4.7 | 4.5 | 4.4 |
| ZR | 0.2* | 0.5* | 0.4 | 0.4 | 0.5 | 0.5 | 0.5 | 1.4 | 0.5 | 0.7 |

ABA; Abscisic acid, SA; Salicylic acid, JA; Jasmonic acid, OPDA; oxo-Phytodienoic acid, Ja-Ile; jasmonoyl-L-isoleucine, IAA; Indole-3-acetic acid, GA1, 3, 7; Gibberellin, ACC; 1-Aminocyclopropane 1-carboxylic acid, IPA; Indole-3-propionic acid, 2iP; 6-(γ,γ-Dimethylallylamino) purine, Z; Zeatin, ZR; zeatin riboside

## 3.3 Transcriptomic analysis of the conserved incompatible 4D-R interaction

To understand the conserved mechanism of resistance in 4D-R compared to 4D-S, consistently upregulated transcripts under both *Z.tritici* inoculations were investigated. 24 transcripts were consistently upregulated at 6 hpi and 33 at 11 dpi. 49 transcripts were consistently downregulated at 6 hpi with 23 downregulated at 11 dpi ($P < 0.05$, log10foldchange > 2). GO-term analysis demonstrated a downregulation of nucleotide and ribonucleotide binding, glutathione binding and ligase activity at 6 hpi (Fig. 5). At 11 dpi 4D-R increased ribonucleotide binding, and protein kinase activity with an increase in protein modification and metabolism (Fig. 5).

These transcripts were investigated in more depth to identify functions not characterised by the GO-term analysis (Table. 2). At 6 hpi, out of the 24 upregulated transcripts these included 11 transcripts associated with disease related proteins and/or protein kinases. This included 3 transcripts with predicted homology to RGA4/5 (Cesari *et al* 2013), as well as other protein kinases associated with hormone-mediated signalling such as INRPK1 (Bassett *et al* 2001) & ER1 (Shen *et al* 2015). Three transcripts were predicted to include F-box domains. Out of the 49 downregulated transcripts there were 19 disease related proteins and/or protein kinases. This included three transcripts with homology to RGA5, although these weren't predicted to have the NB-ARC domain present in the upregulated RGA5 transcripts (Cesari *et al* 2013). Additionally, transcripts with homology to RGA4 (Cesari *et al* 2013) and transcripts with NB-ARC domains were downregulated. Five transcripts associated with oxidoreductive processes were downregulated including two transcripts predicted to transcribe Cytochrome P450 proteins. Other downregulated transcripts included vesicle transport (VAMP711) (Sanderfoot *et al* 2000), transmembrane proteins, glutathione synthetase (GSH2) (Vira *et al* 2002) and Remorin protein (RM29) (Jarsch *et al* 2011) which is responsive to ABA.

At the switch to necrotrophy at 11 dpi 21/24 transcripts upregulated at 6 hpi remained upregulated (logfold > 2). The three transcripts uniquely expressed at 6 hpi encoded a sulfotransferase, cellulase and protein kinase domain. In addition to the consistently upregulated transcripts at both timepoints, at the switch to necrotrophy (11 dpi) 13 additional characterised transcripts were upregulated (Table. 3). Noteworthy transcripts included an additional F-box protein, two additional INRPK1 transcripts, disease related proteins including RGA4 and two oxidoreduction related transcripts. Out of the 49 downregulated transcripts at 6 hpi, 12 were also downregulated at 11 dpi, with 5 additional characterised transcripts

downregulated. Out of the 5 additional downregulated transcripts four were protein kinases and/or disease related proteins (XA21, SIT2, CRK6 & EIX2) (Park & Ronald 2012; Li *et al* 2014; Chern *et al* 2016; Ron & Avni *et al* 2014) with one F-box protein. The consistently downregulated transcripts included RGA4 (Cesari *et al* 2013), two NB-ARC domain proteins, Remorin protein (RM29) (Jarsch *et al* 2011), SIK1 & ER2 protein kinases (Xiong *et al* 2016; Zhang *et al* 2018), 4HBT, VAMP711 (Sanderfoot *et al* 2000), DUF3474 & Sntox1 (Liu *et al* 2012).

No photosynthetic/xanthophyll cycle related transcripts, which were differentially expressed in 4D-R/4D-S NILs, were consistent between isolates. However, there was upregulation of two separate transcripts which were predicted to encode for PsbR at 11 dpi in the 4D-R NIL. Timewise comparison of photosynthetic/xanthophyll cycle related transcripts in 4D-R identified three consistent transcripts in both HT-22 and IPO323 treatments. These included a PetF-ferredoxin which was downregulated from 0 to 6 hours, PsbQ which was upregulated from 0 to 6 hours and 11 days, and PsbW which was upregulated from 0 to 11 days.

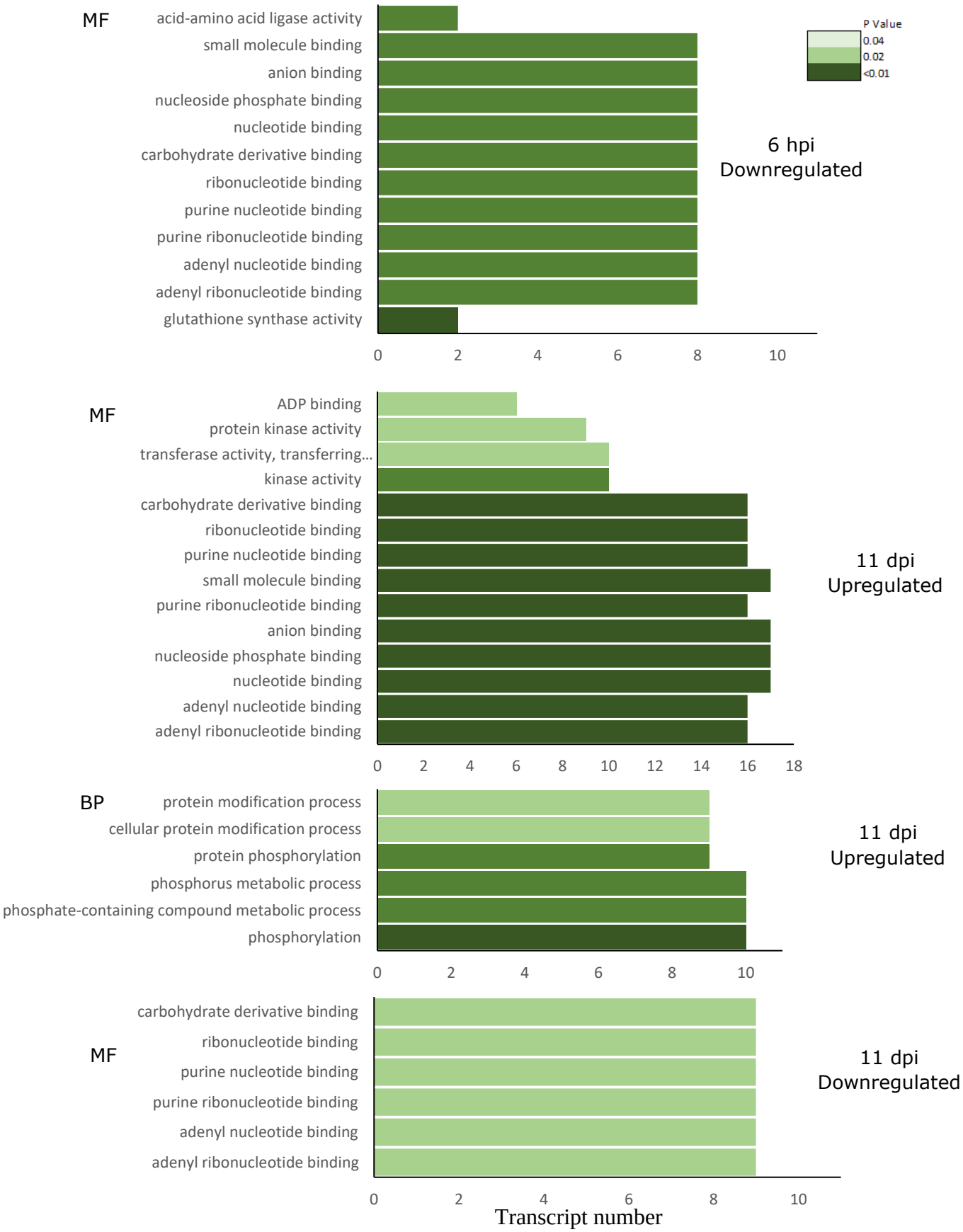



**Figure 5.** GO-term analysis of consistently differential expressed transcripts for both HT-22 and IPO323 inoculations for 4D-R compared to 4D-S. Only significant results are displayed. MF = molecular function, BP = Biological process.

**Table 2a**. Consistently upregulated transcripts in HT-22 and IPO323 treatments in 4D-R compared to 4D-S at 6 hpi. (log10foldchange > 2, P < 0.05). Predicted annotation from UniProtKB & Knetminer.

| Transcript | Predicted annotation | Predicted process | Average TPM | | Average |
|---|---|---|---|---|---|
| | | | 4D-R | 4D-S | logfoldchange |
| **4D-007600** | R3H & SUZ domain | RNA-binding | 757.0 | 0.2 | 11.6 |
| 1B-007100 | protein kinase, membrane binding | hormone-mediated signalling | 191.7 | 0.0 | 10.0 |
| 1B-011500 | DUF3339 domain | unknown | 188.5 | 0.0 | 10.0 |
| 7D-075000 | MED17 | regulated transcription l of RNA polymerase II-dependent genes | 175.5 | 0.2 | 9.5 |
| 7D-075100 | F-box domain | unknown | 82.5 | 0.0 | 8.9 |
| 1B-000100 | NB-ARC domain - RGA4 | disease resistant protein (gene-for-gene) | 73.5 | 0.0 | 8.7 |
| 1B-008500 | protein kinase, membrane binding | unknown | 50.8 | 0.0 | 8.1 |
| 1B-009000 | protein kinase, membrane binding | unknown | 50.2 | 0.0 | 8.1 |
| 1B-000200 | NB-ARC domain - RGA5 | disease resistant protein (gene-for-gene) | 39.6 | 0.0 | 7.8 |
| 4B-392400 | sulfotransferase, SOT1 | Sulfotransferase activity | 37.7 | 0.0 | 7.7 |
| 7D-074900 | NmrA domain - PCBER | Isoflavone reductase | 20.4 | 0.0 | 6.8 |
| 4B-387200 | PGG domain | unknown | 15.8 | 0.0 | 6.5 |
| 1B-007200 | SCF ubiquitin ligase complex - FBL14 F-box protein | unknown | 31.8 | 0.7 | 5.8 |
| 1B-006500 | protein kinase, membrane binding - ER1 | hormone-mediated signalling, thermal tolerance | 32.9 | 1.9 | 5.4 |
| **4D-006300** | protein kinase, membrane binding - INRPK1 | hormone-mediated signalling, photoperiod | 101.6 | 4.7 | 4.6 |
| 4B-396500 | Protein kinase | transmembrane receptor protein tyrosine kinase activity | 52.0 | 2.7 | 4.2 |
| 4D-004100 | protein kinase, membrane binding - RGA4 | hormone-mediated signalling | 216.8 | 12.7 | 4.2 |
| 7D-073400 | GDP-mannose | GDP-mannose metabolic process | 380.6 | 22.2 | 4.2 |
| 1B-007300 | SCF ubiquitin ligase complex - FBL14 - F-box protein | unknown | 128.3 | 11.2 | 3.5 |
| 1B-000800 | peroxisomal membrane | protein import into peroxisome matrix, docking | 2954.8 | 316.4 | 3.2 |
| 4D-003900 | protein kinase | unknown | 77.7 | 9.3 | 3.0 |
| 1B-016400 | cellulase domain | actin filament binding | 91.1 | 12.1 | 3.0 |

**Table 2b**. Consistently downregulated transcripts in HT-22 and IPO323 treatments in 4D-R compared to 4D-S at 6 hpi. (log10foldchange > 2, P < 0.05). Predicted annotation & process from UniProtKB & Knetminer.

| Transcript | Predicted annotation | Predicted process | Average TPM | | Average |
|---|---|---|---|---|---|
| | | | 4D-R | 4D-S | logfoldchange |
| 5D-559300 | cytochrome P450 - CYP71BE54 | oxidoreductase activity | 0.2 | 690.3 | -11.4 |
| 4B-393100 | Clp R domain-containing protein - CLPB1 | cellular response to heat | 0.0 | 387.9 | -10.9 |
| 1B-002900 | PIK-2 | disease resistant protein (gene-for-gene) | 0.0 | 308.6 | -10.7 |
| 5D-560100 | cytochrome P450 - CYP99A2 | oxidoreductase activity | 0.0 | 288.5 | -10.6 |
| **4D-007900** | LRRNT_2 domain - EIX2 | disease resistant protein (gene-for-gene) | 0.0 | 163.7 | -9.8 |
| 4D-002400 | AP2/ERF domain - RGA5 | DNA-binding, disease resistant protein (gene-for-gene) | 0.0 | 142.8 | -9.6 |
| 3A-150500 | chloroplast protein import - Tic22 | protein deubiquitination, transport | 0.0 | 135.8 | -9.5 |
| 1B-004100 | SnTox1 sensitivity protein | sensitivity to Tox1 necrotrophic effector | 0.6 | 310.6 | -9.5 |
| 5D-560200 | AAMT1I | methyltransferase involved in the biosynthesis of methyl anthranilate | 0.0 | 130.8 | -9.5 |
| 4D-002300 | RGA5 | disease resistant protein (gene-for-gene) | 0.0 | 95.0 | -9.0 |
| 7A-434300 | cysteine-rich receptor-like protein kinase 6 | benzothiadiazole-induced immune response. | 0.0 | 77.1 | -8.7 |
| 3A-195800 | Myb_DNA-bind_3 domain | DNA-binding | 0.0 | 75.0 | -8.6 |
| 5D-560500 | NB-ARC domain | disease resistant protein | 0.0 | 45.2 | -7.9 |
| 5D-547100 | RGA4 | disease resistant protein (gene-for-gene) | 0.0 | 36.5 | -7.6 |
| 4B-393000 | remorin protein - RM29 | response to abscisic acid | 0.0 | 33.8 | -7.5 |
| 7A-411100 | remorin protein - RM29 | cytokinin-activated signaling, response to abscisic acid | 0.0 | 31.0 | -7.3 |
| 4D-008000 | GDSL esterase/lipase - AAE | auxin signalling | 1.3 | 137.4 | -7.2 |
| 7B-216200 | 4HBT domain | phylloquinone biosynthetic process, lipid metabolic process | 0.0 | 26.9 | -7.2 |
| 5D-547300 | serine/threonine-protein kinase - SIK1 | defence response | 0.0 | 21.5 | -6.8 |
| 7B-038400 | AT15 | N-acyltransferase activity, cell wall biosynthesis | 0.0 | 19.0 | -6.7 |
| 1B-009800 | protein kinase, membrane binding - ER2 | hormone-mediated signalling | 0.2 | 27.7 | -6.6 |
| 1B-002800 | NB-ARC domain | disease resistant protein | 0.0 | 18.5 | -6.6 |
| 4B-387600 | protein kinase domain - CHARK | defense response to bacterium, cytokinin signalling | 0.0 | 17.7 | -6.5 |
| 7A-442600 | unknown | glutathione synthase | 0.2 | 24.2 | -6.5 |
| 4B-383800 | Inositol-pentakisphosphate 2-kinase | inositol phosphate biosynthetic process | 0.0 | 17.3 | -6.5 |
| 7B-038300 | rieske domain | chlorophyllide a oxygenase activity | 18.6 | 1206.7 | -6.3 |
| 7A-434400 | ternary complex factor MIP1 | metal ion binding | 0.0 | 13.9 | -6.2 |
| 7B-195400 | DUF3474 domain | oxidoreductase activity | 3.1 | 165.2 | -5.9 |
| 7A-136300 | vesicle-associated membrane protein - VAMP711 | vesicle-mediated transport | 4.2 | 215.6 | -5.8 |
| 7A-442500 | glutathione synthetase - GSH2 | glutathione synthetase | 3.0 | 116.9 | -5.7 |
| 7A-392700 | transmembrane protein 230 | integral component of membrane | 1.1 | 34.4 | -5.7 |
| 5D-556400 | pentatricopeptide repeat-containing protein - OGR1 | mitochondrial electron transport | 5.7 | 69.4 | -3.6 |
| **4D-007400** | protein kinase - MSL1 | unknown | 28.1 | 308.7 | -3.5 |
| 7B-185600 | RER1 | protein retention in ER lumen | 25.7 | 176.6 | -2.8 |
| 5D-557700 | RGA5 | disease resistant protein (gene-for-gene) | 12.0 | 64.9 | -2.6 |
| 4B-387800 | THO1 | generation of functional messenger ribonucleoproteins (mRNPs) | 42.2 | 222.4 | -2.4 |
| 7B-130200 | protein kinase | phosphotransferase activity | 55.3 | 273.7 | -2.3 |
| 4B-392700 | small nuclear ribonucleoprotein Sm D3 | spliceosomal snRNP assembly | 134.8 | 528.8 | -2.0 |

**Table 3a**. Consistently upregulated transcripts in HT-22 and IPO323 treatments in 4D-R compared to 4D-S at 11 dpi. (log10foldchange > 2, P < 0.05). Predicted annotation & process from UniProtKB & Knetminer.

| Transcript | Predicted annotation | Predicted process | Average TPM | | Average |
|---|---|---|---|---|---|
| | | | 4D-R | 4D-S | logfoldchange |
| 1B-007100 | protein kinase, membrane binding | hormone-mediated signalling | 510.3 | 0.2 | 10.9 |
| 1B-008500 | protein kinase, membrane binding | unknown | 206.0 | 0.0 | 10.0 |
| **4D-007600** | R3H, SUZ domain | RNA-binding | 819.5 | 0.8 | 9.9 |
| 7D-075000 | MED17 | regulated transcription l of RNA polymerase II-dependent genes | 185.6 | 0.2 | 9.4 |
| 1B-011500 | DUF3339 domain | unknown | 75.7 | 0.0 | 8.6 |
| 7D-075100 | F-box domain | unknown | 56.2 | 0.0 | 8.1 |
| 1B-000100 | NB-ARC domain - RGA4 | disease resistant protein (gene-for-gene) | 52.4 | 0.0 | 8.1 |
| 1B-000200 | NB-ARC domain - RGA5 | disease resistant protein (gene-for-gene) | 46.1 | 0.0 | 7.9 |
| 4B-391900 | FAD-binding PCMH-type domain | oxidoreductase activity | 25.8 | 0.0 | 6.9 |
| 1B-009100 | LRRNT_2 domain - ER2 | unknown | 22.7 | 0.0 | 6.9 |
| 4D-004200 | Unknown | DNA transcription regulation | 47.8 | 0.4 | 6.7 |
| 1B-009000 | protein kinase, membrane binding | unknown | 119.5 | 1.6 | 6.5 |
| 4D-004100 | protein kinase, membrane binding - RGA4 | hormone-mediated signalling | 528.5 | 7.0 | 6.2 |
| 1B-006500 | protein kinase, membrane binding - ER1 | hormone-mediated signalling, thermal tolerance | 135.9 | 2.1 | 6.1 |
| 7D-074900 | NmrA domain - PCBER | isoflavone reductase | 12.3 | 0.0 | 6.0 |
| **4D-006400** | glycosyltransferase | glycosyltransferase activity | 9.9 | 0.0 | 5.6 |
| 1B-007200 | SCF ubiquitin ligase complex - FBL14 - F-box protein | unknown | 31.9 | 0.9 | 5.2 |
| 1D-001500 | protein kinase, membrane binding - INRPK1 | hormone-mediated signalling, photoperiod | 58.6 | 3.0 | 5.0 |
| 4D-006300 | protein kinase, membrane binding - INRPK1 | hormone-mediated signalling, photoperiod | 203.6 | 7.2 | 4.9 |
| 5D-559100 | NB-ARC domain | disease resistant protein | 20.1 | 1.2 | 4.9 |
| 4B-387200 | PGG domain | unknown | 24.0 | 0.9 | 4.8 |
| 1B-007400 | protein kinase, membrane binding - INRPK1 | hormone-mediated signalling, photoperiod | 107.3 | 4.3 | 4.6 |
| 1A-444300 | nucleoside diphosphate kinase - NDK4 | nucleoside diphosphate phosphorylation | 24.9 | 1.6 | 4.1 |
| 4B-396500 | protein kinase | transmembrane receptor protein tyrosine kinase activity | 27.1 | 1.8 | 4.0 |
| 1A-442200 | Flavonoid 3'-monooxygenase - YP75B1 | oxidoreduction process | 97.4 | 7.7 | 3.7 |
| 1B-007300 | SCF ubiquitin ligase complex - FBL14 - F-box protein | unknown | 108.7 | 9.2 | 3.6 |
| 4B-005100 | RGA4 | disease resistant protein (gene-for-gene) | 67.5 | 5.9 | 3.5 |
| 7D-073400 | GDP-mannose | GDP-mannose metabolic process | 426.9 | 48.6 | 3.1 |
| 1B-000800 | peroxisomal membrane | protein import into peroxisome matrix, docking | 3063.6 | 372.3 | 3.0 |
| 3B-474400 | protein kinase, membrane binding - NORK | detection of symbiotic bacterial/fungi | 59.2 | 12.8 | 2.3 |
| 2A-000100 | polycomb group (PcG) protein - EMF2B | histone methylation | 151.7 | 31.6 | 2.3 |
| 1B-008600 | SCF ubiquitin ligase complex - FBL14 - F-box protein | unknown | 59.3 | 13.2 | 2.2 |

**Table 3b**. Consistently downregulated transcripts in HT-22 and IPO323 treatments in 4D-R compared to 4D-S at 11 dpi. (log10foldchange > 2, P < 0.05). Predicted annotation & process from UniProtKB & Knetminer.

| Transcript | Predicted annotation | Predicted process | Average TPM | | Average |
|---|---|---|---|---|---|
| | | | 4D-R | 4D-S | logfoldchange |
| 5D-547300 | serine/threonine-protein kinase - SIK1 | defence response | 0.0 | 256.7 | -9.8 |
| 5D-547400 | protein kinase - XA21 | disease resistant protein (gene-for-gene) | 0.0 | 125.5 | -8.8 |
| 7B-216200 | 4HBT domain | phylloquinone biosynthetic process, lipid metabolic process | 0.0 | 39.9 | -7.8 |
| 1B-009800 | protein kinase, membrane binding - ER2 | hormone-mediated signalling | 2.8 | 380.6 | -7.5 |
| 5D-560500 | NB-ARC domain | disease resistant protein | 0.0 | 31.3 | -7.5 |
| 7A-136300 | vesicle-associated membrane protein - VAMP711 | vesicle-mediated transport | 2.1 | 314.4 | -7.1 |
| 4B-393000 | remorin protein - RM29 | response to abscisic acid | 0.4 | 43.7 | -7.0 |
| 5D-547100 | RGA4 | disease resistant protein (gene-for-gene) | 0.3 | 47.2 | -6.9 |
| 5D-546700 | protein kinase - SIT2 | regulator of salt stress | 0.0 | 20.5 | -6.8 |
| 7A-434100 | protein kinase - CRK6 | defence response | 0.7 | 38.7 | -6.3 |
| 4B-392900 | F-box protein | unknown | 0.9 | 35.1 | -6.1 |
| 7A-411100 | RR29 - remorin protein | cytokinin-activated signaling, response to abscisic acid | 0.7 | 27.0 | -5.8 |
| 1B-004900 | LRRNT_2 domain - EIX2 | disease resistant protein (gene-for-gene) | 0.7 | 39.6 | -5.8 |
| 1B-002800 | NB-ARC domain | disease resistant protein (gene-for-gene) | 0.7 | 25.9 | -5.8 |
| 7B-195400 | DUF3474 domain | oxidoreductase activity | 5.2 | 220.9 | -5.4 |
| 1B-004100 | SnTox1 sensitivity protein | sensitivity to Tox1 necrotrophic effector | 23.9 | 593.9 | -4.7 |
| 5D-557700 | RGA5 | disease resistant protein (gene-for-gene) | 23.2 | 108.3 | -2.3 |

### 3.4 Transcriptomic analysis of the differential response of 4D-R to HT-22 and IPO323

Due to differences in visual phenotype, chlorophyll fluorescence measurements, hormone composition and xanthophyll enzyme expression we expect differences in 4D-Rs response to HT-22 and IPO323 despite both being incompatible interactions. At 6 hpi, 88 transcripts were consistently upregulated and 88 were downregulated in response to HT-22 (Fig. 6). In response to IPO323, 42 transcripts were significantly upregulated in 4D-R compared to 4D-S NILs with 62 downregulated transcripts in response to IPO323 (Fig. 7). GSEA analysis demonstrated differences between HT-22 and IPO323 incompatible interactions. In response to HT-22 there was differential expression of transcripts associated with: detoxification, Alcohol catabolic process, stomatal complex development, auxin regulation, Protein import, molybdopterin metabolism and oxidoreductase activity (Fig. 10). In response to IPO323 there was differential expression of transcripts associated with: dephosphorylation, thiamine synthesis, Peroxisome import, Auxin synthesis and GTP synthesis (Fig. 11). GO term analysis was not suitable at 6 hpi due to the low number of significant GO terms (Fig.8/9).

At 11 dpi 495 transcripts were significantly upregulated in 4D-R compared to 4D-S NILs with 956 downregulated transcripts in response to HT-22 (Fig. 6). In response to IPO323 354 transcripts were significantly upregulated in 4D-R compared to 4D-S NILs and 98 were downregulated (Fig. 7). GSEA analysis highlighted differential expression of transcripts associated with: Hydroxy Behenoyl COA dehydratase activity, nitrate metabolism, Rho GTPase binding and protein kinase activity in response to HT-22. In response to IPO323 there was differential expression of Alpha 12 fucosyltransferase activity, defence response to fungus, Chitinase activity and protein import into mitochondrial membrane. A detailed breakdown of transcripts contributing towards GSEA significance is provided in supplementary table S9a. GO term analysis gave similar results to the GSEA analysis (Fig. 8/9).

Due to large differences in the photoprotective processes as shown by chlorophyll fluorescence measurements, transcripts unique to each incompatible interaction related to PSII, photoprotection and xanthophylls were investigated in more depth.

In the incompatible 4D-R/S HT-22 interaction there was no differential expression of photosynthetic related transcripts at 6 hpi. However, at 11 dpi in the 4D-R NIL compared to the 4D-S NIL there was upregulation of transcripts predicted to encode PNSL1/PsbP, PsbQ, PsbR, Lhca1 and Lhcb1&3. In addition to pairwise comparison of 4D-R and 4D-S NILs,

transcripts differentially expressed between time points in the 4D-R NIL but not the 4D-S NIL were also investigated. From 0 hours to 6 hours post inoculation with HT-22, 4D-R had reduced expression of a transcript associated with Psb28, whilst 2 transcripts associated with PsbW & PsbQ were upregulated. From 6 hours to 11 days there was an upregulation of many photosynthetic related transcripts including: PsbR, PsbP, PsaN, PetC, PetH, lhcb7, lhca1, lhcb3. Investigation of xanthophyll related transcripts showed that from 0 hours to 6 hours transcripts associated with NCED2 & VDE were downregulated at 6 hours, suggesting potential accumulation of neoxanthin and violaxanthin. However, from 6 hours to 11 days the transcript associated with NCED2 increased, suggesting potential accumulation of ABA.

In the incompatible 4D-R/S IPO323 interaction there was no differential expression of photosynthetic related transcripts at 6 hpi. However, at 11 dpi 4D-R downregulated four transcripts associated with Lhcb1.1 expression and three transcripts for CRD1 which is involved in chlorophyll synthesis. In addition to pairwise comparison of 4D-R and 4D-S NILs, transcripts differentially expressed between time points in the 4D-R NIL but not the 4D-S NIL were also investigated. From 0 to 6 hours post inoculation 4D-R downregulated four transcripts including PsaF, PsbZ & lhcb3. From 6 hours to 11 days four transcripts associated with PsbQ were downregulated as well as one for Lhcb4. Investigation of xanthophyll related transcripts highlighted a decreased in phytoene synthesis from 0 to 6 hours and 11 days. From 0 – 11 days a transcript associated with the synthesis of strigol from β-carotene decreased, suggesting potential accumulation of β-carotene.

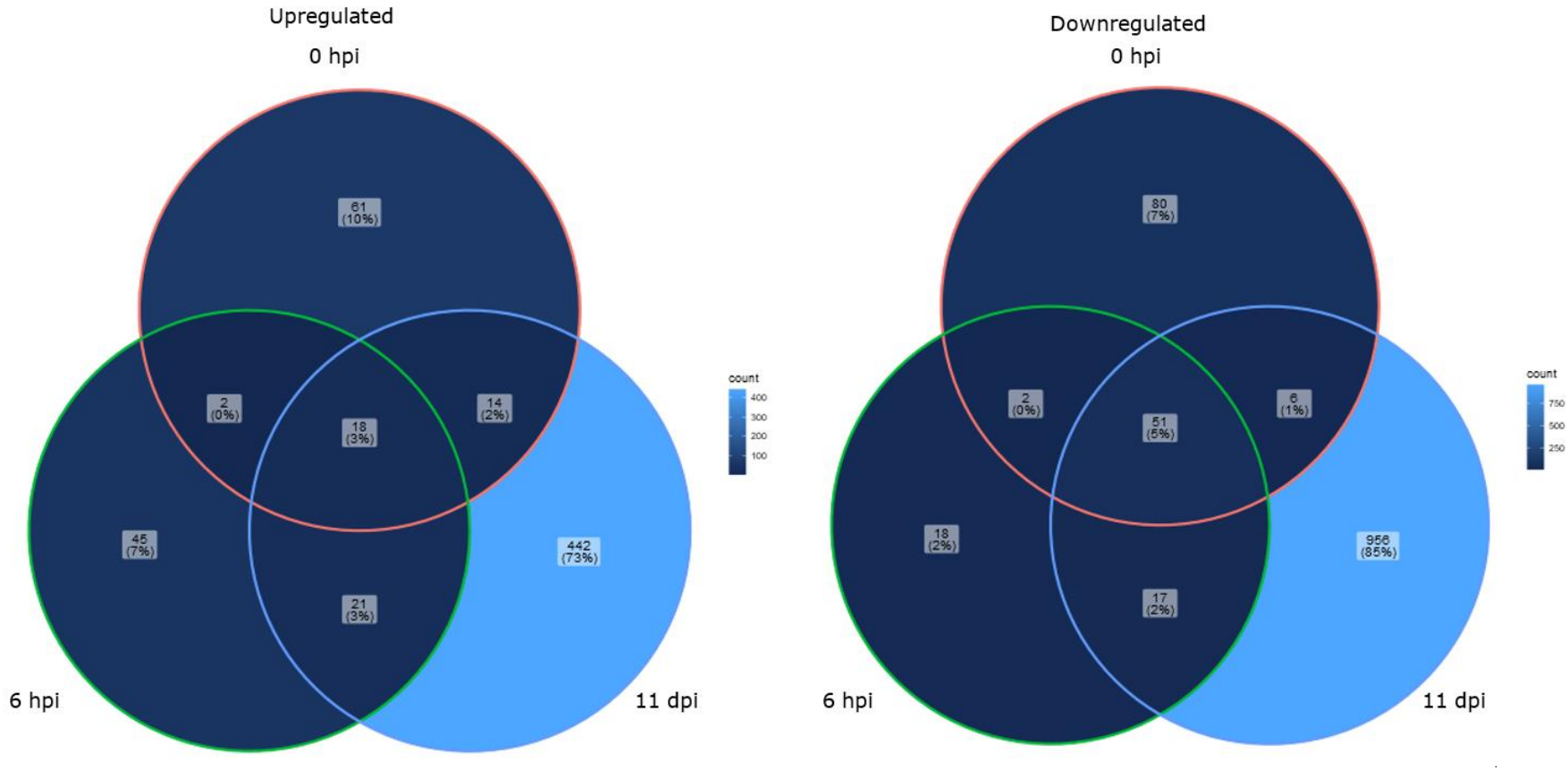



**Figure 6.** Pairwise comparison of 4D-R & 4D-S NILs inoculated with HT-22 at 0 hpi, 6 hpi and 11 dpi. Venn diagrams display differentially expressed transcripts.

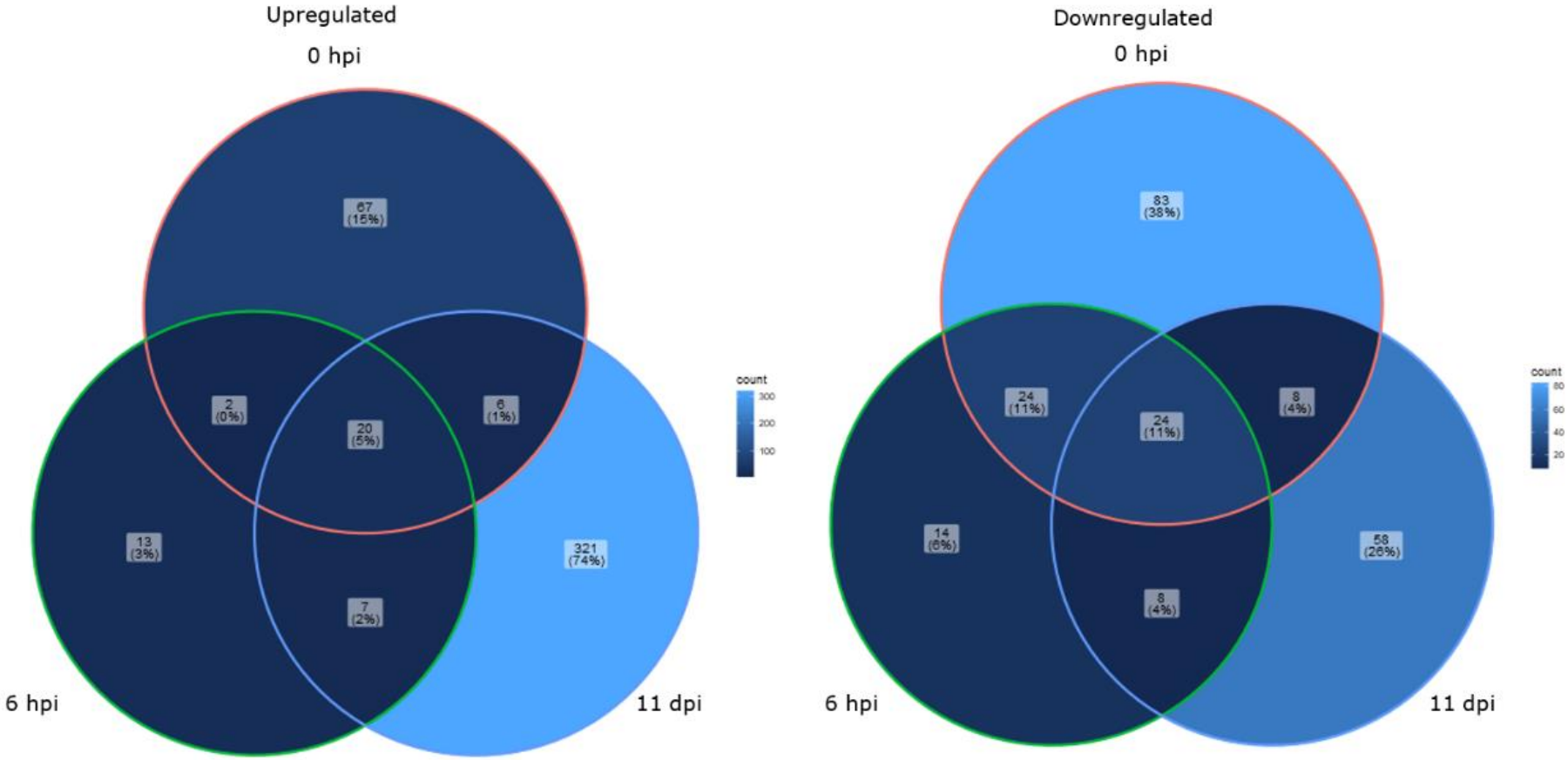



**Figure 7.** Pairwise comparison of 4D-R & 4D-S NILs inoculated with IPO323 at 0 hpi, 6 hpi and 11 dpi. Venn diagrams display differentially expressed transcripts.

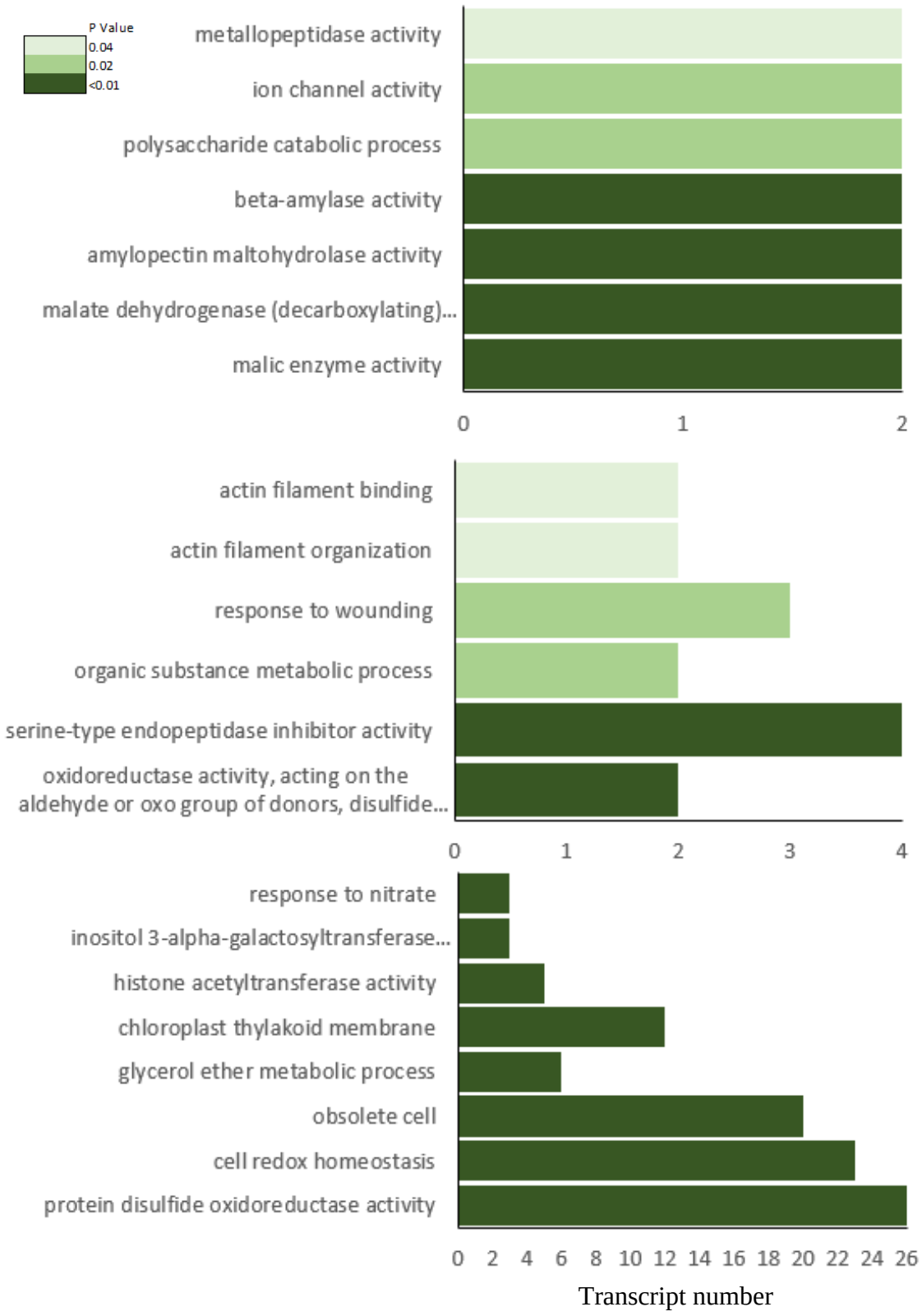



**Figure 8.** Pairwise comparison of 4D-R & 4D-S at 0 hpi (Top), and when inoculated with HT-22 at 6 hpi (Middle) and 11 dpi (Bottom). Top significant GO terms shown.

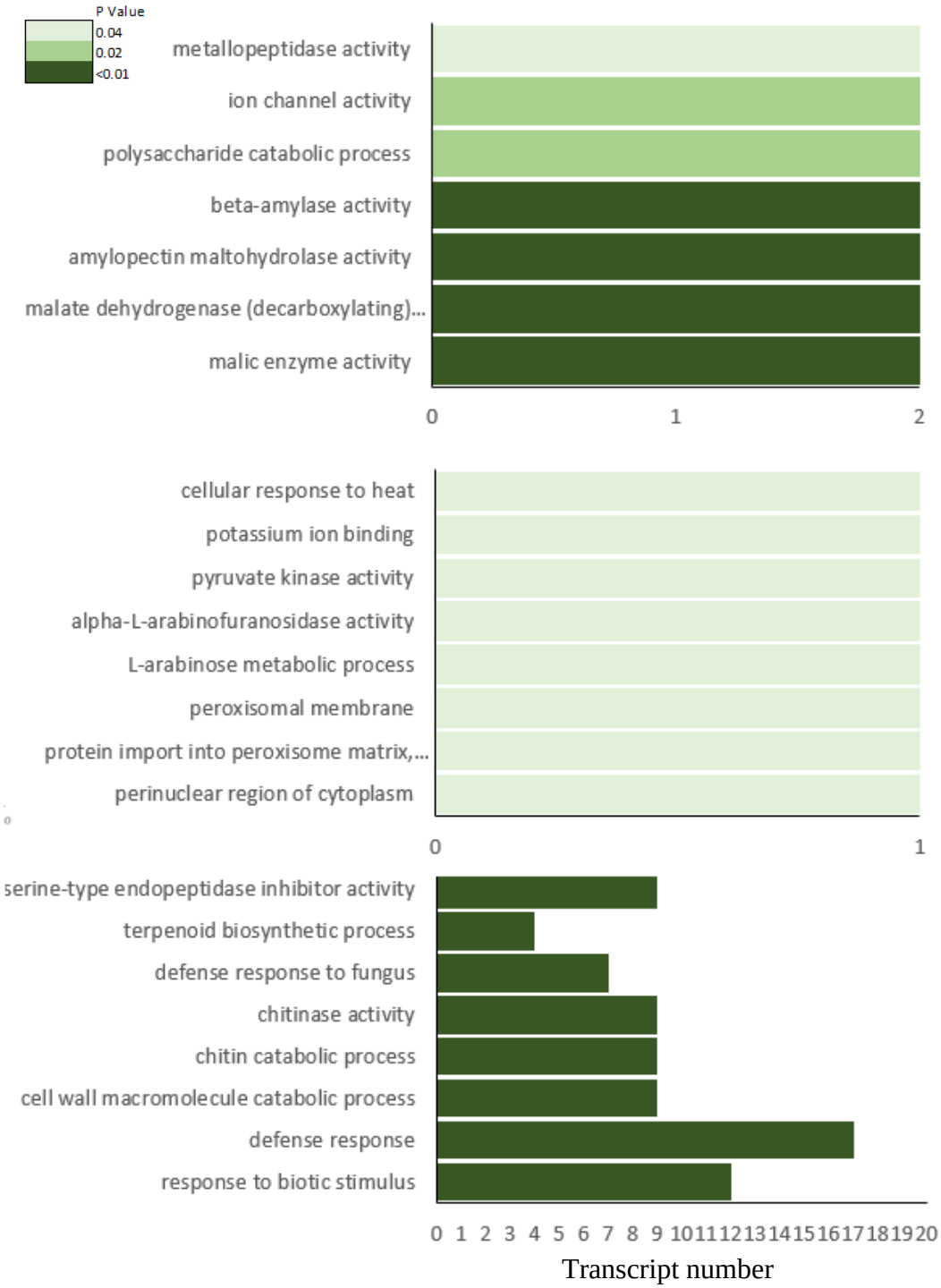



**Figure 9.** Pairwise comparison of 4D-R & 4D-S at 0 hpi (Top), and when inoculated with IPO323 at 6 hpi (Middle) and 11 dpi (Bottom). Top significant GO terms shown.

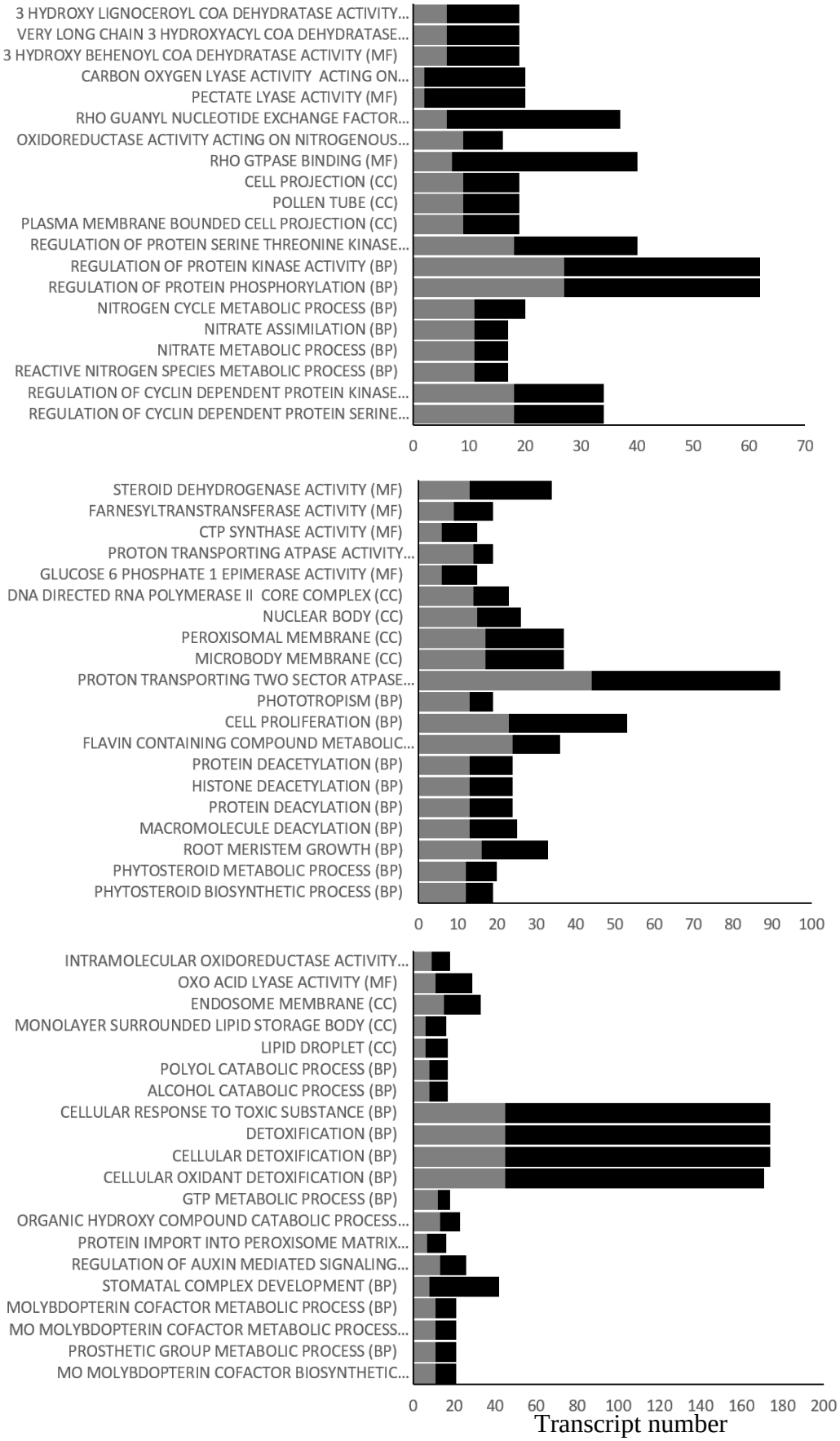



**Figure 10.** Pairwise comparison of 4D-R & 4D-S at 0 hpi (Top), and when inoculated with HT-22 at 6 hpi (Middle) and 11 dpi (Bottom). Top 20 significant GSEA terms shown. Grey = Number of contributing transcripts towards significance. Black = Number of transcripts not contributing towards significance.

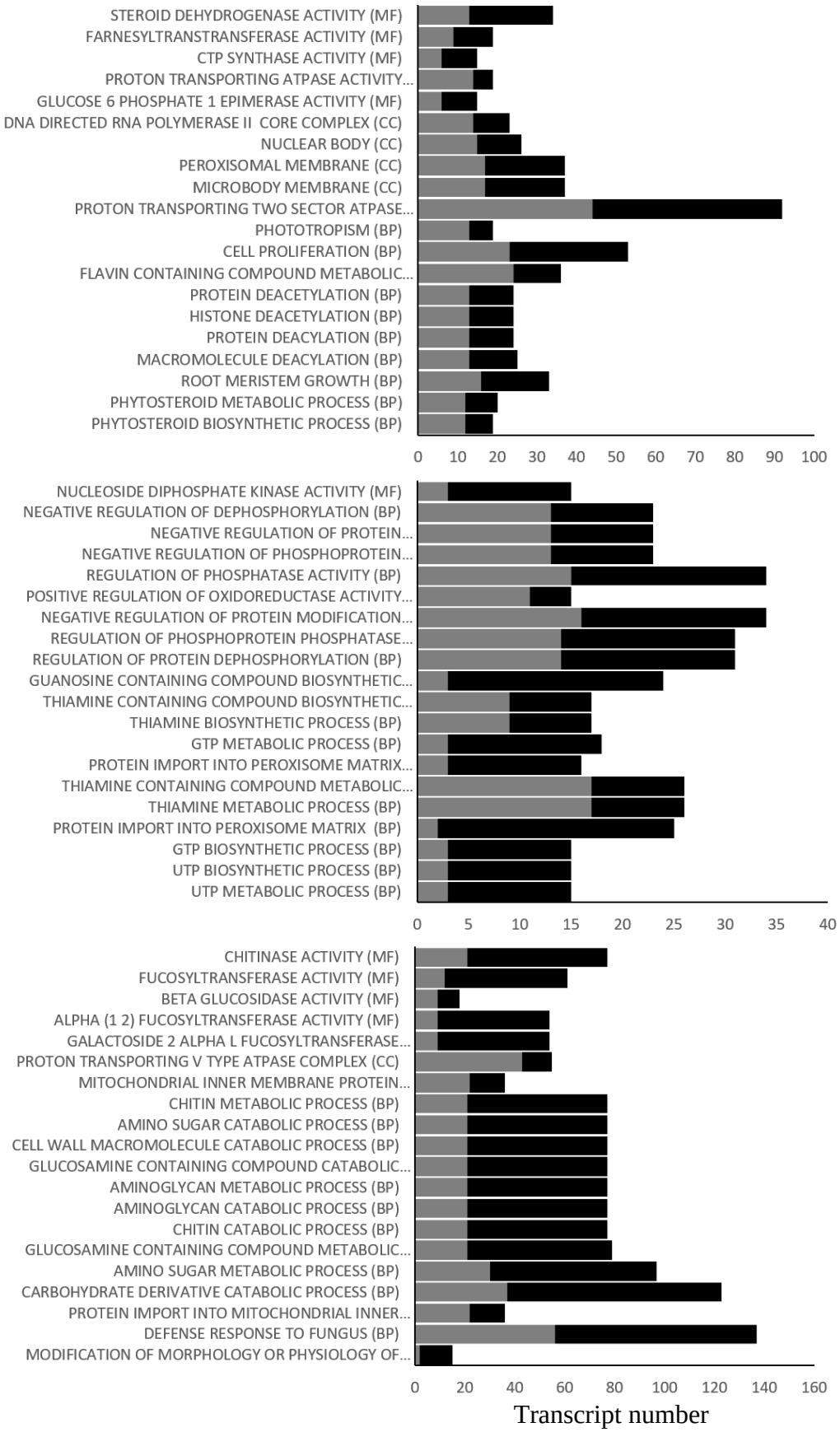



**Figure 11.** Pairwise comparison of 4D-R & 4D-S at 0 hpi (Top), and when inoculated with IPO323 at 6 hpi (Middle) and 11 dpi (Bottom). Top 20 significant GSEA terms shown. Grey = Number of contributing transcripts towards significance. Black = Number of transcripts not contributing towards significance.

### 3.5 Transcriptomic analysis of *Z.tritici* isolates HT-22 & IPO323

Mycgr3T111412 (uncharacterised, upregulated in 4D) & Mycgr3T103215 (HSP104, downregulated in 4D) were the only 2 differentially expressed transcripts in the 4D-R/S comparison at 6 hpi, which was in the HT-22 treatment. At 11 dpi no *Z.tritici* transcripts were upregulated in the 4D-R NIL. 1226 transcripts were downregulated in HT-22 in the interaction with 4D-R compared to 4D-S and 68 for IPO323, with 64 of those transcripts common with HT-22 (Fig. 12).

GO analysis of the 64 consistently upregulated transcripts for both HT-22 & IPO323 on 4D-S NILs compared to 4D-R NILs were weighted towards ribosomal processes and translation (Fig. 12). 6/20 of the top differentially expressed transcripts were characterised with 33/64 total transcripts characterised (Table 4). 15 transcripts encoded for ribosomal proteins. There was 4 transcripts involved in protein folding and processing, 4 peptidases, 2 FAD-binding and 2 helicases. Other transcripts included LysM domain effectors, glutamine synthetase, ammonium transport, Acetoacetyl-CoA reductase and glycosidase.

GO term analysis of differentially expressed transcripts unique to HT-22 on the susceptible NIL (4D-S) showed an upregulation of protein synthesis processes such as ribosome synthesis and translation and initiation (Fig. 12). There were also transcripts associated with mitochondria and carbohydrate metabolism. 17/20 of the top differentially expressed transcripts unique to HT-22 were uncharacterised (Table. 3). Amongst the top 20 characterised transcripts for HT-22 there were 5 Permease transcripts, 4 sugar transport, 3 hydrolases and transcripts involved in iron transport, FAD binding, Cytochrome P450, Peptidase, Transferase, Protease & catalytic activity. Of the 4 transcripts unique to IPO323 and upregulated in the 4D-S NIL compared to 4D-R Mycgr3T104028 was the only characterised protein (rps7, 40S ribosomal protein) (Table. 4).

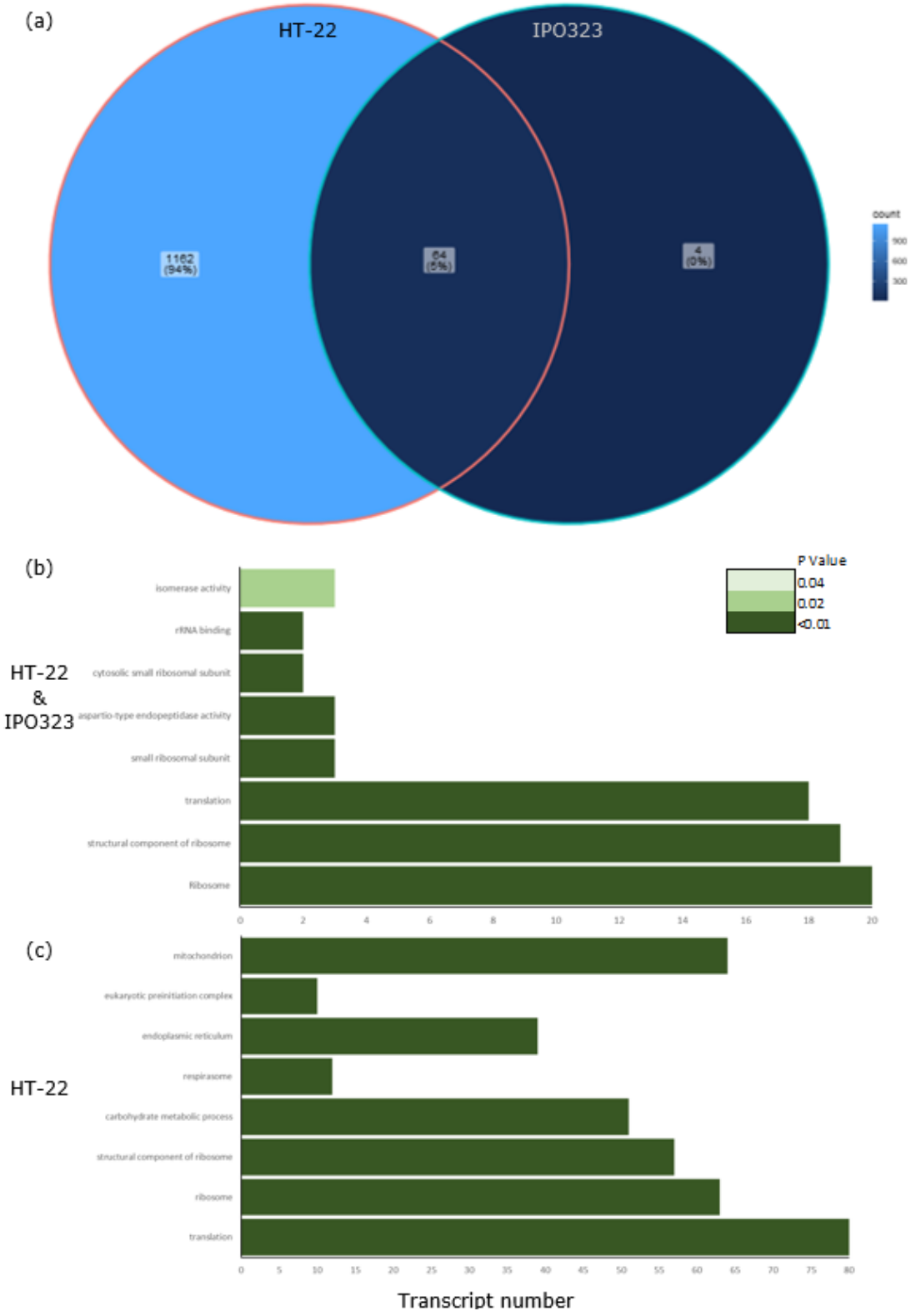



**Figure. 12.** Pairwise comparison of *Z.tritici* transcript expression at 11 dpi in 4D-S compared to 4D-R. Venn diagram display differentially upregulated transcripts (a). GO terms for HT-22 (c) & consistent GO terms between both isolates (b) are displayed.

**Table. 4.** Top 20 downregulated *Z.tritici* HT-22 and IPO323 transcripts at 11 dpi in 4D-R NILs compared to 4D-S NILs.

| | Transcript | Annotation | Effector | Localised | Biological process | TPM | | B-Value |
|---|---|---|---|---|---|---|---|---|
| | | | | | | 4D | No4D | |
| HT-22 | Mycgr3T91471 | Uncharacterised protein | Apoplastic | - | - | 0 | 399 | 8.1 |
| | Mycgr3T109777 | Uncharacterised protein | - | - | - | 0 | 323 | 8.1 |
| | Mycgr3T91662 | Uncharacterised protein | Cytoplasmic | - | - | 0 | 225 | 7.5 |
| | Mycgr3T107758 | Uncharacterised protein | Cytoplasmic | - | - | 0 | 39 | 7.4 |
| | Mycgr3T108482 | Uncharacterised protein | - | - | - | 0 | 87 | 7.3 |
| | Mycgr3T105825 | Uncharacterised protein | Apoplastic | - | - | 0 | 153 | 7.0 |
| | Mycgr3T105151 | Uncharacterised protein | - | - | - | 0 | 203 | 6.9 |
| | Mycgr3T102792 | Uncharacterised protein | Cytoplasmic | Nucleus | - | 1 | 544 | 6.6 |
| | Mycgr3T96951 | Uncharacterised protein | - | - | - | 0 | 23 | 6.3 |
| | Mycgr3T65946 | permease protein (put4) | - | - | Transport | 0 | 17 | 6.3 |
| | Mycgr3T80260 | Uncharacterised protein | - | - | - | 0 | 39 | 6.3 |
| | Mycgr3T103900 | Uncharacterised protein | Apoplastic/cytoplasmic | | - | 0 | 43 | 6.3 |
| | Mycgr3T97034 | Uncharacterised protein | Cytoplasmic | | - | 0 | 105 | 6.3 |
| | Mycgr3T92614 | Uncharacterised protein | - | - | - | 0 | 11 | 6.2 |
| | Mycgr3T73589 | MFS glucose transporter (HGT1) | - | - | Transport | 0 | 8 | 6.1 |
| | Mycgr3T90089 | Uncharacterised protein | Cytoplasmic | Chloroplast/Nucleus | - | 1 | 211 | 5.9 |
| | Mycgr3T105351 | Uncharacterised protein | - | - | - | 0 | 18 | 5.9 |
| | Mycgr3T95478 | Uncharacterised protein | Cytoplasmic | Nucleus | - | 0 | 31 | 5.7 |
| | Mycgr3T107565 | Beta-mannosidase A (mndA) | - | - | Metabolism | 0 | 2 | 5.6 |
| | Mycgr3T39797 | permease protein (put4) | - | - | Transport | 0 | 3 | 5.5 |
| HT-22 & IPO323 | Mycgr3T38460 | oxidoreductase activity | - | - | Stress | 0 | 3 | 2.9 |
| | Mycgr3T88698 | Uncharacterised protein | Apoplastic/cytoplasmic | - | - | 1 | 11 | 2.7 |
| | Mycgr3T107601 | Pyr redox 2 domain containing protein | - | - | Stress | 0 | 2 | 2.6 |
| | Mycgr3T97235 | Uncharacterised protein | - | - | - | 0 | 2 | 2.6 |
| | Mycgr3T42709 | serine-type carboxypeptidase | - | - | Metabolism | 0 | 2 | 2.4 |
| | Mycgr3T105867 | Uncharacterised protein | Apoplastic | - | - | 2 | 16 | 2.4 |
| | Mycgr3T73144 | Ammonium transporter (amt1) | - | - | Transport | 0 | 2 | 2.4 |
| | Mycgr3T90420 | Uncharacterised protein | Apoplastic | - | - | 1 | 16 | 2.3 |
| | Mycgr3T104444 | Uncharacterised protein | Apoplastic | - | - | 8 | 72 | 2.3 |
| | Mycgr3T102617 | Uncharacterised protein | Apoplastic/cytoplasmic | - | - | 1 | 11 | 2.2 |
| | Mycgr3T99257 | Carbohydrate metabolism | - | - | Metabolism | 0 | 2 | 2.2 |
| | Mycgr3T105030 | aspartic-type endopeptidase | - | - | Metabolism | 1 | 6 | 2.2 |
| | Mycgr3T81517 | Uncharacterised protein | - | - | - | 2 | 18 | 2.2 |
| | Mycgr3T109992 | Uncharacterised protein | - | - | - | 1 | 5 | 2.1 |
| | Mycgr3T93075 | Uncharacterised protein | Apoplastic | Chloroplast | - | 3 | 21 | 2.1 |
| | Mycgr3T104404 | Uncharacterised protein | Apoplastic | - | - | 4 | 31 | 2.1 |
| | Mycgr3T102064 | Glutamine synthase | - | - | Metabolism | 0 | 2 | 2.0 |
| | Mycgr3T94290 | Uncharacterised protein | Cytoplasmic/apoplastic | Chloroplast/Nucleus | - | 1 | 5 | 2.0 |
| | Mycgr3T103029 | Uncharacterised protein | - | - | - | 2 | 15 | 1.9 |
| | Mycgr3T89162 | Uncharacterised protein | - | - | - | 1 | 4 | 1.9 |
| IPO323 | Mycgr3T68948 | Uncharacterised protein | - | - | - | 0 | 1 | 3.0 |
| | Mycgr3T104028 | 40S ribosomal protein (rps7) | - | - | metabolism | 0 | 4 | 2.1 |
| | Mycgr3T94526 | Uncharacterised protein | Cytoplasmic | Nucleus | - | 2 | 11 | 1.9 |
| | Mycgr3T104383 | Uncharacterised protein | Apoplastic/cytoplasmic | - | - | 5 | 26 | 1.7 |

### 3.6 *Z.tritici* candidate effector identification

Transcripts were investigated using Localizer, Targetp and EffectorP3 to identify coding sequences which could be involved in effector functionality, as well as providing information on target location in the host. 685 *Z.tritici* transcripts were consistently upregulated from 0-6 hpi for both isolates. 64 contained a signal peptide with 10 localised to the nucleus, 2 to the mitochondria and 2 to the chloroplast. 23 of these transcripts were predicted to be an effector with 3 of these localised to the nucleus (Supp. Table S10). 866 *Z.tritici* transcripts were consistently upregulated from 0-11 dpi for both isolates. 86 contained a signal peptide with 20 localised to the nucleus, 5 to the mitochondria and 4 to the chloroplast. 31 of these transcripts were predicted to be an effector with 6 localised to the nucleus and 1 to the chloroplast (Supp. table S10). Only 31 transcripts were consistently upregulated from 6 hpi to 11 dpi for both isolates (Supp. Table S10). 10 contained a signal peptide with 4 predicted effectors, one of which localised to the nucleus.

Candidate effectors were also identified from *Z.tritici* transcripts which were upregulated in 4D-S compared to 4D-R NILs for both isolates at 11 dpi (Supp. Table S11). 89 transcripts in HT-22 were predicted to be effectors with 9 localised to the nucleus, 2 to the mitochondria and 4 to the chloroplast. Only 2 effectors were identified unique to IPO323 with one localised to the nucleus. Lastly, 17 transcripts in both HT-22 and IPO323 were predicted as effectors with 3 localised to the nucleus, 1 to the mitochondria, and 2 to the chloroplast.

### 3.7 Candidate resistance gene(s) identification

Marker assisted mapping demonstrated that the source of resistance was likely between AX-94733088 (PL: 3609069) and AX-94627860_k (PL: 4361772) with a lower level of confidence that the gene(s) could also reside between AX-95200287_k (PL: 3253229) and AX-89639967_K (PL: 6758600). This lower confidence region encompasses TraesCD4D02G005600 – TraesCD0402013700. Therefore, for candidate gene identification TraesCD4D02G005600 – TraesCD0402013700 was investigated. Three candidate genes were identified by investigating consistently upregulated transcripts in 4D-R NILs compared to 4D-S NILs for both IPO323 and HT-22 (6300 - 3418552-3421822 , 7300 -3691889-3695119 & 7600 - 3724827-3729334). 6300 & 7600 were continuously upregulated whilst 7300 was induced at 11 dpi. Candidate gene expression was confirmed using qRT-PCRs (Fig. 13a-c). All three candidates were upregulated and at all time points. qRT-PCRs were repeated with another set of 4D-R NILs with IPO323 substituted for 508 which has overcome the 4D resistance (Fig. 12 d-e). 4D-R NILs upregulated all three candidate genes in response to 508 at all timepoints except at 0 hpi for 7600. Knetminer was used to identify linked genes and protein domains (Fig. 14).

6300 contains a signal peptide followed by an N-terminal domain, 3 LR repeats a transmembrane peptide and a protein kinase. Predicted proteins include brassinosteroid LRR receptor kinases such as BRL1 & CURL3 (Yamamuro *et al* 2000), receptor kinase Xa21 (Park & Ronald 2012) and FLS2 (Takai, R., *et al* 2008). 6300 also has 2 homologs although neither had any expression in 4D-R/S NILs.

7300 contains a signal peptide followed by an N-terminal domain, 2 LR repeats and a transmembrane peptide. Predicted proteins include Cf-9, a gene-gene receptor protein in tomato conferring resistance to *Cladosporum fulvum* (Kruijt *et al* 2004), EIX1, a receptor protein also in tomato conferring resistance to *Trichoderma viride* (Ron & Avni 2004), and XIAO, a LRR receptor kinase involved in brassinosteroid signalling (Jiang *et al* 2012). Predicted proteins also included FLS2 like with the 6300 candidate (Takai *et al* 2008). 7300 has 2 homologs, with no expression in one and the other having TPM values of 10-100 increasing from 6 hpi to 11 dpi, however there were no differences between 4D-R and 4D-S NILs.

7600 contains a signal peptide, SUZ and R3H domains and a transmembrane peptide. The R3H domain is highly conserved across species and has a role in RNA-binding (Grishin et al 1998).

The R3H domain is also found in DBF1 in Maize and acts as an ethylene response factor and is involved in an ABA-responsive gene rab17 (Saleh *et al* 2006). The SUZ domain is also associated with RNA-binding in addition to centrosome binding (Song *et al* 2008). 7600 also has 2 homologs with TPM values of ~500-1200 with no differences between 4D-R and 4D-S NILs.

**Table. 5.** Tpm Logfoldchange of differentially expressed transcripts in 4D-R NILs compared to 4D-S NILs for the physical location 3253229 (AX-95200287_k) – 6758600 (AX-89639967_K) on chromosome 4D. (Green = upregulated, Red = downregulated)

| Transcript | Logfoldchange 4D v No4D | | | | |
|---|---|---|---|---|---|
| | 0 hpi | 6 hpi - HT-22 | 6 hpi IPO323 | 11 dpi HT-22 | 11 dpi IPO323 |
| 4D-005600 | -0.6 | 0.3 | -2.4 | 1.6 | -0.9 |
| 4D-005900 | 0.3 | -1.3 | -0.2 | -0.2 | -0.2 |
| 4D-006000 | -0.5 | 0.0 | -0.3 | 0.0 | -0.1 |
| 4D-006100 | 0.2 | 0.2 | 0.1 | 0.2 | 0.1 |
| 4D-006200 | 0.3 | 0.5 | 0.3 | 0.4 | 0.0 |
| 4D-006300 | 8.3 | 4.9 | 4.2 | 4.6 | 5.1 |
| 4D-006400 | 7.9 | 0.0 | 0.0 | 5.3 | 6.0 |
| 4D-006500 | 2.0 | 3.1 | 2.5 | 2.0 | 2.3 |
| 4D-006600 | 0.9 | -0.6 | 0.2 | 1.1 | 0.0 |
| 4D-006700 | 0.0 | -0.1 | -0.4 | 0.0 | 0.0 |
| 4D-006900 | 0.0 | 0.3 | 0.2 | -0.2 | 0.1 |
| 4D-007000 | 0.0 | 3.4 | -2.9 | -2.4 | -0.4 |
| 4D-007100 | 0.8 | 0.9 | 1.4 | 0.1 | 1.1 |
| 4D-007200 | 0.0 | 1.8 | 0.0 | 0.0 | 0.0 |
| 4D-007300 | 3.3 | 3.3 | 4.2 | 1.9 | 3.7 |
| 4D-007400 | -2.6 | -3.8 | -3.2 | -0.6 | -0.5 |
| 4D-007500 | -1.8 | -1.9 | -1.7 | -2.0 | -1.8 |
| 4D-007600 | 11.0 | 11.9 | 11.3 | 10.2 | 9.6 |
| 4D-007700 | 0.0 | 0.0 | 0.0 | 0.0 | -1.7 |
| 4D-007900 | -9.5 | -9.8 | -9.8 | -11.0 | -4.3 |
| 4D-008000 | -8.6 | -6.0 | -8.4 | -9.9 | -4.4 |
| 4D-008300 | -0.7 | 1.9 | 0.6 | 4.1 | 1.9 |
| 4D-008400 | -0.2 | 0.0 | -0.2 | 0.1 | -0.2 |
| 4D-008500 | 1.6 | 0.4 | 0.9 | 1.7 | -0.3 |
| 4D-009000 | -0.7 | -0.2 | -0.4 | -0.3 | -0.4 |
| 4D-009100 | -1.6 | -1.8 | -1.8 | -1.3 | -1.7 |
| 4D-009200 | -0.2 | -0.5 | -0.5 | -0.5 | -0.5 |
| 4D-010100 | 0.7 | 0.1 | 0.1 | 0.0 | -0.1 |
| 4D-010200 | -0.1 | 0.1 | 0.0 | 0.0 | 0.0 |
| 4D-010300 | -3.1 | -0.4 | 0.1 | -0.3 | -1.2 |
| 4D-010400 | -2.9 | -0.5 | 0.6 | -0.3 | 0.3 |
| 4D-010700 | 0.3 | -0.2 | 0.0 | 0.2 | 0.2 |
| 4D-011200 | 1.0 | -0.6 | 0.4 | 0.5 | 0.6 |
| 4D-011300 | 0.2 | 0.0 | 0.0 | -0.2 | 0.0 |
| 4D-011700 | -0.3 | -0.2 | 0.0 | 0.2 | -0.1 |
| 4D-011800 | 0.2 | 0.2 | -0.1 | 0.2 | 0.0 |
| 4D-012100 | 0.0 | 0.8 | 0.1 | -0.1 | 0.0 |
| 4D-012200 | 0.2 | 0.1 | -0.4 | 0.0 | 0.2 |
| 4D-012300 | 0.0 | 0.0 | -0.2 | 0.2 | -0.2 |
| 4D-012400 | 0.0 | -0.1 | 0.0 | -0.2 | -0.3 |
| 4D-012500 | 0.2 | 0.2 | 0.2 | 0.5 | -0.1 |
| 4D-012600 | -0.2 | 0.4 | 0.0 | -0.2 | 0.3 |
| 4D-012700 | 0.5 | -0.5 | 0.0 | 0.2 | 0.0 |
| 4D-012900 | -0.9 | 0.3 | 0.1 | -0.4 | 0.3 |
| 4D-013000 | -2.0 | 0.0 | 0.0 | 0.0 | 0.0 |
| 4D-013100 | -1.3 | -0.2 | 0.1 | 4.7 | -1.3 |
| 4D-013200 | -0.2 | -0.1 | -0.2 | 0.2 | 0.0 |
| 4D-013400 | 0.4 | 0.5 | -0.3 | -1.0 | -1.7 |
| 4D-013500 | -4.1 | 3.8 | 1.1 | -0.6 | 0.3 |
| 4D-013600 | 0.0 | -0.4 | 0.3 | 0.2 | -0.5 |
| 4D-013700 | -1.2 | -4.0 | 2.6 | 0.9 | -0.2 |
| 4D-013800 | 2.5 | 3.0 | 3.2 | 0.0 | 0.0 |
| 4D-013900 | 0.3 | -0.4 | 0.2 | -0.1 | 0.2 |
| 4D-014000 | -0.1 | -0.2 | 0.3 | 0.1 | 0.0 |
| 4D-014100 | -0.6 | 0.3 | -0.1 | 0.4 | 0.0 |
| 4D-014200 | -0.3 | 0.1 | -0.2 | -0.2 | 0.1 |
| 4D-014300 | 0.8 | -0.1 | -0.4 | -0.4 | 0.0 |
| 4D-014400 | -0.3 | 0.1 | 0.0 | -0.3 | 0.0 |
| 4D-014500 | -0.8 | -0.1 | -0.3 | -0.3 | -0.2 |
| 4D-014600 | 0.0 | 0.0 | -1.7 | 0.0 | 0.8 |
| 4D-014700 | 3.0 | -2.3 | -3.3 | -0.3 | 1.1 |
| 4D-014800 | -0.2 | 0.3 | 0.0 | -0.1 | 0.3 |
| 4D-014900 | 0.0 | 0.0 | 0.0 | 0.0 | -2.3 |
| 4D-015000 | -2.3 | -1.0 | -2.5 | -1.3 | 0.0 |

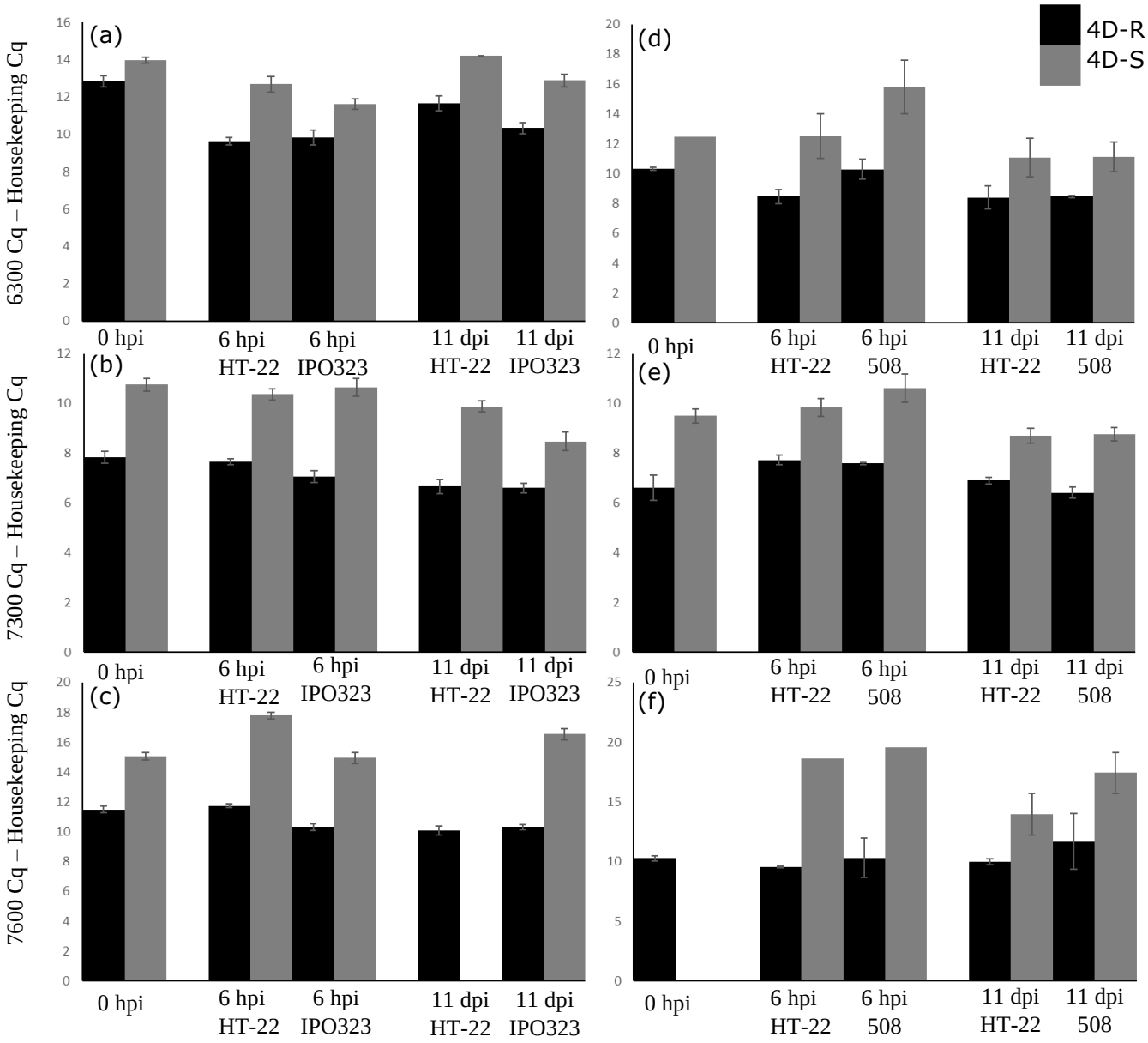



**Figure 13.** qRT-PCR gene expression (Sample-Houskeeping Cq) of candidate transcripts (6300 (a, d), 7300 (b, e), 7600 (c, f)) in 4D-R & 4D-S NILs at 0 hpi and when inoculated with HT-22 (incompatible), IPO323 (incompatible) with the NILs used in this transcriptomic experiment (a, b, c) & a newer set of NILs (d, e, f) inoculated with 508 (compatible) & HT-22 (incompatible) at 6 hpi & 11 dpi. (Black = 4D-R, Grey = 4D-S) (All 4D-R/S comparisons were significant, P <0.05 students T-test) (Expression compared to housekeeping ADP & UBI)

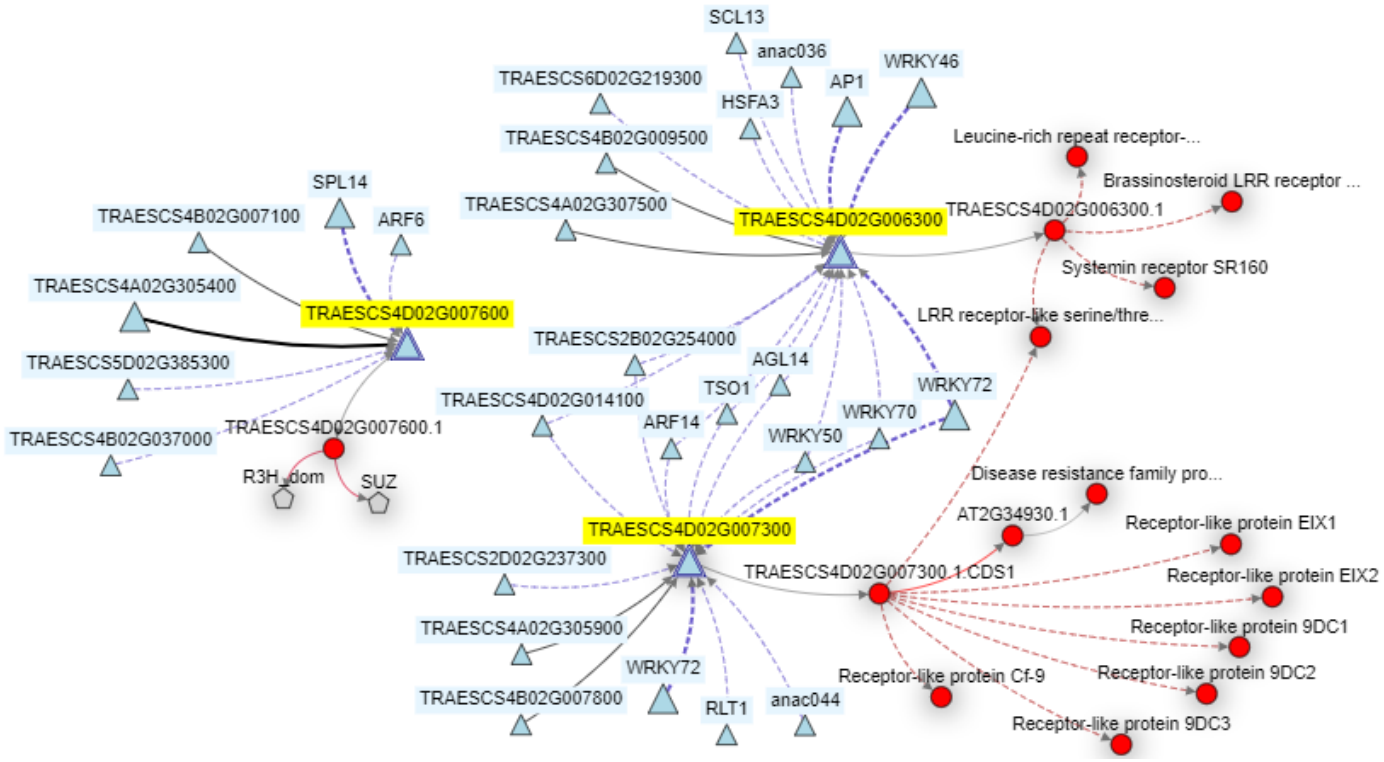



**Figure 14.** Knetminer visual map displaying genes (Light blue), transcripts (Light blue), protein domains (Grey) & proteins (Red) related to the major 4D candidate transcripts (6300, 7300 & 7600). (arrow indicates regulation or associated protein)

### 3.8 Candidate resistance gene(s) SNP 4D-R/S comparison

To investigate these candidate genes further, RNAseq sequencing data was analysed for all three candidate transcripts to identify indels and SNPs which might result in a change in protein function or translation. Phyre2 (Protein fold recognition server) was used to predict protein structure based on differences in SNPs between 4D-R/S NILs (Supp. Fig. 4). However, no SNPs for 6300, 7300, or 7600 was predicted to affect the Phyre2 protein predictions between 4D-R/S NILs (6300 & 7300 c6s6qB model crystal structure of the lrr ectodomain of the plant membrane receptor2 kinase gassho1/schengen3 from *Arabidopsis thaliana* in complex with3 casparian strip integrity factor 2. 7600 R3H domain).

6300 had 8 SNPs between 4D-R/S NILs which involved 3 missense mutations which was predicted using Phyre2 modelling and Hmmer Biosequence analysis to induce no change in the reading frame, protein structure, or signal/transmembrane peptides (Supp. Fig. 1) (Supp.

Fig. 4). However, these SNPs involved an amino acid substitution from aspartic acid to tyrosine within a leuicine rich repeat, substitution of threonine with asparagine in a protein kinase domain, and substitution of histidine with asparagine in an uncharacterised domain.

7300 has 40 SNPs between 4D-R/S NILs with one 1bp deletion causing a frame shift in both the 4D-R and 4D-S NILs relative to Chinese Spring. These mutations affect the reading frame which the 4D-R NIL translates its 2 LRR protein domains (Supp. Fig. 2). Whereas the Chinese Spring reference 7300 transcript contains 1 exon, the SNPs in the 4D-R/S NILs have truncated exons such that the 4D-S NIL has 6 exons and the 4D-R NIL in the reading frame containing the protein kinase has 7 exons (Supp. Fig. 2). If only the first exon is translated then for 4D-S this exon translates a signal peptide, N-terminal domain and 2 LRR protein domains. If the same reading frame is translated for the 4D-R NIL then the first exon only encodes for a signal peptide and an N-terminal domain (Supp. Fig. 2). This suggests that 7300 might be non-functional in both 4D-R/S NILs compared to Chinese Spring due to this frameshift. The other exons for both 4D-R/S NILs contain additional LRR protein domains present in the Chinese Spring reference, however it's uncertain if these are translated.

7600 has 15 SNPs with 15 indels in the 4D-S NIL and 2 indels in the 4D-R NIL compared to the Chinese Spring reference. The NILs were heterozygous for many of the SNPs, however this could be attributed to the detection of another homozygous transcript which is upregulated since 7600 has 2 homologs which were upregulated in this dataset. The Chinese Spring reference contains 8 exons with the first 2 exons containing a signal peptide followed by an exon containing the R3H and SUZ domain and subsequent exons with 3 transmembrane peptides. However, both 4D-R and 4D-S NILs have a reading frame shift for the R3H and SUZ domain (Supp. Fig. 3). Therefore, whilst there are large differences between 4D-R/S NILs they might both be non-functional due to a frameshift compared to the reference in Chinese Spring preventing the translation of the R3H and SUZ domains. Additionally, there were no SNPs between 4D-R/S NILs in the R3H and SUZ domains.

## 4. Discussion.

The major source of resistance in Cougar was effective at reducing necrotic lesion and pycnidia development, although in response to IPO323 there was an increase in chlorotic lesions, suggesting that 4D-R NILs might not confer complete resistance to IPO323. This difference in chlorotic phenotype could explain why there were more differentially expressed genes between 4D-R/S NILs in response to HT-22 compared to IPO323. Additionally, 4D-R NILs exhibited different photoprotective mechanisms to each isolate, reflected by differences in Fv/Fm, NPQ (QE/QI), conductance and PhiPS2.

In the incompatible 4D-R/S HT-22 interaction there was a decrease in $F_v/F_m$ consistent with an increase in the dark NPQ component qI and decrease in qE. Increased qI indicates inactivation of D1 and consequently decreased PS2 activity, whilst decreased qE suggests downregulation of NPQ driven by zeaxanthin and PsbS. This photoinhibitory phenotype was associated with downregulation of additional PetF electron transport transcripts in addition to Psb28 (0-6hpi), which is involved in the reassembly of D1 and the light harvesting complexes. Transcripts involved in VDE & NCED2 from 0-6hpi were also downregulated, suggesting conversion of zeaxanthin into violaxanthin & neoxanthin. However, ZEP and NCED4 qRT-PCR expression was upregulated in 4D-R NILs, suggesting a shift in carotenoid composition from 6 hpi to 11 dpi. GSEA analysis demonstrated that in the incompatible 4D-R/S HT-22 interaction these photoprotective mechanisms were associated with molybdenum metabolism (Llamas *et al* 2006; Leimkuhler *et al* 2003), likely involved in carotenoid biosynthesis, as well as detoxification processes at 6hpi. Despite an increase in SA content in the incompatible 4D-R HT-22 interaction SA was not represented in the GSEA analysis. At 11 dpi, there was a shift to protein kinase activity combined with Psb33 transcript upregulation which is typically involved in PSII stabilisation (Fristedt *et al* 2015). Overall, these findings demonstrate an association between transcripts related to carotenoid metabolism, electron transport, detoxification, PSII related proteins, and photoprotective mechanisms detected utilising chlorophyll fluorescence measurements in the incompatible 4D-R/S HT-22 incompatible interaction.

In the incompatible 4D-R/S IPO323 interaction there were no differences in Fv/Fm and the light NPQ component QE increased. This phenotype was associated with downregulation of Lhcb3, PsbZ & PsaF (0-6hpi). Both Lhcb3 & PsbZ is required for PS2-LHCII supercomplex formation (Eckardt 2001) whilst PsaF is involved in electron transfer to PS1. The absence of a

decrease in Fv/Fm suggests that the 4D NILs response to IPO323 involved a lower photoinhibitory response relative to HT-22. GSEA analysis demonstrated that the incompatible 4D-R/S HT-22 interaction at 6 hpi included ROS scavenging enzymes which constituted of iron superoxide dismutase, which has been previously identified by Ajigboye et al (2021), as well as an increase in thiamine metabolism transcripts, which can be involved in carotenoid precursor synthesis, and an increase in ABA receptor transcripts. At 11 dpi there was a shift towards defence related processes such as defence related proteins and chitinases, as well as an increase in ABA metabolism consistent with Ajigboye *et al* (2021). These included the presence of JA related transcripts, autophagy transcripts, phenylpropanoid metabolism and PS1 related ATP processes. These results could indicate that the 4D-R resistance is acting on the removal and degradation of PAMPs, fungal protein effectors, fungal cell wall degradation and chloroplast recycling. This study demonstrates that whilst the major source of resistance in Cougar impedes necrotic lesion and pycnidia development against both IPO323 and HT-22, there are significant differences in the defence mechanisms as indicated by chlorophyll fluorescence measurements, transcriptomic analysis, xanthophyll gene expression and hormonal analysis.

Investigating conserved responses in both HT-22 and IPO323 4D-R/S incompatible interactions highlights the defence responses likely associated with the major source of resistance in Cougar on 4D, instead of isolate specific responses which don't contribute towards resistance. The conserved incompatible 4D-R/S interaction was associated with a lack of necrotic lesion and pycnidia development and a decrease in PhiPS2 at 6 hpi indicating photoinhibition as demonstrated by Ajigboye *et al* (2021). Time comparisons from 0-6hpi transcripts in the 4D NIL indicated that this photoinhibition of PSII was associated with modification of electron transport (PetF) and PsbQ, the latter being involved in the oxygen-evolving complex (OEC). 4D-R upregulated peroxisome import transcripts, which might be attributed to an increase in reactive oxygen species detoxification protecting PSII from ROS induced damage. The only conserved PSII related transcript was upregulation of PsbR at 11dpi. This protein is a structural component of PSII and facilitates transfer of electrons from $Q_A$ to $Q_B$ (Allahverdiyeva *et al* 2007). Reassembly of the LHCs incorporates PsbR as well as PsbH, M & T to convert RC47a to RC47b where it binds to D2 and subsequently the OEC (Lu 2016). It's possible that PsbR plays a role in preventing the switch to necrotrophy displayed in the 4D-S NIL. A proposed mechanism could involve *Z.tritici* disrupting PSII stability to increase ROS generation for necrotrophy and subsequent pycnidia formation by targeting PsbR. Despite

major differences in the defence response between isolates as captured by the transcriptomics, the most upregulated transcripts remained relatively consistent for both isolates and across both 6 hpi and 11 dpi. These included some protein kinases of unknown function as well as transcripts with predicted annotation for: INRPK1, Receptor like protein involved in photoperiodic-induced flowering (Bassett *et al* 2000), RGA4/5, Disease resistance protein to *X.oryzae pathovars* (Hutin *et al* 2016), PCBER, (Oxidoreductase involved in lignin synthesis (Gang *et al* 1999), FBL14, F-box protein (Viñas-Castells *et al* 2010), ER1/2, regulatory role in plant development (Zhang *et al* 2018) and GDP-Mannose. Overall, the most upregulated transcripts in the incompatible 4D-R/S HT-22/IPO323 interaction were upregulated at both 6 hpi and 11 dpi and involved protein kinases associated with a variety of processes, although the majority appear to be involved in hormone mediated signalling. GO term analysis demonstrated the role of transcripts associated with nucleotide binding at 6 hpi, which could be indicative of differential regulation of specific genes. At 11 dpi this binding GO term remained, although it was accompanied with protein modification processes such as ribosomal nucleotide binding and protein phosphorylation. These results suggests that the major source of resistance in Cougar involves a variety of defence related proteins.

Three candidate resistance genes were identified which were consistently upregulated in both 4D-R/S HT-22/IPO323 incompatible interactions. The candidate '6300' has ~30% homology to proteins Xa21, Fls2 & BRL1 which are all LRR receptor kinases. Xa21 confers broad spectrum immunity in rice to the bacterial pathogen *Xanthomonas oryzae* (Park & Ronald 2012), whereby upon pathogen detection the kinase translocates to the nucleus and interacts with WRKY62 which negatively regulates Xa21 immunity. In this transcriptomic analysis 18 transcripts regulated by WRKY62 were downregulated by more than 2 fold at 11 dpi with HT-22, with none upregulated, suggesting the possibility that this mechanism could be present in 4D-R. BRL1 is involved in brassinosteroid related signalling and internode elongation (Yamamuro *et al* 2000). Lastly, Fls2 is involved in flagellin preceptor induced defence response with overexpression leading to hypersensitive cell death in rice (Takai, R., *et al* 2008). 6300 had 8 SNPs between 4-R/S NILs with 3 inducing an amino acid change in the coding region. Whilst these SNPs didn't affect the Phyre2 protein structure prediction, these SNPs could cause changes in protein function or changes in the molecular interaction between the protein and the avirulence effector. This could be especially important in ETI mediated immunity due to the specificity of the protein-protein interaction required to elicit a defence response.

The candidate 7300 is similar to 6300 since it has similar homology to Fls2 which is also reflected in the Phre2 modelling prediction, although 7300 also has homology to Cf-9 & EIX2. Cf-9 is a gene-gene resistance protein which provides resistance to *Cladosporum fulvum* in tomato (Kruijt *et al* 2004). Candidate effectors were screened to identify any Avr9 homologs in *Z.tritici* transcripts, however none were found. EIX2 is a receptor in tomato inducing ethylene biosynthesis, electrolyte leakage, pathogenesis-related protein expression and hypersensitive cell death response (Ron & Avni 2004). Ethylene related transcripts were not over-represented in the transcriptomic dataset suggesting that 7300 doesn't induce defence through this EIX2 mechanism. 7300 is also the only candidate gene which is induced at 11 dpi in the transcriptomic database. When investigating the SNPs and indels in the 4D-R NIL for potential change in functionality, this transcript may be lacking a functional protein domain or produce a truncated protein. Therefore, even though this candidate gene is upregulated in 4D-R NILs relative to 4D-S NILs it might be non-functional.

Lastly, the candidate '7600' was the most upregulated transcripts out of the entire dataset. 7600 also shared homology to DBF1 which plays a role in the regulation of the ABA-dependent gene rab17 in maize (Saleh *et al* 2006). Due to the potential role of ABA in the 4D-R resistant mechanism in response to both isolates and in response to Cougar (Ajigboye *et al* 2021) 7600 might be involved in regulation of this response and be responsible for the major source of resistance in Cougar. SNPs and indels in the 4D-R NIL have no effect on the R3H & SUZ protein domain of 7600. However, the main change is the shift of translation to different reading frames due to numerous indels. Therefore, like with 7300, 7600 might be non-functional. Future work involving the knockdown of these candidate genes using virus induced gene silencing (VIGS), or transforming a susceptible line with the functional gene is needed to investigate these candidate genes further. It is worth noting that other gene(s) may be responsible for the major source of resistance in Cougar. These could involve genes which aren't differentially expressed between 4D-R/S NILs but have SNPs causing functional changes which elicit the Cougar defence response. It is likely that the major source of resistance is an effector protein kinase due to its quick breakdown in the field (Kildea *et al* 2021).

This study also investigated the HT-22 and IPO323 *Z.tritici* response to the host. The *Z.tritici* transcriptome from HT-22 & IPO323 indicated that both isolates consistently upregulated ribosomal processes and translation, indicating the production of protein effectors into the host. We identified 23 potential effectors which are upregulated at 6 hpi in all treatments and 31 at 11 dpi. In addition, 89 candidate effectors were upregulated in the 4D-S NIL in HT-22, 2 in

IPO323 and 17 were consistently upregulated in both isolates. There were also 7 effectors shown to localise to the chloroplast. Therefore, this paper highlights potential *Z.tritici* avr effectors which could be inducing defence through specific host recognition (ETI).

In conclusion, the major source of resistance in Cougar provided resistance to both HT-22 & IPO323, although IPO323 was more virulent as demonstrated by an increase in chlorotic lesion development. The major source of resistance was associated with a photoprotective defence response, although this varied depending on the isolate, with a decrease in PhiPS2 being the only consistent photoprotective response. Transcriptomic analysis identified three candidate genes which could be responsible for the major source of resistance in Cougar, although further work would be needed to confirm this studies results and identify the resistance gene(s) responsible. This study also identified candidate *Z.tritici* Avr effectors which might be involved in a Cougar ETI defence response. Lastly, the Cougar holistic resistance mechanism was quantified using a combination of hormone, xanthophyll enzyme quantification and transcriptomic analysis, which highlighted differences in the Cougar defence response to HT-22 and IPO323.

# Chapter 4.

## Phenotyping and characterisation of a novel source of resistance to *Zymoseptoria tritici* in Cougar in incompatible and compatible interactions

# 1. Introduction

*Zymoseptoria tritici* is a latent necrotrophic fungal pathogen causing septoria tritici blotch (STB) on wheat (*Triticum aestivum*) (Sanchez-Vallet *et al* 2015). The identification and characterisation of novel sources of resistance to *Z.tritici* is essential in managing the impact of this pathogen on food security whilst minimising the unsustainable and expensive fungicide use for the control of the disease. The molecular and physiological mechanisms involved in defence against *Z.tritici* have not been fully characterised or understood, although significant progress has been made in understanding Stb6 effector triggered immunity (ETI) (Zhong *et al* 2017; Saintenac *et al* 2018).

Spore germination is a key stage in the *Z.tritici* infection life-cycle with stomatal penetration occurring as early as 12-24 hpi (Steinberg *et al* 2015). A vital component of the compatible *Z.tritici*-wheat interactions is the switch from yeast-like growth to hyphal growth. For example, knockdown of *Alg2* (Motteram *et al* 2011) and *Hog1* (Mehrabi *et al* 2006) prevented this developmental switch leading to an incompatible phenotype. Furthermore, knockdown of *CC1* (Choi & Goodwin 2011) lead to a variety of phenotypes involving delayed filamentous growth and unusual hyphal swellings, whilst knockdown of *Fus3* (Cousin *et al* 2006) displayed altered polarized growth, and knockdown of *MST* (Kramer *et al* 2009) prevented the development of filaments required to penetrate stomata. Ajigboye *et al* (2021) demonstrated that on Cougar leaves, *Z.tritici* exhibited reduced germination rate and hyphal branching in contrast to terminal hyphal length, suggesting that the major source of resistance on 4D could alter pathogen behaviour leading to an incompatible phenotype. Furthermore, in the study by Ajigboye *et al* (2021), Cougar had narrower, longer and sparser stomata, suggesting a role of preformed leaf defence traits in *Z.tritici* resistance independent of virulence. Therefore, due to the infection process of *Z.tritici* involving stomatal penetration (Steinberg *et al* 2015), stomatal behaviour is likely important when it comes down to differentiating between compatible and incompatible interactions. In addition to developmental genes involved in the stomatal penetration and the switch to hyphal growth, Orton *et al* (2016) investigated previously identified genes to characterise the molecular basis in *Z.tritici*-wheat compatible and incompatible interactions. However, there were no differences found in gene expression between compatible and incompatible interactions, suggesting that quantifying specific previously discovered genes might not be an effective method to characterise compatible and incompatible *Z.tritici*-wheat interactions.

The accumulation of reactive oxygen species (ROS) has been shown to facilitate compatible wheat-*Z.tritici* interactions (Foyer & Noctor 2005; Choi *et al*., 2016) during the switch from asymptomatic growth of the pathogen in the apoplast and necrotrophy. The main source of ROS in plants is from the photosynthetic apparatus involved in the capture and dissipation of energy required for photosynthesis (Foyer & Noctor 2005). Photoprotective mechanisms have evolved in plants to prevent harmful accumulation of ROS in the chloroplast under stressful environments. One major mechanism of photoprotection is non-photochemical quenching (NPQ) that controls thermal dissipation of unused energy to avoid photo damage (Murchie & Ruban 2020). NPQ forms include a fast-relaxing component (qE) in the light and the slow-relaxing qI component in darkness. qE operates through lumen acidification under high-light, triggering protonation of the protein PsbS and the carotenoid, zeaxanthin. The qI form of NPQ is less well understood although it also involves zeaxanthin and is associated with reorganisation of LHCII and downregulation of light harvesting capacity by reduction of the antennae in photosystem (PSII) complexes. Carotenoids and the xanthophyll cycle are central for NPQ regulation, photoprotection and structural integrity of PSII. For example, LHCII composes of a protein backbone of three transmembrane a-helical domains binded to 8 chlorophyll a's, 6 chlorophyll b's, two luteins, one neoxanthin and one violaxanthin, which can also be substituted with zeaxanthin or antheraxanthin (Lokstein, Renger, & Götze, 2021). Xanthophyll involvement in photoprotective NPQ have previously been investigated in Arabidopsis using knockdown mutants (Dall'Osto *et al* 2007). This study highlighted the importance of both the α and β-branched xanthophylls in maintaining qE & qI with mutants deficient in either branch exhibiting impaired photosynthetic functionality. Chlorophyll fluorescence measurements have also previously been utilised to characterise the NPQ mechanism of resistance in Cougar by Ajigboye *et al* (2021) and Chapter 3 of this thesis. The xanthophyll cycle leads to ABA synthesis through neoxanthin, suggesting that there is a close connection between forms of NPQ and the ABA response in plants infected by *Z.tritici* since ABA is a plant defence hormone which is also tightly associated with stomatal responses (Cao *et al* 2011).

The hormonal regulation of defence to *Z.tritici* is not fully understood with Salicylic acid (SA), and Jasmonic acid (JA) being most frequently implicated in the response. For example, silencing of TaWRKY10, which negatively regulates JA, leads to increased resistance to *Z.tritici* (Campanaro *et al* 2021). Another example includes Le Mire *et al* (2018) which demonstrated that surfactin application induces wheat defence responses by inducing JA and

SA defence pathways. Less is known of the roles of ethylene (ET), auxin, abscisic acid (ABA) or gibberellic acid (GA) in the regulation of defence responses, although application of (GA) has been shown to decrease disease severity under field conditions (El-Mougy *et al* 2022).

The aim of this study was to determine the physiological phenotype, including the mechanism of photoprotection, of 4D-R resistance and susceptibility with a combination of the following: Visual assessments, spore & stomatal staining assays, ROS assays, chlorophyll fluorescence measurements, xanthophyll quantification, xanthophyll gene expression and hormone quantification. In addition, this study characterised the differences between compatible and incompatible wheat-*Z.tritici* interactions utilising these methods. This study uses a set of near isogenic lines (NILs) to build upon findings from Ajigboye *et al* (2021) and chapter 3 of this thesis, with two isolates with differing virulence to 4D-R. This chapter aims to test the following hypothesis:

3) A range of pre-formed and inducible (structural/physiological/biochemical) factors are associated with incompatibility between cv. Cougar and an Avr *Z.tritici* isolate.
4) A range of pre-formed and inducible (structural/physiological/biochemical) factors contribute to isolate-non-specific resistance.

## 2. Materials and methods

### 2.1 Plant material and controlled environmental conditions

Near isogenic lines (NILs) were developed by RAGT and constituted the 4D Cougar resistance region and a background of Cashel (susceptible, not known to carry any Stb genes). Cougar was backcrossed with Cashel to BC3 with marker and phenotyping data used to confirm the presence of the major source of resistance on chromosome 4D as previously identified in Chapter 2. Both NILs did not contain Stb6. These NILs were from a different cross pipeline from chapter 3 since the NILs from chapter 3 failed to display a clear phenotype in response to IPO323 (Low levels of chlorosis in the incompatible IPO3234D-R NIL interaction, Fig 1, Chapter 3), whereas the NILs used here showed a clear phenotype (low levels of chlorosis in the incompatible IPO323 4D-R NIL interaction, Fig 1 Chapter 4) suggesting that there was reduced background sources of resistance in the NILs in this chapter. Seeds were grown in modular trays using Jon Innes No.2 compost and transferred to 8cm deep pots after 10 days. Plants were kept in a tray of water with a bi-weekly application of 15:7:30 Hortifeed and had transparent sleeves fitted to minimize leaf damage. Conditions were 16-22 $^{O}$C for a 16-hour day night cycle with a ~260 μmols $m^{-2}$ $s^{-1}$ Photosynthetic Photon Flux Density (PPFD).

### 2.2 *Z.tritici* inoculations

An isolate with avirulence to the 4D-R resistance (HT-22), and an isolate with virulence to 4D-R (508) were selected to investigate the incompatible and compatible interactions respectively. HT-22 was provided by Dr Kostya Kanyuka (NIAB) and 508 from RAGT. Isolates were stored in 50% glycerol at -80$^{O}$C and grown for 5 days at room temperature on yeast extract peptone dextrose (YPD). Spore concentration was diluted to $1x10^{6}$ concentration using a haemocytometer with ~1 drop of tween added per 100ml to assist with spore adhesion to the leaf. Plants were sprayed till runoff and kept under a humidity tent with trays of water to ensure ~100% humidity before being taken off after 4 days. Plants were taken out of the tent for measurement purposes with effort taken to maintain high levels of humidity.

### 2.3 STB disease and pycnidia assessments

Plants were assessed for percentage chlorotic lesion area, percentage necrotic lesions area and pycnidia presence at 9, 13, 17 & 21 dpi. The same plants and leaves, which were analysed for the chlorophyll fluorescence measurements, were also assessed for disease in addition to 2 other leaves. The 3 most expanded leaves at the time of inoculation were tagged and later

assessed. Assessments shown are from two separate chlorophyll fluorescence phenotyping experiments. Visual assessments from other experiments used for RT-qPCR, ROS and stomatal/fungal staining sections are not included but always conformed to the visual phenotype displayed.

### 2.4 Chlorophyll fluorescence and gas exchange measurements

The infrared gas analyser (IRGA), LI-6400 (LI-COR Biosciences, Nebraska, USA) was used to measure chlorophyll fluorescence and gas exchange. The IRGA had a flow rate of 500 mL $min^{-1}$ and a curvet temperature of 20 °C, $CO_2$ concentration of 400 ppm, and relative humidity of ~60%. Leaves were dark adapted for ~1 h using aluminium foil to ensure maximum oxidation of the reaction centres to get a true measurement for Fo and Fm. The protocol involved applying a low measuring light insufficient to induce significant variable fluorescence ($F_o$), followed by a saturating pulse to get maximum fluorescence ($F_m$). Actinic light (1500 μmol $m^{-2}$ $s^{-1}$) was turned on at 2 min, a saturating pulse of 7000μmol $m^{-2}$ $s^{-1}$ (for 0.8 s) was applied to determine maximum fluorescence ($F_m$'). Actinic light was switched off for 2s with far-red light applied to determine $F_o$'. Application of a series of saturating pulses every 2 min over a period of 14 min under actinic light and for another 12 min under darkness (actinic light turned off), allowed calculation of $F_o'$ and $F_m'$. Chlorophyll fluorescence parameters were calculated directly from LICOR 6400XT software. Measurements obtained included including non-photochemical quenching (NPQ), maximum quantum efficiency of PSII photochemistry ($F_v/F_m$), photochemical quenching (qP), electron transport (ETR) and efficiency of PSII (PhiPS2). The fast relaxing component of NPQ (qE) was calculated as ($F_m/F_m'$) - ($F_m/F_m''$), while the slowly relaxing component (qI) was calculated as ($F_m - F_m''$)/$F_m''$, where $F_m''$ is the maximal yield of fluorescence after 12 min of dark relaxation. We assumed that after 14 min of dark treatment the NPQ consists only of qI. This protocol was reduced in length compared to the transcriptomic chlorophyll fluorescence phenotyping to enable 6 biological replicates to be phenotyped instead of just 3. This experiment was repeated and analysed together to increase confidence in the results by increasing the number of replicates and to ensure reproducibility.

### 2.5 ROS staining

ROS was quantified using histochemical staining for hydrogen peroxide ($H_2O_2$) and superoxide ($O_2^{\bullet-}$). Staining of $H_2O_2$ was carried out using 3,3′-diaminobenzidine (DAB). Leaf sections were vacuum-infiltrated with 1 mg/ml DAB-HCl (pH 3.8) and incubated overnight with gentle shaking at room temperature in the dark. The DAB solution was removed, and the leaf sections

were washed with distilled water. Samples were then boiled for 5 min in 95% ethanol and then were kept in 95% ethanol with gentle shaking until all chlorophyll was removed which took 3-4 days. Generation of superoxide anion ($O_2^{\bullet-}$) in leaves was detected with nitroblue tetrazolium (NBT). Leaf sections were vacuum-infiltrated with 50 mM phosphate buffer (pH 7.8) containing 0.5% NBT and incubated at room temperature for 1h in darkness. Subsequent sample preparation was identical to DAB staining. Leaf samples were collected at 0 hpi, 6 hpi, 24 hpi and 48 hpi. Hydrogen peroxide data is not shown due to non-significant results. Photos were taken using an Iphone11 camera and analysed using a modified ImageJ macro from Stewart *et al* (2016).

### 2.6 Stomatal and fungal staining

Three cuttings of each biological replicate were taken ~4cm long and placed between two filter papers in a petri dish soaked in glacial acetic acid for 2 days to clear the chlorophyll. Leaf cuttings were transferred to an equivalent setup soaked in lactoglycerol for long term storage. Leaf cuttings were transferred to a 2ml Eppendorf tube and covered in 0.1% Tryphan blue for 1 hour at 50$^{O}$C. Cuttings were transferred to a microscope slide and analysed using a Leica2 microscope, CTR 5000 light microscope (Leica Microsystems, Bensheim, Germany). Cuttings were taken at 0 hpi, 6 hpi, 24 hpi & 48 hpi. For stomatal analysis 3 images were taken at 10x magnification per cutting with 3 cuttings per biological replicate and 4 biological replicates per treatment. Number of stomata stained/unstained stomata*100 was used to calculate % stomata open. For spore germination analysis 3 images were taken at 20x magnification per cutting with 3 cuttings per biological replicate and 4 biological replicates per treatment. Images were taken of the first three spores found. Spores were analysed for germination rate and the number of germ tubes from the main spore body.

### 2.7.1 RT-qPCR of xanthophylls cycle enzyme conversion genes

RNA was converted into cDNA using the iScript cDNA synthesis kit (Biorad) and quantified using NanoDrop to ensure consistent DNA concentrations of 20ngul$^{-1}$. Primers at 50 µM concentration were used along with SYBR mix. ADP-ribosylation factor (ADP) housekeeping gene were used. qPCRs consisted of 2 technical replicates. The protocol used was consistent for all primers; 95$^{O}$C for 30s, 40 cycles of 95 $^{O}$C for 15s and 60 $^{O}$C for 30s followed by a melt curve between 65 and 95$^{O}$C. Zeaxanthin epoxidase (ZEP), 9-cis-epoxycarotenoid dioxygenase (NCED) & Violaxanthin depoxidase (VDE) primers were used from Ajigboye *et al* (2021).

Relative expression was calculated as 2^(Sample CQ – Housekeeping CQ). (Candidate gene expression is presented in Chapter 3)

Primers used:

VDE – F (CCCGAGCTAGAAAGGGCTAC) R (ACCACAGGTGTTGTCTGTCC)
ZEP – F (GGACTTCAACGACCCCTTGT) R (TACCCTATTGTACACCCTCGGT)
NCED – F (TAAGTGCTACAAGAGTGACTACC) R (CCTGTAGCGAAGCAGTAGG)

### 2.7.2 Xanthophyll quantification

Carotenoids were extracted in 100% acetone (HPLC grade), placed in amber 1.5 ml Eppendorf tubes for light protection, centrifuged for 2 min at 10,000g at 4 °C, and filtered through a 13 mm diameter 0.2 µm polytetrafluoroethylene (PTFE) syringe filter (Whatman). Dr Dimitra Angelopoulou (University of Nottingham), Dr Petra Ungerer and Dr Vasco Giovagnetti, (Queen Mary University of London) performed the HPLC analysis. Pigment separation was performed by reverse-phase HPLC as described in Färber *et al* (1997). The HPLC analysis was performed using a BioLC HPLC system (Dionex) with LiChrospher 100 RP-18 (5 µm) column (Merck). Three biological replicates were measured. For each sample the amount of each carotenoid was calculated as a percentage of total carotenoids. In wheat the total carotenoids (Car) comprise neoxanthin (Neo), violaxanthin (Vio), antheraxanthin (Anth), lutein (Lut), zeaxanthin (Zea), and β-carotene (βCar). The size of the xanthophyll cycle (XC) pool of carotenoids, expressed as a percentage of total carotenoids, and de-epoxidation state (DEP) of the xanthophyll cycle pigments were calculated from Equations 1 and 2, respectively (Ajigboye *et al* 2021).

1) XCpool/Car (%) = (Zea+Anth+Vio )/(Neo+Vio+Anth+Lut+Zea+ βCar) x 100
2) DEP (%) = (Zea+ 0.5 x Anth)/(Zea+Anth+Vio) x 100

### 2.8 Hormone quantification

The same samples obtained for the Xanthophyll quantification was used for hormonal quantification (see section 2.1). The endogenous contents of hormones, including ABA; Abscisic acid, SA; Salicylic acid, JA; Jasmonic acid, OPDA; oxo-Phytodienoic acid, Ja-Ile; jasmonoyl-L-isoleucine, IAA; Indole-3-acetic acid, GA1, 3, 7; Gibberellin, ACC; 1-Aminocyclopropane 1-carboxylic acid, IPA; Indole-3-propionic acid, 2iP; 6-(γ,γ-

Dimethylallylamino)purine, Z; Zeatin, ZR; zeatin riboside were determined by liquid chromatography coupled to electrospray ionization tandem mass spectrometry (LC/ESI-MS/MS) as described by Müller and Munné-Bosch (2011). 100mg freeze dried leaf sample was extracted using a mixture of methanol:isopropanol:acetic acid, 50:49:1 (v/v/v) using ultra-sonication (Branson 2510 ultrasonic cleaner, Bransonic, Danbury, CT, USA). Deuterium-labeled plant hormones were added to the initial extract to estimate recovery rates. Extract was vortex and centrifuged at 4°C for 10 min at 1300 rpm. Supernatant was collected, pooled and filtered using 0.22-μm hydrophobic PTFE Syringe Filters (Phenomenex, Torrance, CA, USA). This was then injected into the UHPLC/ESI-MS/MS system. All hormones analysed using negative ion mode, except cytokinins (measured using positive ion mode).

### 2.9 Statistical analysis

Experiments were designed as randomised block designs. Visual *Z.tritici* phenotype, chlorophyll fluorescence measurements, qPCRs, ROS staining and carotenoid content were analysed using Genstat 19th edition (VSN international). To assess the impact of compatibility on the wheat defence response the following statistical model using ANOVA was used: Line + Isolate + Compatibility. When applicable, minutes into the protocol was incorporated into the statistical model to account for the effect of the measuring period: minutes*compatibility/Line/Isolate. Summary tables displaying these results are displayed in supplementary tables S12-21. To assess the effect of the Cougar resistance gene on 4D, Student's t-test was carried out to compare 4D-R and 4D-S lines in both HT-22 and 508 inoculated treatments. Residuals were normally distributed so there was no requirement for data transformation.

# 3. Results

## 3.1 Visual assessment of *Z.tritici* isolates HT-22 & 508 symptoms on 4D-R & 4D-S NILs

Chlorotic lesions were visible from 9 dpi (Fig. 1a). 4D-S NILs exhibited significantly greater % chlorotic lesions at 16 dpi when inoculated with 508 before a decrease in chlorosis in both lines being replaced by necrosis increasing in response to 508 in both NILs but being significantly greater in the 4D-S line (Fig1b). Chlorotic lesion development from 13 to 20 dpi was significantly lower in the 4D-R NILs inoculated with HT-22 compared to the 4D-S NILs (Fig. 1a). Necrosis in response to HT-22 developed only in 4D-S (Fig. 1b). There was reduced pycnidia presence and % necrotic lesion coverage on the 4D-R NILs inoculated with HT-22 compared to 508 (Fig. 1bc). HT-22 inoculated 4D-R NILs had reduced pycnidia presence from 13 dpi compared to the 4D-S NIL (Fig. 1bc). There were significant effects of compatibility for chlorotic lesions, necrotic lesions and pycnidia presence (Table S12), demonstrating clear phenotypic differences between compatible (HT-22 – 4D-S, 508 – 4D-S, 508 – 4D-R) and incompatible (HT-22 – 4D-R) interactions. These visual assessments also demonstrate that 4D-R NILs provided complete immunity (lack of necrosis or pycnidia) to HT-22, whilst 508 has overcome that resistance (showing necrosis and pycnidia formation) (Fig. 1d).

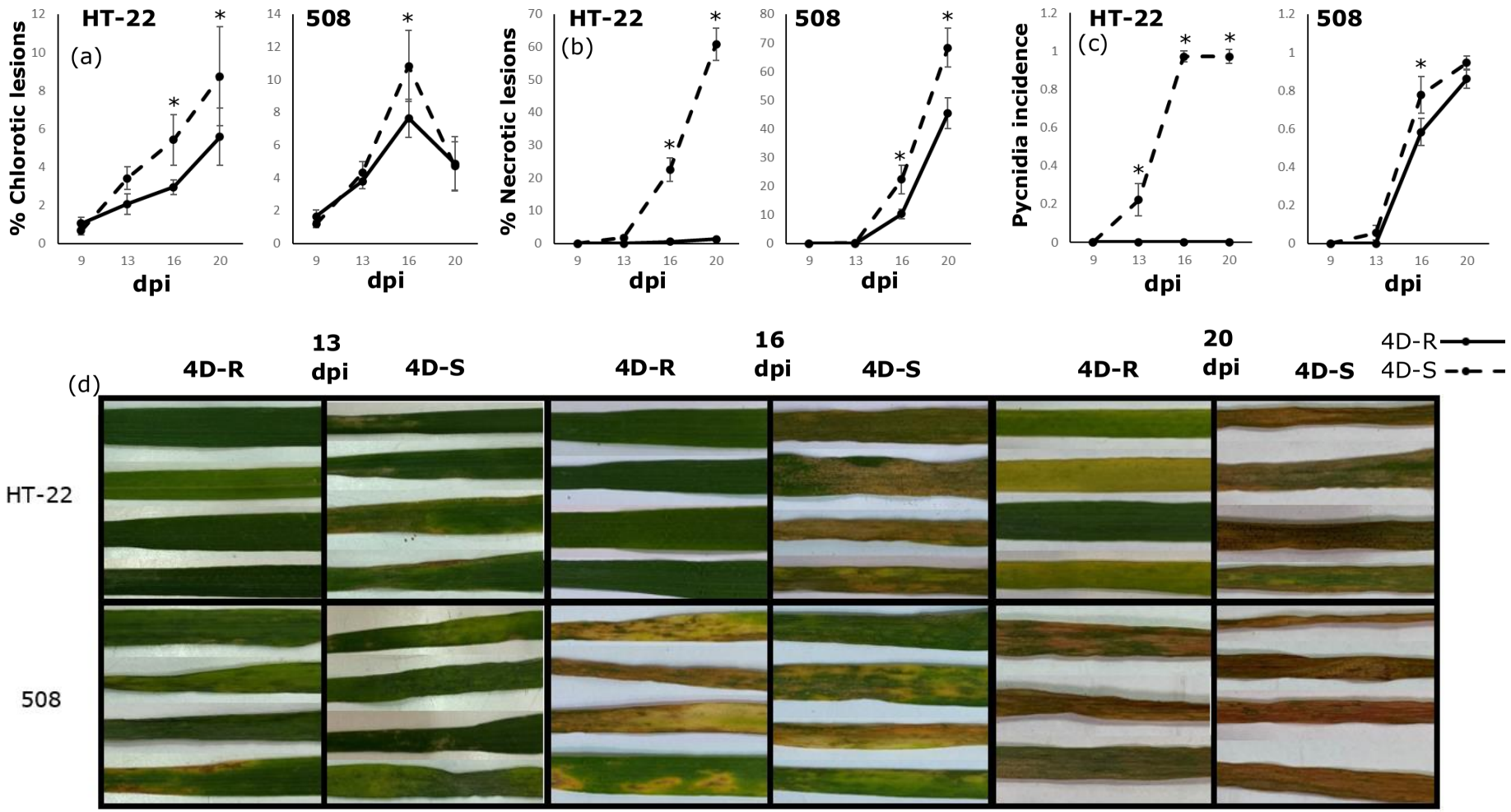



**Figure 1.** Visual assessment phenotype of 4D-R & 4D-S lines when inoculated with HT-22 or 508. 4D-R & 4D-S lines infected by HT-22 or 508 are analysed using student T-tests (Asterix indicates P<0.05) for (a), % Necrotic lesions (b) & pycnidia presence (c) (P <0.05). Effect of compatibility analysed using an ANOVA (Table S12). (d) Visual representative images of *Z.tritici* symptoms. Data are means of 12 biological replicates. SE bars are shown.

### 3.2 Chlorophyll fluorescence measurements

NPQ, qE/qI, $F_v/F_m$, PhiPS2, qP, ETR, conductance and photosynthesis were measured to investigate the physiology of the resistant response in 4D-R NILs as well as how these parameters change in the compatible interaction with 508. There were no differences between 4D-R/S NILs for $F_v/F_m$, with no effect of compatibility. The qI component of NPQ relaxed slower in 4D-R NILs compared to 4D-S NILs in response to HT-22 at 6 hpi (Fig. 2b, 3a), whilst there were no differences in response to 508. At 24 & 48 hpi 4D-R NILs had higher NPQ (Fig. 3cd), although qE differences were not statistically significantly at $P<0.05$. When examining the effect of compatibility on NPQ, compatibility had no significant effect on the maximum qE and qI, whereby 4D-R lines significantly increased qE at 48hpi and qI at 6hpi compared to 4D-S lines in response to HT-22 (Table S13, 14). However, taking into account the whole light response and recovery curve, compatibility was associated with a decrease in NPQ in the dark at 6 hpi and a decrease in response to light at 24 and 48 hpi. At 24 hpi 4D-R NILs decreased qP, ETR, PhiPS2, photosynthetic rate and conductance compared to 4D-S NILs in response to HT-22, whereas in response to 508 only functionality of the stomata decreased in response to light. At 48 hpi these differences were less pronounced for qP, ETR & PhiPS2, with no differences for photosynthetic rate and a slight decrease in conductance in 4D-R lines as part of the dark recovery. There was a significant effect of compatibility for qP, PhiPS2, ETR, photosynthetic rate and conductance at 24 and 48 hpi (Table S15). Additionally, photosynthetic rate and conductance were significantly affected by compatibility at 12 hpi with reduced photosynthesis and conductance in the incompatible interaction.

### 3.3 Fungal and stomatal staining assay

A staining assay was utilised to quantify stomatal and fungal behaviour in addition to LI-COR conductance measurements. At 6 hpi 4D-R NILs opened stomata in response to both HT-22 and 508 (Fig. 6) with no effect of compatibility (Table S16). At 24 hpi 4D-R NILs induced a decrease in germ tube number, and germination rate in response to 508, whereas only germ tube number decreased in response to HT-22 (Fig. 7). There was no effect of compatibility. 508 had a lower germination rate at 6 hpi compared to HT-22 (Table S17).

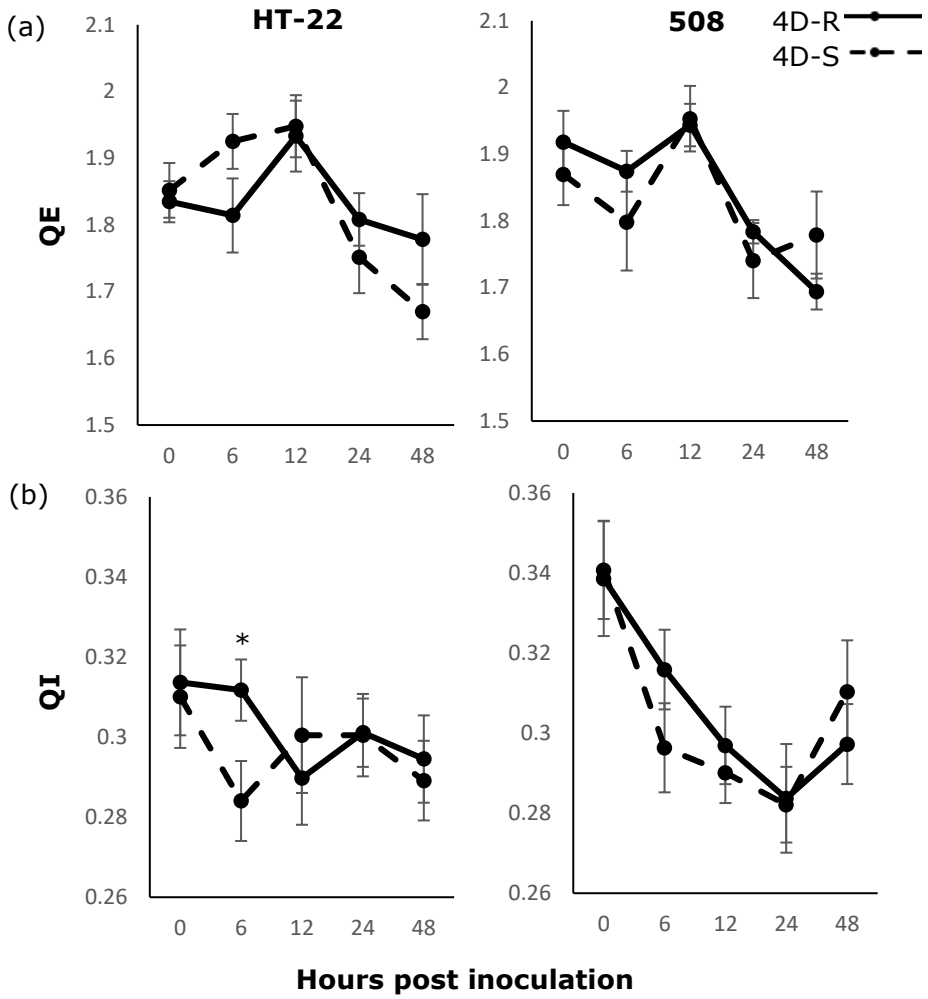



**Figure 2.** qE & qI form of NPQ of 4D-R & 4D-S lines inoculated with HT-22 or 508. 4D-R & 4D-S lines infected by HT-22 or 508 are analysed using student T-tests (Asterix indicates P<0.05). Effect of compatibility analysed using an ANOVA (Table S13). Data are means of 12 biological replicates. SE bars are shown.

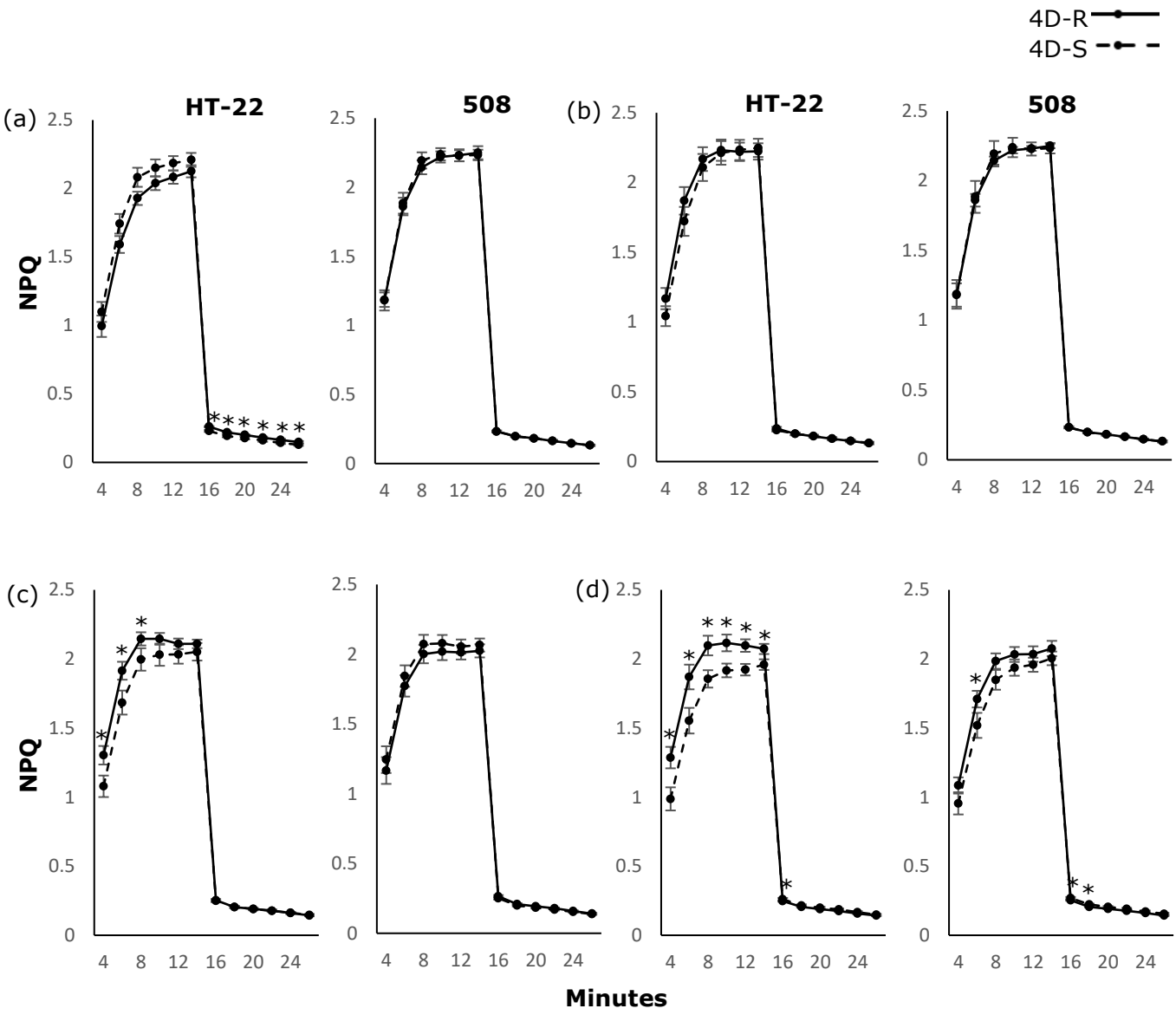



**Figure 3.** NPQ of 4D-R & 4D-S lines inoculated with HT-22 or 508 at 6(a), 12(b), 24(c) & 48(d) hpi. 4D-R & 4D-S lines infected by HT-22 or 508 are analysed using student T-tests (Asterix indicates $P<0.05$). Effect of compatibility analysed using an ANOVA (Table S14). Data are means of 12 biological replicates. SE bars are shown.

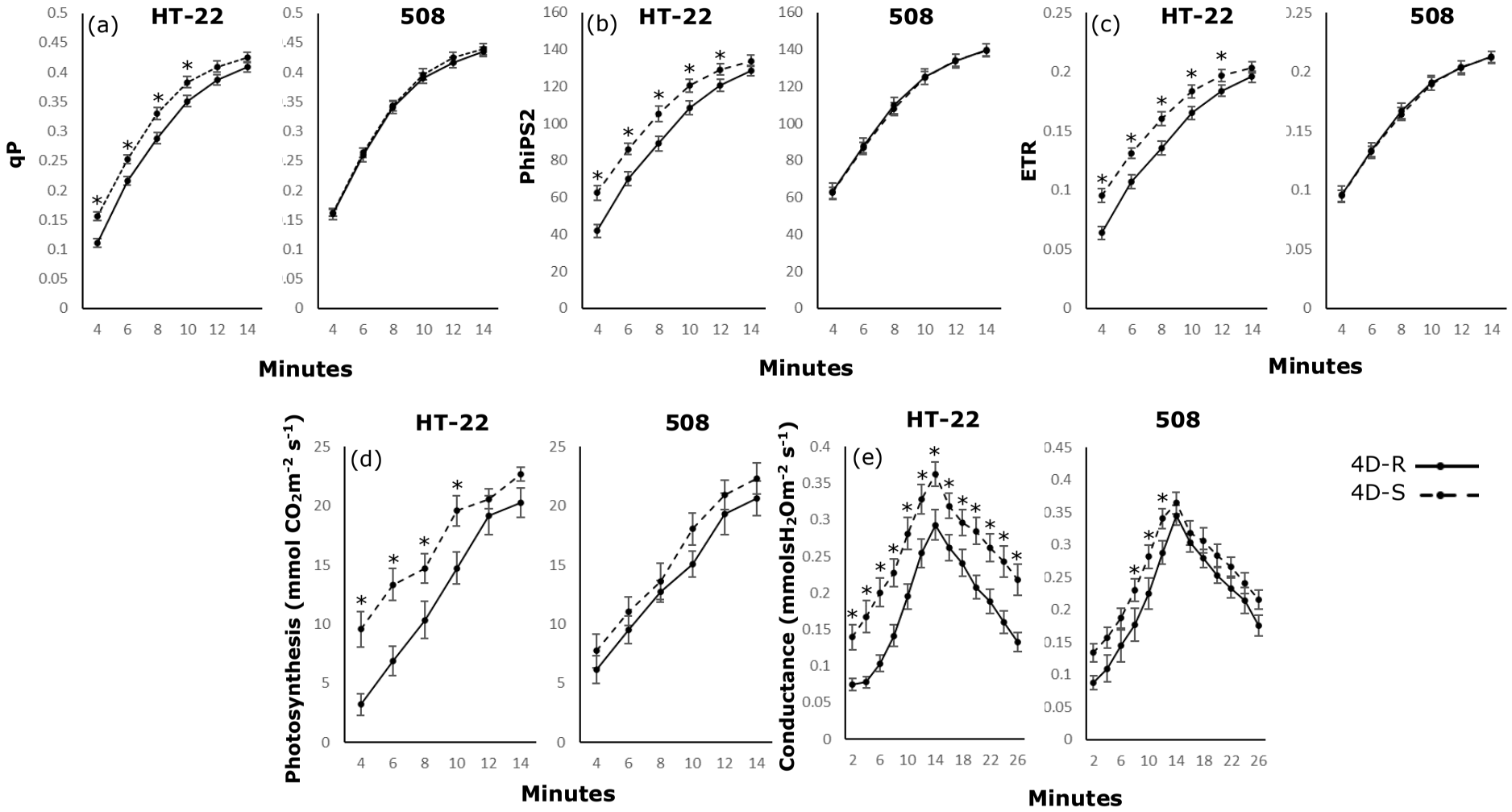



**Figure 4.** LI-COR phenotyping of 4D-R & 4D-S lines inoculated with HT-22 or 508 at 24 hpi for (a) qP, (b) PhiPS2, (c) ETR, (d) Photosynthesis & (e) Conductance. 4D-R & 4D-S lines infected by HT-22 or 508 are analysed using student T-tests (Asterix indicates $P<0.05$). Effect of compatibility analysed using an ANOVA (Table S15). Data are means of 12 biological replicates. SE bars are shown.

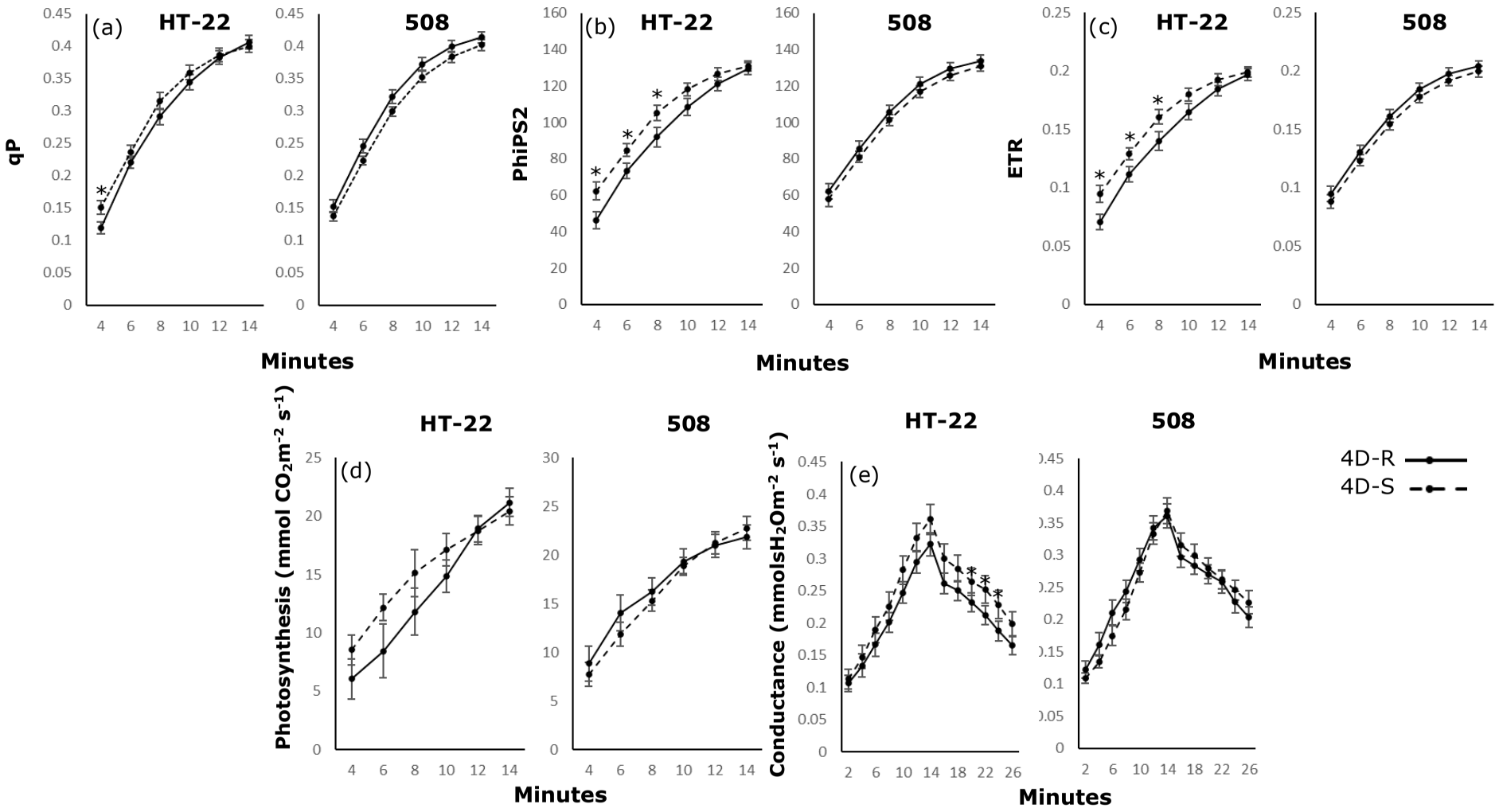



**Figure 5.** LI-COR phenotyping of 4D-R & 4D-S lines inoculated with HT-22 or 508 at 48 hpi for (a) qP, (b) PhiPS2, (c) ETR, (d) Photosynthesis & (e) Conductance. 4D-R & 4D-S lines infected by HT-22 or 508 are analysed using student T-tests (Asterix indicates $P<0.05$). Effect of compatibility analysed using an ANOVA (Table S15). Data are means of 12 biological replicates. SE bars are shown.

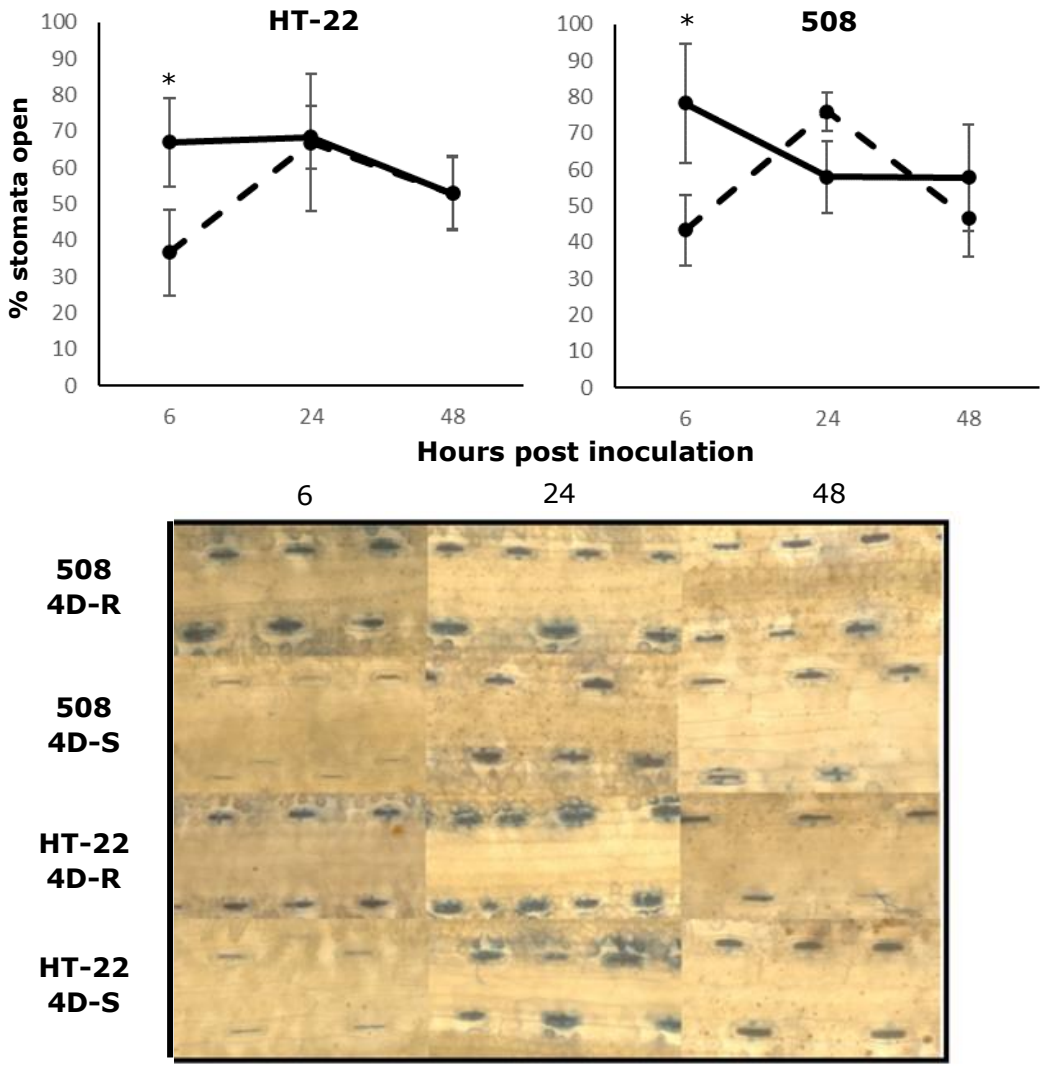



**Figure 6.** Stomatal response to *Z.tritici* isolates HT-22 & 508 on 4D-R & 4D-S NILs. 4D-R & 4D-S lines infected by HT-22 or 508 are analysed using student T-tests (Asterix indicates P<0.05). Effect of compatibility analysed using an ANOVA (Table S16). Data are means of 4 biological replicates. SE bars are shown.

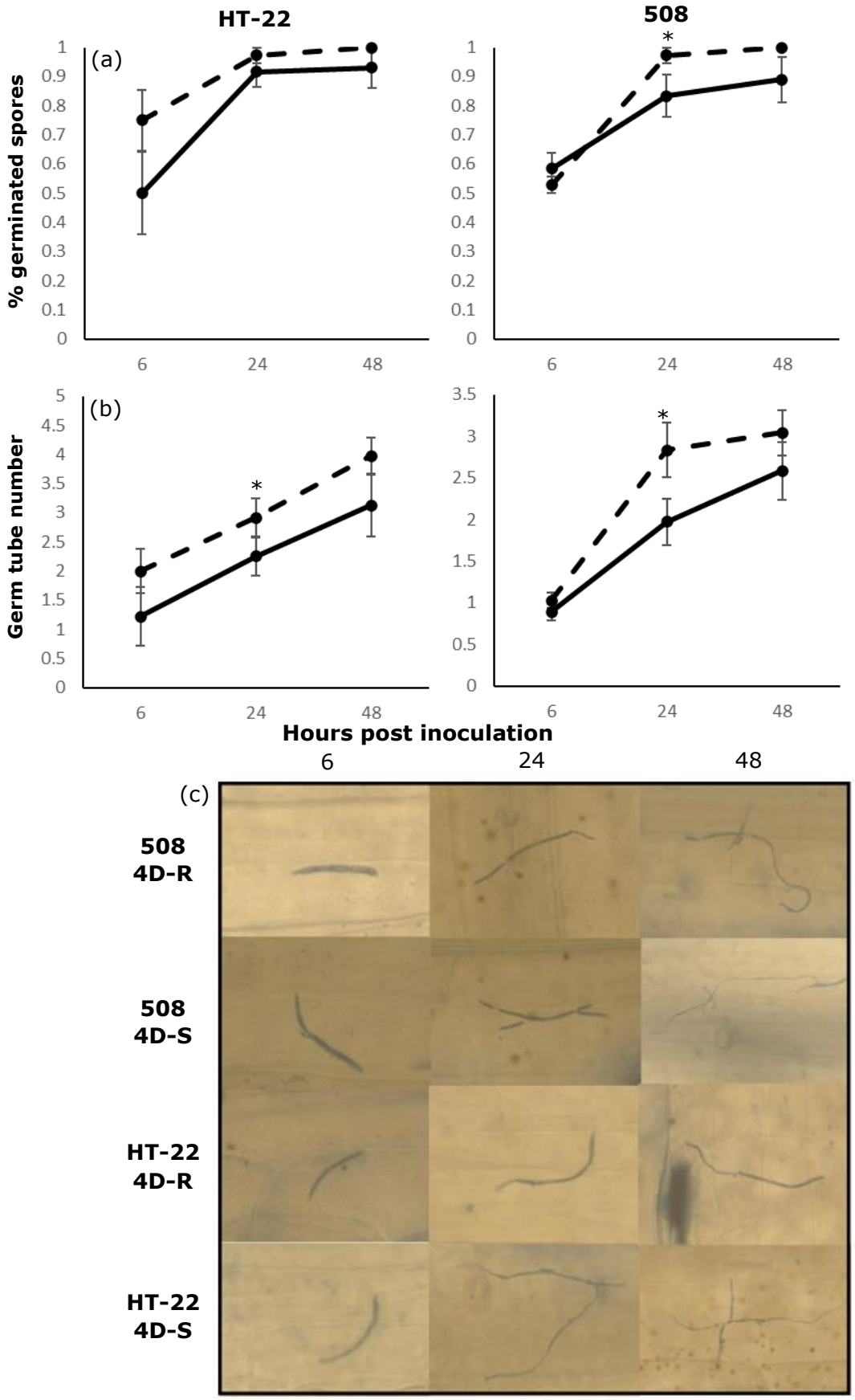



**Figure 7.** *Z.tritici* spore germination assay for isolates HT-22 & 508 on 4D-R and 4D-S NILs. (a) % germinated spores, (b) germ tube number, (c) representative spore germination images. 4D-R & 4D-S lines infected by HT-22 or 508 are analysed using student T-tests (Asterix indicates P<0.05). Effect of compatibility analysed using an ANOVA (Table S17). Data are means of 4 biological replicates. SE bars are shown.

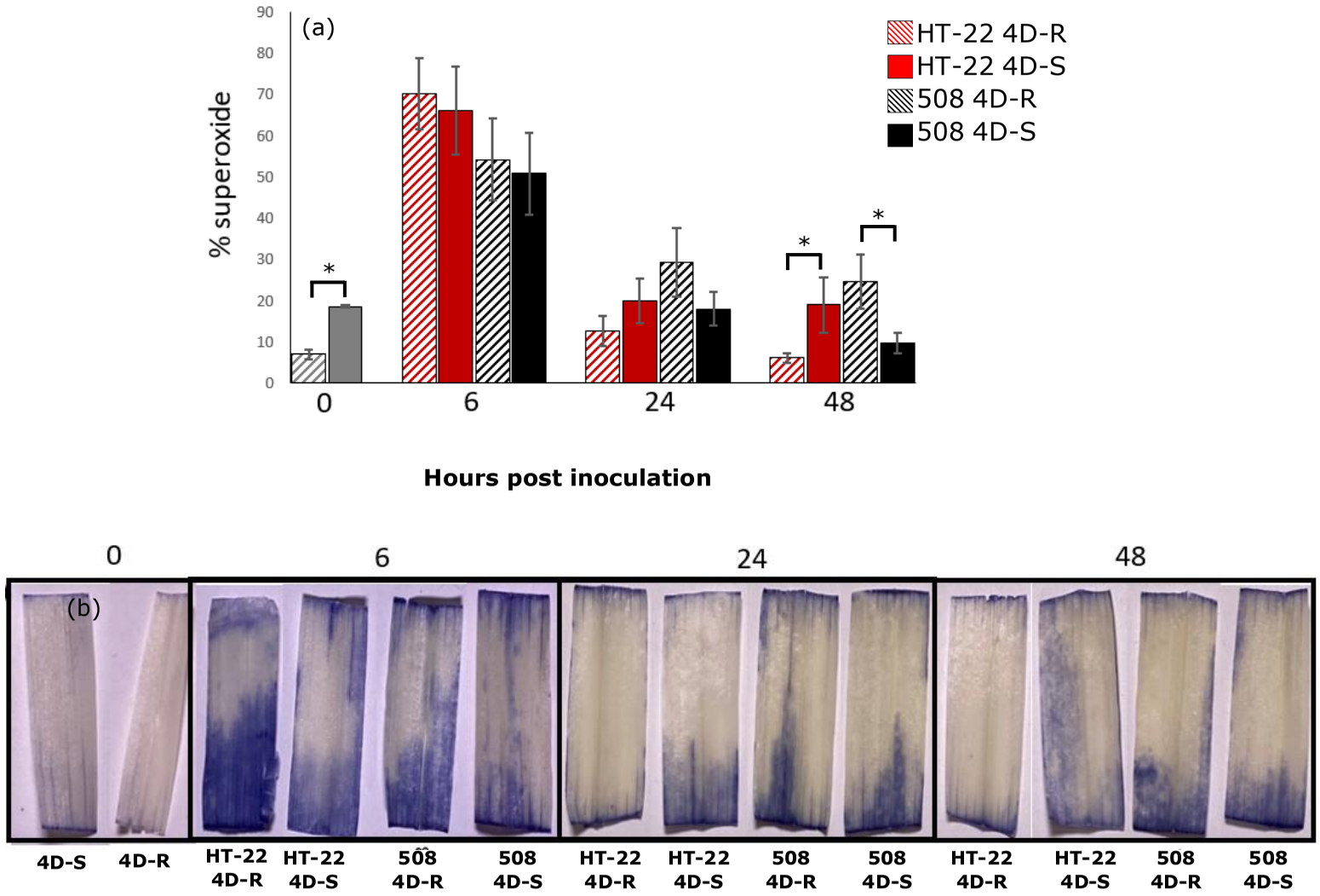



**Figure 8.** Superoxide quantification using Nitroblue tetrazolium (NBT) of 4D-R and 4D-S NILs inoculated with *Z.tritici* isolate HT-22 or 508. (a) Quantification, (b) representative images of staining. 4D-R & 4D-S lines infected by HT-22 or 508 are analysed using student T-tests. Effect of compatibility analysed using an ANOVA (Table S18). Data are means of 4 biological replicates.

### 3.4 Superoxide and hydrogen peroxide ROS assay

4D-R decreased superoxide content compared to 4D-S at 48 hpi in response to HT-22, although in response to 508 superoxide content increased. 4D-R NILs also had lower levels of superoxide before infection by *Z.tritici* (Fig. 8). There was no effect of compatibility on superoxide accumulation (Table S18). There was no differences in hydrogen peroxide content between any treatments.

### 3.5 Carotenoid & Xanthophyll enzyme quantification

Carotenoid quantification of the xanthophyll cycle included lutein, β-carotene, zeaxanthin, antheraxanthin, violaxanthin & neoxanthin (Fig. 9). 6 hpi after HT-22 infection 4D-R NILs increased β-carotene and violaxanthin content whilst decreasing lutein content compared to 4D-S NILs (Fig. 9) which is reflected in an increase in the XC pool (Table 2). 11 dpi after HT-22 infection 4D-R NILs had higher lutein and neoxanthin content whilst zeaxanthin and violaxanthin content decreased compared to 4D-S NILs resulting in a decreased XC pool and DEP state (Table 2). There were no differences between 4D-R/S NILs at both 6hpi and 11dpi in response to 508. At 6 hpi there was no effect of compatibility, however at 11 dpi compatibility was associated with decreased lutein and neoxanthin content and an increase in the XC pool comprising of zeaxanthin and violaxanthin (Table S19).

There were no significant differences between 4D-S/R NILs for xanthophyll conversion enzymes ZEP, VDE and NCED in response to HT-22. However, at 6 hpi ZEP significant increased in 4D-R lines inoculated by HT-22 or 508. Additionally, isolates had an effect on NCED with higher NCED expression in response to 508. At 11 dpi compatibility was associated with an increase in VDE expression (Table S19).

**Table 2.** Pigment content of 4D-R & 4D-S NILs inoculated with HT-22 or 508. 4D-R & 4D-S lines infected by HT-22 or 508 are analysed using student T-tests (Asterix indicates P <0.05 for 4D-R/S comparison). Effect of compatibility analysed using an ANOVA (Table S19). Data are means of 3 biological replicates.

| | 0 hpi | | 6 hpi | | | | 11 dpi | | | |
|---|---|---|---|---|---|---|---|---|---|---|
| Pigment[a] | | | HT-22 | | 508 | | HT-22 | | 508 | |
| | 4D | No4D | 4D | No4D | 4D | No4D | 4D | No4D | 4D | No4D |
| Chl a:b | 5.53 | 2.52 | 2.75 | 1.72 | 2.48 | 2.90 | 2.74 | 2.29 | 2.77 | 3.62 |
| Car:Chl | 0.54 | 0.84 | 0.50 | 0.91 | 0.62 | 0.50 | 1.09 | 0.21 | 0.30 | 0.22 |
| XC pool | 50.87 | 59.33 | 74.25* | 11.29* | 81.24 | 50.82 | 0.00* | 25.42* | 39.70 | 30.33 |
| DEP | 1.55 | 1.26 | 7.33 | 15.23 | 5.80 | 0.46 | 0.00* | 7.02* | 28.41 | 11.23 |

[a]Chl, chlorophylls; Car:Chl, ratio of total carotenoids; XC, xanthophyll cycle; DEP, de-epoxidation state; hpi, hours post inoculation; dpi, days post inoculation

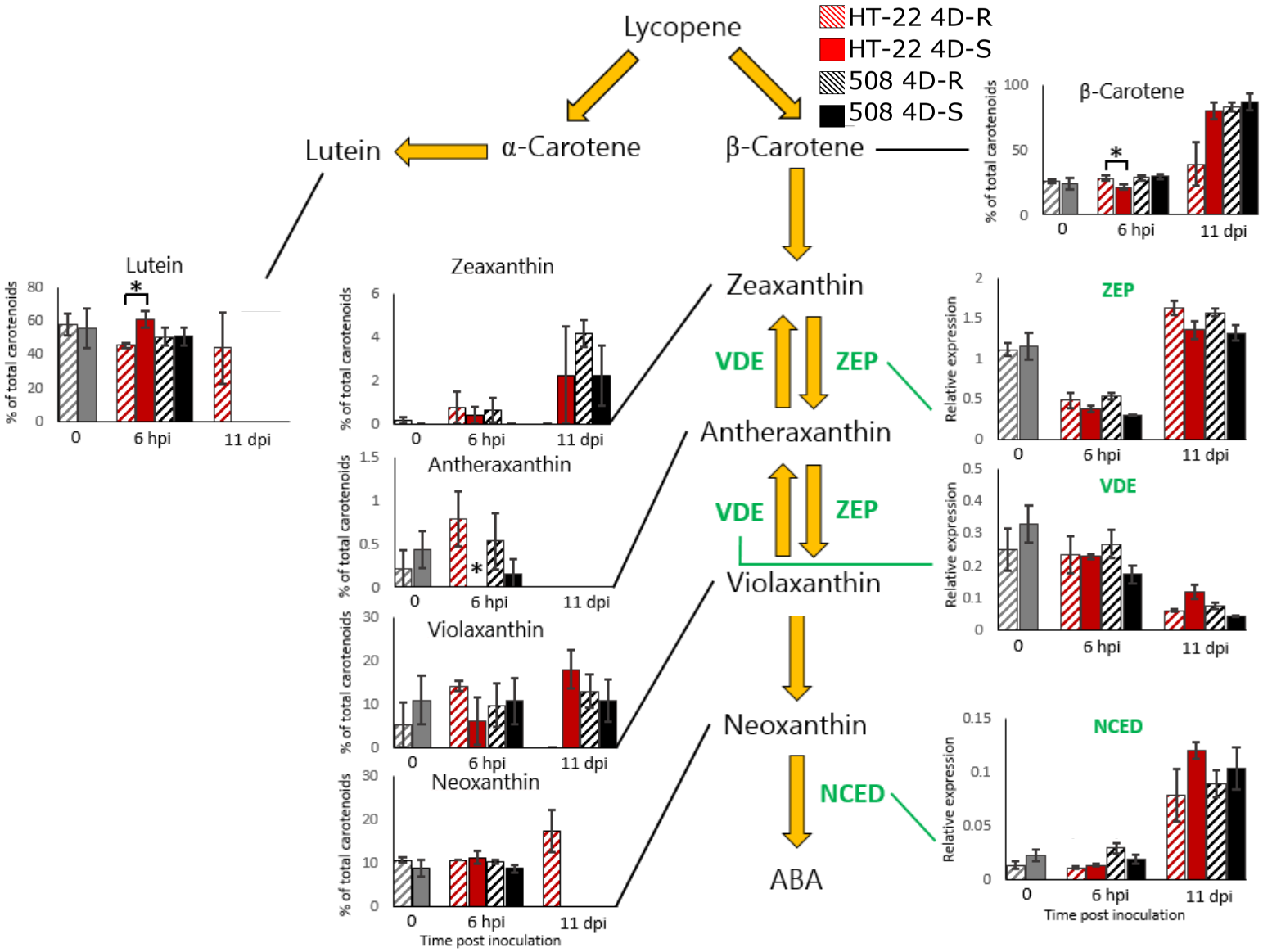



**Figure 9.** Effect of *Z.tritici* isolates HT-22 & 508 on Lycopene derived xanthophyll's and xanthophyll metabolism genes in 4D-R and 4D-S NILs. VDE (Violaxanthin de-epoxidase), ZEP (zeaxanthin epoxidase), NCED (Epoxycarotenoid dioxygenase). SE bars are displayed for 3 biological reps. 4D-R & 4D-S lines infected by HT-22 or 508 are analysed using student T-tests (Asterix indicates $P<0.05$). Effect of compatibility analysed using an ANOVA (Table S19.D20).

### 3.6 Hormone quantification

Hormone quantification included a variety of hormones and hormone precursors which could aid in characterising 4D-R NILs and investigate the effect of compatibility (Table 3, Table S10). 4D-R NILs increased JA content relative to 4D-S NILs at 6 hpi and decreased SA content at 11 dpi. Prior to *Z.tritici* inoculation GA3 content was higher in 4D-R NILs (Table 3). GA3 was affected by compatibility at 6 hpi with increased GA3 content in the incompatible interaction. ZR content significantly increased in 4D-R NILs compared to 4D-S NILs independent of *Z.tritici* inoculation at 6 hpi.

**Table 3.** Hormone content of 4D-R & 4D-S NILs inoculated with HT-22 or 508. 4D-R & 4D-S lines infected by HT-22 or 508 are analysed using student T-tests. (Asterix indicates $P < 0.05$ between 4D-R/S) Effect of compatibility analysed using an ANOVA (Table S21, S22). Data are means of 3 biological replicates.

| Hormone | 0 hpi | | 6hpi | | | | 11 dpi | | | |
|---|---|---|---|---|---|---|---|---|---|---|
| (ng/g DW) | Water | | HT-22 | | 508 | | HT-22 | | 508 | |
| | 4D-R | 4D-S | 4D-R | 4D-S | 4D-R | 4D-S | 4D-R | 4D-S | 4D-R | 4D-S |
| ABA | 16.2 | 14.2 | 11.6 | 10.2 | 8.3 | 7.8 | 7.2 | 8.8 | 8.9 | 7.3 |
| SA | 4111.9 | 3745.8 | 1737.1 | 1744.3 | 1278.9 | 996.0 | 1518.4* | 2940.8* | 2949.7 | 3120.9 |
| JA | 11.3 | 11.2 | 9.9* | 6.2* | 14.8 | 7.6 | 3.8 | 10.1 | 6.4 | 18.8 |
| OPDA | 103.2 | 171.7 | 28.8 | 33.2 | 39.9 | 25.7 | 18.6 | 14.2 | 22.4 | 21.8 |
| Ja-Ile | 0.1 | 0.0 | 0.0 | 0.0 | 0.1 | 0.1 | 0.0 | 0.1 | 0.3 | 0.1 |
| IAA | 8.9 | 7.5 | 11.3 | 13.7 | 10.4 | 10.3 | 5.7 | 6.1 | 5.2 | 10.4 |
| GA1 | 6.8 | 7.2 | 11.6 | 13.0 | 10.6 | 14.4 | 11.4 | 23.4 | 35.4 | 50.3 |
| GA3 | 276.9* | 132.1* | 189.3 | 85.3 | 67.3 | 84.1 | 53.8 | 210.2 | 91.1 | 202.3 |
| GA7 | 23.9 | 53.5 | 34.4 | 9.1 | 6.7 | 29.1 | 5.2 | 5.9 | 6.2 | 7.0 |
| ACC | 59.4 | 79.7 | 58.8 | 55.8 | 74.3 | 64.9 | 60.8 | 103.2 | 128.5 | 120.2 |
| IPA | 1.6 | 1.7 | 1.0 | 1.1 | 1.1 | 0.7 | 0.4 | 0.8 | 0.7 | 0.6 |
| 2iP | 0.5 | 1.0 | 0.5 | 1.2 | 0.8 | 0.5 | 1.4 | 2.4 | 2.8 | 2.7 |
| Z | 6.1 | 10.2 | 4.6 | 5.2 | 5.2 | 5.6 | 11.8 | 10.9 | 12.0 | 16.9 |
| ZR | 7.4 | 13.4 | 10.8 | 2.8 | 22.1 | 4.9 | 6.3 | 5.7 | 21.2 | 8.0 |

ABA; Abscisic acid, SA; Salicylic acid, JA; Jasmonic acid, OPDA; oxo-Phytodienoic acid, Ja-Ile; jasmonoyl-L-isoleucine, IAA; Indole-3-acetic acid, GA1, 3, 7; Gibberellin, ACC; 1-Aminocyclopropane 1-carboxylic acid, IPA; Indole-3-propionic acid, 2iP; 6-(γ,γ-Dimethylallylamino)purine, Z; Zeatin, ZR; zeatin riboside

## 4. Discussion

Visual assessments of *Z.tritici* symptoms demonstrated that the major source of resistance on 4D in Cougar is incompatible with *Z.tritici* isolate HT-22, whilst the interaction with 508 is compatible. These comparisons enable both the specific characterisation of the major source of resistance on 4D in Cougar and the characterisation of incompatible and compatible wheat-*Z.tritici* interactions. Ajigboye *et al* (2021) highlighted numerous traits associated with the Cougar defence response, however its uncertain what traits contributed towards the resistance phenotype. This study improves on the work from Ajigboye *et al* (2021) by characterising the major source of resistance in Cougar, whereby we can infer what traits are associated with the major source of resistance and what are attributed to other qualitative and/or quantitative sources of resistance.

Early in the infection process (6-48hpi) the major source of resistance in Cougar is associated with numerous physiological changes which contribute to the resistant phenotype. Fungal staining assays demonstrated that 4D-R NILs decreased germ tube number similar to shown by Cougar as published by Ajigboye *et al* (2021). However, 4D-R NILs also reduced germination rate and germination tube number of 508 which has overcome the resistance suggesting that these effects on fungal behaviour were as a result of basal resistance from Cougar. Stomata behaviour was also independent of compatibility with 4D-R NILs opening stomata at 6 hpi when inoculated with HT-22 or 508. These results suggests that these preformed defence traits are induced by all isolates of *Z.tritici* irrespective of virulence and does not form part of an effector triggered immunity (ETI) response but rather of pathogen associated molecular pattern triggered immunity (PTI). Although stomata from 4D-R NILs opened at 6 hpi independent of isolate inoculation, compatibility did affect stomatal functionality at 12, 24 & 48 hpi, with reduced conductance in the incompatible interaction suggesting that this response plays a role in ETI.

Chlorophyll fluorescence measurements (CFMs) highlight differences in photoprotective and photosynthetic processes early in the infection process. In the incompatible interaction 4D-R NILs downregulated many photosynthetic processes at 24 & 48 hpi including qP, ETR, PhiPS2 and photosynthetic rate, whilst increasing photoprotective mechanisms (NPQ), namely qI at 6 hpi and qE at 24 & 48 hpi. These results confirm those presented by Ajigboye *et al* (2021), although the qI responses were detected earlier in this study at 6 hpi. Although the incompatible interaction displayed differences in qI this was not significantly associated with compatibility,

however taking the whole light curve into account, compatibility was associated with increased NPQ measured as part of the dark adapted protocol at 6 hpi and in response to light at 24 and 48 hpi. This demonstrates the need to investigate the full light response curve instead of solely utilising the last measurement to calculate qE/qI. This increase in the qI component of NPQ typically indicates reorganisation of the light harvesting complexes possibly by reducing or reassembling specific antennae to downregulate light-harvesting and/or inactivation of D1. D1 typically has a high turnover rate and hence is constantly recycled as part of the D1-repair cycle (Kato *et al* 2012). Phosphorylation and removal of D1 from the thylakoid stacks to the stromal lamella reduces ROS generation and hence acts as a photoprotective mechanism to shield the host against photooxidative damage caused by excessive ROS (Staleva *et al* 2015; Malnoe 2018). qE is better characterised compared to qI and typically indicates re-organisation of the light harvesting complexes into a quenching state facilitated by conversion of violaxanthin to zeaxanthin and protonation of PsbS (Murchie & Ruban 2020). We also acknowledge that our CFMs also encapsulate other quenching processes such as migration of light harvesting complexes from PSII to PSI (state transition; qT), stomatal movement (qM) and the newly termed qH which involves LCNP mediated quenching (Malnoe 2018). The downregulation of photosynthetic quenching combined with upregulation of NPQ processes demonstrates photoinhibitory and photoprotective mechanisms are associated with the major source of resistance in Cougar, however the extent to which this is unique to this source of resistance is unknown.

At 6 hpi, the major source of resistance was associated with an increase in the XC pool through accumulation of antheraxanthin, whilst there was an increase in β-carotene content and decrease in lutein. These changes in xanthophyll composition could reflect changes in light harvesting complex and PSII functionality which we demonstrated through an increase in NPQ and downregulation of qP, ETR and PhiPS2. For example, β-carotene is involved in D1 turnover required in photoprotection (Nayak et al 2002) and quenching of single oxygen species (Telfer *et al* 1994), whilst accumulation of antheraxanthin likely reflects the lack of the qE photoprotective response requiring zeaxanthin at 6 hpi (Färber *et al* 1997). Additionally, carotenoids have antioxidant capabilities suggesting their importance in detoxification of ROS (Jahns & Holzwarth 2012). These changes are likely unique to the major source of resistance in Cougar due to there being no effect of compatibility on carotenoid composition. 4D-R NILs also increased ZEP expression independent of compatibility, suggesting that the major source of resistance is associated with conversion of zeaxanthin into violaxanthin. Investigating these

results compared to Ajigboye *et al* (2021), both this study and Ajigboye *et al* (2021) demonstrated a decrease in lutein and an increase in neoxanthin. Hormone metabolic analysis failed to confirm a significant increase in ABA content demonstrated by Ajigboye *et al* (2021) and chapter 3 of this thesis. However, high levels of variability in the hormone data could explain why many comparisons failed to reach the significance threshold. Additionally, different timings, different plant material and a different *Z.tritici* isolate were used in both studies so the results aren't directly comparable.

At 6 hpi the major source of resistance was associated with an increase in JA, a well characterised plant hormone involved in defence responses and demonstrated to be influential in the wheat-*Z.tritici* incompatible interaction (Campanaro *et al* 2021). ZR was also upregulated in 4D-R NILs however this was in response to both isolates demonstrating that this didn't contribute towards the disease phenotype. Lastly, compatibility was associated with accumulation of GA3 which could be involved in regulation of JA & SA (Navarro *et al* 2008). Interestingly, since GA stimulates degradation of DELLA proteins (Navarro *et al* 2008; Achard *et al* 2006) it is likely that this hormone promotes resistance to biotrophs, which could facilitate incompatibility early in *Z.*tritici's asymptomatic phase (Bari & Jones 2009).

Due to downregulation of photosynthetic processes (qP, ETR, PhiPS2, phototsynthesis, conductance), upregulation of NPQ and changes in carotenoid and hormone composition, this data suggests a decrease in ROS generation and increase in ROS breakdown. This study investigated superoxide and hydrogen peroxide accumulation early in the defence response and demonstrated a decrease in superoxide content at 48 hpi in 4D-R NILs compared to 4D-S NILs in the incompatible interaction. However, there was no effect of compatibility, suggesting that this response is unique to the major source of resistance in Cougar. It is interesting that from 6 – 48 hpi the major source of resistance in Cougar and the incompatible wheat-*Z.tritici* interaction involved numerous processes involved in clearing ROS. During the asymptomatic phase of infection ROS generation would likely lead to premature cell death preceding the necrotrophic phase of infection, which is required for *Z.tritici* compatibility and sexual/asexual propagation (Sánchez-Vallet *et al* 2015).

In addition to characterising the major source of resistance in Cougar and the effect of compatibility at 6 hpi, this study investigated the changes in carotenoid and hormone composition at the switch to necrotrophy (11 dpi). The major source of resistance and incompatibility was associated with increased lutein and neoxanthin accumulation, whereas β-

Carotene content and the XC pool decreased. VDE expression also decreased. Lutein is a core component of LHCII and has potent anti-oxidant capabilities by quenching $^{3}$Chl, in addition to playing a significant role in NPQ (Muller & Niyogi *et al* 2001; Jahns & Holzwarth 2012). Neoxanthin is also a potent anti-oxidant (Giossi *et al* 2020) as well as the precursor to ABA, which plays a significant role in the Cougar resistance (Ajigboye *et al* 2021). These results starkly contrast with the results at 6 hpi, demonstrating a change in carotenoid composition required for incompatibility at the switch to necrotrophy. It is surprising that at 11 dpi the incompatible interaction lacked a XC pool which is required for NPQ processes, suggesting that the anti-oxidant properties of lutein and neoxanthin could be more influential in the defence response. The major source of resistance in Cougar was also associated with a decrease in SA content. Due to the typical role of SA in biotic defence responses (Bari & Jones 2009), it isn't surprising that lower SA levels were associated with resistance. Although, there was no effect of compatibility on any hormone at 11 dpi. These results demonstrate that at different stages in the wheat-*Z.tritici* lifecycle carotenoid composition required for incompatibility is highly dynamic.

Ajigboye *et al* (2021) demonstrated distinct differences between the Cougar and Sacramento defence response. However, it was unknown what differences are a) attributed to the major source of resistance and b) contribute towards incompatibility. By utilising NILs for the major source of resistance and a *Z.tritici* isolate that has overcome this resistance, this study has investigated these limitations. The data from this study suggests that the major source of resistance on 4D in Cougar encodes for preformed defence traits which don't contribute towards ETI immunity. Many differences between Cougar and Sacramento from Ajigboye *et al* (2021) are most likely attributed to other sources of qualitative and/or quantitative genes in Cougar that may or may not contribute towards resistance. Likewise, differences in hydrogen peroxide accumulation might not be attributed towards the major source of resistance in Cougar or contribute towards resistance (Ajigboye *et al* 2021). However, the results from this paper confirms the role of the photoprotective defence response as part of the major defence response on 4D in Cougar, involving downregulation of photosynthetic process and upregulation of both qI and qE NPQ components.

Overall, this study demonstrated that wheat-*Z.tritici* incompatibility was associated with:

- Increased NPQ in the dark at 6 hpi and light at 24 & 48 hpi
- Decrease in qP, ETR and PhiPS2 at 24 & 48 hpi
- Decrease in photosynthesis and conductance at 12, 24 & 48 hpi
- Accumulation of GA3 at 6 hpi
- Increased Lutein and Neoxanthin at 11 dpi
- Decrease of β-Carotene and lack of a XC pool at 11 dpi
- Decrease in VDE expression

Whilst the major source of resistance on 4D in Cougar was specifically associated with:

- Decreasing spore germination rate independent of compatibility
- Stomata opening at 6 hpi independent of compatibility
- Increase in ZR independent of compatibility
- Increased QI at 6 hpi and NPQ in the light at 24 & 48 hpi
- Decrease in qP, ETR and PhiPS2 at 24 & 48 hpi
- Decrease in photosynthesis and conductance at 12, 24 & 48 hpi
- Decrease in Lutein at 6 hpi
- Increase in β-Carotene and Antheraxanthin content at 6 hpi
- Increased Lutein and Neoxanthin accumulation at 11 dpi
- Decrease of β-Carotene and lack of a XC pool at 11 dpi
- Increase in JA at 6 hpi
- Decrease in SA at 11 dpi
- Decrease in superoxide at 48 hpi and at 0 hpi in the absence of *Z,tritici*.

In addition to characterising the major source of resistance on 4D in Cougar and the wheat-*Z.tritici* compatible and incompatible interaction, this study identified what traits characterised in Ajigboye *et al* (2021) were associated with the major source resistance and what traits are likely part of Cougars background resistance, or which fail to contribute towards *Z.tritici* resistance. The work by Ajigboye *et al* (2021) and this study help to identify traits which are associated with background sources of resistance which are likely quantitative, and hence are highly desirable for breeders. Future work investigating other resistance genes would be needed to confirm what aspects of the incompatible defence response presented in this study are unique to the major source of resistance on 4D in Cougar.

# Chapter 6.

# General discussion and conclusions

# 1. General Discussion

Cv. Cougar has been of specific interest to breeders due in part to its high *Z.tritici* resistance rating in 2013 (AHDB RL 2013). Despite Cougar's removal from the recommended list (RL) in 2015 it has been used as a parental line to develop novel cultivars (KWS Firefly, LG Illuminate, RGT Saki, Merit, LG Prince, LG Astronomer, Swallow). Caiazzo *et al* (2019) demonstrated the evolution of *Z.tritici* genotypes with virulence to Cougar resistance, with Kildea *et al* (2021) subsequently showing this in cultivars with Cougar parentage in Ireland, where Cougar hasn't been commercially grown. Furthermore, a decrease in *Z.tritici* resistance ratings was reported by AHDB in 2021/2022 in cultivars with Cougar parentage. This evidence suggests that Cougar contains a major source of resistance which has broken down leading to a ~0.6-1.9 decrease in *Z.tritici* resistance score.

This PhD confirmed the presence of this major source of resistance in Cougar on 4D in 2018 by utilising QTL analyses from STB assessment data and hyperspectral reflectance data. NPQI (Pheophitinization of chlorophyll a to phaeophytin) was the best hyperspectral index to identify the major source of resistance. An increase in RARSc, PSSRa,/b, ND705 (chlorophyll & carotenoid content) and a decrease in NPQI & D2 (chlorophyll fluorescence) in lines containing the major source of resistance suggests that the major source of resistance in Cougar is associated with elevated chlorophyll and carotenoid content and PSII downregulation as demonstrated by Ajigboye *et al* (2021). Interestingly, the major source of resistance on 4D was not detectable in 2019, suggesting an emergence of virulent pathogens in the local pathogen population between 2018 and 2019.

Chapter 2 of this thesis demonstrated the role of chlorophyll fluorescence and hyperspectral reflectance measurements on *Z.tritici* resistance gene identification, having identified 5 additional resistance genes from both Cougar and Scout. Correlations for ND705 (Yu *et al* 2018; Odilbekov *et al* 2018), D2, PSSRa/b & ARI (Odilbekov *et al* 2018) were consistent with previous studies on *Z.tritici*. Additionally, LRDSI1/2 for leaf rust (Ashourloo *et al* 2014), SIPI, PSSRa/b, RARSc and LRDSI1/2 for Fusarium Head Blight (Mustafa *et al* 2022) and PWI/ARI for Powdery Mildew (Feng *et al* 2017) correlated in a similar manner to this study. These results show that whilst these indices correlate with *Z.tritici* disease, they are unlikely to be able to differentiate between different diseases, especially for leaf rusts since LRDSI1/2 (designed to quantify leaf rusts Ashourloo *et al* 2014) were amongst the best indices in this study for detecting *Z.tritici*. However, if the goal for breeders is to select for the best performing

cultivar against a variety diseases then index specificity might be less important. This chapter also highlighted how chlorophyll fluorescence and hyperspectral reflectance measurements can be used to predict future STB disease, which might aid in increasing the phenotyping window for breeders.

Previous work on investigating the mechanisms of resistance to *Z.tritici* has primarily been constrained to understanding the gene-for-gene effector triggered immunity (ETI) response for specific genes such as Stb7, Stb12 (Meile *et al* 2018), Stb6 (Brading *et al* 2002; Saintenac *et al* 2018; Mirzadi Gohari 2015; Zhong *et al* 2017; Kildea *et al* 2021) and Stb16q (Saintenac *et al* 2021). Whilst this has considerably advanced our understanding of the wheat-*Z.tritici* interaction, research regarding the downstream mechanisms of resistance is lacking. Specific genes have been identified which have been shown to be involved in the *Z.tritici*-wheat defence response (Ray *et al* 2003; Adhikari *et al* 2007; Shetty *et al* 2009), however the functionality of some these genes might not be repeatable (Orton *et al* 2017). Transcriptomic analyses are therefore needed to understand the *Z.tritici*-wheat incompatible interaction in a more holistic manner. Odilbekov *et al* (2019) and Benbow *et al* (2020) investigated the transcriptome of wheat in response to *Z.tritici*, with Odilbekov *et al* (2019) linking genes to specific *Z.tritici* QTLs and Benbow *et al* (2020) comparing two cultivars in response to a single isolate.

This PhD builds on this existing knowledge by using two incompatible interactions, using near isogenic lines (NILs) for the major source of resistance in Cougar. 73 transcripts were differentially expressed at 6hpi and 56 at 11dpi in the conserved incompatible interaction. These primarily included transcripts associated with disease related protein kinases, F-box proteins and cytochrome P450 proteins. This transcriptomic analysis also demonstrated a differential defence response to the different *Z.tritici* isolates (IPO323/HT-22) including a range of transcripts associated with hormone regulation, carotenoid metabolism, electron transport, detoxification, PSII related proteins and protein kinases. To gain further insight into the Cougar incompatible resistance mechanism, hormone quantification, chlorophyll fluorescence measurements and RT-qPCR of xanthophyll related genes was carried out. Chlorophyll fluorescence measurements demonstrated a decrease in PhiPS2 at 6 hpi in both incompatible interactions, whilst there was an increase in the qI component of NPQ, consistent with Ajigboye *et al* (2021) in response to HT-22. Hormone quantification also showed differences between isolate resistance responses, with a decrease in SA at 11 dpi associated with incompatibility. Additionally, ZEP and NCED expression increased in 4D-R lines compared to 4D-S lines in response to HT-22 but not to IPO323. These results demonstrate

that the major source of resistance in Cougar is associated with changes in the transcriptome associated with hormone and protein kinase regulation and changes in photosynthetic functionality. Additionally, this study highlights that the resistant incompatible wheat-*Z.tritici* interaction is highly isolate specific, and hence multiple incompatible interactions are needed to filter out isolate specific responses which aren't likely to be associated with resistance.

To further understand the mechanism of resistance for the major source of resistance in Cougar the defence response in response to HT-22 (incompatible interaction) and 508 which is virulent to the major source of resistance in Cougar (compatible interaction) was investigated. This chapter demonstrated that the major source of resistance was associated with changes in photosynthetic functionality, increased photoprotection, decreased superoxide accumulation, changes in SA/JA content and changes in carotenoid composition. This confirmed many findings from previous work on Cougar by Ajigboye *et al* (2021) such as changes in carotenoid content, specifically neoxanthin and lutein, and an increase in the qI and qE component of NPQ. Additionally, this chapter demonstrated that preformed defence traits are induced by all isolates of *Z.tritici* irrespective of virulence and does not form part of an ETI response but rather of pathogen associated molecular pattern triggered immunity PTI. Some findings from Ajigboye *et al* (2021) were not repeatable, however it is worth noting that different timings, different plant material and a different *Z.tritici* isolate were used in both studies and hence the results aren't directly comparable.

QTL analysis from chapter 2 of this thesis identified the major source of resistance in Cougar to be located within a 1.3cm region on 4D at the peak marker AX-94733088 (PL: 3609069), with further mapping by RAGT narrowing it down to between AX-94733088 (PL: 3609069) and AX-94627860_k (PL: 4361772) with a lower level of confidence that the gene(s) could also reside between AX-95200287_k (PL: 3253229) and AX-89639967_K (PL: 6758600). Three candidate resistance genes were identified from the transcriptomic analysis which resided within this region which were TraesCD4D02G006300, TraesCD4D02G007300 and TraesCD4D02G007600. SNP data, which was consistent for both HT-22 & IPO323 incompatible interactions, was collected between 4D-R and 4D-S NILs which identified a range of SNPs which could be impacting protein translation and functionality. TraesCD4D02G006300 and TraesCD4D02G007300 are similar LRR kinases with homology to other disease related kinases, whilst TraesCD4D02G007600 encodes R3H and SUZ domains involved in RNA binding. (A brief summary of the evidence for each candidate gene is summarised in table 1). These results suggest that these candidate genes could be responsible

for the major source of resistance in Cougar. However, further work is required such as virus induced gene silencing (VIGS), work with tilling lines, and cloning like with Stb6 (Saintenac *et al* 2018) and Stb16q (Saintenac *et al* 2021) to confirm or disprove these candidate gene(s) role in the major source of resistance in Cougar.

Overall, this PhD has built on previous work by Caiazzo *et al* (2019) & Kildea *et al* (2021), showing that Cougar has a major source of resistance on 4D which was broken down in 2019, with three candidate resistance gene(s) identified through transcriptomic analysis. A range of methods was used to confirm previous findings by Ajigboye *et al* (2021) and provide more information on Cougar's *Z.tritici* resistance mechanisms. This work also demonstrates the role of hyperspectral reflectance and chlorophyll fluorescence measurements in identifying and characterising novel sources of resistance to *Z.tritici*. The results from this PhD should help in the identification and characterisation of other novel sources of resistance to improve STB management and promote sustainable global food security.

## Table 1. Candidate genes 6300, 7300 & 7600 evidence summary

| Candidate gene | Supporting evidence | Contrasting evidence |
|---|---|---|
| TraesCS3D02G006300 | Upregulated in 4D-R NILS relative to 4D-S NILs at all timepoints in response to both IPO323 and HT-22<br>RT-qPCRs confirmed upregulation at all timepoints<br>LRR receptor with homology to:<br>XA21 - broad scale immunity to *Xanthamanasoryzae* in rice<br>FLS2 - Flagellin perceptor induced defence response<br>CRL1 - Brassinosteroid signalling<br>8 SNPs in 4D-R relative to 4D-S NILs (No change in predicted protein) | Log10foldchange is 8.3 at 0 hpi and decreases to 4.2-5.1 at 6 hpi and 11 dpi<br>RT-qPCRs show upregulation in 4D-R compared to 4D-S NILs when inoculated with 508 which is virulent on 4D-R<br>Medium confidence TraesCS3D02G006300 resides in the QTL interval |
| TraesCS3D02G007300 | High confidence TraesCS3D02G007300 resides in the QTL interval<br>Upregulated in 4D-R NILs relative to 4D-S NILs only at 11dpi in response to both IPO323 and HT-22<br>RT-qPCRs confirmed upregulation at 11 dpi, as well all other timepoints<br>LRR receptor with homology to:<br>FLS2 - Flagellin perceptor induced defence response<br>Cf-9 - Gene-for-gene resistance protein which provides resistance to *Cladosporum fulvum* in tomato<br>EIX2 - Receptor in tomato which induces ethylene biosynthesis, pathogenesis-related rptoein expression and hypersensitive cell death<br>40 SNPs in 4D-R relative to 4D-S NILs | RT-qPCRs show upregulation in 4D-R compared to 4D-S NILs when inoculated with 508 which is virulent on 4D-R<br>Relative to the Chinese Spring reference both 4D-R/S NILs might translate truncated proteins and be non-functional |
| TraesCS3D02G007600 | High confidence TraesCS3D02G007300 resides in the QTL interval<br>Upregulated in 4D-R NILS relative to 4D-S NILs at all timepoints in response to both IPO323 and HT-22<br>Most upregulated transcript out of the entire transcritpome<br>RT-qPCRs confirmed upregulation at all timepoints<br>R3H and SUZ binding domain containing protein (RNA binding protein)<br>Homology to DBF1 which regulates an ABA-dependent gene Rab17 in Maize<br>15 SNPs in 4D-R relative to 4D-S NILs | Low RT-qPCR expression relative to TraesCS3D02G006300 and TraesCS3D02G007300<br>RT-qPCRs show upregulation in 4D-R compared to 4D-S NILs when inoculated with 508 which is virulent on 4D-R |

# Bibliography and supplementary materials

**Table S1.** ANOVA analysis table displaying differences between Cougar X Scout lines over both years.

| Year | STB Assessment | Source of variation | d.f. | s.s. | m.s. | v.r. | F pr. |
|---|---|---|---|---|---|---|---|
| 2018 | GS23-26 | Block stratum | 1 | 124.95 | 124.95 | 7.66 | |
| | | Block.*Units* stratum | | | | | |
| | | Line | 99 | 2402.9 | 24.27 | 1.49 | 0.025 |
| | | Residual | 98 | 1599.05 | 16.32 | | |
| | | Total | 198 | 4113.23 | | | |
| 2018 | GS39 | Block stratum | 1 | 86.21 | 86.21 | 2.51 | |
| | | Block.*Units* stratum | | | | | |
| | | Line | 99 | 17291 | 174.66 | 5.09 | <.001 |
| | | Residual | 98 | 3364.65 | 34.33 | | |
| | | Total | 198 | 20675.29 | | | |
| 2018 | GS55 | Block stratum | 1 | 642.95 | 642.95 | 40.77 | |
| | | Block.*Units* stratum | | | | | |
| | | Line | 99 | 7489.53 | 75.65 | 4.8 | <.001 |
| | | Residual | 98 | 1545.45 | 15.77 | | |
| | | Total | 198 | 9671.58 | | | |
| 2018 | GS61-69 | Block stratum | 1 | 3011.59 | 3011.59 | 146.52 | |
| | | Block.*Units* stratum | | | | | |
| | | Line | 99 | 7881.15 | 79.61 | 3.87 | <.001 |
| | | Residual | 98 | 2014.34 | 20.55 | | |
| | | Total | 198 | 12770.02 | | | |

| | | | | | | | |
|---|---|---|---|---|---|---|---|
| 2018 | GS61-69 FLL | Block stratum | 1 | 126.548 | 126.548 | 31.52 | |
| | | Block.*Units* stratum | | | | | |
| | | Line | 99 | 2833.898 | 28.625 | 7.13 | <.001 |
| | | Residual | 98 | 393.466 | 4.015 | | |
| | | Total | 198 | 3322.739 | | | |
| 2019 | GS23-26 | Block stratum | 2 | 128.3 | 64.15 | 6.02 | |
| | | Block.*Units* stratum | | | | | |
| | | Line | 99 | 2344.32 | 23.68 | 2.22 | <.001 |
| | | Residual | 198 | 2109.63 | 10.65 | | |
| | | Total | 299 | 4582.24 | | | |
| 2019 | GS33 | Block stratum | 2 | 500.16 | 250.08 | 16.76 | |
| | | Block.*Units* stratum | | | | | |
| | | Line | 99 | 7848.61 | 79.28 | 5.31 | <.001 |
| | | Residual | 198 | 2953.91 | 14.92 | | |
| | | Total | 299 | 11302.69 | | | |
| 2019 | GS39 | Block stratum | 2 | 197.24 | 98.62 | 4.23 | |
| | | Block.*Units* stratum | | | | | |
| | | Line | 99 | 6256.44 | 63.2 | 2.71 | <.001 |
| | | Residual | 198 | 4621.28 | 23.34 | | |
| | | Total | 299 | 11074.96 | | | |
| 2019 | GS55 | Block stratum | 2 | 1558.22 | 779.11 | 26.83 | |
| | | Block.*Units* stratum | | | | | |
| | | Line | 99 | 8037.04 | 81.18 | 2.8 | <.001 |
| | | Residual | 198 | 5749.19 | 29.04 | | |
| | | Total | 299 | 15344.44 | | | |

| | | | | | | | |
|---|---|---|---|---|---|---|---|
| 2019 | GS61-69 | Block stratum | 2 | 900.03 | 450.01 | 15.84 | |
| | | Block.*Units* stratum | | | | | |
| | | Line | 99 | 6963.14 | 70.33 | 2.48 | <.001 |
| | | Residual | 198 | 5624.71 | 28.41 | | |
| | | Total | 299 | 13487.89 | | | |
| 2019 | GS71 | Block stratum | 2 | 2264.52 | 1132.26 | 18.23 | |
| | | Block.*Units* stratum | | | | | |
| | | Line | 99 | 39091.95 | 394.87 | 6.36 | <.001 |
| | | Residual | 198 | 12294.74 | 62.09 | | |
| | | Total | 299 | 53651.21 | | | |
| 2019 | GS71 FLL | Block stratum | 2 | 1932.67 | 966.33 | 10.03 | |
| | | Block.*Units* stratum | | | | | |
| | | Line | 99 | 47722 | 482.04 | 5 | <.001 |
| | | Residual | 198 | 19084 | 96.38 | | |
| | | Total | 299 | 68738.67 | | | |

**Table S2a.** Correlation analysis between hyperspectral reflectance indices and STB visual assessments in 2018. Indices not included in main text are shown. r values are displayed.

| Trait Measurments GS | STB assessment GS | NDVI | RNDVI | GNDVI | RARSc | PSSRc | PSNDc | Car(R) | Car(G) | MTCI | CAR1 | CRI1 | CRI2 | SIPI | ND705 | PSSRa | PSSRb | MACRI | RARSb | Sr(car) | NPQI | ARI1 | ARI2 | D2 | PWI | LRDSI2 | LRDSI1 | RARSa | PSRI | PRI | PRIm1 | RBRI |
|---|---|---|---|---|---|---|---|---|---|---|---|---|---|---|---|---|---|---|---|---|---|---|---|---|---|---|---|---|---|---|---|---|
| | GS 23 | - | - | - | - | - | - | - | - | - | - | - | - | - | - | - | - | - | - | - | - | - | - | - | - | - | - | - | - | - | - | - |
| | GS 39 | -0.47*** | -0.47*** | -0.42*** | -0.44*** | -0.44*** | -0.44*** | -0.43*** | -0.45*** | -0.34*** | -0.45*** | -0.41*** | -0.35*** | -0.44*** | -0.45*** | -0.46*** | -0.45*** | -0.46*** | -0.33*** | 0.25*** | 0.41*** | 0.50*** | 0.47*** | 0.46*** | 0.38*** | 0.46*** | 0.45*** | 0.49*** | 0.50*** | 0.50*** | 0.47*** | 0.45*** |
| 33 | GS 55 | - | - | 0.14* | - | 0.14* | - | 0.14* | - | 0.16* | - | - | - | - | - | 0.14* | 0.15* | - | - | - | -0.15* | - | - | - | - | - | -0.16* | - | - | - | - | - |
| | GS 61 | - | - | - | - | - | - | - | - | - | - | - | - | - | - | - | - | -0.14* | - | 0.19** | - | 0.22** | 0.28*** | - | 0.22** | 0.16* | - | - | - | - | - | 0.17* |
| | GS 61 FLL | - | - | - | - | - | - | - | - | - | - | - | - | - | - | - | - | - | - | - | - | - | - | - | - | - | - | - | - | - | - | - |
| | GS 23 | - | - | - | - | - | - | - | - | - | - | - | - | - | - | - | - | -0.15* | - | - | - | - | - | - | -0.14* | - | - | - | - | - | - | 0.16* |
| | GS 39 | -0.39*** | -0.36*** | -0.32*** | -0.36*** | -0.35*** | -0.30*** | -0.32*** | -0.36*** | -0.22** | -0.20*** | - | - | -0.34*** | -0.33*** | -0.41*** | -0.38*** | -0.20** | - | - | 0.16* | 0.19** | 0.23** | 0.37*** | 0.23*** | 0.23** | 0.20** | 0.40*** | 0.41*** | 0.26*** | 0.24*** | 0.17* |
| 39 | GS 55 | - | - | - | - | - | - | - | - | - | - | - | - | - | - | - | - | 0.14* | - | - | - | - | - | - | - | - | - | - | - | - | - | -0.15* |
| | GS 61 | -0.22** | -0.26*** | -0.29*** | -0.27*** | -0.21** | -0.20** | -0.16* | -0.24*** | -0.35*** | - | -0.24*** | -0.23** | -0.20** | -0.34*** | -0.28*** | -0.30*** | 0.19** | -0.24*** | - | 0.19** | 0.26*** | 0.30*** | 0.32*** | 0.38*** | 0.30*** | 0.29*** | - | 0.21** | 0.29*** | 0.18** | -0.20** |
| | GS 61 FLL | - | - | - | - | - | - | - | - | - | - | - | - | - | - | - | - | 0.14* | -0.14* | -0.16* | - | 0.17* | 0.24* | - | - | 0.25*** | 0.24*** | - | - | 0.19** | - | - |
| | GS 23 | -0.18* | - | -0.14* | - | - | - | - | - | - | -0.14* | - | - | - | - | - | - | - | - | - | -0.20** | - | - | - | -0.17* | - | - | - | - | - | - | - |
| | GS 39 | -0.20** | -0.17* | -0.20** | -0.15* | -0.17* | -0.17* | - | - | -0.16* | - | - | - | -0.17* | -0.17* | -0.16* | -0.15* | - | - | - | - | - | - | 0.14* | - | - | - | - | - | - | - | - |
| 55 | GS 55 | - | -0.14* | - | - | - | - | - | - | -0.26*** | 0.15* | - | - | - | -0.23*** | - | -0.14* | 0.17* | -0.16* | -0.30*** | - | 0.28*** | 0.33*** | 0.21** | 0.17* | 0.39*** | 0.38*** | - | 0.31*** | 0.28*** | - | - |
| | GS 61 | -0.17* | -0.24*** | -0.28*** | -0.22** | -0.17* | -0.17* | - | -0.17* | -0.38*** | - | - | - | -0.21** | -0.34*** | -0.22** | -0.24*** | 0.17* | -0.15* | - | 0.24*** | 0.23** | 0.26*** | 0.30*** | 0.36*** | 0.24*** | 0.20** | - | - | 0.15* | - | - |
| | GS 61 FLL | - | - | - | - | - | - | - | - | - | - | - | 0.18* | - | - | - | - | - | - | - | - | - | - | - | - | 0.15* | - | - | - | - | - | - |
| | GS 23 | -0.14* | - | -0.17* | - | - | - | - | - | -0.19** | - | - | - | - | -0.16* | -0.15* | -0.15* | 0.16* | -0.15* | -0.24*** | -0.32*** | - | - | - | - | 0.16* | 0.20** | - | - | 0.20** | - | - |
| | GS 39 | - | - | - | - | - | - | - | - | - | 0.17* | - | - | - | - | - | - | - | - | -0.20** | - | - | - | - | 0.15* | - | - | 0.16* | - | - | - |
| 61 | GS 55 | -0.22** | -0.24*** | -0.24*** | -0.19** | -0.14* | -0.15* | - | - | -0.31*** | - | - | - | - | -0.30*** | -0.23*** | -0.24*** | - | - | -0.30*** | - | 0.31*** | 0.32*** | 0.33*** | 0.25*** | 0.42*** | 0.40** | - | 0.29*** | 0.26*** | - | - |
| | GS 61 | -0.21** | -0.24*** | -0.25*** | -0.25*** | -0.16* | -0.16* | - | -0.16* | -0.32*** | - | - | - | -0.18* | -0.30*** | -0.23*** | -0.24*** | 0.11* | -0.14* | -0.24*** | - | 0.19** | 0.29*** | 0.30*** | 0.38*** | 0.38*** | 0.34*** | - | 0.27*** | 0.22** | - | - |
| | GS 61 FLL | - | - | - | - | - | - | - | - | -0.17* | - | - | - | - | - | - | - | - | - | -0.17* | - | - | - | - | - | 0.15* | 0.14* | - | - | - | - | - |
| | GS 23 | - | - | -0.15* | - | - | - | -0.14* | - | - | -0.15* | -0.19** | -0.24*** | - | - | - | - | - | -0.23*** | - | -0.22** | - | - | - | - | - | - | - | - | - | - | -0.16* |
| | GS 39 | - | - | - | - | - | - | - | - | - | - | - | - | - | - | - | - | - | - | - | - | - | - | - | - | - | - | - | - | - | - | - |
| 71 | GS 55 | -0.32*** | -0.33*** | -0.31*** | -0.27*** | -0.25*** | -0.27*** | -0.21** | -0.26*** | -0.35*** | -0.18** | -0.25*** | - | -0.21** | -0.35*** | -0.30*** | -0.30*** | -0.17* | -0.33*** | -0.28*** | -0.30*** | 0.23** | 0.20** | 0.34*** | 0.32*** | 0.42*** | 0.42*** | 0.28*** | 0.36*** | 0.36*** | 0.25*** | - |
| | GS 61 | -0.38*** | -0.40*** | -0.37*** | -0.37*** | -0.34*** | -0.34*** | -0.29*** | -0.36*** | -0.42*** | -0.24*** | -0.25*** | - | -0.33*** | -0.41*** | -0.40*** | -0.40*** | -0.32*** | -0.28*** | -0.21** | -0.20** | 0.38*** | 0.31*** | 0.40*** | 0.46*** | 0.46*** | 0.44*** | 0.37*** | 0.41*** | 0.40*** | 0.34*** | 0.25*** |
| | GS 61 FLL | - | - | - | - | - | - | - | - | - | - | - | - | - | - | - | - | - | - | - | - | 0.15* | - | - | - | - | - | - | - | - | - | - |

(NS = -, P<0.001 ***, P<0.01 **, P<0.05 *). Cells are shaded from light green to dark based on positive R values, cells are shaded from light brown to dark brown based on negative R values.

**Table S2b.** Correlation analysis between hyperspectral reflectance indices and STB visual assessments in 2019. Indices not included in main text are shown. r values are displayed.

| Trait Measurments GS | STB assessment GS | NDVI | RNDVI | GNDVI | RARSc | PSSRc | PSNDc | Car(R) | Car(G) | MTCI | CAR1 | CRI1 | CRI2 | SIPI | ND705 | PSSRa | PSSRb | MACRI | RARSb | Sr(car) | NPQI | ARI1 | ARI2 | D2 | PWI | LRDSI2 | LRDSI1 | RARSa | PSRI | PRI | PRIm1 | RBRI |
|---|---|---|---|---|---|---|---|---|---|---|---|---|---|---|---|---|---|---|---|---|---|---|---|---|---|---|---|---|---|---|---|---|
| | GS 26 | -0.20* | -0.23* | - | - | - | - | - | - | - | - | - | - | - | -0.21* | - | - | - | - | - | - | 0.27** | 0.33*** | 0.21* | 0.24* | 0.23* | - | - | 0.29** | - | - | - |
| | GS 33 | - | - | - | - | - | - | - | - | - | - | 0.20* | 0.22* | - | - | - | - | -0.12* | 0.20* | - | - | 0.28** | - | - | - | - | - | - | - | - | - | 0.26* |
| | GS 39 | - | - | - | - | - | - | - | - | - | - | - | 0.22* | - | - | - | - | -0.12* | - | - | - | 0.42*** | - | - | - | - | - | - | - | - | - | 0.21* |
| 26 | GS 55 | - | - | - | - | - | - | - | - | - | - | - | - | - | - | - | - | - | - | - | 0.25* | 0.29** | - | - | - | - | - | - | - | - | - | 0.21* |
| | GS 69 | - | - | - | - | - | - | - | - | - | - | - | - | - | - | - | - | - | - | - | - | - | - | - | - | - | - | - | - | - | - | 0.21* |
| | GS 71 | - | - | - | - | - | - | - | - | - | - | - | - | - | - | - | - | - | 0.20* | - | - | - | - | - | - | - | - | - | - | - | - | 0.29** |
| | GS 71 FLL | - | - | - | - | - | - | - | - | - | - | - | - | - | - | - | - | - | 0.25* | - | - | - | - | - | -0.23* | - | - | - | - | - | - | 0.34*** |
| | GS 26 | - | - | - | - | - | - | - | - | - | - | - | - | - | - | - | - | -0.13* | - | - | - | - | - | - | - | - | - | - | - | - | - | - |
| | GS 33 | -0.49*** | -0.50*** | -0.45*** | -0.32** | -0.25* | -0.27** | -0.20* | -0.27** | -0.51*** | - | - | - | -0.22* | -0.54*** | -0.47*** | -0.49*** | -0.25*** | - | - | 0.27* | 0.59*** | 0.56*** | 0.55*** | 0.40*** | 0.48*** | 0.48*** | 0.36*** | 0.64*** | 0.59*** | - | 0.31*** |
| | GS 39 | -0.31** | -0.29** | -0.26** | -0.21* | - | - | - | - | -0.34*** | - | - | - | - | -0.35*** | -0.29** | -0.30** | - | - | - | - | 0.47*** | 0.45*** | 0.40*** | 0.21* | 0.40*** | 0.39*** | - | 0.44*** | 0.37*** | - | 0.22*** |
| 33 | GS 55 | -0.27** | -0.29** | -0.20* | - | - | - | - | - | -0.28** | - | - | - | - | -0.31** | -0.29** | -0.30** | -0.15** | - | - | 0.20* | 0.51*** | 0.52*** | 0.38*** | - | 0.36*** | 0.33*** | 0.21* | 0.45*** | 0.45*** | - | 0.24* |
| | GS 69 | -0.23* | -0.26* | - | - | - | - | - | - | -0.23* | - | - | - | - | -0.27** | -0.26** | -0.25* | -0.16** | - | - | - | 0.33*** | 0.36*** | 0.29** | 0.23* | - | - | 0.22* | 0.32** | 0.37*** | - | - |
| | GS 71 | -0.34*** | -0.36*** | - | -0.27** | -0.26** | -0.27** | -0.25* | -0.28** | - | -0.28** | - | - | -0.25* | -0.23* | -0.36*** | -0.32*** | -0.26* | - | 0.24* | - | 0.33*** | 0.29** | 0.27** | 0.25* | - | - | 0.45*** | 0.34*** | 0.27** | 0.33*** | 0.36*** |
| | GS 71 FLL | -0.37*** | -0.38*** | -0.24* | -0.30** | -0.29** | -0.30** | -0.28** | -0.31** | - | -0.30** | - | - | -0.26** | -0.28** | -0.37*** | -0.33*** | -0.24* | - | 0.25* | - | 0.29** | 0.24* | 0.29** | 0.27** | - | - | 0.45*** | 0.31** | 0.26* | 0.34*** | 0.33*** |
| | GS 26 | - | - | - | - | - | - | - | - | - | - | - | - | - | - | - | - | - | - | - | - | 0.20* | 0.22* | - | - | - | - | - | 0.20* | - | - | - |
| | GS 33 | -0.28** | -0.33*** | - | - | - | - | - | -0.22* | -0.17* | -0.21* | - | - | - | - | -0.29** | -0.30** | - | - | - | - | - | - | 0.27** | - | - | - | 0.32** | - | 0.24* | 0.26** | 0.20* |
| | GS 39 | -0.28** | -0.37*** | - | - | - | - | - | -0.24* | - | -0.23* | -0.21* | - | - | -0.20* | -0.31* | -0.32*** | - | - | - | - | 0.27** | 0.30** | 0.32** | - | - | - | 0.35*** | 0.23* | 0.37*** | 0.35*** | - |
| 39 | GS 55 | - | -0.24** | - | - | - | - | - | - | - | - | - | - | - | - | -0.21* | -0.21* | - | - | - | - | 0.28** | 0.31** | 0.22* | - | - | 0.20* | 0.27** | 0.29** | 0.32** | 0.24* | - |
| | GS 69 | -0.22* | -0.27** | - | - | - | - | - | - | - | - | - | - | - | - | -0.26** | -0.24* | - | - | - | - | - | 0.23* | 0.23* | - | - | - | 0.33*** | 0.22* | 0.29** | 0.27** | - |
| | GS 71 | -0.24* | -0.27** | - | -0.21* | - | - | -0.20* | -0.23* | -0.32*** | -0.28** | - | - | - | - | -0.26** | -0.23* | - | - | 0.28** | - | - | - | - | - | - | - | 0.41*** | - | - | 0.37*** | 0.25* |
| | GS 71 FLL | -0.28** | -0.32** | - | -0.25* | -0.22* | - | -0.25* | -0.29** | -0.23*** | -0.34*** | - | - | - | - | -0.31** | -0.29** | - | - | 0.33*** | - | - | - | 0.25* | - | - | - | 0.47*** | - | - | 0.44*** | 0.26** |
| | GS 26 | - | - | - | - | - | - | - | - | - | - | - | - | - | - | - | - | - | - | - | - | - | - | - | - | - | 0.21* | - | - | - | - | - |
| | GS 33 | -0.41*** | -0.38*** | -0.27** | -0.31** | -0.24* | -0.26* | -0.28** | -0.34*** | - | -0.24* | - | - | - | -0.28** | -0.35*** | -0.41*** | -0.26* | - | - | - | 0.38*** | 0.38*** | 0.35*** | - | - | - | - | 0.23*** | 0.45*** | 0.23* | - |
| | GS 39 | -0.43*** | -0.37*** | -0.30** | -0.32* | -0.22* | -0.23* | -0.27** | -0.34*** | -0.24** | -0.25* | - | - | - | -0.32** | -0.32** | -0.44*** | - | - | -0.31** | - | 0.39*** | 0.41*** | 0.44*** | - | 0.26** | 0.30** | - | - | 0.58*** | - | - |
| 55 | GS 55 | -0.46*** | -0.47*** | -0.38*** | -0.37*** | -0.32*** | -0.33*** | -0.30** | -0.37*** | -0.34*** | -0.25* | - | - | -0.29** | -0.44*** | -0.45*** | -0.47*** | - | - | - | - | 0.39*** | 0.40*** | 0.49*** | 0.21* | 0.26** | 0.26** | - | 0.32** | 0.41*** | - | - |
| | GS 69 | -0.49*** | -0.52*** | -0.47*** | -0.48*** | -0.47*** | -0.45*** | -0.43*** | -0.47*** | -0.43*** | -0.35*** | -0.23* | - | -0.47*** | -0.52*** | -0.54*** | -0.52*** | - | - | - | - | 0.20* | 0.20* | 0.51*** | 0.31** | - | - | 0.27** | - | 0.21* | 0.23* | - |
| | GS 71 | -0.40*** | -0.44*** | -0.29** | -0.41*** | -0.35*** | -0.35*** | -0.35*** | -0.39*** | - | -0.40*** | - | - | -0.34*** | -0.32** | -0.43*** | -0.42*** | -0.29*** | - | - | - | 0.22* | - | 0.44*** | - | - | - | 0.39*** | - | 0.27*** | 0.37*** | 0.23* |
| | GS 71 FLL | -0.42*** | -0.44*** | -0.28** | -0.43*** | -0.37*** | -0.36*** | -0.39*** | -0.42*** | - | -0.46*** | - | - | -0.36*** | -0.29** | -0.41*** | -0.43*** | -0.21*** | - | - | - | 0.22* | - | 0.44*** | - | - | - | 0.36*** | - | 0.27*** | 0.41*** | 0.27** |
| | GS 26 | - | - | - | -0.21* | -0.20* | -0.21* | -0.23* | -0.22* | - | -0.22* | - | - | -0.22* | - | - | - | - | - | - | - | - | - | 0.21* | - | - | - | - | - | - | - | - |
| | GS 33 | - | - | - | - | - | - | - | - | - | - | - | - | - | - | - | - | - | - | - | - | 0.38*** | 0.25* | - | - | - | - | - | 0.31** | 0.20* | - | - |
| | GS 39 | - | - | - | - | - | - | - | - | - | - | - | - | - | - | - | - | - | - | - | - | 0.29** | - | - | - | - | - | - | - | - | - | - |
| 69 | GS 55 | -0.23* | -0.26** | - | - | - | - | - | - | - | - | - | - | - | -0.22* | -0.22* | -0.22* | - | - | - | 0.23* | 0.41*** | 0.20* | 0.30** | - | - | - | - | 0.23* | 0.26* | - | - |
| | GS 69 | -0.25* | -0.30** | -0.20* | -0.24* | -0.22* | -0.22* | - | - | - | - | - | - | -0.21* | -0.23* | -0.25* | -0.23* | - | - | - | - | 0.38*** | - | 0.31** | 0.24* | - | - | - | 0.23* | 0.39*** | 0.21* | 0.21* |
| | GS 71 | -0.46*** | -0.53*** | -0.39*** | -0.40*** | 0.37*** | -0.37*** | -0.31** | -0.39*** | -0.36*** | -0.21* | - | - | -0.33*** | -0.45*** | -0.50*** | -0.47*** | - | - | - | 0.20* | 0.39*** | 0.33*** | 0.47*** | 0.38*** | - | 0.21* | 0.28** | 0.32*** | 0.54*** | 0.24*** | - |
| | GS 71 FLL | -0.41*** | -0.48*** | -0.33*** | -0.37*** | -0.36*** | -0.35*** | -0.28** | -0.35*** | -0.28** | -0.24* | - | - | -0.31** | -0.38*** | -0.45*** | -0.41*** | - | - | - | 0.23* | 0.37*** | 0.27** | 0.43*** | 0.28*** | - | - | 0.31** | 0.29** | 0.56*** | 0.30** | - |
| | GS 26 | - | - | - | - | - | - | - | - | - | - | - | - | - | - | - | - | -0.13* | - | - | - | - | - | - | - | - | - | - | - | - | - | - |
| | GS 33 | -0.32*** | -0.35*** | -0.31** | -0.30** | -0.26** | -0.28** | -0.24* | -0.30** | -0.31** | - | - | 0.24* | -0.28** | -0.35*** | -0.33*** | -0.32** | -0.23* | 0.12 | - | - | 0.46*** | 0.31** | 0.34*** | 0.36*** | 0.34*** | 0.27** | 0.30** | 0.37*** | 0.33*** | 0.25* | 0.36*** |
| | GS 39 | -0.22* | -0.26** | -0.28** | -0.27** | -0.27** | -0.27** | -0.25* | -0.28** | -0.29** | - | - | - | -0.31** | -0.29** | -0.28** | -0.28** | - | - | - | - | 0.22* | 0.14 | 0.26** | 0.32** | - | - | - | 0.20* | - | - | - |
| 71 | GS 55 | -0.44*** | -0.45*** | -0.45*** | -0.39*** | -0.36*** | -0.37*** | -0.30** | -0.37*** | -0.49*** | - | - | - | -0.33*** | -0.49*** | -0.44*** | -0.44*** | - | - | -0.25* | - | 0.41*** | 0.32** | 0.45*** | 0.45*** | 0.48** | 0.44*** | 0.26** | 0.44*** | 0.43*** | 0.21* | - |
| | GS 69 | -0.56*** | -0.57*** | -0.54*** | -0.48*** | -0.44*** | -0.46*** | -0.35*** | -0.45*** | -0.59*** | -0.25* | - | - | -0.39*** | -0.59*** | -0.57*** | -0.56*** | -0.11* | - | -0.40*** | - | 0.54*** | 0.45*** | 0.58*** | 0.50*** | 0.60*** | 0.58*** | 0.39*** | 0.57*** | 0.65*** | 0.29** | 0.21* |
| | GS 71 | -0.76*** | -0.77** | -0.69*** | -0.68*** | -0.63*** | -0.65*** | -0.56*** | -0.65*** | -0.70*** | -0.47*** | - | - | -0.57*** | -0.76*** | -0.73*** | -0.72*** | -0.27*** | - | -0.21* | - | 0.63*** | 0.46*** | 0.75*** | 0.62*** | 0.68*** | 0.62*** | 0.66*** | 0.77*** | 0.75*** | 0.56** | 0.36*** |
| | GS 71 FLL | -0.73*** | -0.76*** | -0.67*** | -0.67*** | -0.62*** | -0.63*** | -0.55*** | -0.65*** | -0.70*** | -0.44*** | -0.21* | - | -0.56*** | -0.75*** | -0.74*** | -0.72*** | -0.25*** | - | -0.22* | - | 0.65*** | 0.53*** | 0.73*** | 0.65*** | 0.67*** | 0.61*** | 0.66*** | 0.77*** | 0.76*** | 0.56** | 0.32*** |

(NS = -, P<0.001 ***, P<0.01 **, P<0.05 *). Cells are shaded from light green to dark based on positive R values, cells are shaded from light brown to dark brown based on negative R values.

**Table S3.** Correlation analysis between chlorophyll fluorescence measurements and STB visual assessments in 2019. r values are displayed.

| Trait Measurments GS | STB assessment GS | DIoRC | EToRC | TRoRC | ABSRC | Fv'/Fm' | NPQt | Phi2 | PhiNO | PhiNPQ |
|---|---|---|---|---|---|---|---|---|---|---|
| | GS 23 | - | - | -0.14* | - | - | - | 0.14* | - | - |
| | GS 39 | - | - | - | - | - | - | - | - | - |
| 39 | GS 55 | - | 0.14* | - | - | - | - | - | - | -0.15* |
| | GS 61 | - | 0.18** | - | - | 0.14* | - | 0.16* | - | -0.23** |
| | GS 61 FLL | - | - | - | - | - | - | - | - | - |
| | GS 23 | - | - | - | - | - | - | - | - | - |
| | GS 39 | - | - | - | - | - | - | - | - | - |
| 55 | GS 55 | 0.15* | - | - | - | -0.16* | 0.17* | - | -0.17* | 0.18** |
| | GS 61 | 0.27*** | - | - | 0.26*** | -0.28*** | 0.23** | -0.18** | -0.15* | 0.28*** |
| | GS 61 FLL | - | - | - | - | - | - | - | -0.15* | - |
| | GS 23 | - | - | - | - | - | - | - | - | 0.14* |
| | GS 39 | - | - | - | - | - | - | - | - | - |
| 61 | GS 55 | - | 0.17* | - | - | - | - | -0.16* | - | - |
| | GS 61 | - | 0.14* | - | - | -0.18* | - | -0.16* | - | - |
| | GS 61 FLL | - | 0.18* | - | - | - | - | - | - | - |

| Trait Measurments GS | STB assessment GS | DIoRC | EToRC | TRoRC | ABSRC | Fv'/Fm' | NPQt | Phi2 | PhiNO | PhiNPQ |
|---|---|---|---|---|---|---|---|---|---|---|
| | GS 26 | -0.28** | - | - | -0.26** | 0.31** | -0.32** | 0.25* | - | -0.37*** |
| | GS 33 | - | - | -0.26* | - | - | -0.34*** | - | 0.22* | -0.33*** |
| | GS 39 | -0.21* | - | -0.30** | -0.27** | 0.23* | -0.36*** | 0.41*** | - | -0.47*** |
| 33 | GS 55 | - | - | - | - | - | - | - | - | - |
| | GS 69 | 0.26** | - | - | 0.21* | -0.30** | - | - | - | - |
| | GS 71 | - | - | - | - | - | - | - | - | - |
| | GS 71 FLL | - | - | - | - | - | - | - | - | - |
| | GS 26 | - | - | - | - | - | - | - | - | - |
| | GS 33 | - | - | - | - | - | - | - | - | - |
| | GS 39 | - | - | - | - | - | - | - | - | - |
| 39 | GS 55 | - | - | - | - | - | - | - | - | - |
| | GS 69 | - | - | - | - | - | - | - | - | - |
| | GS 71 | - | - | - | - | - | - | - | - | - |
| | GS 71 FLL | - | - | - | - | - | - | - | - | - |
| | GS 26 | 0.21* | - | - | - | -0.20* | - | - | - | - |
| | GS 33 | - | - | - | - | - | - | - | - | - |
| | GS 39 | - | - | - | - | - | - | - | - | - |
| 55 | GS 55 | - | - | - | - | - | - | - | - | - |
| | GS 69 | - | - | - | - | - | - | - | - | - |
| | GS 71 | - | - | - | - | - | - | - | - | - |
| | GS 71 FLL | - | - | - | - | - | - | - | - | - |
| | GS 26 | - | - | - | - | - | - | - | 0.20* | - |
| | GS 33 | - | - | - | - | - | - | - | - | - |
| | GS 39 | - | - | - | - | -0.20* | - | - | - | - |
| 69 | GS 55 | - | - | - | - | - | - | - | - | - |
| | GS 69 | - | - | - | - | - | - | - | - | - |
| | GS 71 | - | - | - | - | - | - | - | - | - |
| | GS 71 FLL | - | - | - | - | - | - | - | - | - |

(NS = -, P<0.001 ***, P<0.01 **, P<0.05 *). Cells are shaded from light green to dark based on positive R values, cells are shaded from light brown to dark brown based on negative R values.

**Table S4.** ANOVA analysis of area under the disease progress curve analysis (AUDPC) with assessment method (Visual/ImageJ) as a treatment factor with line (4D-R/4D-S)

| Treatment | Source of variation | d.f. | s.s. | m.s. | v.r. | F pr. |
|---|---|---|---|---|---|---|
| Spray | Rep stratum | 4 | 5132.7 | 1283.2 | 4.45 | |
| | Rep.*Units* stratum | | | | | |
| | 4D | 1 | 10718.4 | 10718.4 | 37.15 | <.001 |
| | Assessment method | 1 | 15.6 | 15.6 | 0.05 | 0.817 |
| | 4D.Assessment method | 1 | 2842.3 | 2842.3 | 9.85 | 0.002 |
| | Residual | 72 | 20773.7 | 288.5 | | |
| | Total | 79 | 39482.7 | | | |
| Infiltration | Rep stratum | 4 | 464.71 | 116.18 | 1.7 | |
| | Rep.*Units* stratum | | | | | |
| | 4D | 1 | 809.16 | 809.16 | 11.84 | <.001 |
| | Assessment method | 1 | 7503.01 | 7503.01 | 109.77 | <.001 |
| | 4D.Assessment method | 1 | 328.08 | 328.08 | 4.8 | 0.032 |
| | Residual | 72 | 4921.42 | 68.35 | | |
| | Total | 79 | 14026.38 | | | |

**Table S5.** ANOVA analysis of percentage chlorotic lesions, necrotic lesions & Pycnidia incidence (Visual) / Pycnidia count (ImageJ) for Spray (Figure 4) and Infiltration (Figure 5) treatments comparing four 4D-R & 4D-S lines.

| Measurement | Inoculation | Assessment | Source of variation | d.f. | s.s. | m.s. | v.r. | F pr. |
|---|---|---|---|---|---|---|---|---|
| | | | Experiment strat | 1 | 421.7 | 421.7 | 1.72 | |
| | | | Experiment.Rep strat | 8 | 1961.1 | 245.1 | 1.26 | |
| | | | Experiment.Rep.*Units* strat | | | | | |
| Chlorosis | Spray | Visual | %4D | 1 | 18292.6 | 18292.6 | 94.04 | <.001 |
| | | | dpi | 6 | 61429.3 | 10238.2 | 52.63 | <.001 |
| | | | %4D.dpi | 6 | 4164.8 | 694.1 | 3.57 | 0.002 |
| | | | Residual | 536 | 104265.8 | 194.5 | | |
| | | | Total | 558 | 190440.8 | | | |
| | | | Experiment strat | 1 | 10298.6 | 10298.6 | 16.76 | |
| | | | Experiment.Rep strat | 8 | 4916.8 | 614.6 | 3.34 | |
| | | | Experiment.Rep.*Units* strat | | | | | |
| Necrosis | Spray | Visual | %4D | 1 | 713.6 | 713.6 | 3.88 | 0.049 |
| | | | dpi | 6 | 68784.7 | 11464.1 | 62.27 | <.001 |
| | | | %4D.dpi | 6 | 1627.5 | 271.2 | 1.47 | 0.185 |
| | | | Residual | 536 | 98672.3 | 184.1 | | |
| | | | Total | 558 | 184948.7 | | | |
| | | | Experiment strat | 1 | 0.26051 | 0.26051 | 1.06 | |
| | | | Experiment.Rep strat | 8 | 1.97463 | 0.24683 | 3.07 | |
| | | | Experiment.Rep.*Units* strat | | | | | |
| Pycnidia | Spray | Visual | %4D | 1 | 0.57355 | 0.57355 | 7.12 | 0.008 |
| | | | dpi | 6 | 46.37628 | 7.72938 | 96.01 | <.001 |
| | | | %4D.dpi | 6 | 0.77261 | 0.12877 | 1.6 | 0.145 |
| | | | Residual | 536 | 43.15128 | 0.08051 | | |
| | | | Total | 558 | 93.09123 | | | |

| | | | | | | | | |
|---|---|---|---|---|---|---|---|---|
| | | | Rep strat | 4 | 1179.3 | 294.8 | 2.59 | |
| | | | Rep.*Units* strat | | | | | |
| | | | %4D | 1 | 300.9 | 300.9 | 2.64 | 0.105 |
| Chlorosis | Spray | ImageJ | dpi | 5 | 24370.7 | 4874.1 | 42.84 | <.001 |
| | | | %4D.dpi | 5 | 1097.1 | 219.4 | 1.93 | 0.091 |
| | | | Residual | 222 | 25260.2 | 113.8 | | |
| | | | Total | 237 | 51835.2 | | | |
| | | | Rep strat | 4 | 4131.2 | 1032.8 | 5.78 | |
| | | | Rep.*Units* strat | | | | | |
| | | | %4D | 1 | 486.5 | 486.5 | 2.72 | 0.1 |
| Necrosis | Spray | ImageJ | dpi | 5 | 27378.1 | 5475.6 | 30.67 | <.001 |
| | | | %4D.dpi | 5 | 2977.7 | 595.5 | 3.34 | 0.006 |
| | | | Residual | 222 | 39636.1 | 178.5 | | |
| | | | Total | 237 | 74303.7 | | | |
| | | | Rep strat | 4 | 847.4 | 211.9 | 1.46 | |
| | | | Rep.*Units* strat | | | | | |
| | | | %4D | 1 | 234.3 | 234.3 | 1.62 | 0.205 |
| Pycnidia | Spray | ImageJ | dpi | 5 | 11518.4 | 2303.7 | 15.88 | <.001 |
| | | | %4D.dpi | 5 | 956.2 | 191.2 | 1.32 | 0.257 |
| | | | Residual | 222 | 32200.9 | 145 | | |
| | | | Total | 237 | 45455.7 | | | |
| | | | Experiment.Rep strat | 4 | 2941.47 | 735.37 | 7.66 | |
| | | | Experiment.Rep.*Units* strat | | | | | |
| | | | %4D | 1 | 571.96 | 571.96 | 5.96 | 0.015 |
| Chlorosis | Infiltration | Visual | dpi | 5 | 43298.57 | 8659.71 | 90.22 | <.001 |
| | | | %4D.dpi | 5 | 261.81 | 52.36 | 0.55 | 0.742 |
| | | | Residual | 224 | 21499.53 | 95.98 | | |
| | | | Total | 239 | 68573.34 | | | |

| | | | | | | | |
|---|---|---|---|---|---|---|---|
| | | | Experiment.Rep strat | 4 | 76.171 | 19.043 | 2.19 | |
| | | | Experiment.Rep.*Units* strat | | | | | |
| | | | %4D | 1 | 14.341 | 14.341 | 1.65 | 0.2 |
| Necrosis | Infiltration | Visual | dpi | 5 | 1466.894 | 293.379 | 33.73 | <.001 |
| | | | %4D.dpi | 5 | 14.527 | 2.905 | 0.33 | 0.892 |
| | | | Residual | 224 | 1948.048 | 8.697 | | |
| | | | Total | 239 | 3519.981 | | | |
| | | | Experiment.Rep strat | 4 | 0.28981 | 0.07245 | 1.81 | |
| | | | Experiment.Rep.*Units* strat | | | | | |
| | | | %4D | 1 | 0.22407 | 0.22407 | 5.58 | 0.019 |
| Pycnidia count | Infiltration | Visual | dpi | 5 | 5.28704 | 1.05741 | 26.35 | <.001 |
| | | | %4D.dpi | 5 | 0.29259 | 0.05852 | 1.46 | 0.205 |
| | | | Residual | 224 | 8.98796 | 0.04012 | | |
| | | | Total | 239 | 15.08148 | | | |
| | | | Rep strat | 4 | 0.105157 | 0.026289 | 4.47 | |
| | | | Rep.*Units* strat | | | | | |
| | | | %4D | 1 | 0.011891 | 0.011891 | 2.02 | 0.157 |
| Chlorosis | Infiltration | ImageJ | dpi | 4 | 1.917721 | 0.47943 | 81.5 | <.001 |
| | | | %4D.dpi | 4 | 0.012226 | 0.003057 | 0.52 | 0.721 |
| | | | Residual | 186 | 1.094095 | 0.005882 | | |
| | | | Total | 199 | 3.14109 | | | |
| | | | Rep strat | 4 | 95.56 | 23.89 | 1.26 | |
| | | | Rep.*Units* strat | | | | | |
| | | | %4D | 1 | 109.23 | 109.23 | 5.76 | 0.017 |
| Necrosis | Infiltration | ImageJ | dpi | 4 | 1164.2 | 291.05 | 15.34 | <.001 |
| | | | %4D.dpi | 4 | 328.86 | 82.22 | 4.33 | 0.002 |
| | | | Residual | 185 | 3510.89 | 18.98 | | |
| | | | Total | 198 | 5208.67 | | | |

| | | | | | | | | |
|---|---|---|---|---|---|---|---|---|
| | | | Rep strat | 4 | 0.94 | 0.235 | 0.06 | |
| | | | Rep.*Units* strat | | | | | |
| | | | %4D | 1 | 7.076 | 7.076 | 1.89 | 0.171 |
| Pycnidia count | Infiltration | ImageJ | dpi | 4 | 122.403 | 30.601 | 8.17 | <.001 |
| | | | %4D.dpi | 4 | 37.559 | 9.39 | 2.51 | 0.044 |
| | | | Residual | 185 | 692.817 | 3.745 | | |
| | | | Total | 198 | 860.566 | | | |

**Table S6a.** Repeated measurement analysis of 4D-R & 4D-S lines over the time course (0.167 dpi – 16 dpi) for Chlorophyll fluorescence measurements utilising a Fluorpen and MultispeQ. Spray treatment results are shown for two experiments. ANOVA tables are displayed.

| Measurement | Source of variation | d.f. | s.s. | m.s. | v.r. | F pr. |
|---|---|---|---|---|---|---|
| ABS/RC | Experiment stratum | 1 | 18.1836 | 18.1836 | 55.77 | |
| | Experiment.Block stratum | 4 | 1.3042 | 0.3261 | 2.12 | |
| | Experiment.Block.Subject stratum | | | | | |
| | %4D | 1 | 0.4052 | 0.4052 | 2.64 | 0.112 |
| | Residual | 41 | 6.3005 | 0.1537 | 1.11 | |
| | Experiment.Block.Subject.Time stratum | | | | | |
| | d.f. correction factor 0.1876 | | | | | |
| | Time | 8 | 35.533 | 4.4416 | 32.03 | <.001 |
| | Time.%4D | 8 | 1.5186 | 0.1898 | 1.37 | 0.258 |
| | Residual | 366 | 50.761 | 0.1387 | | |
| | Total | 429 | 113.7774 | | | |
| DIo/RC | Experiment stratum | 1 | 2.7956 | 2.7956 | 14.74 | |
| | Experiment.Block stratum | 4 | 0.75861 | 0.18965 | 2.61 | |
| | Experiment.Block.Subject stratum | | | | | |
| | %4D | 1 | 0.12312 | 0.12312 | 1.69 | 0.2 |
| | Residual | 41 | 2.97914 | 0.07266 | 1.01 | |
| | Experiment.Block.Subject.Time stratum | | | | | |
| | d.f. correction factor 0.1463 | | | | | |
| | Time | 8 | 8.49169 | 1.06146 | 14.81 | <.001 |
| | Time.%4D | 8 | 0.62422 | 0.07803 | 1.09 | 0.312 |
| | Residual | 366 | 26.23742 | 0.07169 | | |
| | Total | 429 | 41.95118 | | | |

| | | | | | | |
|---|---|---|---|---|---|---|
| ETo/RC | Experiment stratum | 1 | 0.357177 | 0.35718 | 85.71 | |
| | Experiment.Block stratum | | | | | |
| | | 4 | 0.016668 | 0.00417 | 0.59 | |
| | Experiment.Block.Subject stratum | | | | | |
| | %4D | 1 | 0.006411 | 0.00641 | 0.9 | 0.347 |
| | Residual | 41 | 0.290704 | 0.00709 | 1.17 | |
| | Experiment.Block.Subject.Time stratum | | | | | |
| | d.f. correction factor 0.7676 | | | | | |
| | Time | 8 | 1.271458 | 0.15893 | 26.24 | <.001 |
| | Time.%4D | 8 | 0.030434 | 0.0038 | 0.63 | 0.712 |
| | Residual | 366 | 2.21686 | 0.00606 | | |
| | Total | 429 | 4.180036 | | | |
| Tro/RC | Experiment stratum | 1 | 6.71639 | 6.71639 | 218.4 | |
| | Experiment.Block stratum | | | | | |
| | | 4 | 0.123 | 0.03075 | 1.15 | |
| | Experiment.Block.Subject stratum | | | | | |
| | %4D | 1 | 0.08153 | 0.08153 | 3.04 | 0.089 |
| | Residual | 41 | 1.10033 | 0.02684 | 1.41 | |
| | Experiment.Block.Subject.Time stratum | | | | | |
| | d.f. correction factor 0.3434 | | | | | |
| | Time | 8 | 9.41569 | 1.17696 | 61.99 | <.001 |
| | Time.%4D | 8 | 0.22374 | 0.02797 | 1.47 | 0.228 |
| | Residual | 366 | 6.94862 | 0.01899 | | |
| | Total | 429 | 24.55331 | | | |

| | | | | | | |
|---|---|---|---|---|---|---|
| NPQt | Experiment stratum | 1 | 1.16945 | 1.16945 | 7.36 | |
| | Experiment.Block stratum | | | | | |
| | | 4 | 0.63599 | 0.159 | 3.11 | |
| | Experiment.Block.Subject stratum | | | | | |
| | %4D | 1 | 0.00479 | 0.00479 | 0.09 | 0.761 |
| | Residual | 41 | 2.09796 | 0.05117 | 1.67 | |
| | Experiment.Block.Subject.Time stratum | | | | | |
| | d.f. correction factor 0.2164 | | | | | |
| | Time | 8 | 9.40796 | 1.176 | 38.38 | <.001 |
| | Time.%4D | 8 | 0.11513 | 0.01439 | 0.47 | 0.599 |
| | Residual | 367 | 11.2451 | 0.03064 | | |
| | Total | 430 | 24.66114 | | | |
| PhiNPQ | Experiment stratum | 1 | 0.18724 | 0.18724 | 16 | |
| | Experiment.Block stratum | | | | | |
| | | 4 | 0.046818 | 0.0117 | 2.53 | |
| | Experiment.Block.Subject stratum | | | | | |
| | %4D | 1 | 0.003015 | 0.00302 | 0.65 | 0.424 |
| | Residual | 41 | 0.189876 | 0.00463 | 1.82 | |
| | Experiment.Block.Subject.Time stratum | | | | | |
| | d.f. correction factor 0.2910 | | | | | |
| | Time | 8 | 1.126437 | 0.14081 | 55.41 | <.001 |
| | Time.%4D | 8 | 0.01328 | 0.00166 | 0.65 | 0.545 |
| | Residual | 366 | 0.930088 | 0.00254 | | |
| | Total | 429 | 2.494085 | | | |

| | | | | | | |
|---|---|---|---|---|---|---|
| PhiNO | Experiment stratum | 1 | 0.056755 | 0.05676 | 22.72 | |
| | Experiment.Block stratum | | | | | |
| | | 4 | 0.009992 | 0.0025 | 1.3 | |
| | Experiment.Block.Subject stratum | | | | | |
| | %4D | 1 | 0.006552 | 0.00655 | 3.42 | 0.072 |
| | Residual | 41 | 0.078528 | 0.00192 | 1.09 | |
| | Experiment.Block.Subject.Time stratum | | | | | |
| | d.f. correction factor 0.8013 | | | | | |
| | Time | 8 | 0.026583 | 0.00332 | 1.89 | 0.078 |
| | Time.%4D | 8 | 0.012157 | 0.00152 | 0.86 | 0.529 |
| | Residual | 367 | 0.646901 | 0.00176 | | |
| | Total | 430 | 0.837237 | | | |
| Phi2 | Experiment stratum | 1 | 0.451639 | 0.45164 | 58.66 | |
| | Experiment.Block stratum | | | | | |
| | | 4 | 0.030797 | 0.0077 | 1.27 | |
| | Experiment.Block.Subject stratum | | | | | |
| | %4D | 1 | 0.018173 | 0.01817 | 3 | 0.091 |
| | Residual | 41 | 0.248582 | 0.00606 | 1.38 | |
| | Experiment.Block.Subject.Time stratum | | | | | |
| | d.f. correction factor 0.7896 | | | | | |
| | Time | 8 | 1.23479 | 0.15435 | 35.11 | <.001 |
| | Time.%4D | 8 | 0.032165 | 0.00402 | 0.91 | 0.488 |
| | Residual | 367 | 1.613427 | 0.0044 | | |
| | Total | 430 | 3.629084 | | | |

**Table S6b.** Repeated measurement analysis of 4D-R & 4D-S lines over the time course (0.167 dpi – 16 dpi) for Chlorophyll fluorescence measurements utilising a Fluorpen and MultispeQ. Infiltration treatment results are shown for two experiments. ANOVA tables are displayed.

| Measurment | Source of variation | d.f. | s.s. | m.s. | v.r. | F pr. |
|---|---|---|---|---|---|---|
| ABS/RC | Experiment stratum | 1 | 0.2941 | 0.2941 | 0.63 | |
| | Experiment.Block stratum | 4 | 1.8807 | 0.4702 | 0.86 | |
| | Experiment.Block.Subject stratum | | | | | |
| | %4D | 1 | 1.1264 | 1.1264 | 2.06 | 0.159 |
| | Residual | 41 | 22.4003 | 0.5463 | 2.9 | |
| | Experiment.Block.Subject.Time stratum | | | | | |
| | d.f. correction factor 0.2509 | | | | | |
| | Time | 8 | 139.279 | 17.4099 | 92.39 | <.001 |
| | Time.%4D | 8 | 1.2567 | 0.1571 | 0.83 | 0.438 |
| | Residual | 367 | 69.1566 | 0.1884 | | |
| | Total | 430 | 235.0627 | | | |
| DIo/RC | Experiment stratum | 1 | 1.1323 | 1.1323 | 9.83 | |
| | Experiment.Block stratum | 4 | 0.4605 | 0.1151 | 0.39 | |
| | Experiment.Block.Subject stratum | | | | | |
| | %4D | 1 | 0.5303 | 0.5303 | 1.79 | 0.188 |
| | Residual | 41 | 12.1193 | 0.2956 | 2.69 | |
| | Experiment.Block.Subject.Time stratum | | | | | |
| | d.f. correction factor 0.2115 | | | | | |
| | Time | 8 | 48.2922 | 6.0365 | 54.89 | <.001 |
| | Time.%4D | 8 | 0.5426 | 0.0678 | 0.62 | 0.516 |
| | Residual | 367 | 40.3603 | 0.11 | | |
| | Total | 430 | 103.0711 | | | |

| | | | | | | |
|---|---|---|---|---|---|---|
| ETo/RC | Experiment stratum | 1 | 0.025753 | 0.02575 | 1.87 | |
| | Experiment.Block stratum | | | | | |
| | | 4 | 0.055098 | 0.01377 | 1.38 | |
| | Experiment.Block.Subject stratum | | | | | |
| | %4D | 1 | 0.002693 | 0.00269 | 0.27 | 0.606 |
| | Residual | 41 | 0.408639 | 0.00997 | 2.24 | |
| | Experiment.Block.Subject.Time stratum | | | | | |
| | d.f. correction factor 0.7643 | | | | | |
| | Time | 8 | 1.496771 | 0.1871 | 41.97 | <.001 |
| | Time.%4D | 8 | 0.083535 | 0.01044 | 2.34 | 0.031 |
| | Residual | 367 | 1.636031 | 0.00446 | | |
| | Total | 430 | 3.70455 | | | |
| Tro/RC | Experiment stratum | 1 | 0.16264 | 0.16264 | 1.04 | |
| | Experiment.Block stratum | | | | | |
| | | 4 | 0.62533 | 0.15633 | 2.62 | |
| | Experiment.Block.Subject stratum | | | | | |
| | %4D | 1 | 0.11252 | 0.11252 | 1.88 | 0.177 |
| | Residual | 41 | 2.44877 | 0.05973 | 2.88 | |
| | Experiment.Block.Subject.Time stratum | | | | | |
| | d.f. correction factor 0.4995 | | | | | |
| | Time | 7 | 21.90191 | 3.12884 | 150.9 | <.001 |
| | Time.%4D | 7 | 0.22451 | 0.03207 | 1.55 | 0.198 |
| | Residual | 321 | 6.65526 | 0.02073 | | |
| | Total | 382 | 32.12962 | | | |

| | | | | | | |
|---|---|---|---|---|---|---|
| NPQt | Experiment stratum | 1 | 0.72296 | 0.72296 | 6.6 | |
| | Experiment.Block stratum | | | | | |
| | | 4 | 0.43789 | 0.10947 | 1.01 | |
| | Experiment.Block.Subject stratum | | | | | |
| | %4D | 1 | 0.0589 | 0.0589 | 0.54 | 0.466 |
| | Residual | 41 | 4.46057 | 0.10879 | 2.51 | |
| | Experiment.Block.Subject.Time stratum | | | | | |
| | d.f. correction factor 0.2026 | | | | | |
| | Time | 8 | 25.45136 | 3.18142 | 73.36 | <.001 |
| | Time.%4D | 8 | 0.25523 | 0.0319 | 0.74 | 0.456 |
| | Residual | 367 | 15.91642 | 0.04337 | | |
| | Total | 430 | 47.26596 | | | |
| PhiNPQ | Experiment stratum | 1 | 0.013456 | 0.01346 | 1.08 | |
| | Experiment.Block stratum | | | | | |
| | | 4 | 0.049914 | 0.01248 | 1.55 | |
| | Experiment.Block.Subject stratum | | | | | |
| | %4D | 1 | 0.007425 | 0.00743 | 0.92 | 0.342 |
| | Residual | 41 | 0.329426 | 0.00804 | 3.92 | |
| | Experiment.Block.Subject.Time stratum | | | | | |
| | d.f. correction factor 0.4063 | | | | | |
| | Time | 8 | 2.305245 | 0.28816 | 140.6 | <.001 |
| | Time.%4D | 8 | 0.012594 | 0.00157 | 0.77 | 0.523 |
| | Residual | 367 | 0.752094 | 0.00205 | | |
| | Total | 430 | 3.466894 | | | |

| | | | | | | |
|---|---|---|---|---|---|---|
| PhiNO | Experiment stratum | 1 | 0.039701 | 0.0397 | 9.72 | |
| | Experiment.Block stratum | | | | | |
| | | 4 | 0.01634 | 0.00409 | 1.8 | |
| | Experiment.Block.Subject stratum | | | | | |
| | %4D | 1 | 0.000105 | 0.00011 | 0.05 | 0.831 |
| | Residual | 41 | 0.093291 | 0.00228 | 1.23 | |
| | Experiment.Block.Subject.Time stratum | | | | | |
| | d.f. correction factor 0.7573 | | | | | |
| | Time | 8 | 0.031024 | 0.00388 | 2.1 | 0.053 |
| | Time.%4D | 8 | 0.01378 | 0.00172 | 0.93 | 0.472 |
| | Residual | 367 | 0.677283 | 0.00185 | | |
| | Total | 430 | 0.871523 | | | |
| Phi2 | Experiment stratum | 1 | 0.006826 | 0.00683 | 0.35 | |
| | Experiment.Block stratum | | | | | |
| | | 4 | 0.077754 | 0.01944 | 1.92 | |
| | Experiment.Block.Subject stratum | | | | | |
| | %4D | 1 | 0.005741 | 0.00574 | 0.57 | 0.456 |
| | Residual | 41 | 0.415866 | 0.01014 | 2.57 | |
| | Experiment.Block.Subject.Time stratum | | | | | |
| | d.f. correction factor 0.7482 | | | | | |
| | Time | 8 | 1.988096 | 0.24851 | 62.89 | <.001 |
| | Time.%4D | 8 | 0.030285 | 0.00379 | 0.96 | 0.454 |
| | Residual | 367 | 1.450263 | 0.00395 | | |
| | Total | 430 | 3.971766 | | | |

**Table S7a.** Chlorophyll fluorescence measurement comparison of 4D-R & 4D-S NILs inoculated with HT-22. Maximum value for ETR, qP and photosynthesis at 16 min are displayed. Students T-test P-value and SE are displayed.

| Isolate | Measurement | HPI | Maximum value | | SE | | Pvalue | |
|---|---|---|---|---|---|---|---|---|
| | | | 4D | No4D | 4D | No4D | 4D<No4D | 4D>No4D |
| HT-22 | QE | 6 | 1.78 | 2.01 | 0.110 | 0.104 | 0.104 | 0.896 |
| | | 12 | 1.94 | 2.07 | 0.085 | 0.085 | 0.165 | 0.835 |
| | | 24 | 1.87 | 1.95 | 0.178 | 0.0757 | 0.35 | 0.65 |
| | | 48 | 1.82 | 1.79 | 0.179 | 0.059 | 0.565 | 0.435 |
| | QI | 6 | 0.302 | 0.253 | 0.0209 | 0.0170 | 0.928 | 0.072 |
| | | 12 | 0.287 | 0.246 | 0.0169 | 0.0139 | 0.933 | 0.067 |
| | | 24 | 0.296 | 0.269 | 0.0173 | 0.0207 | 0.805 | 0.195 |
| | | 48 | 0.266 | 0.295 | 0.00374 | 0.00756 | 0.013 | 0.987 |
| | ETR | 6 | 130 | 149 | 9.77 | 6.04 | 0.092 | 0.908 |
| | | 12 | 121 | 135 | 9.89 | 9.16 | 0.17 | 0.83 |
| | | 24 | 132 | 147 | 13.4 | 1.80 | 0.201 | 0.799 |
| | | 48 | 141 | 146 | 14.5 | 3.53 | 0.377 | 0.623 |
| | qP | 6 | 0.409 | 0.458 | 0.0230 | 0.0110 | 0.062 | 0.938 |
| | | 12 | 0.394 | 0.439 | 0.0235 | 0.0263 | 0.137 | 0.863 |
| | | 24 | 0.410 | 0.461 | 0.0299 | 0.00475 | 0.114 | 0.886 |
| | | 48 | 0.427 | 0.443 | 0.0309 | 0.00509 | 0.319 | 0.681 |
| | Photosynthesis | 6 | 15.4 | 17.6 | 4.23 | 4.02 | 0.366 | 0.634 |
| | | 12 | 14.1 | 12.3 | 1.77 | 0.666 | 0.805 | 0.195 |
| | | 24 | 16.1 | 19.2 | 2.25 | 1.55 | 0.159 | 0.841 |
| | | 48 | 14.8 | 16.7 | 0.519 | 3.79 | 0.333 | 0.667 |

**Table S7b.** Chlorophyll fluorescence measurement comparison of 4D-R & 4D-S NILs inoculated with IPO323. Maximum value for ETR, qP and photosynthesis at 16 min are displayed. Students T-test P-value and SE are displayed.

| Isolate | Measurement | HPI | Maximum value | | SE | | Pvalue | |
|---|---|---|---|---|---|---|---|---|
| | | | 4D | No4D | 4D | No4D | 4D<No4D | 4D>No4D |
| IPO323 | QE | 6 | 2.04 | 1.86 | 0.0695 | 0.0560 | 0.949 | 0.051 |
| | | 12 | 2.15 | 2.15 | 0.0743 | 0.0475 | 0.519 | 0.481 |
| | | 24 | 1.84 | 1.90 | 0.0519 | 0.0697 | 0.293 | 0.707 |
| | | 48 | 1.71 | 1.96 | 0.122 | 0.0594 | 0.07 | 0.93 |
| | QI | 6 | 0.251 | 0.272 | 0.0119 | 0.0171 | 0.184 | 0.816 |
| | | 12 | 0.251 | 0.265 | 0.0116 | 0.00899 | 0.196 | 0.804 |
| | | 24 | 0.304 | 0.289 | 0.0172 | 0.0146 | 0.734 | 0.266 |
| | | 48 | 0.262 | 0.299 | 0.0300 | 0.00530 | 0.142 | 0.858 |
| | ETR | 6 | 145 | 156 | 3.87 | 9.74 | 0.165 | 0.835 |
| | | 12 | 127 | 128 | 6.80 | 4.59 | 0.488 | 0.512 |
| | | 24 | 144 | 142 | 4.70 | 8.68 | 0.578 | 0.422 |
| | | 48 | 158 | 129 | 13.1 | 2.64 | 0.952 | 0.048 |
| | qP | 6 | 0.461 | 0.492 | 0.0103 | 0.0226 | 0.139 | 0.861 |
| | | 12 | 0.433 | 0.418 | 0.0205 | 0.0120 | 0.718 | 0.282 |
| | | 24 | 0.454 | 0.451 | 0.0207 | 0.0216 | 0.528 | 0.472 |
| | | 48 | 0.469 | 0.414 | 0.0283 | 0.0140 | 0.921 | 0.079 |
| | Photosynthesis | 6 | 17.5 | 17.8 | 0.888 | 1.77 | 0.45 | 0.55 |
| | | 12 | 13.2 | 12.2 | 0.310 | 2.04 | 0.663 | 0.337 |
| | | 24 | 18.1 | 19.7 | 2.91 | 1.46 | 0.324 | 0.676 |
| | | 48 | 14.6 | 21.4 | 4.34 | 0.524 | 0.13 | 0.87 |

**Table S8a.** Effect of *Z.tritici* isolates HT-22 & IPO323 at 6 hpi on ABA; Abscisic acid, SA; Salicylic acid, JA; Jasmonic acid, OPDA; oxo-Phytodienoic acid, Ja-Ile; jasmonoyl-L-isoleucine, IAA; Indole-3-acetic acid, GA1, 3, 7; Gibberellin, ACC; 1-Aminocyclopropane 1-carboxylic acid, IPA; Indole-3-propionic acid, 2iP; 6-(γ,γ-Dimethylallylamino)purine, Z; Zeatin and ZR; zeatin riboside content in 4D-R and 4D-S NILs. 4D-R & 4D-S lines infected by HT-22 or IPO323 are analysed using student T-tests (Table 3). Effect of compatibility analysed using an

| hpi | Hormone | Source of variation | d.f. | s.s. | m.s. | v.r. | F pr. |
|---|---|---|---|---|---|---|---|
| 6 | %2iP | Rep stratum | 2 | 13.381 | 6.69 | 1.1 | |
| | | Rep.*Units* stratum | | | | | |
| | | Compatibility | 1 | 6.162 | 6.162 | 1.01 | 0.348 |
| | | Inoculation | 1 | 1.764 | 1.764 | 0.29 | 0.607 |
| | | Residual | 7 | 42.632 | 6.09 | | |
| | | Total | 11 | 63.939 | | | |
| 6 | ABA | Rep stratum | 2 | 119.3 | 59.6 | 0.47 | |
| | | Rep.*Units* stratum | | | | | |
| | | Compatibility | 1 | 81.2 | 81.2 | 0.64 | 0.451 |
| | | Inoculation | 1 | 60.5 | 60.5 | 0.47 | 0.513 |
| | | Residual | 7 | 893.8 | 127.7 | | |
| | | Total | 11 | 1154.8 | | | |
| 6 | ACC | Rep stratum | 2 | 10877 | 5439 | 0.89 | |
| | | Rep.*Units* stratum | | | | | |
| | | Compatibility | 1 | 1296 | 1296 | 0.21 | 0.659 |
| | | Inoculation | 1 | 1740 | 1740 | 0.29 | 0.61 |
| | | Residual | 7 | 42660 | 6094 | | |
| | | Total | 11 | 56574 | | | |
| 6 | GA1 | Rep stratum | 2 | 2309 | 1154 | 0.12 | |
| | | Rep.*Units* stratum | | | | | |
| | | Compatibility | 1 | 627 | 627 | 0.07 | 0.804 |
| | | Inoculation | 1 | 1588 | 1588 | 0.17 | 0.695 |
| | | Residual | 7 | 66358 | 9480 | | |
| | | Total | 11 | 70881 | | | |

| | | | | | | | |
|---|---|---|---|---|---|---|---|
| | | Rep stratum | 2 | 27640 | 13820 | 2.29 | |
| | | Rep.*Units* stratum | | | | | |
| 6 | GA3 | Compatibility | 1 | 3165 | 3165 | 0.52 | 0.492 |
| | | Inoculation | 1 | 37706 | 37706 | 6.25 | 0.041 |
| | | Residual | 7 | 42226 | 6032 | | |
| | | Total | 11 | 110737 | | | |
| | | Rep stratum | 2 | 360613 | 180306 | 0.6 | |
| | | Rep.*Units* stratum | | | | | |
| 6 | GA4 | Compatibility | 1 | 95698 | 95698 | 0.32 | 0.59 |
| | | Inoculation | 1 | 25921 | 25921 | 0.09 | 0.777 |
| | | Residual | 7 | 2100660 | 300094 | | |
| | | Total | 11 | 2582892 | | | |
| | | Rep stratum | 2 | 12294 | 6147 | 1.43 | |
| | | Rep.*Units* stratum | | | | | |
| 6 | GA7 | Compatibility | 1 | 1222 | 1222 | 0.28 | 0.611 |
| | | Inoculation | 1 | 1467 | 1467 | 0.34 | 0.578 |
| | | Residual | 7 | 30106 | 4301 | | |
| | | Total | 11 | 45089 | | | |
| | | Rep stratum | 2 | 256873 | 128437 | 1.64 | |
| | | Rep.*Units* stratum | | | | | |
| 6 | IAA | Compatibility | 1 | 39283 | 39283 | 0.5 | 0.502 |
| | | Inoculation | 1 | 8430 | 8430 | 0.11 | 0.752 |
| | | Residual | 7 | 547738 | 78248 | | |
| | | Total | 11 | 852324 | | | |
| | | Rep stratum | 2 | 1451.1 | 725.6 | 3.02 | |
| 6 | IPA | Rep.*Units* stratum | | | | | |
| | | Compatibility | 1 | 1005.6 | 1005.6 | 4.18 | 0.08 |
| | | Inoculation | 1 | 1500.1 | 1500.1 | 6.24 | 0.041 |

| | | | | | | | |
|---|---|---|---|---|---|---|---|
| | | Residual | 7 | 1682.1 | 240.3 | | |
| | | Total | 11 | 5638.9 | | | |
| 6 | JA_Ile | Rep stratum | 2 | 0.016082 | 0.008041 | 1.02 | |
| | | Rep.*Units* stratum | | | | | |
| | | Compatibility | 1 | 0.000448 | 0.000448 | 0.06 | 0.818 |
| | | Inoculation | 1 | 0.010529 | 0.010529 | 1.34 | 0.285 |
| | | Residual | 7 | 0.054916 | 0.007845 | | |
| | | Total | 11 | 0.081974 | | | |
| 6 | JA | Rep stratum | 2 | 34.704 | 17.352 | 1.86 | |
| | | Rep.*Units* stratum | | | | | |
| | | Compatibility | 1 | 0.616 | 0.616 | 0.07 | 0.805 |
| | | Inoculation | 1 | 2.43 | 2.43 | 0.26 | 0.626 |
| | | Residual | 7 | 65.392 | 9.342 | | |
| | | Total | 11 | 103.143 | | | |
| 6 | Mel | Rep stratum | 2 | 72.24 | 36.12 | 0.39 | |
| | | Rep.*Units* stratum | | | | | |
| | | Compatibility | 1 | 60.18 | 60.18 | 0.65 | 0.446 |
| | | Inoculation | 1 | 17.77 | 17.77 | 0.19 | 0.674 |
| | | Residual | 7 | 647.61 | 92.52 | | |
| | | Total | 11 | 797.79 | | | |
| 6 | OPDA | Rep stratum | 2 | 2.5165 | 1.2583 | 1.98 | |
| | | Rep.*Units* stratum | | | | | |
| | | Compatibility | 1 | 0.2549 | 0.2549 | 0.4 | 0.547 |
| | | Inoculation | 1 | 2.2034 | 2.2034 | 3.47 | 0.105 |
| | | Residual | 7 | 4.4485 | 0.6355 | | |
| | | Total | 11 | 9.4233 | | | |

| | | | | | | | |
|---|---|---|---|---|---|---|---|
| | | Rep stratum | 2 | 21058 | 10529 | 0.61 | |
| | | Rep.*Units* stratum | | | | | |
| 6 | SA | Compatibility | 1 | 49019 | 49019 | 2.83 | 0.136 |
| | | Inoculation | 1 | 96631 | 96631 | 5.58 | 0.05 |
| | | Residual | 7 | 121195 | 17314 | | |
| | | Total | 11 | 287903 | | | |
| | | Rep stratum | 2 | 9.55 | 4.77 | 0.23 | |
| | | Rep.*Units* stratum | | | | | |
| 6 | Z | Compatibility | 1 | 6.11 | 6.11 | 0.3 | 0.603 |
| | | Inoculation | 1 | 1.34 | 1.34 | 0.07 | 0.806 |
| | | Residual | 7 | 144.47 | 20.64 | | |
| | | Total | 11 | 161.47 | | | |
| | | Rep stratum | 2 | 0.0881 | 0.04405 | 0.67 | |
| | | Rep.*Units* stratum | | | | | |
| 6 | ZR | Compatibility | 1 | 0.00675 | 0.00675 | 0.1 | 0.758 |
| | | Inoculation | 1 | 0.02976 | 0.02976 | 0.45 | 0.522 |
| | | Residual | 7 | 0.4584 | 0.06549 | | |
| | | Total | 11 | 0.58301 | | | |

**Table S8b.** Effect of *Z.tritici* isolates HT-22 & IPO323 at 11 dpi on ABA; Abscisic acid, SA; Salicylic acid, JA; Jasmonic acid, OPDA; oxo-Phytodienoic acid, Ja-Ile; jasmonoyl-L-isoleucine, IAA; Indole-3-acetic acid, GA1, 3, 7; Gibberellin, ACC; 1-Aminocyclopropane 1-carboxylic acid, IPA; Indole-3-propionic acid, 2iP; 6-(γ,γ-Dimethylallylamino)purine, Z; Zeatin and ZR; zeatin riboside content in 4D-R and 4D-S NILs. 4D-R & 4D-S lines infected by HT-22 or IPO323 are analysed using student T-tests (Table 3). Effect of compatibility analysed using an

| dpi | Hormone | Source of variation | d.f. | s.s. | m.s. | v.r. | F pr. |
|---|---|---|---|---|---|---|---|
| 11 | %2iP | Rep stratum | 2 | 25.26 | 12.63 | 0.64 | |
| | | Rep.*Units* stratum | | | | | |
| | | Compatibility | 1 | 10.58 | 10.58 | 0.53 | 0.489 |
| | | Inoculation | 1 | 0.02 | 0.02 | 0 | 0.979 |
| | | Residual | 7 | 138.96 | 19.85 | | |
| | | Total | 11 | 174.81 | | | |
| 11 | ABA | Rep stratum | 2 | 125.7 | 62.8 | 0.51 | |
| | | Rep.*Units* stratum | | | | | |
| | | Compatibility | 1 | 482.7 | 482.7 | 3.91 | 0.089 |
| | | Inoculation | 1 | 345.5 | 345.5 | 2.8 | 0.138 |
| | | Residual | 7 | 864.6 | 123.5 | | |
| | | Total | 11 | 1818.5 | | | |
| 11 | ACC | Rep stratum | 2 | 2403 | 1201 | 0.2 | |
| | | Rep.*Units* stratum | | | | | |
| | | Compatibility | 1 | 10551 | 10551 | 1.79 | 0.223 |
| | | Inoculation | 1 | 1390 | 1390 | 0.24 | 0.642 |
| | | Residual | 7 | 41214 | 5888 | | |
| | | Total | 11 | 55558 | | | |
| 11 | GA1 | Rep stratum | 2 | 104198 | 52099 | 0.24 | |
| | | Rep.*Units* stratum | | | | | |
| | | Compatibility | 1 | 19494 | 19494 | 0.09 | 0.772 |
| | | Inoculation | 1 | 8155 | 8155 | 0.04 | 0.851 |
| | | Residual | 7 | 1503700 | 214814 | | |
| | | otal | 11 | 1635548 | | | |

| | | | | | | | |
|---|---|---|---|---|---|---|---|
| | | Rep stratum | 2 | 3757 | 1879 | 0.46 | |
| | | Rep.*Units* stratum | | | | | |
| 11 | GA3 | Compatibility | 1 | 581 | 581 | 0.14 | 0.718 |
| | | Inoculation | 1 | 3995 | 3995 | 0.97 | 0.357 |
| | | Residual | 7 | 28775 | 4111 | | |
| | | Total | 11 | 37108 | | | |
| | | Rep stratum | 2 | 481489 | 240744 | 0.63 | |
| | | Rep.*Units* stratum | | | | | |
| 11 | GA4 | Compatibility | 1 | 139489 | 139489 | 0.36 | 0.565 |
| | | Inoculation | 1 | 957 | 957 | 0 | 0.962 |
| | | Residual | 7 | 2681473 | 383068 | | |
| | | Total | 11 | 3303408 | | | |
| | | Rep stratum | 2 | 4744 | 2372 | 0.82 | |
| | | Rep.*Units* stratum | | | | | |
| 11 | GA7 | Compatibility | 1 | 739 | 739 | 0.25 | 0.63 |
| | | Inoculation | 1 | 1909 | 1909 | 0.66 | 0.444 |
| | | Residual | 7 | 20342 | 2906 | | |
| | | Total | 11 | 27734 | | | |
| | | Rep stratum | 2 | 142055 | 71027 | 2.42 | |
| | | Rep.*Units* stratum | | | | | |
| | | Compatibility | 1 | 417 | 417 | 0.01 | 0.908 |
| | | Inoculation | 1 | 21644 | 21644 | 0.74 | 0.419 |
| 11 | IAA | Residual | 7 | 205218 | 29317 | | |
| | | Total | 11 | 369334 | | | |
| 11 | IPA | Rep stratum | 2 | 178.5 | 89.2 | 0.19 | |

| | | | | | | |
|---|---|---|---|---|---|---|
| | | Rep.*Units* stratum | | | | |
| | | Compatibility | 1 | 202.5 | 202.5 | 0.43 | 0.532 |
| | | Inoculation | 1 | 17.4 | 17.4 | 0.04 | 0.852 |
| | | Residual | 7 | 3273.5 | 467.6 | | |
| | | Total | 11 | 3671.9 | | | |
| 11 | JA_Ile | Rep stratum | 2 | 0.04717 | 0.02358 | 0.96 | |
| | | Rep.*Units* stratum | | | | | |
| | | Compatibility | 1 | 0.03715 | 0.03715 | 1.51 | 0.259 |
| | | Inoculation | 1 | 0.04693 | 0.04693 | 1.91 | 0.21 |
| | | Residual | 7 | 0.17204 | 0.02458 | | |
| | | Total | 11 | 0.3033 | | | |
| 11 | JA | Rep stratum | 2 | 2571 | 1286 | 0.67 | |
| | | Rep.*Units* stratum | | | | | |
| | | Compatibility | 1 | 3675 | 3675 | 1.91 | 0.209 |
| | | Inoculation | 1 | 3408 | 3408 | 1.77 | 0.225 |
| | | Residual | 7 | 13442 | 1920 | | |
| | | Total | 11 | 23096 | | | |
| 11 | Mel | Rep stratum | 2 | 664.5 | 332.3 | 0.7 | |
| | | Rep.*Units* stratum | | | | | |
| | | Compatibility | 1 | 6.3 | 6.3 | 0.01 | 0.911 |
| | | Inoculation | 1 | 0 | 0 | 0 | 0.998 |
| | | Residual | 7 | 3313.9 | 473.4 | | |
| | | Total | 11 | 3984.7 | | | |
| 11 | OPDA | Rep stratum | 2 | 0.297 | 0.148 | 0.09 | |
| | | Rep.*Units* stratum | | | | | |
| | | Compatibility | 1 | 0.61 | 0.61 | 0.37 | 0.564 |
| | | Inoculation | 1 | 2.274 | 2.274 | 1.37 | 0.281 |
| | | Residual | 7 | 11.648 | 1.664 | | |

| | | | | | | | |
|---|---|---|---|---|---|---|---|
| | | Total | 11 | 14.829 | | | |
| 11 | SA | Rep stratum | 2 | 18419 | 9210 | 3.28 | |
| | | Rep.*Units* stratum | | | | | |
| | | Compatibility | 1 | 43720 | 43720 | 15.55 | 0.006 |
| | | Inoculation | 1 | 503 | 503 | 0.18 | 0.685 |
| | | Residual | 7 | 19683 | 2812 | | |
| | | Total | 11 | 82325 | | | |
| 11 | Z | Rep stratum | 2 | 18.083 | 9.041 | 1.43 | |
| | | Rep.*Units* stratum | | | | | |
| | | Compatibility | 1 | 2.265 | 2.265 | 0.36 | 0.568 |
| | | Inoculation | 1 | 3.996 | 3.996 | 0.63 | 0.452 |
| | | Residual | 7 | 44.195 | 6.314 | | |
| | | Total | 11 | 68.539 | | | |
| 11 | ZR | Rep stratum | 2 | 0.4879 | 0.244 | 0.6 | |
| | | Rep.*Units* stratum | | | | | |
| | | Compatibility | 1 | 0.9191 | 0.9191 | 2.25 | 0.177 |
| | | Inoculation | 1 | 0.5018 | 0.5018 | 1.23 | 0.304 |
| | | Residual | 7 | 2.8542 | 0.4077 | | |
| | | Total | 11 | 4.763 | | | |

**Table S9a.** GSEA analysis breakdown for HT-22 inoculated 4D-R/S NILs. UniProt utilised to characterise transcripts. Transcripts displayed significantly contributed towards GSEA significance.

| Time | GO-Term | Transcript No. | Gene | Process | Reference |
|---|---|---|---|---|---|
| 6 hpi | Detoxification | 53 | DHAR1 | Peroxidase | Sasaki-Sekimoto *et al* 2005 |
| | | | SODCC2 | Peroxidase | Gaudet *et al* 2011 |
| | | | APX4 | Peroxidase | Gaudet *et al* 2011 |
| | | | PNC1 | Peroxidase | Gaudet *et al* 2011 |
| | | | SODA4 | Peroxidase | Scandalios 1994 |
| | | | APX1 | Peroxidase | Davletova *et al* 2005 |
| | | | SPC4 | Peroxidase | Dicko *et al* 2006 |
| | | | RBOHC | Peroxidase | Foreman *et al* 2003 |
| | | | CAT1 | Peroxidase | Xing *et al* 2008 |
| | | | NTR1 | Peroxidase | Jean-Pierre Jacquot *et al* 1994 |
| | | | NDPK1 | Peroxidase | Fukamatsu *et al* 2003 |
| | Alcohol catabolic process | 5 | N/A | Ascorbate biosynthesis | Gaudet *et al* 2011 |
| | Stomatal complex development | 7 | EPF4 | Epidermal pattern factor | Kondo *et al* 2010 |
| | | | EPF4 | Epidermal pattern factor | Kondo *et al* 2010 |
| | Regulation of auxin mediated signalling pathway | 13 | HAG3 | Auxin signalling | Nelissen *et al* 2010 |
| | | | FBX6 | Auxin signalling | Song *et al* 2012 |
| | | | BIG-GRAIN-1 | Auxin signalling | Liu *et al* 2015 |
| | | | SCI1B | Auxin signalling | Depaoli *et al* 2012 |
| | | | ELP4 | Auxin signalling | Nelissen *et al* 2005 |
| | Protein important into peroxisome matrix | 15 | ESCRT-I | Peroxisomal sorting and protein degradation | Wang *et al* 2017 |
| | | | ESCRT-2 | Peroxisomal sorting and protein degradation | Wang *et al* 2017 |
| | Molybdopterin cofactor metabolism | 10 | CNX1 | Molybdopterin synthesis | Llamas *et al* 2006 |
| | | | MOCS2 | Molybdopterin synthesis | Leimkühler *et al* 2003 |
| | | | ABA3 | Sulfation of molybdopterin | Bittner *et al* 2001 |
| | Oxidoreductase activity transposing C=C bonds | 6 | IPP1 | Isoprenoid synthesis | Phillips *et al* 2008 |
| | | | IPP2 | Isoprenoid production | Phillips *et al* 2008 |
| 11 dpi | Hydroxy Behenoyl COA dehydratase activity | 6 | PAS2 | membrane lipid synthesis | Bellec *et al* 2002 |
| | Nitrate assimilation & metabolism | 11 | SOX1 | Nitrate reductase (Molybdopterin metabolism) | Gaudet *et al* 2011 |
| | | | Psb33 | PSII assembly and stabilization | Fristedt *et al* 2015 |
| | | | NIA | Nitrate reductase (Molybdopterin metabolism) | Gaudet *et al* 2011 |
| | Rho GTPase binding | 7 | ROPGEF4 | ABA mediated stomatal closure | Li & Liu 2012 |
| | | | SKIP32 | degradation of target proteins | Calderón-Villalobos *et al* 2007 |
| | Protein kinase activity | 26 | BAK1 | brassinosteroid receptor pathway | Li *et al* 2009 |
| | | | CYCU1 | cyclin kinases formation | Gaudet *et al* 2011 |
| | | | MAT1 | cyclin kinases formation | Gaudet *et al* 2011 |
| | | | CKB2 | degradation of PIF1 (ABA and GA signalling; Bu *et a*l 2011) | Dennis & Browning 2009 |
| | | | CKB4 | degradation of PIF1 (ABA and GA signalling; Bu *et a*l 2011) | Dennis & Browning 2009 |

**Table S9b.** GSEA analysis breakdown for IPO323 inoculated 4D-R/S NILs. UniProt utilised to characterise transcripts. Transcripts displayed significantly contributed towards GSEA significance.

| Time | GO-Term | Transcript No. | Gene | Process | Reference |
|---|---|---|---|---|---|
| 6 hpi | Negative regulation of dephosphorylation | 14 | PYL3 | ABA receptor | Zhang *et al* 2012 |
| | | | PYL9 | ABA receptor | Hao *et al* 2011 |
| | | | PYL2 | ABA receptor | Hao *et al* 2011 |
| | | | Betv1 | ABA receptor | Gaudet *et al* 2011 |
| | | | CPN20 | Activation of iron superoxide dismutase and ABA signalling | Bonshtien *et al* 2007; Zhang *et al* 2013 |
| | Thiamine biosynthesis | 19 | THI1 | Chloroplastic triazole synthesis | Li *et al* 2016 |
| | | | THI2 | Chloroplastic triazole synthesis | Li *et al* 2016 |
| | | | THIC | Chloroplastic triazole synthesis | Kong *et al* 2008 |
| | | | THIM | Thiamine salvaging | Yazdani *et al* 2013 |
| | | | TPK2 | Phosphorylation of Thiamine to Thiamine pyrophosphate (TPP) | Ajjawi *et al* 2007; Takahashi et al 1998 |
| | Peroxisome import | 3 | PEX14 | Peroxisome import | Lanyon-Hogg *et al* 2014 |
| | Auxin biosynthetic process | 1 | SIC | Auxin biosynthetic process | Zhan *et al* 2012 |
| | GTP biosynthetic process | 3 | NDPK1 | Peroxidase activity | Fukamatsu *et al* 2003 |
| 11 dpi | Alpha 12 fucosyltransferase activity | 4 | FUT | Fucosyltransferases | Gaudet *et al* 2011 |
| | | | FT1 | Fucosyltransferases | Gaudet *et al* 2011 |
| | Defence responses to fungus | 56 | AOC1 | OPDA synthesis | Stenzel *et al* 2003 |
| | | | AOC2 | OPDA synthesis | Stenzel *et al* 2003 |
| | | | AOC3 | OPDA synthesis | Stenzel *et al* 2003 |
| | | | AOC4 | OPDA synthesis | Stenzel *et al* 2003 |
| | | | OCP3 | JA detection | Coego *et al* 2005 |
| | | | RCF3 | Basal mediator of JA related defences | Thatcher *et al* 2015 |
| | | | ATG18A | Autophagy | Xiong *et al* 2005 |
| | | | ATG5 | Autophagy | Thompson *et al* 2005 |
| | | | ATG6 | Autophagy | Patel *et al* 2008 |
| | | | ATG7 | Autophagy | Sakuraba *et al* 2014 |
| | | | ATG9 | Autophagy | Sakuraba *et al* 2014 |
| | | | SERK2 | Required for immunity mediated by Xa21 and Fls22 | McAndrew *et al* 2014 |
| | | | 4CL3 | Phenylpropanoid metabolism | Rgen Ehlting *et al* 1999 |
| | | | AAE3 | Oxalate ligase | Foster *et al* 2012 |
| | | | BG1 | Auxin transport | Liu *et al* 2015 |
| | | | CESA1 | Cellulose synthase | Arioli *et al* 1998 |
| | | | DOX1 | Alpha-dioxygenase | Leo *et al* 2002 |
| | | | DSP2 | Tyrosine phosphatase | Romá-Mateo *et al* 2007 |
| | | | MOS4 | splicing factor SPF27 | Xu *et al* 2012 |
| | | | Patatin | lipolytic acyl hydrolase | la Camera *et al* 2009 |
| | | | PRT1 | E3 ubiquitin-protein ligase | Potuschak *et al* 1998 |
| | | | RACK1B | MAPK protein | Guo & Chen 2008 |
| | | | RH10 | RNA chaperone | Wang *et al* 2016 |
| | | | THO1 | THO subcomplex | Jauvion *et al* 2010 |
| | | | Hevein | Chitinase | Bertini *et al* 2012 |
| | Chitinase activity | 26 | CDA1 | Cytidine deaminiase, required for UMP synthesis | Dong *et al* 2019 |
| | | | CDA7 | Cytidine deaminiase, required for UMP synthesis | Dong *et al* 2019 |
| | | | CDA8 | Cytidine deaminiase, required for UMP synthesis | Dong *et al* 2019 |
| | Protein import into mitochondrial membrane | 58 | TIM22-2 | Chloroplast inner membrane transport | Rossig *et al* 2013 |
| | | | HP30-1 | Chloroplast inner membrane transport | Rossig *et al* 2013 |
| | | | TIM9 | mitochondrial chaperone protein | Gaudet *et al* 2011 |
| | | | OEP163 | Chloroplastic/mitochondria outer envelope pore protein | Gaudet *et al* 2011 |
| | V-Type ATPase subunits | | | Conversion of ADP to ATP | Gaudet *et al* 2011 |

**Supp. Table. 10.** Effector candidates for transcripts consistently upregulated in all treatments.

| Comparison | ensembl_peptide_id | signalp | tmhmm | TargetP2 | Localize | residues | %_cysteine | EffectorP3 |
|---|---|---|---|---|---|---|---|---|
| 0-6 | Mycgr3P80332 | SignalP-noTM | | noTP | ---\|---\|--- | 76 | 7.895 | Apoplastic effector |
| 0-6 | Mycgr3P83064 | SignalP-noTM | | noTP | ---\|---\|--- | 75 | 8 | Apoplastic effector |
| 0-6 | Mycgr3P102047 | SignalP-noTM | | noTP | ---\|---\|--- | 441 | 2.268 | Apoplastic effector |
| 0-6 | Mycgr3P104697 | SignalP-noTM | | noTP | ---\|---\|--- | 149 | 2.685 | Apoplastic effector |
| 0-6 | Mycgr3P105182 | SignalP-noTM | | noTP | ---\|---\|--- | 143 | 4.196 | Apoplastic effector |
| 0-6 | Mycgr3P105677 | SignalP-noTM | | noTP | ---\|---\|--- | 198 | 2.02 | Apoplastic effector |
| 0-6 | Mycgr3P106335 | SignalP-noTM | | noTP | ---\|---\|--- | 238 | 2.101 | Apoplastic effector |
| 0-6 | Mycgr3P39947 | SignalP-noTM | | noTP | ---\|---\|--- | 149 | 2.685 | Apoplastic effector |
| 0-6 | Mycgr3P99161 | SignalP-noTM | | noTP | ---\|---\|--- | 164 | 10.976 | Apoplastic effector |
| 0-6 | Mycgr3P102849 | SignalP-noTM | | noTP | ---\|---\|--- | 285 | 2.105 | Apoplastic effector |
| 0-6 | Mycgr3P103950 | SignalP-noTM | | noTP | ---\|---\|--- | 470 | 2.766 | Apoplastic effector |
| 0-6 | Mycgr3P102341 | SignalP-noTM | TMhelix | noTP | ---\|---\|Nuc | 459 | 1.525 | Apoplastic effector |
| 0-6 | Mycgr3P62211 | SignalP-noTM | TMhelix | noTP | ---\|---\|--- | 428 | 1.869 | Cytoplasmic effector |
| 0-6 | Mycgr3P100167 | SignalP-noTM | | noTP | ---\|---\|--- | 142 | 1.408 | Cytoplasmic effector |
| 0-6 | Mycgr3P101365 | SignalP-noTM | | noTP | ---\|---\|--- | 363 | 1.102 | Cytoplasmic effector |
| 0-6 | Mycgr3P110887 | SignalP-noTM | | noTP | ---\|---\|--- | 283 | 4.947 | Cytoplasmic effector |
| 0-6 | Mycgr3P100250 | SignalP-noTM | | noTP | ---\|---\|--- | 387 | 1.034 | Cytoplasmic effector |
| 0-6 | Mycgr3P104009 | SignalP-noTM | | noTP | ---\|---\|--- | 483 | 0 | Cytoplasmic effector |
| 0-6 | Mycgr3P72138 | SignalP-noTM | | noTP | ---\|---\|--- | 178 | 2.247 | Cytoplasmic effector |
| 0-6 | Mycgr3P100063 | SignalP-noTM | | noTP | ---\|---\|--- | 395 | 1.266 | Cytoplasmic effector |
| 0-6 | Mycgr3P83835 | SignalP-noTM | | noTP | ---\|---\|Nuc | 659 | 0.303 | Cytoplasmic effector |
| 0-6 | Mycgr3P68144 | SignalP-noTM | | noTP | ---\|---\|Nuc | 431 | 0.232 | Cytoplasmic effector |
| 0-6 | Mycgr3P104794 | SignalP-noTM | | noTP | ---\|---\|--- | 157 | 2.548 | Cytoplasmic/apoplastic effector |
| 0-11 | Mycgr3P104283 | SignalP-noTM | TMhelix | noTP | ---\|---\|--- | 226 | 5.31 | Apoplastic effector |
| 0-11 | Mycgr3P101235 | SignalP-noTM | | noTP | ---\|---\|--- | 426 | 1.174 | Apoplastic effector |
| 0-11 | Mycgr3P88451 | SignalP-noTM | | noTP | ---\|---\|--- | 237 | 0.844 | Apoplastic effector |
| 0-11 | Mycgr3P96543 | SignalP-noTM | | noTP | ---\|---\|--- | 143 | 5.594 | Apoplastic effector |
| 0-11 | Mycgr3P102047 | SignalP-noTM | | noTP | ---\|---\|--- | 441 | 2.268 | Apoplastic effector |
| 0-11 | Mycgr3P104697 | SignalP-noTM | | noTP | ---\|---\|--- | 149 | 2.685 | Apoplastic effector |
| 0-11 | Mycgr3P105182 | SignalP-noTM | | noTP | ---\|---\|--- | 143 | 4.196 | Apoplastic effector |
| 0-11 | Mycgr3P111221 | SignalP-noTM | | noTP | ---\|---\|--- | 232 | 3.879 | Apoplastic effector |
| 0-11 | Mycgr3P102016 | SignalP-noTM | | noTP | ---\|---\|--- | 339 | 2.36 | Apoplastic effector |
| 0-11 | Mycgr3P102849 | SignalP-noTM | | noTP | ---\|---\|--- | 285 | 2.105 | Apoplastic effector |
| 0-11 | Mycgr3P103950 | SignalP-noTM | | noTP | ---\|---\|--- | 470 | 2.766 | Apoplastic effector |
| 0-11 | Mycgr3P106127 | SignalP-noTM | | noTP | ---\|---\|--- | 97 | 6.186 | Apoplastic effector |
| 0-11 | Mycgr3P102341 | SignalP-noTM | TMhelix | noTP | ---\|---\|Nuc | 459 | 1.525 | Apoplastic effector |
| 0-11 | Mycgr3P62211 | SignalP-noTM | TMhelix | noTP | ---\|---\|--- | 428 | 1.869 | Cytoplasmic effector |
| 0-11 | Mycgr3P100167 | SignalP-noTM | | noTP | ---\|---\|--- | 142 | 1.408 | Cytoplasmic effector |
| 0-11 | Mycgr3P101365 | SignalP-noTM | | noTP | ---\|---\|--- | 363 | 1.102 | Cytoplasmic effector |
| 0-11 | Mycgr3P101587 | SignalP-noTM | | noTP | ---\|---\|--- | 508 | 1.181 | Cytoplasmic effector |
| 0-11 | Mycgr3P104009 | SignalP-noTM | | noTP | ---\|---\|--- | 483 | 0 | Cytoplasmic effector |
| 0-11 | Mycgr3P72138 | SignalP-noTM | | noTP | ---\|---\|--- | 178 | 2.247 | Cytoplasmic effector |
| 0-11 | Mycgr3P90776 | SignalP-noTM | | noTP | ---\|---\|--- | 242 | 0 | Cytoplasmic effector |
| 0-11 | Mycgr3P100063 | SignalP-noTM | | noTP | ---\|---\|--- | 395 | 1.266 | Cytoplasmic effector |
| 0-11 | Mycgr3P106329 | SignalP-noTM | | noTP | ---\|---\|--- | 135 | 0.741 | Cytoplasmic effector |
| 0-11 | Mycgr3P102792 | SignalP-noTM | | noTP | ---\|---\|Nuc | 114 | 7.018 | Cytoplasmic effector |
| 0-11 | Mycgr3P54172 | SignalP-noTM | | noTP | ---\|---\|Nuc | 690 | 0.58 | Cytoplasmic effector |
| 0-11 | Mycgr3P83835 | SignalP-noTM | | noTP | ---\|---\|Nuc | 659 | 0.303 | Cytoplasmic effector |
| 0-11 | Mycgr3P109991 | SignalP-noTM | | noTP | ---\|---\|Nuc | 235 | 0 | Cytoplasmic effector |
| 0-11 | Mycgr3P58400 | SignalP-noTM | | noTP | ---\|---\|Nuc | 456 | 1.316 | Cytoplasmic effector |
| 0-11 | Mycgr3P77055 | SignalP-noTM | | noTP | Chl\|---\|--- | 193 | 0 | Cytoplasmic effector |
| 0-11 | Mycgr3P104000 | SignalP-noTM | | noTP | ---\|---\|--- | 180 | 3.333 | Cytoplasmic/apoplastic effector |
| 0-11 | Mycgr3P109137 | SignalP-noTM | | noTP | ---\|---\|--- | 154 | 2.597 | Cytoplasmic/apoplastic effector |
| 0-11 | Mycgr3P104794 | SignalP-noTM | | noTP | ---\|---\|--- | 157 | 2.548 | Cytoplasmic/apoplastic effector |
| 6-11 | Mycgr3P101235 | SignalP-noTM | | noTP | ---\|---\|--- | 426 | 1.174 | Apoplastic effector |
| 6-11 | Mycgr3P96543 | SignalP-noTM | | noTP | ---\|---\|--- | 143 | 5.594 | Apoplastic effector |
| 6-11 | Mycgr3P109991 | SignalP-noTM | | noTP | ---\|---\|Nuc | 235 | 0 | Cytoplasmic effector |
| 6-11 | Mycgr3P104000 | SignalP-noTM | | noTP | ---\|---\|--- | 180 | 3.333 | Cytoplasmic/apoplastic effector |

**Supp. Table. 11.** Candidate effectors for upregulated *Z.tritici* transcripts in 4D-R NILs compared to 4D-S NILs. (11dpi)

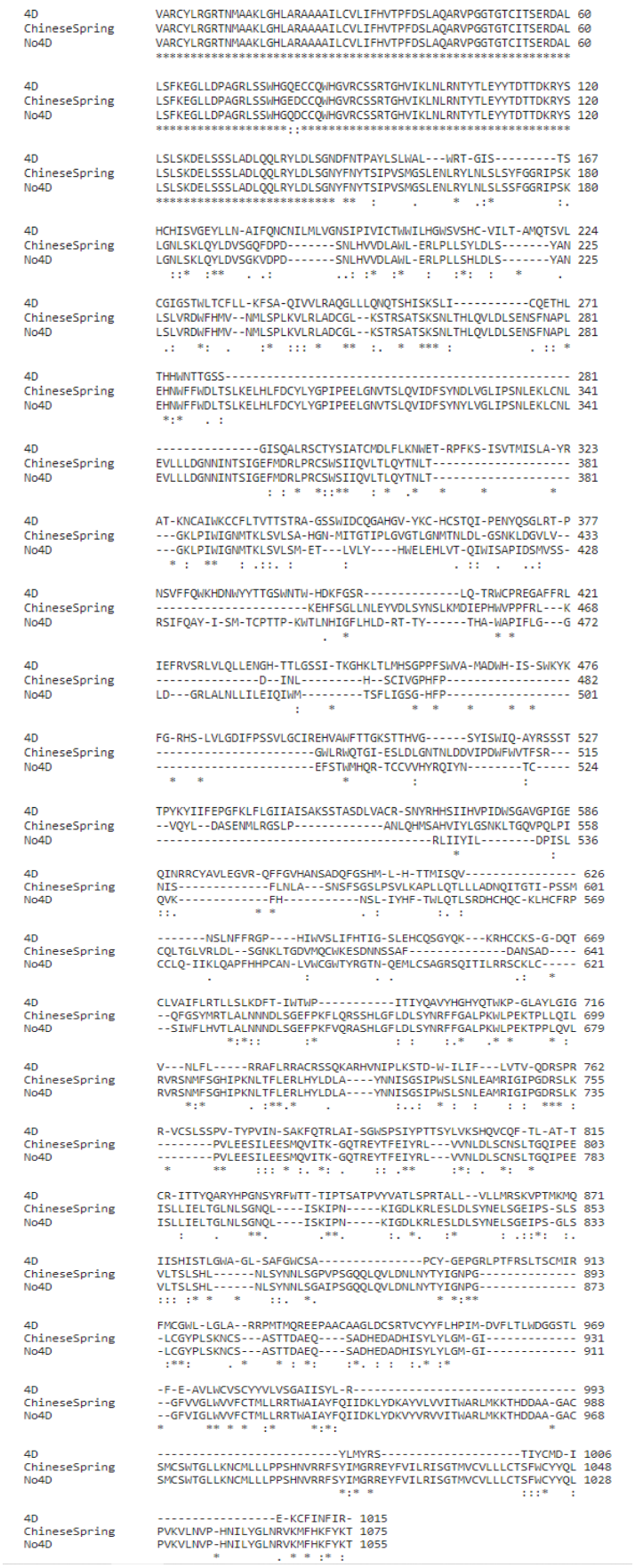
| Isolate | Peptide | Q-Value | B-Value | TPM 4D | TPM No4D | signalp | Transmembrane helix | TargetP2 | Localize | Protein No. | %_cysteine | Effector |
|---|---|---|---|---|---|---|---|---|---|---|---|---|
| | Mycgr3G91471 | <0.001 | -8.1 | 0 | 399 | SignalP-noTM | | SP | - | 154 | 3.90 | Apoplastic |
| | Mycgr3G91662 | <0.001 | -7.5 | 0 | 225 | SignalP-noTM | | noTP | - | 126 | 6.35 | Cytoplasmic |
| | Mycgr3G107758 | <0.001 | -7.4 | 0 | 39 | SignalP-noTM | | noTP | - | 269 | 0.74 | Cytoplasmic |
| | Mycgr3G108482 | <0.001 | -7.3 | 0 | 87 | SignalP-noTM | | noTP | - | 108 | 9.26 | Apoplastic |
| | Mycgr3G105825 | <0.001 | -7.0 | 0 | 153 | SignalP-noTM | | SP | - | 67 | 8.96 | Apoplastic |
| | Mycgr3G102792 | <0.001 | -6.6 | 1 | 544 | SignalP-noTM | | noTP | Nucleus | 114 | 7.02 | Cytoplasmic |
| | Mycgr3G103900 | <0.001 | -6.3 | 0 | 43 | SignalP-noTM | | noTP | - | 129 | 6.20 | Apoplastic/cytoplasmic |
| | Mycgr3G97034 | <0.001 | -6.3 | 0 | 105 | SignalP-noTM | | noTP | - | 117 | 1.71 | Cytoplasmic |
| | Mycgr3G90089 | <0.001 | -5.9 | 1 | 211 | SignalP-TM | | noTP | Chloroplast/Mitochondria | 196 | 1.53 | Cytoplasmic |
| | Mycgr3G95478 | <0.001 | -5.7 | 0 | 31 | SignalP-noTM | | noTP | Nucleus | 236 | 0.00 | Cytoplasmic |
| | Mycgr3G70396 | <0.001 | -5.4 | 0 | 46 | SignalP-noTM | | noTP | - | 331 | 2.42 | Apoplastic |
| | Mycgr3G111636 | <0.001 | -5.2 | 0 | 30 | SignalP-noTM | | noTP | - | 159 | 2.52 | Apoplastic |
| | Mycgr3G89647 | <0.001 | -5.1 | 1 | 88 | SignalP-noTM | | noTP | - | 109 | 7.34 | Apoplastic |
| | Mycgr3G95537 | <0.001 | -5.0 | 0 | 11 | SignalP-noTM | | noTP | - | 155 | 2.58 | Apoplastic |
| | Mycgr3G97449 | <0.001 | -5.0 | 1 | 66 | SignalP-noTM | | noTP | - | 105 | 5.71 | Apoplastic |
| | Mycgr3G106445 | <0.001 | -4.9 | 0 | 5 | SignalP-noTM | | noTP | - | 119 | 8.40 | Apoplastic |
| | Mycgr3G83064 | 0.001 | -4.8 | 1 | 40 | SignalP-noTM | | noTP | - | 75 | 8.00 | Apoplastic |
| | Mycgr3G95672 | <0.001 | -4.7 | 0 | 11 | SignalP-noTM | | noTP | - | 141 | 4.26 | Apoplastic |
| | Mycgr3G97031 | <0.001 | -4.7 | 0 | 44 | SignalP-noTM | | noTP | - | 118 | 8.48 | Apoplastic |
| | Mycgr3G96389 | <0.001 | -4.7 | 0 | 32 | SignalP-noTM | | noTP | - | 109 | 6.42 | Apoplastic/cytoplasmic |
| | Mycgr3G89705 | <0.001 | -4.6 | 0 | 15 | SignalP-noTM | | noTP | Chloroplast | 133 | 3.01 | Apoplastic |
| | Mycgr3G96882 | <0.001 | -4.6 | 0 | 22 | SignalP-TM | | noTP | - | 106 | 4.72 | Apoplastic |
| | Mycgr3G103091 | <0.001 | -4.5 | 0 | 38 | SignalP-noTM | | noTP | - | 82 | 1.22 | Cytoplasmic |
| | Mycgr3G91164 | <0.001 | -4.5 | 0 | 12 | SignalP-noTM | | noTP | - | 126 | 7.94 | Apoplastic/cytoplasmic |
| HT-22 | Mycgr3G108877 | <0.001 | -4.4 | 0 | 12 | SignalP-noTM | | noTP | - | 111 | 5.41 | Apoplastic |
| | Mycgr3G94107 | <0.001 | -4.4 | 0 | 17 | SignalP-noTM | | noTP | Nucleus | 109 | 5.51 | Apoplastic |
| | Mycgr3G99124 | <0.001 | -4.4 | 0 | 6 | SignalP-noTM | | noTP | - | 112 | 6.25 | Apoplastic |
| | Mycgr3G92640 | 0.003 | -4.3 | 2 | 67 | SignalP-noTM | | noTP | - | 120 | 3.33 | Cytoplasmic |
| | Mycgr3G104867 | 0.006 | -4.3 | 0 | 9 | SignalP-noTM | | noTP | - | 170 | 2.35 | Apoplastic |
| | Mycgr3G83081 | <0.001 | -4.2 | 0 | 5 | SignalP-noTM | | SP | - | 53 | 11.32 | Apoplastic |
| | Mycgr3G106436 | <0.001 | -4.2 | 0 | 10 | SignalP-noTM | TMhelix | SP | - | 83 | 9.64 | Cytoplasmic |
| | Mycgr3G76589 | <0.001 | -4.2 | 0 | 3 | SignalP-noTM | | noTP | - | 240 | 5.83 | Apoplastic |
| | Mycgr3G105896 | <0.001 | -4.1 | 0 | 5 | SignalP-noTM | | noTP | - | 192 | 1.56 | Cytoplasmic |
| | Mycgr3G105826 | <0.001 | -4.1 | 0 | 17 | SignalP-noTM | | noTP | - | 98 | 8.16 | Apoplastic |
| | Mycgr3G111221 | <0.001 | -4.1 | 0 | 36 | SignalP-noTM | | noTP | - | 232 | 3.88 | Apoplastic |
| | Mycgr3G95665 | 0.001 | -4.0 | 0 | 14 | SignalP-noTM | | noTP | - | 102 | 4.90 | Apoplastic/cytoplasmic |
| | Mycgr3G80332 | 0.001 | -3.9 | 0 | 7 | SignalP-noTM | | noTP | - | 76 | 7.90 | Apoplastic |
| | Mycgr3G105323 | 0.002 | -3.9 | 0 | 1 | SignalP-noTM | | noTP | - | 319 | 0.63 | Apoplastic |
| | Mycgr3G105682 | <0.001 | -3.9 | 0 | 18 | SignalP-noTM | TMhelix | noTP | - | 95 | 8.42 | Apoplastic |
| | Mycgr3G110220 | <0.001 | -3.9 | 0 | 12 | SignalP-noTM | | noTP | - | 131 | 4.58 | Apoplastic/cytoplasmic |
| | Mycgr3G107738 | 0.001 | -3.9 | 0 | 5 | SignalP-noTM | TMhelix | noTP | - | 399 | 2.26 | Apoplastic |
| | Mycgr3G93045 | <0.001 | -3.9 | 0 | 3 | SignalP-noTM | TMhelix | noTP | Chloroplast/Mitochondria | 231 | 4.76 | Apoplastic |
| | Mycgr3G105265 | <0.001 | -3.8 | 0 | 2 | SignalP-noTM | | noTP | - | 199 | 5.03 | Apoplastic |
| | Mycgr3G107904 | 0.004 | -3.7 | 0 | 7 | SignalP-noTM | | noTP | - | 170 | 3.53 | Apoplastic |
| | Mycgr3G97526 | 0.013 | -3.7 | 0 | 2 | SignalP-noTM | | noTP | - | 205 | 5.85 | Apoplastic |
| | Mycgr3G95416 | 0.014 | -3.6 | 0 | 12 | SignalP-noTM | | noTP | - | 135 | 2.22 | Cytoplasmic/apoplastic |
| | Mycgr3G83835 | <0.001 | -3.4 | 0 | 13 | SignalP-noTM | | noTP | Nucleus | 659 | 0.30 | Cytoplasmic |
| | Mycgr3G111008 | 0.012 | -3.4 | 0 | 7 | SignalP-noTM | | noTP | - | 219 | 1.83 | Apoplastic |
| | Mycgr3G106125 | <0.001 | -3.4 | 0 | 7 | SignalP-noTM | | SP | - | 70 | 8.57 | Apoplastic |

| | | | | | | | | | | | | |
|---|---|---|---|---|---|---|---|---|---|---|---|---|
| | Mycgr3G79286 | <0.001 | -3.4 | 0 | 13 | SignalP-noTM | | SP | - | 63 | 12.70 | Apoplastic |
| | Mycgr3G94383 | <0.001 | -3.1 | 1 | 24 | SignalP-noTM | | noTP | - | 112 | 7.14 | Cytoplasmic/apoplastic |
| | Mycgr3G95035 | 0.030 | -3.0 | 1 | 20 | SignalP-noTM | | noTP | - | 106 | 7.55 | Cytoplasmic/apoplastic |
| | Mycgr3G67799 | <0.001 | -3.0 | 0 | 9 | SignalP-noTM | | noTP | - | 272 | 2.57 | Apoplastic |
| | Mycgr3G66023 | 0.027 | -3.0 | 0 | 1 | SignalP-noTM | | noTP | Nucleus | 426 | 3.29 | Apoplastic |
| | Mycgr3G87205 | 0.022 | -3.0 | 1 | 23 | SignalP-noTM | | SP | - | 55 | 16.36 | Apoplastic |
| | Mycgr3G79161 | 0.012 | -3.0 | 1 | 18 | SignalP-noTM | | SP | - | 68 | 10.29 | Apoplastic |
| | Mycgr3G111223 | <0.001 | -3.0 | 0 | 3 | SignalP-noTM | | noTP | - | 554 | 1.26 | Cytoplasmic |
| | Mycgr3G105223 | <0.001 | -2.8 | 0 | 5 | SignalP-noTM | | noTP | - | 188 | 2.66 | Apoplastic |
| | Mycgr3G109961 | 0.004 | -2.7 | 0 | 2 | SignalP-noTM | TMhelix | noTP | Nucleus | 441 | 0.45 | Cytoplasmic |
| | Mycgr3G111203 | 0.021 | -2.7 | 0 | 1 | SignalP-noTM | | noTP | - | 154 | 3.90 | Cytoplasmic |
| | Mycgr3G101652 | <0.001 | -2.6 | 0 | 9 | SignalP-noTM | | SP | - | 77 | 10.39 | Apoplastic/cytoplasmic |
| | Mycgr3G109679 | 0.018 | -2.6 | 0 | 1 | SignalP-noTM | TMhelix | noTP | - | 197 | 1.52 | Apoplastic |
| | Mycgr3G100063 | <0.001 | -2.6 | 1 | 9 | SignalP-noTM | | noTP | - | 395 | 1.27 | Cytoplasmic |
| | Mycgr3G95831 | 0.013 | -2.5 | 0 | 5 | SignalP-noTM | | noTP | - | 183 | 2.19 | Apoplastic |
| | Mycgr3G111027 | 0.040 | -2.5 | 0 | 1 | SignalP-noTM | | noTP | - | 151 | 2.65 | Apoplastic |
| | Mycgr3G98257 | 0.002 | -2.5 | 0 | 3 | SignalP-noTM | TMhelix | noTP | - | 214 | 0.94 | Cytoplasmic |
| | Mycgr3G88451 | <0.001 | -2.5 | 1 | 12 | SignalP-noTM | | noTP | - | 237 | 0.84 | Apoplastic |
| | Mycgr3G106260 | 0.010 | -2.5 | 0 | 3 | SignalP-noTM | | SP | - | 109 | 14.68 | Apoplastic/cytoplasmic |
| | Mycgr3G106127 | 0.000 | -2.4 | 2 | 21 | SignalP-noTM | | noTP | - | 97 | 6.19 | Apoplastic |
| | Mycgr3G70376 | 0.034 | -2.3 | 1 | 8 | SignalP-noTM | | noTP | - | 202 | 1.98 | Apoplastic |
| | Mycgr3G109137 | <0.001 | -2.3 | 1 | 12 | SignalP-noTM | | noTP | - | 154 | 2.60 | Cytoplasmic/apoplastic |
| | Mycgr3G58400 | <0.001 | -2.3 | 0 | 3 | SignalP-noTM | | noTP | Nucleus | 456 | 1.32 | Cytoplasmic |
| | Mycgr3G102744 | 0.001 | -2.2 | 0 | 1 | SignalP-noTM | | noTP | Nucleus | 545 | 1.47 | Cytoplasmic |
| | Mycgr3G100391 | 0.013 | -2.2 | 0 | 2 | SignalP-noTM | | noTP | - | 425 | 2.12 | Cytoplasmic |
| | Mycgr3G78786 | <0.001 | -2.2 | 0 | 5 | SignalP-noTM | | noTP | - | 189 | 1.06 | Cytoplasmic |
| | Mycgr3G82936 | <0.001 | -2.1 | 1 | 6 | SignalP-noTM | TMhelix | noTP | - | 155 | 1.94 | Apoplastic |
| | Mycgr3G104794 | 0.031 | -1.7 | 3 | 20 | SignalP-noTM | | noTP | - | 157 | 2.55 | Cytoplasmic/apoplastic |
| | Mycgr3G102956 | 0.050 | -1.7 | 1 | 4 | SignalP-noTM | | noTP | - | 258 | 1.55 | Apoplastic |
| | Mycgr3G62211 | 0.006 | -1.7 | 0 | 2 | SignalP-noTM | TMhelix | noTP | - | 428 | 1.87 | Cytoplasmic |
| | Mycgr3G72138 | 0.007 | -1.5 | 1 | 4 | SignalP-noTM | | noTP | - | 178 | 2.25 | Cytoplasmic |
| | Mycgr3G100250 | 0.008 | -1.4 | 0 | 1 | SignalP-noTM | | noTP | - | 387 | 1.03 | Cytoplasmic |
| | Mycgr3G104283 | 0.002 | -1.4 | 1 | 5 | SignalP-noTM | TMhelix | noTP | - | 226 | 5.31 | Apoplastic |
| | Mycgr3G101365 | 0.006 | -1.4 | 1 | 3 | SignalP-noTM | | noTP | - | 363 | 1.10 | Cytoplasmic |
| | Mycgr3G77055 | 0.009 | -1.3 | 4 | 17 | SignalP-noTM | | noTP | Chloroplast | 193 | 0.00 | Cytoplasmic |
| | Mycgr3G104000 | 0.005 | -1.3 | 4 | 15 | SignalP-noTM | | noTP | - | 180 | 3.33 | Cytoplasmic/apoplastic |
| | Mycgr3G106456 | 0.033 | -1.2 | 1 | 4 | SignalP-noTM | TMhelix | noTP | - | 193 | 0.00 | Apoplastic |
| | Mycgr3G104697 | 0.036 | -1.1 | 7 | 22 | SignalP-noTM | | noTP | - | 149 | 2.69 | Apoplastic |
| | Mycgr3G102341 | 0.007 | -0.7 | 4 | 9 | SignalP-noTM | TMhelix | noTP | Nucleus | 459 | 1.53 | Apoplastic |
| | Mycgr3G94290 | 0.035 | -2.0 | 1 | 5 | SignalP-noTM | | noTP | Chloroplast/Nucleus | 184 | 3.26 | Cytoplasmic/apoplastic effector |
| | Mycgr3G91409 | 0.008 | -1.8 | 2 | 14 | SignalP-noTM | TMhelix | noTP | - | 130 | 4.62 | Cytoplasmic/apoplastic effector |
| | Mycgr3G90776 | <0.001 | -1.9 | 1 | 8 | SignalP-noTM | | noTP | - | 242 | 0.00 | Cytoplasmic effector |
| | Mycgr3G104754 | 0.003 | -1.7 | 1 | 6 | SignalP-noTM | | noTP | - | 163 | 0.61 | Cytoplasmic effector |
| | Mycgr3G100167 | 0.034 | -1.5 | 1 | 4 | SignalP-noTM | | noTP | - | 142 | 1.41 | Cytoplasmic effector |
| HT-22 & IPO323 | Mycgr3G94232 | 0.020 | -1.4 | 3 | 12 | SignalP-noTM | | noTP | - | 178 | 4.49 | Cytoplasmic effector |
| | Mycgr3G71216 | 0.016 | -1.3 | 7 | 28 | SignalP-noTM | | noTP | Nucleus | 196 | 0.51 | Cytoplasmic effector |
| | Mycgr3G101587 | 0.020 | -1.3 | 1 | 6 | SignalP-noTM | | noTP | - | 508 | 1.18 | Cytoplasmic effector |
| | Mycgr3G88698 | 0.025 | -2.7 | 1 | 11 | SignalP-noTM | | noTP | - | 159 | 5.03 | Apoplastic/cytoplasmic effector |
| | Mycgr3G102617 | <0.001 | -2.2 | 1 | 11 | SignalP-noTM | | noTP | - | 158 | 8.23 | Apoplastic/cytoplasmic effector |
| | Mycgr3G82925 | 0.008 | -1.1 | 4 | 11 | SignalP-noTM | | noTP | - | 57 | 10.53 | Apoplastic/cytoplasmic effector |
| | Mycgr3G105867 | <0.001 | -2.4 | 2 | 16 | SignalP-noTM | | noTP | - | 116 | 6.03 | Apoplastic effector |
| | Mycgr3G90420 | 0.001 | -2.3 | 1 | 16 | SignalP-noTM | | noTP | - | 122 | 2.46 | Apoplastic effector |

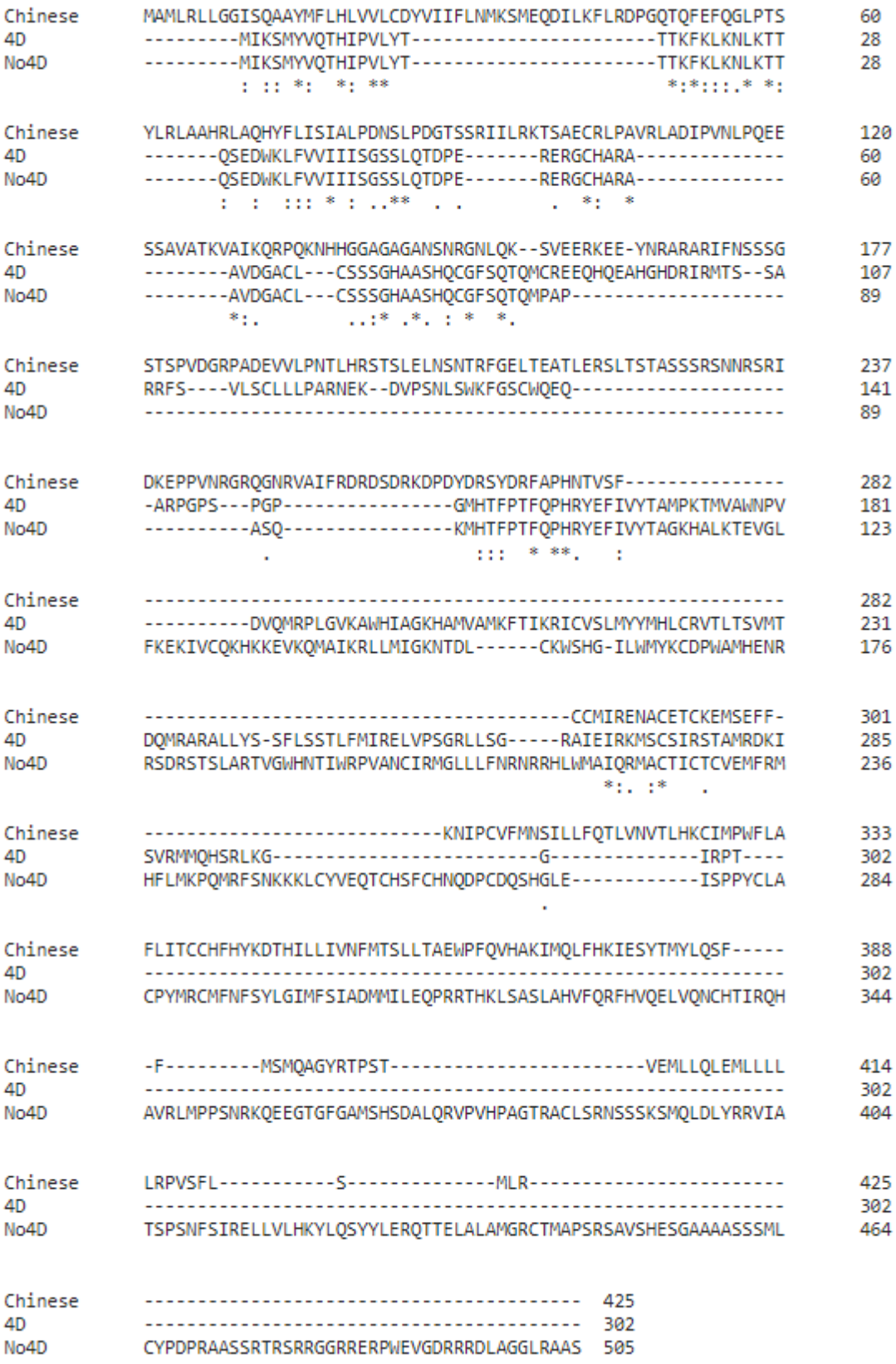
| | | | | | | | | | | | |
|---|---|---|---|---|---|---|---|---|---|---|---|
| | Mycgr3G104444 | 0.016 | -2.3 | 8 | 72 | SignalP-noTM | noTP | - | 79 | 12.66 | Apoplastic effector |
| | Mycgr3G93075 | 0.001 | -2.1 | 3 | 21 | SignalP-noTM | noTP | Chloroplast | 193 | 5.18 | Apoplastic effector |
| | Mycgr3G104404 | 0.015 | -2.1 | 4 | 31 | SignalP-noTM | noTP | - | 179 | 2.24 | Apoplastic effector |
| | Mycgr3G105487 | 0.014 | -1.4 | 2 | 10 | SignalP-noTM | noTP | - | 97 | 4.12 | Apoplastic effector |
| IPO323 | Mycgr3G104383 | 0.029 | -1.7 | 5 | 26 | SignalP-noTM | SP | - | 74 | 10.81 | Apoplastic/cytoplasmic effector |
| | Mycgr3G94526 | 0.001 | -1.9 | 2 | 11 | SignalP-noTM | noTP | Nucleus | 174 | 0.58 | Cytoplasmic effector |



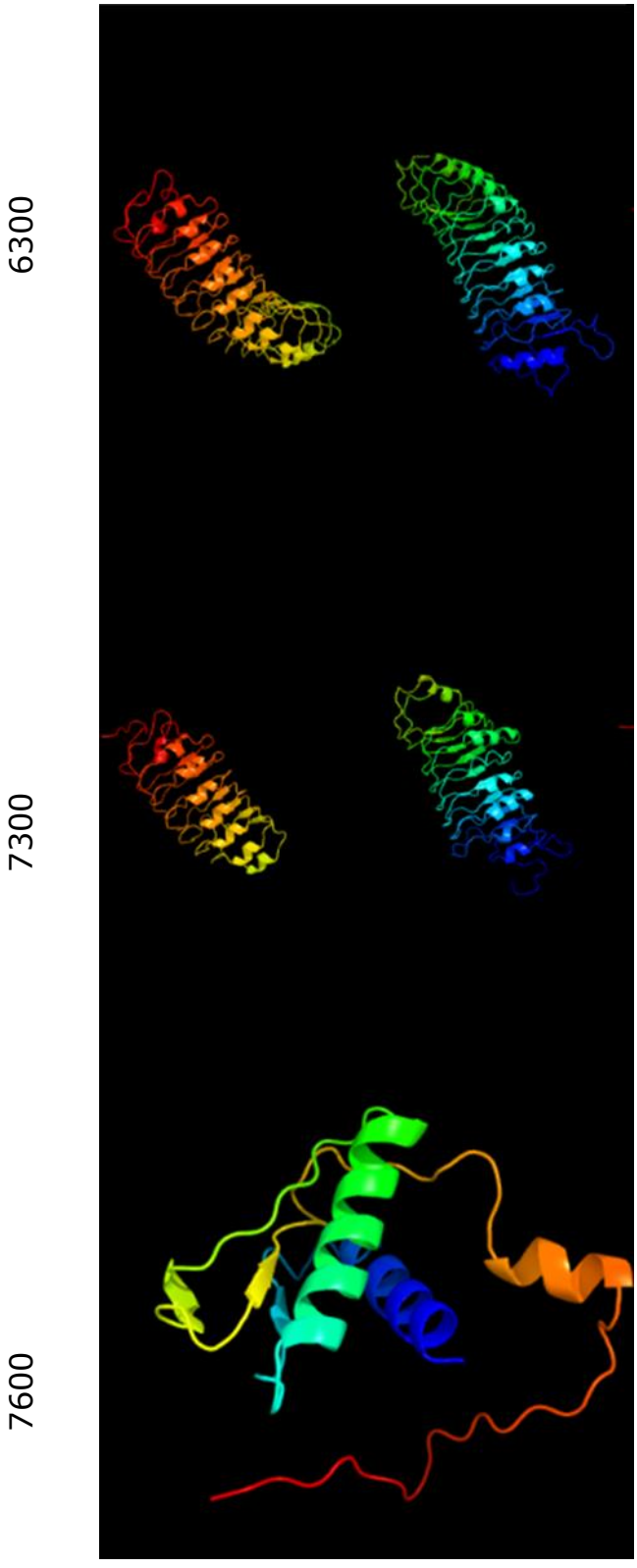

**Supp. Figure 1.** Protein alignment of 6300 candidate gene protein reading frame.




**Supp. Figure 2.** Protein alignment of 7300 candidate gene protein reading frame. (5'3' Frame 1)




**Supp. Figure 3.** Protein alignment of 7600 candidate gene protein reading frame. (5'3' Frame 1)




**Supp. Figure. 4.** Phyre2 model prediction for protein exons in candidate genes. (6300 & 7300 c6s6qB model crystal structure of the lrr ectodomain of the plant membrane receptor2 kinase gassho1/schengen3 from arabidopsis thaliana in complex with3 casparian strip integrity factor 2.) (7600 R3H domain)

**Table S12.** Visual assessment phenotype of 4D-R & 4D-S lines when inoculated with HT-22 or 508. 4D-R & 4D-S lines infected by HT-22 or 508 are analysed using student T-tests (Figure 1) (Asterix indicates P<0.05) for (a), % Necrotic lesions (b) & pycnidia presence (c) (P <0.05). Effect of compatibility analysed using an ANOVA.

| *Z.tritici* visual measurement | Source of variation | d.f | s.s. | m.s. | v.r. | F pr. |
|---|---|---|---|---|---|---|
| % chlorotic lesion coverage | Exp stratum | 1 | 21.56 | 21.56 | 3.08 | |
| | Exp.rep stratum | 10 | 69.98 | 7 | 0.42 | |
| | Exp.rep.*Units* stratum | | | | | |
| | Compatibility | 1 | 124.38 | 124.38 | 7.44 | 0.007 |
| | dpi | 3 | 934.74 | 311.58 | 18.63 | <.001 |
| | Gene | 1 | 5.74 | 5.74 | 0.34 | 0.559 |
| | Isolate | 1 | 11.57 | 11.57 | 0.69 | 0.407 |
| | Compatibility.dpi | 3 | 133.63 | 44.54 | 2.66 | 0.05 |
| | dpi.Gene | 3 | 28.47 | 9.49 | 0.57 | 0.637 |
| | dpi.Isolate | 3 | 268.05 | 89.35 | 5.34 | 0.002 |
| | Residual | 165 | 2759.6 | 16.72 | | |
| | Total | 191 | 4357.72 | | | |
| % necrotic lesion coverage | Exp stratum | 1 | 20.2 | 20.2 | 0.22 | |
| | Exp.rep stratum | 10 | 928 | 92.8 | 0.88 | |
| | Exp.rep.*Units* stratum | | | | | |
| | Compatibility | 1 | 12797.3 | 12797.3 | 121.45 | <.001 |
| | dpi | 3 | 61169.2 | 20389.7 | 193.5 | <.001 |
| | Gene | 1 | 2085.5 | 2085.5 | 19.79 | <.001 |
| | Isolate | 1 | 49.6 | 49.6 | 0.47 | 0.494 |
| | Compatibility.dpi | 3 | 19244.1 | 6414.7 | 60.88 | <.001 |
| | dpi.Gene | 3 | 2037.5 | 679.2 | 6.45 | <.001 |
| | dpi.Isolate | 3 | 302.7 | 100.9 | 0.96 | 0.414 |
| | Residual | 165 | 17386.5 | 105.4 | | |
| | Total | 191 | 116020.6 | | | |
| Pycnidia incidence | Exp stratum | 1 | 0.48669 | 0.48669 | 33.64 | |
| | Exp.rep stratum | 10 | 0.14468 | 0.01447 | 0.75 | |
| | Exp.rep.*Units* stratum | | | | | |

| | | | | | |
|---|---|---|---|---|---|
| Compatibility | 1 | 7.18538 | 7.18538 | 371.34 | <.001 |
| dpi | 3 | 17.69618 | 5.89873 | 304.85 | <.001 |
| Gene | 1 | 0.52816 | 0.52816 | 27.3 | <.001 |
| Isolate | 1 | 0.1956 | 0.1956 | 10.11 | 0.002 |
| Compatibility.dpi | 3 | 5.89873 | 1.96624 | 101.62 | <.001 |
| dpi.Gene | 3 | 0.36227 | 0.12076 | 6.24 | <.001 |
| dpi.Isolate | 3 | 0.19792 | 0.06597 | 3.41 | 0.019 |
| Residual | 165 | 3.19271 | 0.01935 | | |
| Total | 191 | 35.88831 | | | |

**Table S13.** qE & qI form of NPQ of 4D-R & 4D-S lines inoculated with HT-22 or 508. 4D-R & 4D-S lines infected by HT-22 or 508 are analysed using student T-tests (Figure 2). Effect of compatibility analysed using an ANOVA.

| NPQ component | hours post inoculation | Source of variation | d.f | s.s. | m.s. | v.r. | F pr. |
|---|---|---|---|---|---|---|---|
| QE | 6 | Rep stratum | 5 | 0.20222 | 0.04044 | 1.22 | |
| | | Rep.*Units* stratum | | | | | |
| | | %4D | 1 | 0.10528 | 0.10528 | 3.18 | 0.082 |
| | | Isolate | 1 | 0.0134 | 0.0134 | 0.41 | 0.528 |
| | | Compatibility | 1 | 0.00361 | 0.00361 | 0.11 | 0.743 |
| | | Residual | 39 | 1.28983 | 0.03307 | | |
| | | Total | 47 | 1.61434 | | | |
| | 12 | Rep stratum | 5 | 0.0496 | 0.00992 | 0.28 | |
| | | Rep.*Units* stratum | | | | | |
| | | %4D | 1 | 0.00008 | 0.00008 | 0 | 0.962 |
| | | Isolate | 1 | 0.00076 | 0.00076 | 0.02 | 0.885 |
| | | Compatibility | 1 | 0.00179 | 0.00179 | 0.05 | 0.824 |
| | | Residual | 39 | 1.39763 | 0.03584 | | |
| | | Total | 47 | 1.44986 | | | |
| | 24 | Rep stratum | 5 | 0.1553 | 0.03106 | 1.27 | |
| | | Rep.*Units* stratum | | | | | |
| | | %4D | 1 | 0.00054 | 0.00054 | 0.02 | 0.883 |
| | | Isolate | 1 | 0.00379 | 0.00379 | 0.15 | 0.696 |
| | | Compatibility | 1 | 0.02985 | 0.02985 | 1.22 | 0.277 |
| | | Residual | 39 | 0.95586 | 0.02451 | | |
| | | Total | 47 | 1.14534 | | | |
| | 48 | Rep stratum | 5 | 0.09114 | 0.01823 | 0.74 | |
| | | Rep.*Units* stratum | | | | | |
| | | %4D | 1 | 0.11164 | 0.11164 | 4.55 | 0.039 |
| | | Isolate | 1 | 0.00182 | 0.00182 | 0.07 | 0.787 |

| | | | | | | | |
|---|---|---|---|---|---|---|---|
| | | Compatibility | 1 | 0.00163 | 0.00163 | 0.07 | 0.798 |
| | | Residual | 39 | 0.95598 | 0.02451 | | |
| | | Total | 47 | 1.16222 | | | |
| QI | 6 | Rep stratum | 5 | 0.014567 | 0.002913 | 2.32 | |
| | | Rep.*Units* stratum | | | | | |
| | | %4D | 1 | 0.006694 | 0.006694 | 5.32 | 0.026 |
| | | Isolate | 1 | 0.000809 | 0.000809 | 0.64 | 0.427 |
| | | Compatibility | 1 | 0.0002 | 0.0002 | 0.16 | 0.692 |
| | | Residual | 39 | 0.04907 | 0.001258 | | |
| | | Total | 47 | 0.07134 | | | |
| | 12 | Rep stratum | 5 | 0.013659 | 0.002732 | 2.91 | |
| | | Rep.*Units* stratum | | | | | |
| | | %4D | 1 | 4.56E-05 | 4.56E-05 | 0.05 | 0.827 |
| | | Isolate | 1 | 3.17E-05 | 3.17E-05 | 0.03 | 0.855 |
| | | Compatibility | 1 | 0.000922 | 0.000922 | 0.98 | 0.328 |
| | | Residual | 39 | 0.036659 | 0.00094 | | |
| | | Total | 47 | 0.051317 | | | |
| | 24 | Rep stratum | 5 | 0.008718 | 0.001744 | 1.2 | |
| | | Rep.*Units* stratum | | | | | |
| | | %4D | 1 | 0.000014 | 0.000014 | 0.01 | 0.921 |
| | | Isolate | 1 | 0.003838 | 0.003838 | 2.63 | 0.113 |
| | | Compatibility | 1 | 0.000003 | 0.000003 | 0 | 0.965 |
| | | Residual | 39 | 0.05682 | 0.001457 | | |
| | | Total | 47 | 0.069394 | | | |
| | 48 | Rep stratum | 5 | 0.009302 | 0.00186 | 1.44 | |
| | | Rep.*Units* stratum | | | | | |
| | | %4D | 1 | 0.000178 | 0.000178 | 0.14 | 0.712 |
| | | Isolate | 1 | 0.001724 | 0.001724 | 1.33 | 0.255 |
| | | Compatibility | 1 | 0.001026 | 0.001026 | 0.79 | 0.379 |

| | | | |
|---|---|---|---|
| Residual | 39 | 0.050421 | 0.001293 |
| Total | 47 | 0.062651 | |

**Table S14.** NPQ of 4D-R & 4D-S lines inoculated with HT-22 or 508 at 6, 12, 24 & 48 hpi. 4D-R & 4D-S lines infected by HT-22 or 508 are analysed using student T-tests (Figure 3). Effect of compatibility analysed using an ANOVA.

| NPQ (Light/Dark) | Hours post inoculation | Source of variation | d.f | s.s. | m.s. | v.r. | F pr. |
|---|---|---|---|---|---|---|---|
| Light | 6 | Rep stratum | 5 | 1.61542 | 0.32308 | 6.52 | |
| | | Rep.*Units* stratum | | | | | |
| | | %4D | 1 | 0.57744 | 0.57744 | 11.65 | <.001 |
| | | Isolate | 1 | 0.06176 | 0.06176 | 1.25 | 0.265 |
| | | Compatibility | 1 | 0.05731 | 0.05731 | 1.16 | 0.283 |
| | | Min | 5 | 41.17978 | 8.23596 | 166.22 | <.001 |
| | | %4D.Min | 5 | 0.0309 | 0.00618 | 0.12 | 0.987 |
| | | Isolate.Min | 5 | 0.13713 | 0.02743 | 0.55 | 0.736 |
| | | Compatibility.Min | 5 | 0.01134 | 0.00227 | 0.05 | 0.999 |
| | | Residual | 259 | 12.8332 | 0.04955 | | |
| | | Total | 287 | 56.50428 | | | |
| Dark | 6 | Rep stratum | 5 | 0.023975 | 0.004795 | 9.38 | |
| | | Rep.*Units* stratum | | | | | |
| | | %4D | 1 | 0.022859 | 0.022859 | 44.74 | <.001 |
| | | Isolate | 1 | 0.001027 | 0.001027 | 2.01 | 0.158 |
| | | Compatibility | 1 | 0.002658 | 0.002658 | 5.2 | 0.023 |
| | | Min | 5 | 0.339038 | 0.067808 | 132.71 | <.001 |
| | | %4D.Min | 5 | 0.000495 | 0.000099 | 0.19 | 0.965 |
| | | Isolate.Min | 5 | 0.000303 | 6.06E-05 | 0.12 | 0.988 |
| | | Compatibility.Min | 5 | 0.000177 | 3.53E-05 | 0.07 | 0.997 |
| | | Residual | 259 | 0.132339 | 0.000511 | | |
| | | Total | 287 | 0.522871 | | | |
| Light | 12 | Rep stratum | 5 | 0.36876 | 0.07375 | 1.67 | |
| | | Rep.*Units* stratum | | | | | |
| | | %4D | 1 | 0.02789 | 0.02789 | 0.63 | 0.427 |
| | | Isolate | 1 | 0.08302 | 0.08302 | 1.89 | 0.171 |
| | | Compatibility | 1 | 0.07671 | 0.07671 | 1.74 | 0.188 |
| | | Min | 5 | 45.03871 | 9.00774 | 204.52 | <.001 |

| | | | | | | |
|---|---|---|---|---|---|---|
| | | %4D.Min | 5 | 0.06247 | 0.01249 | 0.28 | 0.922 |
| | | Isolate.Min | 5 | 0.07598 | 0.0152 | 0.35 | 0.885 |
| | | Compatibility.Min | 5 | 0.10922 | 0.02184 | 0.5 | 0.779 |
| | | Residual | 259 | 11.40696 | 0.04404 | | |
| | | Total | 287 | 57.24973 | | | |
| Dark | 12 | Rep stratum | 5 | 0.01572 | 0.003144 | 7.93 | |
| | | Rep.*Units* stratum | | | | | |
| | | %4D | 1 | 0.000005 | 0.000005 | 0.01 | 0.911 |
| | | Isolate | 1 | 1.48E-05 | 1.48E-05 | 0.04 | 0.847 |
| | | Compatibility | 1 | 9E-07 | 9E-07 | 0 | 0.961 |
| | | Min | 5 | 0.312782 | 0.062557 | 157.78 | <.001 |
| | | %4D.Min | 5 | 0.0005 | 9.99E-05 | 0.25 | 0.939 |
| | | Isolate.Min | 5 | 4.21E-05 | 8.4E-06 | 0.02 | 1 |
| | | Compatibility.Min | 5 | 0.000674 | 0.000135 | 0.34 | 0.888 |
| | | Residual | 259 | 0.102686 | 0.000397 | | |
| | | Total | 287 | 0.432425 | | | |
| Light | 24 | Rep stratum | 5 | 0.80585 | 0.16117 | 3.55 | |
| | | Rep.*Units* stratum | | | | | |
| | | %4D | 1 | 0.11986 | 0.11986 | 2.64 | 0.105 |
| | | Isolate | 1 | 0.03045 | 0.03045 | 0.67 | 0.414 |
| | | Compatibility | 1 | 0.74175 | 0.74175 | 16.34 | <.001 |
| | | Min | 5 | 28.77028 | 5.75406 | 126.75 | <.001 |
| | | %4D.Min | 5 | 0.05266 | 0.01053 | 0.23 | 0.948 |
| | | Isolate.Min | 5 | 0.03818 | 0.00764 | 0.17 | 0.974 |
| | | Compatibility.Min | 5 | 0.11592 | 0.02318 | 0.51 | 0.768 |
| | | Residual | 259 | 11.75761 | 0.0454 | | |
| | | Total | 287 | 42.43255 | | | |
| Dark | 24 | Rep stratum | 5 | 0.013546 | 0.002709 | 5.97 | |
| | | Rep.*Units* stratum | | | | | |
| | | %4D | 1 | 0.001325 | 0.001325 | 2.92 | 0.089 |
| | | Isolate | 1 | 0.000281 | 0.000281 | 0.62 | 0.432 |
| | | Compatibility | 1 | 0.001362 | 0.001362 | 3 | 0.084 |
| | | Min | 5 | 0.375644 | 0.075129 | 165.53 | <.001 |

| | | | | | | | |
|---|---|---|---|---|---|---|---|
| | | %4D.Min | 5 | 0.000646 | 0.000129 | 0.28 | 0.921 |
| | | Isolate.Min | 5 | 0.001248 | 0.00025 | 0.55 | 0.738 |
| | | Compatibility.Min | 5 | 8.15E-05 | 1.63E-05 | 0.04 | 0.999 |
| | | Residual | 259 | 0.117551 | 0.000454 | | |
| | | Total | 287 | 0.511684 | | | |
| | | Rep stratum | 5 | 1.19409 | 0.23882 | 5.13 | |
| | | Rep.*Units* stratum | | | | | |
| | | %4D | 1 | 2.08802 | 2.08802 | 44.85 | <.001 |
| | | Isolate | 1 | 0.17291 | 0.17291 | 3.71 | 0.055 |
| | | Compatibility | 1 | 0.20738 | 0.20738 | 4.45 | 0.036 |
| Light | 48 | Min | 5 | 33.31623 | 6.66325 | 143.13 | <.001 |
| | | %4D.Min | 5 | 0.21148 | 0.0423 | 0.91 | 0.476 |
| | | Isolate.Min | 5 | 0.16885 | 0.03377 | 0.73 | 0.605 |
| | | Compatibility.Min | 5 | 0.02583 | 0.00517 | 0.11 | 0.99 |
| | | Residual | 259 | 12.05721 | 0.04655 | | |
| | | Total | 287 | 49.44199 | | | |
| | | Rep stratum | 5 | 0.008377 | 0.001675 | 3.6 | |
| | | Rep.*Units* stratum | | | | | |
| | | %4D | 1 | 0.01084 | 0.01084 | 23.32 | <.001 |
| | | Isolate | 1 | 0.001382 | 0.001382 | 2.97 | 0.086 |
| | | Compatibility | 1 | 0.000264 | 0.000264 | 0.57 | 0.452 |
| Dark | 48 | Min | 5 | 0.363417 | 0.072683 | 156.4 | <.001 |
| | | %4D.Min | 5 | 0.000262 | 5.24E-05 | 0.11 | 0.989 |
| | | Isolate.Min | 5 | 0.000141 | 2.82E-05 | 0.06 | 0.998 |
| | | Compatibility.Min | 5 | 9.53E-05 | 1.91E-05 | 0.04 | 0.999 |
| | | Residual | 259 | 0.120368 | 0.000465 | | |
| | | Total | 287 | 0.505146 | | | |

**Table S15.** LI-COR phenotyping of 4D-R & 4D-S lines inoculated with HT-22 or 508 at 48 hpi for qP, PhiPS2, ETR, Photosynthesis & Conductance. 4D-R & 4D-S lines infected by HT-22 or 508 are analysed using student T-tests (Figure 4 &5). Effect of compatibility analysed using an ANOVA

| Measurement | hours post inoculation | Source of variation | d.f | s.s. | m.s. | v.r. | F pr. |
|---|---|---|---|---|---|---|---|
| qP | 6 | Rep stratum | 5 | 0.057644 | 0.011529 | 9.07 | |
| | | Rep.*Units* stratum | | | | | |
| | | %4D | 1 | 0.011559 | 0.011559 | 9.09 | 0.003 |
| | | Isolate | 1 | 0.025504 | 0.025504 | 20.06 | <.001 |
| | | Compatibility | 1 | 0.002222 | 0.002222 | 1.75 | 0.187 |
| | | Min | 5 | 3.336647 | 0.667329 | 524.96 | <.001 |
| | | %4D.Min | 5 | 0.001176 | 0.000235 | 0.18 | 0.968 |
| | | Isolate.Min | 5 | 0.001716 | 0.000343 | 0.27 | 0.929 |
| | | Compatibility.Min | 5 | 0.000218 | 0.000044 | 0.03 | 0.999 |
| | | Residual | 259 | 0.329238 | 0.001271 | | |
| | | Total | 287 | 3.765924 | | | |
| | 12 | Rep stratum | 5 | 0.05879 | 0.011758 | 9.66 | |
| | | Rep.*Units* stratum | | | | | |
| | | %4D | 1 | 0.002605 | 0.002605 | 2.14 | 0.145 |
| | | Isolate | 1 | 0.004787 | 0.004787 | 3.93 | 0.048 |
| | | Compatibility | 1 | 0.000366 | 0.000366 | 0.3 | 0.584 |
| | | Min | 5 | 3.292015 | 0.658403 | 541.16 | <.001 |
| | | %4D.Min | 5 | 0.000488 | 0.000098 | 0.08 | 0.995 |
| | | Isolate.Min | 5 | 0.000766 | 0.000153 | 0.13 | 0.986 |
| | | Compatibility.Min | 5 | 0.001014 | 0.000203 | 0.17 | 0.975 |
| | | Residual | 259 | 0.315112 | 0.001217 | | |
| | | Total | 287 | 3.675944 | | | |
| | 24 | Rep stratum | 5 | 0.021642 | 0.004329 | 4.9 | |
| | | Rep.*Units* stratum | | | | | |
| | | %4D | 1 | 0.024105 | 0.024105 | 27.29 | <.001 |
| | | Isolate | 1 | 0.049399 | 0.049399 | 55.93 | <.001 |
| | | Compatibility | 1 | 0.014385 | 0.014385 | 16.29 | <.001 |
| | | Min | 5 | 2.786214 | 0.557243 | 630.89 | <.001 |
| | | %4D.Min | 5 | 0.001525 | 0.000305 | 0.35 | 0.885 |

| | | | | | | |
|---|---|---|---|---|---|---|
| | Isolate.Min | 5 | 0.001249 | 0.00025 | 0.28 | 0.922 |
| | Compatibility.Min | 5 | 0.002664 | 0.000533 | 0.6 | 0.698 |
| | Residual | 259 | 0.228767 | 0.000883 | | |
| | Total | 287 | 3.12995 | | | |
| | Rep stratum | 5 | 0.04147 | 0.008294 | 8.13 | |
| | Rep.*Units* stratum | | | | | |
| | %4D | 1 | 0.000269 | 0.000269 | 0.26 | 0.608 |
| | Isolate | 1 | 0.004229 | 0.004229 | 4.14 | 0.043 |
| | Compatibility | 1 | 0.018649 | 0.018649 | 18.27 | <.001 |
| 48 | Min | 5 | 2.5083 | 0.50166 | 491.49 | <.001 |
| | %4D.Min | 5 | 0.002124 | 0.000425 | 0.42 | 0.837 |
| | Isolate.Min | 5 | 0.000334 | 0.000067 | 0.07 | 0.997 |
| | Compatibility.Min | 5 | 0.003955 | 0.000791 | 0.77 | 0.569 |
| | Residual | 259 | 0.26436 | 0.001021 | | |
| | Total | 287 | 2.843689 | | | |
| | Rep stratum | 5 | 8200.5 | 1640.1 | 9.35 | |
| | Rep.*Units* stratum | | | | | |
| | %4D | 1 | 148.6 | 148.6 | 0.85 | 0.358 |
| | Isolate | 1 | 3074.3 | 3074.3 | 17.52 | <.001 |
| | Compatibility | 1 | 67.5 | 67.5 | 0.38 | 0.536 |
| 6 | Min | 5 | 258886.9 | 51777.4 | 295.02 | <.001 |
| | %4D.Min | 5 | 28.7 | 5.7 | 0.03 | 0.999 |
| | Isolate.Min | 5 | 207.6 | 41.5 | 0.24 | 0.946 |
| | Compatibility.Min | 5 | 10.6 | 2.1 | 0.01 | 1 |
| | Residual | 259 | 45455.5 | 175.5 | | |
| ETR | Total | 287 | 316080.3 | | | |
| | Rep stratum | 5 | 8917.9 | 1783.6 | 10.32 | |
| | Rep.*Units* stratum | | | | | |
| 12 | %4D | 1 | 592.3 | 592.3 | 3.43 | 0.065 |
| | Isolate | 1 | 842.1 | 842.1 | 4.87 | 0.028 |
| | Compatibility | 1 | 78.4 | 78.4 | 0.45 | 0.501 |
| | Min | 5 | 239815.9 | 47963.2 | 277.64 | <.001 |
| | %4D.Min | 5 | 39.9 | 8 | 0.05 | 0.999 |

| | | | | | | | |
|---|---|---|---|---|---|---|---|
| | | Isolate.Min | 5 | 76.7 | 15.3 | 0.09 | 0.994 |
| | | Compatibility.Min | 5 | 81.8 | 16.4 | 0.09 | 0.993 |
| | | Residual | 259 | 44743.5 | 172.8 | | |
| | | Total | 287 | 295188.4 | | | |
| | 24 | Rep stratum | 5 | 6595.2 | 1319 | 9.81 | |
| | | Rep.*Units* stratum | | | | | |
| | | %4D | 1 | 2813.5 | 2813.5 | 20.93 | <.001 |
| | | Isolate | 1 | 7006.2 | 7006.2 | 52.11 | <.001 |
| | | Compatibility | 1 | 3317.7 | 3317.7 | 24.68 | <.001 |
| | | Min | 5 | 215426.4 | 43085.3 | 320.47 | <.001 |
| | | %4D.Min | 5 | 396.1 | 79.2 | 0.59 | 0.708 |
| | | Isolate.Min | 5 | 91.4 | 18.3 | 0.14 | 0.984 |
| | | Compatibility.Min | 5 | 568.5 | 113.7 | 0.85 | 0.518 |
| | | Residual | 259 | 34821.4 | 134.4 | | |
| | | Total | 287 | 271036.3 | | | |
| | 48 | Rep stratum | 5 | 6917.2 | 1383.4 | 9.55 | |
| | | Rep.*Units* stratum | | | | | |
| | | %4D | 1 | 531.9 | 531.9 | 3.67 | 0.056 |
| | | Isolate | 1 | 1441.4 | 1441.4 | 9.95 | 0.002 |
| | | Compatibility | 1 | 3330.4 | 3330.4 | 22.99 | <.001 |
| | | Min | 5 | 195489.3 | 39097.9 | 269.87 | <.001 |
| | | %4D.Min | 5 | 347.1 | 69.4 | 0.48 | 0.792 |
| | | Isolate.Min | 5 | 100.6 | 20.1 | 0.14 | 0.983 |
| | | Compatibility.Min | 5 | 536.4 | 107.3 | 0.74 | 0.594 |
| | | Residual | 259 | 37523.5 | 144.9 | | |
| | | Total | 287 | 246217.7 | | | |
| PhiPS2 | 6 | Rep stratum | 5 | 0.01895 | 0.00379 | 9.29 | |
| | | Rep.*Units* stratum | | | | | |
| | | %4D | 1 | 0.000347 | 0.000347 | 0.85 | 0.357 |
| | | Isolate | 1 | 0.007143 | 0.007143 | 17.52 | <.001 |
| | | Compatibility | 1 | 0.000154 | 0.000154 | 0.38 | 0.539 |
| | | Min | 5 | 0.601049 | 0.12021 | 294.76 | <.001 |
| | | %4D.Min | 5 | 0.000066 | 1.32E-05 | 0.03 | 0.999 |

| | | | | | | |
|---|---|---|---|---|---|---|
| | Isolate.Min | 5 | 0.000485 | 0.000097 | 0.24 | 0.946 |
| | Compatibility.Min | 5 | 2.57E-05 | 5.1E-06 | 0.01 | 1 |
| | Residual | 259 | 0.105625 | 0.000408 | | |
| | Total | 287 | 0.733845 | | | |
| 12 | Rep stratum | 5 | 0.020729 | 0.004146 | 10.35 | |
| | Rep.*Units* stratum | | | | | |
| | %4D | 1 | 0.001372 | 0.001372 | 3.42 | 0.065 |
| | Isolate | 1 | 0.001962 | 0.001962 | 4.9 | 0.028 |
| | Compatibility | 1 | 0.00018 | 0.00018 | 0.45 | 0.504 |
| | Min | 5 | 0.556892 | 0.111378 | 277.93 | <.001 |
| | %4D.Min | 5 | 9.01E-05 | 0.000018 | 0.04 | 0.999 |
| | Isolate.Min | 5 | 0.00018 | 3.61E-05 | 0.09 | 0.994 |
| | Compatibility.Min | 5 | 0.000193 | 3.86E-05 | 0.1 | 0.993 |
| | Residual | 259 | 0.103793 | 0.000401 | | |
| | Total | 287 | 0.685393 | | | |
| 24 | Rep stratum | 5 | 0.015364 | 0.003073 | 9.84 | |
| | Rep.*Units* stratum | | | | | |
| | %4D | 1 | 0.006536 | 0.006536 | 20.94 | <.001 |
| | Isolate | 1 | 0.016265 | 0.016265 | 52.11 | <.001 |
| | Compatibility | 1 | 0.007711 | 0.007711 | 24.7 | <.001 |
| | Min | 5 | 0.500413 | 0.100083 | 320.63 | <.001 |
| | %4D.Min | 5 | 0.000933 | 0.000187 | 0.6 | 0.702 |
| | Isolate.Min | 5 | 0.000214 | 4.28E-05 | 0.14 | 0.984 |
| | Compatibility.Min | 5 | 0.001321 | 0.000264 | 0.85 | 0.518 |
| | Residual | 259 | 0.080846 | 0.000312 | | |
| | Total | 287 | 0.629602 | | | |
| 48 | Rep stratum | 5 | 0.015999 | 0.0032 | 9.49 | |
| | Rep.*Units* stratum | | | | | |
| | %4D | 1 | 0.00124 | 0.00124 | 3.68 | 0.056 |
| | Isolate | 1 | 0.00335 | 0.00335 | 9.93 | 0.002 |
| | Compatibility | 1 | 0.007764 | 0.007764 | 23.03 | <.001 |
| | Min | 5 | 0.453784 | 0.090757 | 269.16 | <.001 |
| | %4D.Min | 5 | 0.00082 | 0.000164 | 0.49 | 0.786 |

| | | | | | | | |
|---|---|---|---|---|---|---|---|
| | | Isolate.Min | 5 | 0.000239 | 4.79E-05 | 0.14 | 0.982 |
| | | Compatibility.Min | 5 | 0.001229 | 0.000246 | 0.73 | 0.602 |
| | | Residual | 259 | 0.087331 | 0.000337 | | |
| | | Total | 287 | 0.571755 | | | |
| | 6 | Rep stratum | 5 | 1046.23 | 209.25 | 8.34 | |
| | | Rep.*Units* stratum | | | | | |
| | | %4D | 1 | 21.74 | 21.74 | 0.87 | 0.353 |
| | | Isolate | 1 | 182.49 | 182.49 | 7.27 | 0.007 |
| | | Compatibility | 1 | 1.56 | 1.56 | 0.06 | 0.803 |
| | | Min | 5 | 10554.2 | 2110.84 | 84.12 | <.001 |
| | | %4D.Min | 5 | 72.66 | 14.53 | 0.58 | 0.716 |
| | | Isolate.Min | 5 | 38.04 | 7.61 | 0.3 | 0.911 |
| | | Compatibility.Min | 5 | 33.28 | 6.66 | 0.27 | 0.932 |
| | | Residual | 251 | 6298.29 | 25.09 | | |
| | | Total | 279 | 17402.91 | | | |
| Photosynthesis | 12 | Rep stratum | 5 | 502.53 | 100.51 | 4.49 | |
| | | Rep.*Units* stratum | | | | | |
| | | %4D | 1 | 51.21 | 51.21 | 2.29 | 0.132 |
| | | Isolate | 1 | 31.05 | 31.05 | 1.39 | 0.24 |
| | | Compatibility | 1 | 410.09 | 410.09 | 18.32 | <.001 |
| | | Min | 5 | 8672.68 | 1734.54 | 77.48 | <.001 |
| | | %4D.Min | 5 | 8.22 | 1.64 | 0.07 | 0.996 |
| | | Isolate.Min | 5 | 20.67 | 4.13 | 0.18 | 0.968 |
| | | Compatibility.Min | 5 | 33.59 | 6.72 | 0.3 | 0.912 |
| | | Residual | 249 | 5574.32 | 22.39 | | |
| | | Total | 277 | 14527.15 | | | |
| | 24 | Rep stratum | 5 | 188.67 | 37.73 | 1.91 | |
| | | Rep.*Units* stratum | | | | | |
| | | %4D | 1 | 669.22 | 669.22 | 33.95 | <.001 |
| | | Isolate | 1 | 3.02 | 3.02 | 0.15 | 0.696 |
| | | Compatibility | 1 | 128.35 | 128.35 | 6.51 | 0.011 |
| | | Min | 5 | 8072.62 | 1614.52 | 81.9 | <.001 |
| | | %4D.Min | 5 | 77.78 | 15.56 | 0.79 | 0.558 |

| | | | | | | |
|---|---|---|---|---|---|---|
| | Isolate.Min | 5 | 13.31 | 2.66 | 0.14 | 0.984 |
| | Compatibility.Min | 5 | 74.61 | 14.92 | 0.76 | 0.582 |
| | Residual | 255 | 5026.65 | 19.71 | | |
| | Total | 283 | 13761.94 | | | |
| | Rep stratum | 5 | 927.37 | 185.47 | 8.59 | |
| | Rep.*Units* stratum | | | | | |
| | %4D | 1 | 33.52 | 33.52 | 1.55 | 0.214 |
| | Isolate | 1 | 341.35 | 341.35 | 15.8 | <.001 |
| | Compatibility | 1 | 112.48 | 112.48 | 5.21 | 0.023 |
| 48 | Min | 5 | 6581.8 | 1316.36 | 60.94 | <.001 |
| | %4D.Min | 5 | 14.4 | 2.88 | 0.13 | 0.985 |
| | Isolate.Min | 5 | 33.05 | 6.61 | 0.31 | 0.909 |
| | Compatibility.Min | 5 | 133.58 | 26.72 | 1.24 | 0.292 |
| | Residual | 254 | 5486.26 | 21.6 | | |
| | Total | 282 | 13211.9 | | | |
| | Rep stratum | 5 | 0.551748 | 0.11035 | 27.74 | |
| | Rep.*Units* stratum | | | | | |
| | %4D | 1 | 0.013113 | 0.013113 | 3.3 | 0.07 |
| | Isolate | 1 | 0.002569 | 0.002569 | 0.65 | 0.422 |
| | Compatibility | 1 | 0.007566 | 0.007566 | 1.9 | 0.168 |
| 6 | Min | 12 | 3.526746 | 0.293896 | 73.89 | <.001 |
| | %4D.Min | 12 | 0.004486 | 0.000374 | 0.09 | 1 |
| | Isolate.Min | 12 | 0.014699 | 0.001225 | 0.31 | 0.988 |
| | Compatibility.Min | 12 | 0.006652 | 0.000554 | 0.14 | 1 |
| | Residual | 567 | 2.255318 | 0.003978 | | |
| Conductance | Total | 623 | 6.382897 | | | |
| | Rep stratum | 5 | 0.101259 | 0.020252 | 6.32 | |
| | Rep.*Units* stratum | | | | | |
| 12 | %4D | 1 | 0.005527 | 0.005527 | 1.72 | 0.19 |
| | Isolate | 1 | 0.003481 | 0.003481 | 1.09 | 0.298 |
| | Compatibility | 1 | 0.096781 | 0.096781 | 30.2 | <.001 |
| | Min | 12 | 1.979408 | 0.164951 | 51.48 | <.001 |
| | %4D.Min | 12 | 0.011852 | 0.000988 | 0.31 | 0.988 |

| | | | | | | |
|---|---|---|---|---|---|---|
| | Isolate.Min | 12 | 0.006293 | 0.000524 | 0.16 | 0.999 |
| | Compatibility.Min | 12 | 0.012308 | 0.001026 | 0.32 | 0.986 |
| | Residual | 567 | 1.816939 | 0.003204 | | |
| | Total | 623 | 4.033847 | | | |
| 24 | Rep stratum | 5 | 0.267996 | 0.053599 | 15.39 | |
| | Rep.*Units* stratum | | | | | |
| | %4D | 1 | 0.450247 | 0.450247 | 129.28 | <.001 |
| | Isolate | 1 | 0.019988 | 0.019988 | 5.74 | 0.017 |
| | Compatibility | 1 | 0.082354 | 0.082354 | 23.65 | <.001 |
| | Min | 12 | 2.585079 | 0.215423 | 61.85 | <.001 |
| | %4D.Min | 12 | 0.007742 | 0.000645 | 0.19 | 0.999 |
| | Isolate.Min | 12 | 0.021332 | 0.001778 | 0.51 | 0.909 |
| | Compatibility.Min | 12 | 0.01183 | 0.000986 | 0.28 | 0.992 |
| | Residual | 567 | 1.974757 | 0.003483 | | |
| | Total | 623 | 5.421324 | | | |
| 48 | Rep stratum | 5 | 0.077309 | 0.015462 | 4.67 | |
| | Rep.*Units* stratum | | | | | |
| | %4D | 1 | 0.048295 | 0.048295 | 14.59 | <.001 |
| | Isolate | 1 | 0.02885 | 0.02885 | 8.71 | 0.003 |
| | Compatibility | 1 | 0.062741 | 0.062741 | 18.95 | <.001 |
| | Min | 12 | 3.000496 | 0.250041 | 75.52 | <.001 |
| | %4D.Min | 12 | 0.006613 | 0.000551 | 0.17 | 0.999 |
| | Isolate.Min | 12 | 0.016572 | 0.001381 | 0.42 | 0.957 |
| | Compatibility.Min | 12 | 0.036476 | 0.00304 | 0.92 | 0.528 |
| | Residual | 567 | 1.87724 | 0.003311 | | |
| | Total | 623 | 5.154593 | | | |

**Table S16.** Stomatal response to *Z.tritici* isolates HT-22 & 508 on 4D-R & 4D-S NILs. 4D-R & 4D-S lines infected by HT-22 or 508 are analysed using student T-tests (Figure 6). Effect of compatibility analysed using an ANOVA.

| Hours post inoculation | Source of variation | d.f | s.s. | m.s. | v.r. | F pr. |
|---|---|---|---|---|---|---|
| 6 | Rep stratum | 3 | 3149.9 | 1050 | 2 | |
| | Rep.*Units* stratum | | | | | |
| | Genotype | 1 | 4274.2 | 4274.2 | 8.15 | 0.019 |
| | Isolate | 1 | 320 | 320 | 0.61 | 0.455 |
| | Compatibility | 1 | 20 | 20 | 0.04 | 0.85 |
| | Residual | 9 | 4722.3 | 524.7 | | |
| | Total | 15 | 12486.3 | | | |
| 24 | Rep stratum | 3 | 3808.2 | 1269.4 | 4.06 | |
| | Rep.*Units* stratum | | | | | |
| | Genotype | 1 | 269.7 | 269.7 | 0.86 | 0.377 |
| | Isolate | 1 | 1.8 | 1.8 | 0.01 | 0.942 |
| | Compatibility | 1 | 378.3 | 378.3 | 1.21 | 0.3 |
| | Residual | 9 | 2810.9 | 312.3 | | |
| | Total | 15 | 7268.9 | | | |
| 48 | Rep stratum | 3 | 568.7 | 189.6 | 0.3 | |
| | Rep.*Units* stratum | | | | | |
| | Genotype | 1 | 130.5 | 130.5 | 0.2 | 0.662 |
| | Isolate | 1 | 2.2 | 2.2 | 0 | 0.954 |
| | Compatibility | 1 | 128.9 | 128.9 | 0.2 | 0.664 |
| | Residual | 9 | 5737.8 | 637.5 | | |
| | Total | 15 | 6568.1 | | | |

**Table S17.** *Z.tritici* spore germination assay for isolates HT-22 & 508 on 4D-R and 4D-S NILs. % germinated spores, and germ tube number. 4D-R & 4D-S lines infected by HT-22 or 508 are analysed using student T-tests (Figure 7). Effect of compatibility analysed using an ANOVA.

| Spore germination measurement | hours post inoculation | Source of variation | d.f | s.s. | m.s. | v.r. | F pr. |
|---|---|---|---|---|---|---|---|
| Germinated spores | 6 | Rep stratum | 3 | 0.07022 | 0.02341 | 0.62 | |
| | | Rep.*Units* stratum | | | | | |
| | | Genotype | 1 | 0.03781 | 0.03781 | 1 | 0.343 |
| | | Isolate | 1 | 0.01929 | 0.01929 | 0.51 | 0.493 |
| | | Compatibility | 1 | 0.09336 | 0.09336 | 2.47 | 0.151 |
| | | Residual | 9 | 0.34028 | 0.03781 | | |
| | | Total | 15 | 0.56096 | | | |
| | 24 | Rep stratum | 3 | 0.033179 | 0.01106 | 1.23 | |
| | | Rep.*Units* stratum | | | | | |
| | | Genotype | 1 | 0.037809 | 0.037809 | 4.2 | 0.071 |
| | | Isolate | 1 | 0.006944 | 0.006944 | 0.77 | 0.403 |
| | | Compatibility | 1 | 0.006944 | 0.006944 | 0.77 | 0.403 |
| | | Residual | 9 | 0.081019 | 0.009002 | | |
| | | Total | 15 | 0.165895 | | | |
| | 48 | Rep stratum | 3 | 0.01755 | 0.00585 | 0.46 | |
| | | Rep.*Units* stratum | | | | | |
| | | Genotype | 1 | 0.0326 | 0.0326 | 2.56 | 0.144 |
| | | Isolate | 1 | 0.00174 | 0.00174 | 0.14 | 0.72 |
| | | Compatibility | 1 | 0.00174 | 0.00174 | 0.14 | 0.72 |
| | | Residual | 9 | 0.11439 | 0.01271 | | |
| | | Total | 15 | 0.16802 | | | |

| | | | | | | |
|---|---|---|---|---|---|---|
| | | Rep stratum | 3 | 2.3542 | 0.7847 | 2.62 | |
| | | Rep.*Units* stratum | | | | | |
| | | Genotype | 1 | 0.8403 | 0.8403 | 2.81 | 0.128 |
| | 6 | Isolate | 1 | 1.7045 | 1.7045 | 5.7 | 0.041 |
| | | Compatibility | 1 | 0.4082 | 0.4082 | 1.36 | 0.273 |
| | | Residual | 9 | 2.6921 | 0.2991 | | |
| | | Total | 15 | 7.9992 | | | |
| | | Rep stratum | 3 | 2.6134 | 0.8711 | 3.66 | |
| | | Rep.*Units* stratum | | | | | |
| | | Genotype | 1 | 2.3341 | 2.3341 | 9.8 | 0.012 |
| Germ tube number | 24 | Isolate | 1 | 0.1304 | 0.1304 | 0.55 | 0.478 |
| | | Compatibility | 1 | 0.0378 | 0.0378 | 0.16 | 0.7 |
| | | Residual | 9 | 2.1427 | 0.2381 | | |
| | | Total | 15 | 7.2585 | | | |
| | | Rep stratum | 3 | 2.1991 | 0.733 | 1.36 | |
| | | Rep.*Units* stratum | | | | | |
| | | Genotype | 1 | 1.7045 | 1.7045 | 3.17 | 0.109 |
| | 48 | Isolate | 1 | 2.1674 | 2.1674 | 4.03 | 0.076 |
| | | Compatibility | 1 | 0.1512 | 0.1512 | 0.28 | 0.609 |
| | | Residual | 9 | 4.8364 | 0.5374 | | |
| | | Total | 15 | 11.0586 | | | |

**Table S18.** Superoxide quantification using Nitroblue tetrazolium (NBT) of 4D-R and 4D-S NILs inoculated with *Z.tritici* isolate HT-22 or 508. 4D-R & 4D-S lines infected by HT-22 or 508 are analysed using student T-tests (Figure 8). Effect of compatibility analysed using an ANOVA.

| hours post inoculation | Source of variation | d.f | s.s. | m.s. | v.r. | F pr. |
|---|---|---|---|---|---|---|
| 6 | rep stratum | 3 | 1400.7 | 466.9 | 0.47 | |
| | rep.*Units* stratum | | | | | |
| | Gene | 1 | 57.6 | 57.6 | 0.06 | 0.815 |
| | isolate | 1 | 992.6 | 992.6 | 1 | 0.344 |
| | Compatibility | 1 | 0.5 | 0.5 | 0 | 0.982 |
| | Residual | 9 | 8954 | 994.9 | | |
| | Total | 15 | 11405.5 | | | |
| 24 | rep stratum | 3 | 1298.8 | 432.9 | 1.65 | |
| | rep.*Units* stratum | | | | | |
| | Gene | 1 | 15.8 | 15.8 | 0.06 | 0.812 |
| | isolate | 1 | 214.2 | 214.2 | 0.81 | 0.39 |
| | Compatibility | 1 | 350.5 | 350.5 | 1.33 | 0.278 |
| | Residual | 9 | 2366.7 | 263 | | |
| | Total | 15 | 4246 | | | |
| 48 | rep stratum | 3 | 911.3 | 303.8 | 1.02 | |
| | rep.*Units* stratum | | | | | |
| | Gene | 1 | 4 | 4 | 0.01 | 0.91 |
| | isolate | 1 | 85.8 | 85.8 | 0.29 | 0.605 |
| | Compatibility | 1 | 770.3 | 770.3 | 2.58 | 0.142 |
| | Residual | 9 | 2682.3 | 298 | | |
| | Total | 15 | 4453.6 | | | |

**Table S19.** Effect of *Z.tritici* isolates HT-22 & 508 on Lycopene derived xanthophyll's and xanthophyll metabolism genes in 4D-R and 4D-S NILs. 4D-R & 4D-S lines infected by HT-22 or 508 are analysed using student T-tests (Figure 9). Effect of compatibility analysed using an ANOVA.

| time post inoculation | Carotenoid or Enzyme | Source of variation | d.f | s.s. | m.s. | v.r. | F pr. |
|---|---|---|---|---|---|---|---|
| 6 hpi | Antheraxanthin | Rep stratum | 2 | 0.0642 | 0.0321 | 0.15 | |
| | | Rep.*Units* stratum | | | | | |
| | | Gene | 1 | 1.0041 | 1.0041 | 4.64 | 0.075 |
| | | Isolate | 1 | 0.0074 | 0.0074 | 0.03 | 0.86 |
| | | Compatibility | 1 | 0.1296 | 0.1296 | 0.6 | 0.468 |
| | | Residual | 6 | 1.2975 | 0.2163 | | |
| | | Total | 11 | 2.5028 | | | |
| | Lutein | Rep stratum | 2 | 69.88 | 34.94 | 0.49 | |
| | | Rep.*Units* stratum | | | | | |
| | | Gene | 1 | 187.01 | 187.01 | 2.61 | 0.157 |
| | | Isolate | 1 | 21.36 | 21.36 | 0.3 | 0.605 |
| | | Compatibility | 1 | 167.67 | 167.67 | 2.34 | 0.177 |
| | | Residual | 6 | 429.66 | 71.61 | | |
| | | Total | 11 | 875.58 | | | |
| | Neoxanthin | Rep stratum | 2 | 0.648 | 0.324 | 0.12 | |
| | | Rep.*Units* stratum | | | | | |
| | | Gene | 1 | 0.869 | 0.869 | 0.32 | 0.593 |
| | | Isolate | 1 | 6.456 | 6.456 | 2.36 | 0.175 |
| | | Compatibility | 1 | 4.041 | 4.041 | 1.48 | 0.27 |
| | | Residual | 6 | 16.402 | 2.734 | | |
| | | Total | 11 | 28.417 | | | |

| | | | | | | |
|---|---|---|---|---|---|---|
| | Rep stratum | 2 | 59.15 | 29.58 | 0.39 | |
| | Rep.*Units* stratum | | | | | |
| | Gene | 1 | 37.91 | 37.91 | 0.5 | 0.505 |
| Violaxanthin | Isolate | 1 | 0.05 | 0.05 | 0 | 0.979 |
| | Compatibility | 1 | 61.29 | 61.29 | 0.81 | 0.402 |
| | Residual | 6 | 453.33 | 75.56 | | |
| | Total | 11 | 611.74 | | | |
| | Rep stratum | 2 | 48.07 | 24.04 | 0.3 | |
| | Rep.*Units* stratum | | | | | |
| | Gene | 1 | 64.45 | 64.45 | 0.8 | 0.404 |
| XC carotenoid pool | Isolate | 1 | 0.08 | 0.08 | 0 | 0.976 |
| | Compatibility | 1 | 63.44 | 63.44 | 0.79 | 0.408 |
| | Residual | 6 | 480.95 | 80.16 | | |
| | Total | 11 | 656.99 | | | |
| | Rep stratum | 2 | 1.0483 | 0.5241 | 0.62 | |
| | Rep.*Units* stratum | | | | | |
| | Gene | 1 | 0.7546 | 0.7546 | 0.89 | 0.382 |
| Zeaxanthin | Isolate | 1 | 0.1806 | 0.1806 | 0.21 | 0.661 |
| | Compatibility | 1 | 0.0501 | 0.0501 | 0.06 | 0.816 |
| | Residual | 6 | 5.0914 | 0.8486 | | |
| | Total | 11 | 7.1249 | | | |
| | Rep stratum | 2 | 1.675 | 0.8375 | 2.68 | |
| | Rep.*Units* stratum | | | | | |
| | Gene | 1 | 0.2899 | 0.2899 | 0.93 | 0.373 |
| Chl a:b ratio | Isolate | 1 | 0.6299 | 0.6299 | 2.01 | 0.206 |
| | Compatibility | 1 | 1.5727 | 1.5727 | 5.02 | 0.066 |
| | Residual | 6 | 1.8784 | 0.3131 | | |
| | Total | 11 | 6.0459 | | | |

| | | | | | | | |
|---|---|---|---|---|---|---|---|
| | | Rep stratum | 2 | 448.4 | 224.2 | 1.05 | |
| | | Rep.*Units* stratum | | | | | |
| | | Gene | 1 | 4.9 | 4.9 | 0.02 | 0.885 |
| | DEPs | Isolate | 1 | 199.4 | 199.4 | 0.93 | 0.372 |
| | | Compatibility | 1 | 131.5 | 131.5 | 0.61 | 0.463 |
| | | Residual | 6 | 1286.2 | 214.4 | | |
| | | Total | 11 | 2070.4 | | | |
| | | Rep stratum | 2 | 1204 | 602 | 0.13 | |
| | | Rep.*Units* stratum | | | | | |
| | | Gene | 1 | 6540 | 6540 | 1.41 | 0.28 |
| | XC pool | Isolate | 1 | 1624 | 1624 | 0.35 | 0.576 |
| | | Compatibility | 1 | 794 | 794 | 0.17 | 0.694 |
| | | Residual | 6 | 27862 | 4644 | | |
| | | Total | 11 | 38023 | | | |
| | | Rep stratum | 2 | 0 | 0 | | |
| | | Rep.*Units* stratum | | | | | |
| | | Gene | 1 | 0 | 0 | | |
| | Antheraxanthin | Isolate | 1 | 0 | 0 | | |
| | | Compatibility | 1 | 0 | 0 | | |
| | | Residual | 6 | 0 | 0 | | |
| | | Total | 11 | 0 | | | |
| 11 dpi | | Rep stratum | 2 | 662.5 | 331.2 | 1 | |
| | | Rep.*Units* stratum | | | | | |
| | | Gene | 1 | 1432.5 | 1432.5 | 4.32 | 0.083 |
| | Lutein | Isolate | 1 | 1432.5 | 1432.5 | 4.32 | 0.083 |
| | | Compatibility | 1 | 1432.5 | 1432.5 | 4.32 | 0.083 |
| | | Residual | 6 | 1987.4 | 331.2 | | |
| | | Total | 11 | 6947.4 | | | |

| | | | | | | |
|---|---|---|---|---|---|---|
| | Rep stratum | 2 | 36.44 | 18.22 | 1 | |
| | Rep.*Units* stratum | | | | | |
| | Gene | 1 | 227.66 | 227.66 | 12.49 | 0.012 |
| Neoxanthin | Isolate | 1 | 227.66 | 227.66 | 12.49 | 0.012 |
| | Compatibility | 1 | 227.66 | 227.66 | 12.49 | 0.012 |
| | Residual | 6 | 109.32 | 18.22 | | |
| | Total | 11 | 828.75 | | | |
| | Rep stratum | 2 | 247.7 | 123.85 | 7.55 | |
| | Rep.*Units* stratum | | | | | |
| | Gene | 1 | 190.1 | 190.1 | 11.6 | 0.014 |
| Violaxanthin | Isolate | 1 | 25.92 | 25.92 | 1.58 | 0.255 |
| | Compatibility | 1 | 303.45 | 303.45 | 18.51 | 0.005 |
| | Residual | 6 | 98.37 | 16.39 | | |
| | Total | 11 | 865.55 | | | |
| | Rep stratum | 2 | 344.07 | 172.04 | 5.44 | |
| | Rep.*Units* stratum | | | | | |
| | Gene | 1 | 197.44 | 197.44 | 6.25 | 0.047 |
| XC carotenoid pool | Isolate | 1 | 75.7 | 75.7 | 2.39 | 0.173 |
| | Compatibility | 1 | 442.37 | 442.37 | 13.99 | 0.01 |
| | Residual | 6 | 189.66 | 31.61 | | |
| | Total | 11 | 1249.24 | | | |
| | Rep stratum | 2 | 13.675 | 6.837 | 1.36 | |
| | Rep.*Units* stratum | | | | | |
| | Gene | 1 | 0.069 | 0.069 | 0.01 | 0.91 |
| Zeaxanthin | Isolate | 1 | 13.026 | 13.026 | 2.59 | 0.158 |
| | Compatibility | 1 | 13.051 | 13.051 | 2.6 | 0.158 |
| | Residual | 6 | 30.126 | 5.021 | | |
| | Total | 11 | 69.948 | | | |

| | | | | | | |
|---|---|---|---|---|---|---|
| | Rep stratum | 2 | 0.0745 | 0.0372 | 0.07 | |
| | Rep.*Units* stratum | | | | | |
| | Gene | 1 | 0.1232 | 0.1232 | 0.24 | 0.643 |
| Chl a:b ratio | Isolate | 1 | 1.3903 | 1.3903 | 2.69 | 0.152 |
| | Compatibility | 1 | 1.2745 | 1.2745 | 2.46 | 0.168 |
| | Residual | 6 | 3.1029 | 0.5172 | | |
| | Total | 11 | 5.9654 | | | |
| | Rep stratum | 2 | 101 | 50.5 | 0.27 | |
| | Rep.*Units* stratum | | | | | |
| | Gene | 1 | 77.3 | 77.3 | 0.41 | 0.546 |
| DEPs | Isolate | 1 | 798.3 | 798.3 | 4.22 | 0.086 |
| | Compatibility | 1 | 439.3 | 439.3 | 2.32 | 0.179 |
| | Residual | 6 | 1136.1 | 189.4 | | |
| | Total | 11 | 2552 | | | |
| | Rep stratum | 2 | 4149.9 | 2074.9 | 4.26 | |
| | Rep.*Units* stratum | | | | | |
| | Gene | 1 | 193.3 | 193.3 | 0.4 | 0.552 |
| XC pool | Isolate | 1 | 1492.9 | 1492.9 | 3.07 | 0.131 |
| | Compatibility | 1 | 907.8 | 907.8 | 1.86 | 0.221 |
| | Residual | 6 | 2922.1 | 487 | | |
| | Total | 11 | 9666 | | | |

**Table S20.** Effect of *Z.tritici* isolates HT-22 & 508 on VDE (Violaxanthin de-epoxidase), ZEP (zeaxanthin epoxidase) and NCED (Epoxycarotenoid dioxygenase) expression in 4D-R and 4D-S NILs.. 4D-R & 4D-S lines infected by HT-22 or 508 are analysed using student T-tests (Table 2). Effect of compatibility analysed using an ANOVA.

| time post inoculation | Enzyme | Source of variation | d.f | s.s. | m.s. | v.r. | F pr. |
|---|---|---|---|---|---|---|---|
| 6 hpi | VDE | Rep stratum | 2 | 0.004894 | 0.002447 | 0.31 | |
| | | Rep.*Units* stratum | | | | | |
| | | Gene | 1 | 0.0073 | 0.0073 | 0.93 | 0.373 |
| | | Isolate | 1 | 0.000343 | 0.000343 | 0.04 | 0.841 |
| | | Compatibility | 1 | 0.005824 | 0.005824 | 0.74 | 0.423 |
| | | Residual | 6 | 0.047235 | 0.007873 | | |
| | | Total | 11 | 0.065596 | | | |
| | ZEP | Rep stratum | 2 | 0.0186 | 0.0093 | 0.69 | |
| | | Rep.*Units* stratum | | | | | |
| | | Gene | 1 | 0.08448 | 0.08448 | 6.23 | 0.047 |
| | | Isolate | 1 | 0.00057 | 0.00057 | 0.04 | 0.844 |
| | | Compatibility | 1 | 0.01381 | 0.01381 | 1.02 | 0.352 |
| | | Residual | 6 | 0.08132 | 0.01355 | | |
| | | Total | 11 | 0.19878 | | | |
| | NCED | Rep stratum | 2 | 9.38E-05 | 4.69E-05 | 1.09 | |
| | | Rep.*Units* stratum | | | | | |
| | | Gene | 1 | 4.45E-05 | 4.45E-05 | 1.03 | 0.349 |
| | | Isolate | 1 | 0.000411 | 0.000411 | 9.53 | 0.021 |
| | | Compatibility | 1 | 0.000116 | 0.000116 | 2.7 | 0.151 |
| | | Residual | 6 | 0.000259 | 4.31E-05 | | |
| | | Total | 11 | 0.000924 | | | |

| | | | | | | |
|---|---|---|---|---|---|---|
| | VDE | Rep stratum | 2 | 0.000826 | 0.000413 | 0.5 | |
| | | Rep.*Units* stratum | | | | | |
| | | Gene | 1 | 0.000601 | 0.000601 | 0.73 | 0.425 |
| | | Isolate | 1 | 0.00277 | 0.00277 | 3.37 | 0.116 |
| | | Compatibility | 1 | 0.005805 | 0.005805 | 7.06 | 0.038 |
| | | Residual | 6 | 0.004931 | 0.000822 | | |
| | | Total | 11 | 0.014933 | | | |
| 11 dpi | ZEP | Rep stratum | 2 | 0.07477 | 0.03738 | 1.01 | |
| | | Rep.*Units* stratum | | | | | |
| | | Gene | 1 | 0.21106 | 0.21106 | 5.7 | 0.054 |
| | | Isolate | 1 | 0.00683 | 0.00683 | 0.18 | 0.682 |
| | | Compatibility | 1 | 0.00053 | 0.00053 | 0.01 | 0.908 |
| | | Residual | 6 | 0.22203 | 0.03701 | | |
| | | Total | 11 | 0.51522 | | | |
| | NCED | Rep stratum | 2 | 0.00135 | 0.000675 | 0.43 | |
| | | Rep.*Units* stratum | | | | | |
| | | Gene | 1 | 0.002353 | 0.002353 | 1.49 | 0.268 |
| | | Isolate | 1 | 0.000025 | 0.000025 | 0.02 | 0.904 |
| | | Compatibility | 1 | 0.000589 | 0.000589 | 0.37 | 0.564 |
| | | Residual | 6 | 0.009471 | 0.001578 | | |
| | | Total | 11 | 0.013787 | | | |

**Table S21.** Effect of *Z.tritici* isolates HT-22 & 508 on ABA; Abscisic acid, SA; Salicylic acid, JA; Jasmonic acid, OPDA; oxo-Phytodienoic acid, Ja-Ile; jasmonoyl-L-isoleucine, IAA; Indole-3-acetic acid, GA1, 3, 7; Gibberellin, ACC; 1-Aminocyclopropane 1-carboxylic acid, IPA; Indole-3-propionic acid, 2iP; 6-(γ,γ-Dimethylallylamino)purine, Z; Zeatin and ZR; zeatin riboside content in 4D-R and 4D-S NILs. 4D-R & 4D-S lines infected by HT-22 or 508 are analysed using student T-tests (Table 3). Effect of compatibility analysed using an ANOVA.

| time post inoculation | Hormone | Source of Variation | d.f | s.s. | m.s. | v.r. | F pr. |
|---|---|---|---|---|---|---|---|
| 6 hpi | 2iP | Rep stratum | 2 | 0.0647 | 0.0324 | 0.13 | |
| | | Rep.*Units* stratum | | | | | |
| | | Compatibility | 1 | 0.2809 | 0.2809 | 1.16 | 0.322 |
| | | Genotype | 1 | 0 | 0 | 0 | 0.99 |
| | | Treatment | 1 | 0.7563 | 0.7563 | 3.13 | 0.127 |
| | | Residual | 6 | 1.4504 | 0.2417 | | |
| | | Total | 11 | 2.5524 | | | |
| 6 hpi | ABA | Rep stratum | 2 | 3.99 | 1.99 | 0.17 | |
| | | Rep.*Units* stratum | | | | | |
| | | Compatibility | 1 | 18.77 | 18.77 | 1.64 | 0.247 |
| | | Genotype | 1 | 0.97 | 0.97 | 0.08 | 0.781 |
| | | Treatment | 1 | 8.3 | 8.3 | 0.73 | 0.427 |
| | | Residual | 6 | 68.64 | 11.44 | | |
| | | Total | 11 | 100.66 | | | |
| 6 hpi | ACC | Rep stratum | 2 | 681.2 | 340.6 | 1.42 | |
| | | Rep.*Units* stratum | | | | | |
| | | Compatibility | 1 | 88.5 | 88.5 | 0.37 | 0.566 |
| | | Genotype | 1 | 387.6 | 387.6 | 1.62 | 0.251 |
| | | Treatment | 1 | 124 | 124 | 0.52 | 0.499 |
| | | Residual | 6 | 1437.9 | 239.7 | | |
| | | Total | 11 | 2719.2 | | | |

| | | | | | | | |
|---|---|---|---|---|---|---|---|
| | | Rep stratum | 2 | 21.22 | 10.61 | 0.53 | |
| | | Rep.*Units* stratum | | | | | |
| | | Compatibility | 1 | 2.63 | 2.63 | 0.13 | 0.731 |
| 6 hpi | GA1 | Genotype | 1 | 18.96 | 18.96 | 0.94 | 0.37 |
| | | Treatment | 1 | 2.6 | 2.6 | 0.13 | 0.732 |
| | | Residual | 6 | 121.21 | 20.2 | | |
| | | Total | 11 | 166.61 | | | |
| | | Rep stratum | 2 | 3131 | 1565 | 0.44 | |
| | | Rep.*Units* stratum | | | | | |
| | | Compatibility | 1 | 27399 | 27399 | 7.65 | 0.033 |
| 6 hpi | GA3 | Genotype | 1 | 604 | 604 | 0.17 | 0.695 |
| | | Treatment | 1 | 2 | 2 | 0 | 0.981 |
| | | Residual | 6 | 21482 | 3580 | | |
| | | Total | 11 | 52618 | | | |
| | | Rep stratum | 2 | 2793.4 | 1396.7 | 4.87 | |
| | | Rep.*Units* stratum | | | | | |
| | | Compatibility | 1 | 847.1 | 847.1 | 2.96 | 0.136 |
| 6 hpi | GA7 | Genotype | 1 | 307.8 | 307.8 | 1.07 | 0.34 |
| | | Treatment | 1 | 602.6 | 602.6 | 2.1 | 0.197 |
| | | Residual | 6 | 1719.5 | 286.6 | | |
| | | Total | 11 | 6270.5 | | | |
| | | Rep stratum | 2 | 20.04 | 10.02 | 0.49 | |
| | | Rep.*Units* stratum | | | | | |
| | | Compatibility | 1 | 0.03 | 0.03 | 0 | 0.969 |
| | | Genotype | 1 | 5.33 | 5.33 | 0.26 | 0.629 |
| 6 hpi | IAA | Treatment | 1 | 17.7 | 17.7 | 0.86 | 0.389 |
| | | Residual | 6 | 123.32 | 20.55 | | |
| | | Total | 11 | 166.42 | | | |

| | | | | | | | |
|---|---|---|---|---|---|---|---|
| | | Rep stratum | 2 | 0.053 | 0.0265 | 0.35 | |
| | | Rep.*Units* stratum | | | | | |
| | | Compatibility | 1 | 0.00561 | 0.00561 | 0.07 | 0.796 |
| 6 hpi | IPA | Genotype | 1 | 0.08041 | 0.08041 | 1.05 | 0.345 |
| | | Treatment | 1 | 0.30301 | 0.30301 | 3.96 | 0.094 |
| | | Residual | 6 | 0.45932 | 0.07655 | | |
| | | Total | 11 | 0.90135 | | | |
| | | Rep stratum | 2 | 0.003576 | 0.001788 | 0.38 | |
| | | Rep.*Units* stratum | | | | | |
| | | Compatibility | 1 | 0.007662 | 0.007662 | 1.63 | 0.249 |
| 6 hpi | Ja_ile | Genotype | 1 | 0.003406 | 0.003406 | 0.72 | 0.428 |
| | | Treatment | 1 | 0.003521 | 0.003521 | 0.75 | 0.421 |
| | | Residual | 6 | 0.028269 | 0.004712 | | |
| | | Total | 11 | 0.046435 | | | |
| | | Rep stratum | 2 | 27.09 | 13.55 | 0.47 | |
| | | Rep.*Units* stratum | | | | | |
| | | Compatibility | 1 | 0.4 | 0.4 | 0.01 | 0.91 |
| 6 hpi | JA | Genotype | 1 | 126.07 | 126.07 | 4.4 | 0.081 |
| | | Treatment | 1 | 2.83 | 2.83 | 0.1 | 0.764 |
| | | Residual | 6 | 171.83 | 28.64 | | |
| | | Total | 11 | 328.21 | | | |
| | | Rep stratum | 2 | 36.2 | 18.1 | 0.16 | |
| | | Rep.*Units* stratum | | | | | |
| | | Compatibility | 1 | 39.2 | 39.2 | 0.35 | 0.575 |
| | | Genotype | 1 | 217 | 217 | 1.94 | 0.213 |
| 6 hpi | OPDA | Treatment | 1 | 84.6 | 84.6 | 0.76 | 0.418 |
| | | Residual | 6 | 671.1 | 111.8 | | |
| | | Total | 11 | 1048.1 | | | |

| | | | | | | | |
|---|---|---|---|---|---|---|---|
| 6 hpi | SA | Rep stratum | 2 | 236743 | 118371 | 0.25 | |
| | | Rep.*Units* stratum | | | | | |
| | | Compatibility | 1 | 355311 | 355311 | 0.75 | 0.42 |
| | | Genotype | 1 | 16636 | 16636 | 0.04 | 0.858 |
| | | Treatment | 1 | 839954 | 839954 | 1.77 | 0.232 |
| | | Residual | 6 | 2845070 | 474178 | | |
| | | Total | 11 | 4293714 | | | |
| 6 hpi | Z | Rep stratum | 2 | 9.556 | 4.778 | 0.53 | |
| | | Rep.*Units* stratum | | | | | |
| | | Compatibility | 1 | 1.203 | 1.203 | 0.13 | 0.728 |
| | | Genotype | 1 | 0.045 | 0.045 | 0.01 | 0.946 |
| | | Treatment | 1 | 0.248 | 0.248 | 0.03 | 0.874 |
| | | Residual | 6 | 54.264 | 9.044 | | |
| | | Total | 11 | 65.316 | | | |
| 6 hpi | ZR | Rep stratum | 2 | 76.11 | 38.05 | 0.64 | |
| | | Rep.*Units* stratum | | | | | |
| | | Compatibility | 1 | 0.09 | 0.09 | 0 | 0.97 |
| | | Genotype | 1 | 829.33 | 829.33 | 13.91 | 0.02 |
| | | Treatment | 1 | 6.9 | 6.9 | 0.12 | 0.751 |
| | | Residual | 4 | 238.51 | 59.63 | | |
| | | Total | 9 | 628.41 | | | |
| 11 dpi | 2iP | Rep stratum | 2 | 14.097 | 7.049 | 1.54 | |
| | | Rep.*Units* stratum | | | | | |
| | | Compatibility | 1 | 3.553 | 3.553 | 0.78 | 0.412 |
| | | Genotype | 1 | 0.152 | 0.152 | 0.03 | 0.862 |
| | | Treatment | 1 | 0.179 | 0.179 | 0.04 | 0.85 |
| | | Residual | 6 | 27.497 | 4.583 | | |
| | | Total | 11 | 45.477 | | | |

| | | | | | | |
|---|---|---|---|---|---|---|
| | | Rep stratum | 2 | 18.45 | 9.23 | 0.74 | |
| | | Rep.*Units* stratum | | | | | |
| | | Compatibility | 1 | 3.13 | 3.13 | 0.25 | 0.635 |
| 11 dpi | ABA | Genotype | 1 | 1.56 | 1.56 | 0.12 | 0.736 |
| | | Treatment | 1 | 3.04 | 3.04 | 0.24 | 0.64 |
| | | Residual | 6 | 75.17 | 12.53 | | |
| | | Total | 11 | 101.36 | | | |
| | | Rep stratum | 2 | 5365 | 2682 | 0.5 | |
| | | Rep.*Units* stratum | | | | | |
| | | Compatibility | 1 | 7182 | 7182 | 1.34 | 0.292 |
| 11 dpi | ACC | Genotype | 1 | 565 | 565 | 0.11 | 0.757 |
| | | Treatment | 1 | 433 | 433 | 0.08 | 0.786 |
| | | Residual | 6 | 32227 | 5371 | | |
| | | Total | 11 | 45771 | | | |
| | | Rep stratum | 2 | 4241.2 | 2120.6 | 2.14 | |
| | | Rep.*Units* stratum | | | | | |
| | | Compatibility | 1 | 413.2 | 413.2 | 0.42 | 0.564 |
| 11 dpi | GA1 | Genotype | 1 | 514.7 | 514.7 | 0.52 | 0.523 |
| | | Treatment | 1 | 283.9 | 283.9 | 0.29 | 0.629 |
| | | Residual | 3 | 2967 | 989 | | |
| | | Total | 8 | 6769.7 | | | |
| | | Rep stratum | 2 | 68450 | 34225 | 2.7 | |
| | | Rep.*Units* stratum | | | | | |
| | | Compatibility | 1 | 29240 | 29240 | 2.31 | 0.179 |
| | | Genotype | 1 | 26508 | 26508 | 2.09 | 0.198 |
| 11 dpi | GA3 | Treatment | 1 | 93 | 93 | 0.01 | 0.934 |
| | | Residual | 6 | 75932 | 12655 | | |
| | | Total | 11 | 200224 | | | |

| | | | | | | | |
|---|---|---|---|---|---|---|---|
| 11 dpi | | Rep stratum | 2 | 21.05 | 10.53 | 0.83 | |
| | | Rep.*Units* stratum | | | | | |
| | | Compatibility | 1 | 2.76 | 2.76 | 0.22 | 0.657 |
| | GA7 | Genotype | 1 | 0.09 | 0.09 | 0.01 | 0.935 |
| | | Treatment | 1 | 1.76 | 1.76 | 0.14 | 0.723 |
| | | Residual | 6 | 76.2 | 12.7 | | |
| | | Total | 11 | 101.86 | | | |
| | | Rep stratum | 2 | 0.3 | 0.15 | 0.01 | |
| | | Rep.*Units* stratum | | | | | |
| | | Compatibility | 1 | 4.88 | 4.88 | 0.35 | 0.574 |
| 11 dpi | IAA | Genotype | 1 | 18.98 | 18.98 | 1.37 | 0.285 |
| | | Treatment | 1 | 28.56 | 28.56 | 2.07 | 0.2 |
| | | Residual | 6 | 82.85 | 13.81 | | |
| | | Total | 11 | 135.57 | | | |
| | | Rep stratum | 2 | 0.3826 | 0.1913 | 1 | |
| | | Rep.*Units* stratum | | | | | |
| | | Compatibility | 1 | 0.2495 | 0.2495 | 1.31 | 0.297 |
| 11 dpi | IPA | Genotype | 1 | 0.0014 | 0.0014 | 0.01 | 0.934 |
| | | Treatment | 1 | 0.0577 | 0.0577 | 0.3 | 0.602 |
| | | Residual | 6 | 1.1456 | 0.1909 | | |
| | | Total | 11 | 1.8368 | | | |
| | | Rep stratum | 2 | 0.076 | 0.038 | 0.82 | |
| | | Rep.*Units* stratum | | | | | |
| | | Compatibility | 1 | 0.05773 | 0.05773 | 1.25 | 0.315 |
| | | Genotype | 1 | 0.11552 | 0.11552 | 2.49 | 0.175 |
| 11 dpi | Ja_ile | Treatment | 1 | 0.00051 | 0.00051 | 0.01 | 0.92 |
| | | Residual | 5 | 0.23172 | 0.04634 | | |
| | | Total | 10 | 0.43466 | | | |

| | | | | | | | |
|---|---|---|---|---|---|---|---|
| | | Rep stratum | 2 | 580.7 | 290.4 | 2.7 | |
| | | Rep.*Units* stratum | | | | | |
| | | Compatibility | 1 | 143.1 | 143.1 | 1.33 | 0.293 |
| 11 dpi | JA | Genotype | 1 | 129.1 | 129.1 | 1.2 | 0.315 |
| | | Treatment | 1 | 113.5 | 113.5 | 1.06 | 0.344 |
| | | Residual | 6 | 645.4 | 107.6 | | |
| | | Total | 11 | 1611.8 | | | |
| | | Rep stratum | 2 | 118.2 | 59.1 | 0.24 | |
| | | Rep.*Units* stratum | | | | | |
| | | Compatibility | 1 | 1.8 | 1.8 | 0.01 | 0.936 |
| 11 dpi | OPDA | Genotype | 1 | 40 | 40 | 0.16 | 0.703 |
| | | Treatment | 1 | 86.8 | 86.8 | 0.35 | 0.578 |
| | | Residual | 6 | 1503.3 | 250.6 | | |
| | | Total | 11 | 1750.1 | | | |
| | | Rep stratum | 2 | 5125779 | 2562890 | 1.17 | |
| | | Rep.*Units* stratum | | | | | |
| | | Compatibility | 1 | 4964235 | 4964235 | 2.27 | 0.182 |
| | | Genotype | 1 | 13180 | 13180 | 0.01 | 0.941 |
| 11 dpi | SA | Treatment | 1 | 48676 | 48676 | 0.02 | 0.886 |
| | | Residual | 6 | 13098931 | 2183155 | | |
| | | Total | 11 | 23250800 | | | |
| | | Rep stratum | 2 | 505.65 | 252.82 | 3.8 | |
| | | Rep.*Units* stratum | | | | | |
| | | Compatibility | 1 | 4.96 | 4.96 | 0.07 | 0.794 |
| 11 dpi | Z | Genotype | 1 | 7.41 | 7.41 | 0.11 | 0.75 |
| | | Treatment | 1 | 55.45 | 55.45 | 0.83 | 0.397 |
| | | Residual | 6 | 399.22 | 66.54 | | |
| | | Total | 11 | 972.68 | | | |

| | | | | | | | |
|---|---|---|---|---|---|---|---|
| | | Rep stratum | 2 | 355.2 | 177.6 | 0.97 | |
| | | Rep.*Units* stratum | | | | | |
| | | Compatibility | 1 | 65 | 65 | 0.36 | 0.573 |
| 11 dpi | ZR | Genotype | 1 | 410.6 | 410.6 | 2.24 | 0.185 |
| | | Treatment | 1 | 7.4 | 7.4 | 0.04 | 0.848 |
| | | Residual | 6 | 1098.1 | 183 | | |
| | | Total | 11 | 1936.2 | | | |

# References:


1. Abrinbana, M., Mozafari, J., Shams-bakhsh, M. and Mehrabi, R. (2010). Genetic structure of Mycosphaerella graminicola populations in Iran. Plant Pathology, 59, 829-838.
2. Achard P, Renou JP, Berthome R, Harberd NP, Genschik P (2008). Plant DELLAs restrain growth and promote survival of adversity by reducing the levels of reactive oxygen species. Curr Biol. 18, 656–660.
3. Adhikari T.B., J.M. Anderson, S.B. Goodwin (2003). Identification and molecular mapping of a gene in wheat conferring resistance to Mycosphaerella graminicola Phytopathology. 93, 1158-1164
4. Adhikari T.B., Yang, X., Cavaletto, J.R., Hu, X., Buechley, G., Ohm, H.W., Shaner, G., Goodwin, S.B., (2004a). Molecular mapping of Stb1, a potentially durable gene for resistance to Septoria tritici blotch in wheat. Theor. Appl. Genet. 109, 944–953.
5. Adhikari T.B., Balaji B, Breeden J, Goodwin SB, (2007). Resistance to wheat Mycosphaerella graminicola involves early and late peaks of gene expression. Physiological and Molecular Plant Pathology. 71, 55–68.
6. AHDB 2021, Septoria tritici disease resistance in winter wheat (https://ahdb.org.uk/news/septoria-tritici-disease-resistance-in-winter-wheat)
7. AHBD, Septoria: 'Cougar' effect in RL winter wheat trials (2022) https://ahdb.org.uk/news/septoria-cougar-effect-in-rl-winter-wheat-trials
8. Ajigboye O. O., Bousquet Louise, Murchie Erik H., Ray Rumiana V. (2016). Chlorophyll fluorescence parameters allow the rapid detection and differentiation of plant responses in three different wheat pathosystems. Functional Plant Biology. 43, 356-369.
9. Ajigboye O.O., Ray, R.V., Murchie, E.H. (2018). Chlorophyll Fluorescence on the Fast Timescale. In: Covshoff, S. (eds) Photosynthesis. Methods in Molecular Biology, vol 1770. Humana Press, New York, NY.
10. Ajigboye O. O., Jayaweera, D. P., Angelopoulou, D., Ruban, A. V., Murchie, E. H., Pastor, V., … Ray, R. V. (2021). The role of photoprotection in defence of two wheat genotypes against Zymoseptoria tritici. Plant Pathology, 70(6), 1421-1435.
11. Ajjawi, I., Milla, M. A. R., Cushman, J., & Shintani, D. K. (2007). Thiamin pyrophosphokinase is required for thiamin cofactor activation in Arabidopsis. Plant Molecular Biology. 65(1–2), 151–162.

12. Alazem, M., & Lin, N. S. (2015). Roles of plant hormones in the regulation of host-virus interactions. Molecular Plant Pathology. 26(5), 529-540.
13. Allahverdiyeva, Y., Mamedov, F., Suorsa, M., Styring, S., Vass, I., & Aro, E. M. (2007). Insights into the function of PsbR protein in Arabidopsis thaliana. Biochimica et Biophysica Acta - Bioenergetics, 1767(6), 677–685.
14. Allen AM, Winfield MO, Burridge AJ, Downie RC, Benbow HR, Barker GL, Wilkinson PA, Coghill J, Waterfall C, Davassi A, Scopes G, Pirani A, Webster T, Brew F, Bloor C, Griffiths S, Bentley AR, Alda M, Jack P, Phillips AL, Edwards KJ. (2017). Characterization of a Wheat Breeders' Array suitable for high-throughput SNP genotyping of global accessions of hexaploid bread wheat (Triticum aestivum). Plant Biotechnol. 15(3), 390-401.
15. Allioui N, Siah A, Brinis L, Reignault P, Halama P. (2013). Assessment of the cytochrome B substitution G143A in the Algerian population of Mycosphaerella graminicola. Commun Agric Appl Biol Sci. 78(3), 613-6.
16. Allioui N, Ali Siah, Louhichi Brinis, Philippe Reignault & Patrice Halama (2014). Mating type distribution provides evidence for sexual reproduction of Mycosphaerella graminicola in Algeria, Canadian Journal of Plant Pathology. 36(4), 475-481.
17. Anderegg J, Hund Andreas, Karisto Petteri, Mikaberidze Alexey (2019). In-Field Detection and Quantification of Septoria Tritici Blotch in Diverse Wheat Germplasm Using Spectral–Temporal Features, Frontiers in Plant Science, 10.
18. Arioli T, Peng L, Betzner AS, Burn J, Wittke W, Herth W, Camilleri C, Höfte H, Plazinski J, Birch R, Cork A, Glover J, Redmond J, Williamson RE. (1998). Molecular analysis of cellulose biosynthesis in Arabidopsis. Science. 279(5351), 717-20.
19. Armour, T. & Viljanen, Suvi & SF, Chng & Butler, R.C. & Jamieson, Peter & Zyskowski, Robert. (2004). Examining the latent period of Septoria tritici blotch in a field trial of winter wheat. New Zealand Plant Protection. 57(57), 116-120.
20. Arraiano L.S., A.J. Worland, C. Ellerbrook, J.K.M. Brown (2001). Chromosomal location of a gene for resistance to Septoria trictici blotch (Mycosphaerella graminicola) in the hexaploid wheat ‘Synthetic 6x’ Theor. Appl. Genet. 103, 758-764.
21. Arraiano L.S., J.K.M. Brown (2006). Identification of isolate-specific and partial resistance to spetoria tritici blotch in 238 European wheat cultivars and breeding lines Plant. Pathol. 55, 54-61

22. Arraiano L.S., L. Chartrain, E. Bossolini, H.N. Slatter, B. Keller, J.K.M. Brown (2007). A gene in European wheat cultivars for resistance to an African isolate of Mycosphaerella graminicola Plant. Pathol. 56, 73-78.
23. Arraiano, L.S., Balaam, N., Fenwick, P.M., Chapman, C., Feuerhelm, D., Howell, P., Smith, S.J., Widdowson, J.P., Brown, J.K.M., (2009). Contributions of disease resistance and escape to the control of Septoria tritici blotch of wheat. Plant. Pathol. 58, 910–922.
24. Arraiano, L.S. and Brown, J.K.M. (2017). Sources of resistance and susceptibility to Septoria tritici blotch of wheat. Molecular Plant Pathology. 18, 276-292.
25. Ashourloo, D., Mobasheri, M. R., & Huete, A. (2014). Developing two spectral disease indices for detection of wheat leaf rust (Pucciniatriticina). Remote Sensing. 6(6), 4723–4740.
26. Atkins, S. D., King, K. M., Fraaije, B. A. and Newton, A. C. (2010). Rynchosporium secalis: a historical perspective. Proceedings Dundee Conference on Crop Protection in Northern Britain, Dundee. 23-24, 103-108
27. Bailey, K. L., Gossen, B. D., Lafond, G. P., Watson, P. R., & Derksen, D. A. (2001). Effect of tillage and crop rotation on root and foliar diseases of wheat and pea in Saskatchewan from 1991 to 1998: Univariate and multivariate analyses. Canadian Journal of Plant Science. 81(4), 789–803.
28. Bari, R., Jones, J.D.G. (2009). Role of plant hormones in plant defence responses. Plant Mol Biol. 69, 473–488.
29. Bassett CL, Nickerson ML, Cohen RA, Rajeevan MS. (2000). Alternative transcript initiation and novel post-transcriptional processing of a leucine-rich repeat receptor-like protein kinase gene that responds to short-day photoperiodic floral induction in morning glory (Ipomoea nil). Plant Mol Biol. May. 43(1), 43-58.
30. Bassett, C. L., Nickerson, M. L., Cohen, R. A., & Rajeevan, M. S. (2001). Erratum: Alternative transcript initiation and novel post-transcriptional processing of a leucine-rich repeat receptor-like protein kinase gene that responds to short-day photoperiodic floral induction in morning glory (Ipomoea nil). Plant Molecular Biology. 46(6), 761–762.
31. Baltazar, B., A.L. Scharen, and W.E. Kronstad. (1990). Associations and resistance to Septoria between dwarfing genes Rht1and Rht2 tritici blotch in winter wheat (Triticum aestivum L. em Thell). Theor. Appl. Genet. 79, 422–426.

32. Bannon, F. J., & Cooke, B. M. (1998). Studies on dispersal of Septoria tritici pycnidiospores in wheat-clover intercrops. Plant Pathology. 47(1), 49–56.
33. Banke S, Peschon A, McDonald BA. (2004). Phylogenetic analysis of globally distributed Mycosphaerella graminicola populations based on three DNA sequence loci, Fungal Genet Biol. 41, 226-238.
34. Bankina, B., Ruža, A., Paura, L., & Priekule, I. (2015). The effects of soil tillage and crop rotation on the development of winter wheat leaf diseases. Zemdirbyste-Agriculture. 102(1), 67–72.
35. Bankina, B., Bimšteine, G., Arhipova, I., Kaņeps, J., & Stanka, T. (2018). Importance of agronomic practice on the control of wheat leaf diseases. Agriculture (Switzerland). 8(4), 1–8.
36. Battache M., Lebrun Marc-Henri, Sakai Kaori, Soudière Olivier, Cambon Florence, Langin Thierry, Saintenac Cyrille (2022). Blocked at the Stomatal Gate, a Key Step of Wheat Stb16q-Mediated Resistance to Zymoseptoria tritici. Frontiers in Plant Science 13.
37. Bathgate, J. A., & Loughman, R. (2001). Ascospores are a source of inoculum of Phaeosphaeria nodorum, P. Avenaria f. sp. Avenaria and Mycosphaerella graminicola in Western Australia. Australasian Plant Pathology. 30(4), 317–322.
38. Barthel S, Isendahl C, Vis BN, Drescher A, Evans DL, van Timmeren (2019). A. Global urbanization and food production in direct competition for land: Leverage places to mitigate impacts on SDG2 and on the Earth System. The Anthropocene Review. 6(1-2), 71-97.
39. Bayles, R. A., Clarkson, J. D. S. and Slater, S. E. (1997). The UK Cereal Pathogen Virulence Survey. In: Crute, I. R., Holub, E. B. and Burdon, J. J. (Eds) The Gene-for-Gene Relationship in Plant-Parasite Interactions. CAB International, Wallingford. 103–117.
40. Bertini, L., Proietti, S., Aleandri, M. P., Mondello, F., Sandini, S., & Caporale, C. (2012). Modular structure of HEL protein from Arabidopsis reveals new potential functions for PR-4 proteins. Biological Chemistry, 1–14.
41. Bellec, Y., Harrar, Y., Butaeye, C., Darnet, S., Bellini, C., & Faure Ã, J.-D. (2002). Pasticcino2 is a protein tyrosine phosphatase-like involved in cell proliferation and differentiation in Arabidopsis. 32, 713-722.
42. Ben M'Barek, S., Cordewener, J. H. G., Tabib Ghaffary, S. M., van der Lee, T. A. J., Liu, Z., Mirzadi Gohari, A., … Kema, G. H. J. (2015). FPLC and liquid-

chromatography mass spectrometry identify candidate necrosis-inducing proteins from culture filtrates of the fungal wheat pathogen Zymoseptoria tritici. Fungal Genetics and Biology. 79, 54–62.

43. Benbow HR, Brennan CJ, Zhou B, Christodoulou T, Berry S, Uauy C, Mullins E, Doohan FM. (2020). Insights into the resistance of a synthetically-derived wheat to Septoria tritici blotch disease: less is more. BMC Plant Biol. 20, 407.
44. Benjamini, Yoav, and Yosef Hochberg. "Controlling the False Discovery Rate: A Practical and Powerful Approach to Multiple Testing." Journal of the Royal Statistical Society. Series B (Methodological), vol. 57, no. 1, 1995, pp. 289–300.
45. Beyer, M., Kiesner, F., Verreet, J. A., & Klink, H. (2011). Fungicide sensitivity of Septoria tritici field isolates is affected by an interaction between fungicidal mode of action and time. Journal of Plant Pathology. 93(SUPPL. 1), 7–14.
46. Bharadwaj Revuru, Kumar Sarma R., Sharma Ashutosh, Sathishkumar Ramalingam (2021). Plant Metabolic Gene Clusters: Evolution, Organization, and Their Applications in Synthetic Biology. Frontiers in Plant Science. 12.
47. Bharath, P; Gahir, S and Raghavendra, AS (2021). Abscisic Acid-Induced Stomatal Closure: An Important Component of Plant Defense Against Abiotic and Biotic Stress. Frontiers in Plant Science. 12.
48. Bittner, F., Oreb, M., & Mendel, R. R. (2001). ABA3 Is a Molybdenum Cofactor Sulfurase Required for Activation of Aldehyde Oxidase and Xanthine Dehydrogenase in Arabidopsis thaliana. Journal of Biological Chemistry. 276(44), 40381–40384.
49. Blackburn A., G. (1998). Quantifying Chlorophylls and Caroteniods at Leaf and Canopy Scales: An Evaluation of Some Hyperspectral Approaches (Vol. 66).
50. Blake, J.J.; Gosling, P.; Fraaije, B.A.; Burnett, F.J.; Knight, S.M.; Kildea, S.; Paveley, N.D. (2018). Changes in field dose-response curves for demethylation inhibitor (DMI) and quinone outside inhibitor (QoI) fungicides against Zymoseptoria tritici, related to laboratory. sensitivity phenotyping and genotyping assays. Pest Manag. Sci. 74, 302–313.
51. Bohnenkamp, David & Behmann, Jan & Paulus, Stefan & Steiner, Ulrike & Mahlein, Anne-Katrin. (2021). A Hyperspectral Library of Foliar Diseases of Wheat. Phytopathology. 111.
52. Bonshtien, A. L., Weiss, C., Vitlin, A., Niv, A., Lorimer, G. H., & Azem, A. (2007). Significance of the N-terminal domain for the function of chloroplast cpn20 chaperonin. Journal of Biological Chemistry. 282(7), 4463–4469.

53. Brading, P.A., Verstappen, E.C.P., Kema, G.H.J., Brown, J.K.M., (2002). A gene-for-gene relationship between wheat and Mycosphaerella graminicola, the Septoria tritici blotch pathogen. Phytopathology. 92, 439–445.
54. Brown, J. K. M. (1994). Chance and selection in the evolution of barley mildew. Trends in Microbiology. 2(12), 470–475.
55. Brown JK, Chartrain L, Lasserre-Zuber P, Saintenac C. (2015). Genetics of resistance to Zymoseptoria tritici and applications to wheat breeding. Fungal Genet Biol. 79, 33-41.
56. Brown JK (2021). Achievements in breeding cereals with durable disease resistance in Northwest Europe. Burleigh dodds.
57. Brown, J.K.M. and Rant, J.C. (2013). Fitness costs and trade-offs of disease resistance and their consequences for breeding arable crops. Plant Pathol. 62, 83-95.
58. Brunner PC, Stefanato FL, McDonald BA. (2008) Evolution of the CYP51 gene in Mycosphaerella graminicola: evidence for intragenic recombination and selective replacement. Mol Plant Pathol. 9(3), 305-16.
59. Caiazzo, R.C.B., Corsi, B., Di Lenarda, S., Naska, E., Webb, A., Elliott, D. et al (2019). Investigating a potential new variant of Zymoseptoria tritici, causal agent of septoria leaf blotch, and implications for U.K. winter wheat varieties. AHDB Project Report No. 604.
60. Calderón-Villalobos, L. I. A., Nill, C., Marrocco, K., Kretsch, T., & Schwechheimer, C. (2007). The evolutionarily conserved Arabidopsis thaliana F-box protein AtFBP7 is required for efficient translation during temperature stress. Gene. 392(1–2), 106–116.
61. Campanaro, A., Srivastava, A.K., Zhang, C., Lee, J., Millyard, L., Gatehouse, A.M.R., Byrne, E. and Sadanandom, A. (2021). TaWRKY10 transcription factor is a novel jasmonic acid signalling regulator involved in immunity against Septoria tritici blotch disease in wheat. Plant Pathol. 70, 1397-1408.
62. Cao, F.Y., Yoshioka, K. & Desveaux, D. (2011). The roles of ABA in plant–pathogen interactions. J Plant Res. 124, 489–499.
63. Cesari, S., Thilliez, G., Ribot, C., Chalvon, V., Michel, C., Jauneau, A., … Kroj, T. (2013). The rice resistance protein pair RGA4/RGA5 recognizes the Magnaporthe oryzae effectors AVR-Pia and AVR1-CO39 by direct binding. Plant Cell. 25(4), 1463–1481.

64. Camacho Casas, M.A., W.E. Kronstad, and A.L. Scharen. (1995). Sep- toria tritici resistance and associations with agronomic traits in wheat cross. Crop Sci. 35, 971–976.
65. Campos, L.J.M., de Almeida, R.E.M., da Silva, D.D. et al. (2021). Physiological and biophysical alterations in maize plants caused by Colletotrichum graminicola infection verified by OJIP study. Trop. plant pathol. 46, 674–683.
66. Carbonell, E. A., Gerig, T. M., Balansard, E., & Asins, M. J. (1992). Interval Mapping in the Analysis of Nonadditive Quantitative Trait Loci. Biometrics. 48(1), 305–315.
67. Celsa G., David Marshall (1992). Observations on the ascogenous stage of Septoria tritici in Texas, Mycological Research. 96, 65-70.
68. Czembor P, Radecka Janusik M, Ma kowski D (2010) Virulence spectrum of Mycosphaerella graminicola isolates on wheat genotypes carrying known resistance genes to septoria tritici blotch. J Phytopathol.159(3), 146-154.
69. Chappelle E. W., Moon S Kim, James E McMurtrey. (1992). Ratio analysis of reflectance spectra (RARS): An algorithm for the remote estimation of the concentrations of chlorophyll A, chlorophyll B, and carotenoids in soybean leaves, Remote Sensing of Environment. 39(3), 239-247.
70. Chartrain, L., Berry, S.T., Brown, J.K.M., (2005a). Resistance of wheat line Kavkaz-K4500 L.6.A.4 to Septoria tritici blotch controlled by isolate-specific resistance genes. Phytopathology. 95, 664–671.
71. Chartrain, L., Joaquim, P., Berry, S.T., Arraiano, L.S., Azanza, F., Brown, J.K.M., (2005b). Genetics of resistance to Septoria tritici blotch in the Portuguese wheat breeding line TE9111. Theor. Appl. Genet. 110, 1138–1144.
72. Chartrain, L., Sourdille, P., Bernard, M., Brown, J.K.M., (2009). Identification and location of Stb9, a gene for resistance to Septoria tritici blotch in wheat cultivars Courtot and Tonic. Plant. Pathol. 58, 547–555.
73. Chávez-Arias, Cristhian C., Sandra Gómez-Caro, and Hermann Restrepo-Díaz. (2019). "Physiological, Biochemical and Chlorophyll Fluorescence Parameters of Physalis Peruviana L. Seedlings Exposed to Different Short-Term Waterlogging Periods and Fusarium Wilt Infection" Agronomy 9, no. 5: 213.
74. Chern M, Xu Q, Bart RS, Bai W, Ruan D, Sze-To WH, Canlas PE, Jain R, Chen X, Ronald PC. (2016). A Genetic Screen Identifies a Requirement for Cysteine-Rich-

Receptor-Like Kinases in Rice NH1 (OsNPR1)-Mediated Immunity. PLoS Genet. 12(5).

75. Choi, Y. E., Lee, C., & Goodwin, S. B. (2016). Generation of Reactive Oxygen Species via NOXa Is Important for Development and Pathogenicity of Mycosphaerella graminicola. Mycobiology. 44(1), 38–47.

76. Choi, Y.-E., & Goodwin, S. B. (2011). Gene encoding a c-type cyclin in Mycosphaerella graminicola is involved in aerial mycelium formation, filamentous growth, hyphal swelling, melanin biosynthesis, stress response, and pathogenicity. Molecular Plant-Microbe Interactions: MPMI. 24(4), 469–77.

77. Chungu C, Gilbert J, Townley-Smith F. (2001). Septoria tritici Blotch Development as Affected by Temperature, Duration of Leaf Wetness, Inoculum Concentration, and Host. Plant Dis. 85(4), 430-435.

78. Coego, A., Ramirez, V., Gil, M. J., Flors, V., Mauch-Mani, B., & Vera, P. (2005). An arabidopsis homeodomain transcription factor, overexpressor of cationic peroxidase 3, mediates resistance to infection by necrotrophic pathogens. Plant Cell. 17(7), 2123–2137.

79. Cordo C. O, C. I. Mónaco, R. Altamirano, A. E. Perelló, S. Larrán, N. I. Kripelz, M. R. Simón, (2017). "Weather Conditions Associated with the Release and Dispersal of Zymoseptoria tritici Spores in the Argentine Pampas Region", International Journal of Agronomy, Article ID 1468580.

80. Cousin, A., Mehrabi, R., Guilleroux, M., Dufresne, M., Van Der Lee, T., Waalwijk, C., … Kema, G. H. J. (2006). The MAP kinase-encoding gene MgFus3 of the non-appressorium phytopathogen Mycosphaerella graminicola is required for penetration and in vitro pycnidia formation. Molecular Plant Pathology. 7(4), 269–278.

81. Cowger. C., and James K.M. Brown (2019). Durability of Quantitative Resistance in Crops: Greater Than We Know? Annual Review of Phytopathology. 57, 253-277.

82. Cousin, A., Mehrabi, R., Guilleroux, M., Dufresne, M., Van Der Lee, T., Waalwijk, C., … Kema, G. H. J. (2006). The MAP kinase-encoding gene MgFus3 of the non-appressorium phytopathogen Mycosphaerella graminicola is required for penetration and in vitro pycnidia formation. Molecular Plant Pathology. 7(4), 269–278.

83. Cowling, S. G. (2006). Identification and mapping of host resistance genes to septoria tritici blotch of wheat. Available online at: https://mspace.lib.umanitoba.ca/xmlui/handle/1993/20699

84. Crop Prospects and Food Situation - No.2, 07 (2022) GIEWS - Global Information and Early Warning System on Food and Agriculture, FAO.
85. Dall'Osto, L., Fiore, A., Cazzaniga, S., Giuliano, G., & Bassi, R. (2007). Different roles of α- and β-branch xanthophylls in photosystem assembly and photoprotection. Journal of Biological Chemistry. 282(48), 35056–35068.
86. Dall'Osto L, Cazzaniga S, Wada M, Bassi R (2014). On the origin of a slowly reversible fluorescence decay component in the Arabidopsis npq4 mutant. Philos Trans R Soc Lond B Biol Sci. 369, 20130221.
87. Dalvand, M., Soleimani Pari, M.J. & Zafari, D. (2018). Evaluating the efficacy of STB resistance genes to Iranian Zymoseptoria tritici isolates. J Plant Dis Prot. 125, 27–32.
88. Dash, J. and Curran, P.J. (2004). The MERIS terrestrial chlorophyll index. International Journal of Remote Sensing. 25(23), 5403-5413.
89. Datt, B. (1998). Remote Sensing of Chlorophyll a, Chlorophyll b, Chlorophyll a+b, and Total Carotenoid Content in Eucalyptus Leaves. Remote Sensing of Environment. 66, 111-121.
90. Davletova, S., Rizhsky, L., Liang, H., Shengqiang, Z., Oliver, D. J., Coutu, J., … Mittler, R. (2005). Cytosolic ascorbate peroxidase 1 is a central component of the reactive oxygen gene network of Arabidopsis. Plant Cell. 17(1), 268–281.
91. De Torres Zabala M, Littlejohn G, Jayaraman S, Studholme D, Bailey T, Lawson T, Tillich M, Licht D, Bölter B, Delfino L, Truman W, Mansfield J, Smirnoff N, Grant M. (2015). Chloroplasts play a central role in plant defence and are targeted by pathogen effectors. Nat Plants. 1(1), 15074.
92. Dennis MD, Browning KS. (2009). Differential phosphorylation of plant translation initiation factors by Arabidopsis thaliana CK2 holoenzymes. J Biol Chem. 284(31), 20602-14.
93. Depaoli, H. C., Goldman, G. H., & Goldman, M. H. S. (2012). SCI1, the first member of the tissue-specific inhibitors of CDK (TIC) class, is probably connected to the auxin signaling pathway. Plant Signaling and Behavior. 7(1), 53–58.
94. Dicko, M. H., Gruppen, H., Hilhorst, R., Voragen, A. G. J., & Van Berkel, W. J. H. (2006). Biochemical characterization of the major sorghum grain peroxidase. FEBS Journal. 273(10), 2293–2307.

95. Dong Q., Zhang Y.X., Zhou Q., Liu Q.E., Chen D.B., Wang H., et al. (2019). UMP kinase regulates chloroplast development and cold response in rice. Int. J. Mol. Sci. 20, 2107.
96. Dubos, T., Pasquali, M., Pogoda, F., Casanova, A., Hoffmann, L., & Beyer, M. (2013). Differences between the succinate dehydrogenase sequences of isopyrazam sensitive Zymoseptoria tritici and insensitive Fusarium graminearum strains. Pesticide Biochemistry and Physiology. 105(1), 28–35.
97. Duncan, K. E., & Howard, R. J. (2000). Cytological analysis of wheat infection by the leaf blotch pathogen Mycosphaerella graminicola. Mycological Research. 104(9), 1074–1082.
98. Eckardt, N. A. (2001). A role for PsbZ in the core complex of photosystem II. The Plant Cell. 13(6), 1245–1248.
99. Elbekali, A. Y., Siah, A., Ramdani, A., Chartouni, L. El, Tisserant, B., Deweer, C., … Halama, P. (2012). First Report of the Mating Types Mat1-1 and Mat1-2 of Mycosphaerella Graminicola in Morocco. Journal of Plant Pathology. 94(1), 243–247.
100. Eriksen, L., Shaw, M. W., & Ostergård, H. (2001). A Model of the Effect of Pseudothecia on Genetic Recombination and Epidemic Development in Populations of Mycosphaerella graminicola. Phytopathology. 91(3), 240–8.
101. Eriksen L., F. Borum, A. Jahoor (2003). Inheritance and localisation of resistance to Mycosphaerella graminicola causing Septoria tritici blotch and plant height in the wheat (Triticum aestivum L.) genome with DNA markers Theor. Appl. Genet. 107, 515-527.
102. Eriksen, L & Munk, L (2003). 'The occurrence of Mycosphaerella graminicola and its anamorph Septoria tritici in winter wheat during the growing season', European Journal of Plant Pathology. 109(3), 253-259.
103. Eyal Z (1981). Integrated control of Septoria diseases of wheat. Plant Disease. 65, 763–768.
104. Eyal Z, Scharen AL, Prescott JM, Van Ginkel M (1987). 'The Septoria diseases of wheat: concepts and methods of disease management.' (CIMMYT: Mexico)
105. Färber A, Peter Jahns, (1998). The xanthophyll cycle of higher plants: influence of antenna size and membrane organization, Biochimica et Biophysica Acta (BBA) – Bioenergetics. 1363, 47-58.
106. Feng Wei, Qi Shuangli, Heng Yarong, Zhou Yi, Wu Yapeng, Liu Wandai, He Li, Li Xiao (2017). Canopy Vegetation Indices from In situ Hyperspectral Data to Assess

Plant Water Status of Winter Wheat under Powdery Mildew Stress. Frontiers in Plant Science. 8, 1664-462.

107. Fernandez, M. R., Zentner, R. P., McConkey, B. G., & Campbell, C. a. (1998). Effects of crop rotations and fertilizer management on leaf spotting diseases of spring wheat in southwestern Saskatchewan. Canadian Journal of Plant Science. 78(3), 489–496.

108. Fernández-Calleja, Miriam, Arantxa Monteagudo, Ana M. Casas, Christophe Boutin, Pierre A. Pin, Fermín Morales, and Ernesto Igartua. (2020). "Rapid On-Site Phenotyping via Field Fluorimeter Detects Differences in Photosynthetic Performance in a Hybrid—Parent Barley Germplasm Set" Sensors. 20(5), 1486.

109. Fichman, Y. and Mittler, R. (2020). Rapid systemic signalling during abiotic and biotic stresses: is the ROS wave master of all trades? Plant J. 102, 887-896.

110. Flor HH. (1956). The complementary genic systems in flax and flax rust. Advances in Genetics Incorporating Molecular Genetic Medicine. 8, 29–54.

111. Fones, H. N., Eyles, C. J., Kay, W., Cowper, J., & Gurr, S. J. (2017). A role for random, humidity-dependent epiphytic growth prior to invasion of wheat by Zymoseptoria tritici. Fungal Genetics and Biology. 106, 51–60.

112. Foreman, J., Demidchik, V., Bothwell, J. H. F., Mylona, P., Miedema, H., Torresk{, M. A., … Dolan, L. (2003). Reactive oxygen species produced by NADPH oxidase regulate plant cell growth. Nature. 422(6930), 442-6.

113. Foster, J., Kim, H. U., Nakata, P. A., & Browse, J. (2012). A previously unknown Oxalyl-CoA synthetase is important for oxalate catabolism in Arabidopsis. Plant Cell. 24(3), 1217–1229.

114. Foyer, C. H., & Noctor, G. (2005). Oxidant and antioxidant signalling in plants: a re-evaluation of the concept of oxidative stress in a physiological context. Plant, Cell and Environment (Vol. 28).

115. Fraaije, B.A.; Cools, H.J.; Kim, S.-H.; Motteram, J.; Clark,W.S.; Lucas, J.A. (2007). A novel substitution I381V in the sterol 14-demethylase(CYP51) of Mycosphaerella graminicola is differentially selected by azole fungicides. Mol. Plant Pathol. 8, 245–254.

116. Fradgley, N., Gardner, K. A., Cockram, J., Elderfield, J., Hickey, J. M., Howell, P., Jackson, R. and Mackay, I. J. (2019). A large-scale pedigree resource of wheat reveals evidence for adaptation and selection by breeders. PLoS Biology. 17(2)

117. Frels F., Mary Guttieri, Brian Joyce, Bryan Leavitt, P. Stephen Baenziger, (2018). Evaluating canopy spectral reflectance vegetation indices to estimate nitrogen. Field Crops Research, 217, 82-92.
118. Frankart C., P Eullaffroy, G Vernet, (2003). Comparative effects of four herbicides on non-photochemical fluorescence quenching in Lemna minor. Environmental and Experimental Botany. 49(2), 159-168.
119. Friedrichroda, Germany, 24–28 April 2016; Deising, H.B., Fraaije, B., Mehl, A., Oerke, E.C., Sierotzki, H., Stammler, G., Eds.; Deutsche
120. Fristedt, R., Herdean, A., Blaby-Haas, C. E., Mamedov, F., Merchant, S. S., Last, R. L., & Lundin, B. (2015). PHOTOSYSTEM II PROTEIN33, a protein conserved in the plastid lineage, is associated with the chloroplast thylakoid membrane and provides stability to photosystem II supercomplexes in arabidopsis. Plant Physiology. 167(2), 481–492.
121. Fukamatsu, Y., Yabe, N., & Hasunuma, K. (2003). Arabidopsis NDK1 is a Component of ROS Signaling by Interacting with Three Catalases. Plant Cell Physiol (Vol. 44).
122. Galvez-Valdivieso, G., and Mullineaux, P. M. (2010). The role of reactiveoxygen species in signalling from chloroplasts to the nucleus. Physiol.Plant. 138, 430-439.
123. Gang DR, Kasahara H, Xia ZQ, Vander Mijnsbrugge K, Bauw G, Boerjan W, Van Montagu M, Davin LB, Lewis NG. (1999). Evolution of plant defense mechanisms. Relationships of phenylcoumaran benzylic ether reductases to pinoresinol-lariciresinol and isoflavone reductases. J Biol Chem. 274(11), 7516-27.
124. Gamon, A., Pe uelas, J., & Field, C. B. (1992). A Narrow-Waveband Spectral Index That Tracks Diurnal Changes in Photosynthetic Efficiency* (Vol. 41).
125. Gaudet, P., Livstone, M. S., Lewis, S. E., & Thomas, P. D. (2011). Phylogenetic-based propagation of functional annotations within the Gene Ontology consortium. Briefings in Bioinformatics. 12(5), 449–462.
126. Gerard, G.S. et al., (2017). Genome-wide association mapping of genetic factors controlling Septoria tritici blotch resistance and their associations with plant height and heading date in wheat. Euphytica, 213(1).
127. Gilbert, G.S. and Parker, I.M. (2010). Rapid evolution in a plant-pathogen interaction and the consequences for introduced host species. Evolutionary Applications. 3, 144-156.

128. Gisi, U.; Sierotzki, H.; Cook A. & McCaffery, A. (2002). Mechanisms influencing the evoliution of resistance to Qo inhibitor fungicides. Pest Management Science. 58(9), 859-867.
129. Gitelson, A. A., Merzlyak, M. N., & Chivkunova, O. B. (2001). Optical Properties and Nondestructive Estimation of Anthocyanin Content in Plant Leaves. In Photochemistry and Photobiology, 74(1).
130. Gitelson, A.A., Zur, Y., Chivkunova, O.B. and Merzlyak, M.N. (2002). Assessing Carotenoid Content in Plant Leaves with Reflectance Spectroscopy. Photochemistry and Photobiology. 75: 272-281.
131. Giossi C, Cartaxana P, Cruz S. (2020). Photoprotective Role of Neoxanthin in Plants and Algae. Molecules. 25(20), 4617.
132. GLADDERS, P., PAVELEY, N. D., BARRIE, I. A., HARDWICK, N. V, HIMS, M. J., LANGTON, S., & TAYLOR, M. C. (2001). Agronomic and meteorological factors affecting the severity of leaf blotch caused by Mycosphaerella graminicola in commercial wheat crops in England. Annals of Applied Biology. 138(3), 301–311.
133. Goodwin, S.B. (2007). Back to basics and beyond: increasing the level of resistance to Septoria tritici blotch in wheat. Australasian Plant Pathology. 36, 532–538.
134. Goodwin, S. B., Barek, S. B. M., Dhillon, B., Wittenberg, A. H. J., Charles, F., Hane, J. K., … Burgt, A. Van Der. (2011). Finished Genome of the Fungal Wheat Pathogen Mycosphaerella graminicola Reveals Dispensome Structure , Chromosome Plasticity , and Stealth Pathogenesis. 7(6).
135. Goudemand E., V. Laurent, L. Duchalais, S.M. Tabib Ghaffary, G.H.J. Kema, P. Lonnet, E. Margale, O. Robert (2013). Association mapping and meta-analysis: two complementary approaches for the detection of reliable Septoria tritici blotch quantitative resistance in bread wheat (Triticum aestivum L.) Mol. Breed. 32, 563-584.
136. Gough, F. J., & Lee, T. S. (1984). Moisture Effects on the Discharge and Survival of Conidia of Septoria tritici. Phytopathology. 75, 180–182.
137. Gough FJ (1978). Effect of wheat host cultivars on pycnidiospore production by Septoria tritici. Phytopathology. 68, 1343–1345.
138. Grimmer, M.K., Boyd, L.A., Clarke, S.M., Paveley, N.D., (2015). Pyramiding of partial disease resistance genes has a predictable, but diminishing, benefit to efficacy. Plant. Pathol.

139. Grzybowski M., Nuwan K. Wijewardane, Abbas Atefi, Yufeng Ge, James C. Schnable. (2021). Hyperspectral reflectance-based phenotyping for quantitative genetics in crops: Progress and challenges. Plant Communications. 2(4).
140. Guo, J., & Chen, J. G. (2008). RACK1 genes regulate plant development with unequal genetic redundancy in Arabidopsis. BMC Plant Biology. 8.
141. Hagerty, C. H., Anderson, N. P., and Mundt, C. C. (2017). Temporal dynamics and spatial variation of Zymoseptoria tritici azoxystrobin and propiconazole fungicide resistance: a hierarchical survey of commercial winter wheat fields in the Willametter Valley of Oregon. Phytopathology. 107, 345-352.
142. Hardwick, N.V., Jones, D.R. and Slough, J.E. (2001). Factors affecting diseases ofwinter wheat in England and Wales. Plant Pathol. 50, 453–462.
143. Haueisen, J., Möller, M., Eschenbrenner, C. J., Grandaubert, J., Seybold, H., Adamiak, H., & Stukenbrock, E. H. (2019). Highly flexible infection programs in a specialized wheat pathogen. Ecology and Evolution. 9(1), 275–294.
144. Hawkins NJ, Fraaije BA. (2016). Predicting Resistance by Mutagenesis: Lessons from 45 Years of MBC Resistance. Front Microbiol. 15(7), 1814.
145. Hazem M. Kalaji, Abdallah Oukarroum, Vladimir Alexandrov, Margarita Kouzmanova, Marian Brestic, Marek Zivcak, Izabela A. Samborska, Magdalena D. Cetner, Suleyman I. Allakhverdiev, Vasilij Goltsev, (2014). Identification of nutrient deficiency in maize and tomato plants by in vivo chlorophyll a fluorescence measurements, Plant Physiology and Biochemistry. 81, 16-25,
146. Hao Q, Yin P, Li W, et al. (2011). The molecular basis of ABA-independent inhibition of PP2Cs by a subclass of PYL proteins. Molecular Cell. 42(5), 662-672.
147. Hazrati S., Zeinolabedin Tahmasebi-Sarvestani, Seyed Ali Mohammad Modarres-Sanavy, Ali Mokhtassi-Bidgoli, Silvana Nicola, Effects of water stress and light intensity on chlorophyll fluorescence parameters and pigments of Aloe vera L., Plant Physiology and Biochemistry. 106, 141-148.
148. Hellin, P., Duvivier, M., Heick, T.M., Fraaije, B.A., Bataille, C., Clinckemaillie, A., Legrève, A., Jørgensen, L.N., Andersson, B., Samils, B., Rodemann, B., Berg, G., Hutton, F., Garnault, M., El Jarroudi, M., Couleaud, G. and Kildea, S. (2021). Spatio-temporal distribution of DMI and SDHI fungicide resistance of Zymoseptoria tritici throughout Europe based on frequencies of key target-site alterations. Pest Manag Sci. 77, 5576-5588.

149. Hernández-Clemente R., Rafael M. Navarro-Cerrillo, Lola Suárez, Fermín Morales, Pablo J. Zarco-Tejada (2011) Assessing structural effects on PRI for stress detection in conifer forests, Remote Sensing of Environment, 115(9), 2360-2375.
150. Hoorne C., L. Lamari, G. M. Ballance & J. Gilbert (2002). First report of Mycosphaerella graminicola, the sexual state of Septoria tritici, in Manitoba, Canada, Canadian Journal of Plant Pathology. 24(4), 445-449.
151. Hunter, T., Coker, R. R., & Royle, D. J. (1999). The teleomorph stage, Mycosphaerella graminicola, in epidemics of septoria tritici blotch on winter wheat in the UK. Plant Pathology. 48(1), 51–57.
152. Hutin M, Césari S, Chalvon V, Michel C, Tran TT, Boch J, Koebnik R, Szurek B, Kroj T. (2016). Ectopic activation of the rice NLR heteropair RGA4/RGA5 confers resistance to bacterial blight and bacterial leaf streak diseases. Plant J. 88, 43-55.
153. IPCC WGII Sixth Assessment Report (2021) Chapter 5: Food, Fibre, and other Ecosystem Products.
154. Iakovidis M, Teixeira PJPL, Exposito-Alonso M, Cowper MG, Law TF, et al. (2016). Effector-triggered immune response in Arabidopsis thaliana is a quantitative trait. Genetics. 204, 337–53.
155. Jauvion, V., Elmayan, T., & Vaucheret, H. (2010). The conserved RNA trafficking proteins HPR1 and TEX1 are involved in the production of endogenous and exogenous small interfering RNA in arabidopsis. Plant Cell. 22(8), 2697–2709.
156. Jackson LF, Dubcovsky J, Gallagher LW, Wennig RL, Heaton J,Vogt H, et al. (2000). Regional barley and common and durum wheat performance tests in California. Agron Prog Rep, 272, 1–56.
157. Jahns, P., & Holzwarth, A. R. (2012). The role of the xanthophyll cycle and of lutein in photoprotection of photosystem II. Biochimica et Biophysica Acta – Bioenergetics. 1817(1), 182–193.
158. Jarsch IK, Ott T. (2011). Perspectives on remorin proteins, membrane rafts, and their role during plant-microbe interactions. Mol Plant Microbe Interact. 24(1), 7-12.
159. Jiang Y, Bao L, Jeong SY, et al. (2012). XIAO is involved in the control of organ size by contributing to the regulation of signaling and homeostasis of brassinosteroids and cell cycling in rice. The Plant Journal: for Cell and Molecular Biology. 70(3), 398-408.

160. Jin, N., Huang, W., Ren, Y., Luo, J., Wu, Y., Jing, Y., & Wang, D. (2013). Hyperspectral identification of cotton verticillium disease severity. Optik, 124(16), 2569–2573.
161. Johnson R (1984). A critical analysis of durable resistance. Annu Rev Phytopathol. 22, 309–330
162. Jørgensen, J. H. (1994). Genetics of powdery mildew resistance in barley. Critical Reviews in Plant Sciences. 13(1), 97–119.
163. Jørgensen, L.N.; Matzen, N.; Heick, T.M.; Havis, N.; Holdgate, S.; Clark, B.; Blake, J.; Glazek, M.; Korbas, M.; Danielewicz, J.; et al. (2021). Decreasing azole sensitivity of Z. tritici in Europe contributes to reduced and varying field efficacy. J. Plant Dis. Prot. 128, 287–301.
164. Katamadze, M., & Paura, L. (2015). CROP ROTATION – THE MAIN FACTOR INFLUENCING THE DEVELOPMENT OF WHEAT LEAF BLOTCH, 65–69.
165. Katanić, Zorana, Selma Mlinarić, Nataša Katanić, Josipa Ćosić, and Valentina Španić. (2021). "Photosynthetic Efficiency in Flag Leaves and Ears of Winter Wheat during Fusarium Head Blight Infection" Agronomy. 11(12), 2415.
166. Kabbage, M., Leslie, J. F., Hulbert, S. H., & Bockus, W. W. (2009). Comparison of natural populations of Mycosphaerella graminicola from single fields in Kansas and California. Physiological and Molecular Plant Pathology. 74(1), 55–59.
167. Karisto, P., Hund, A., Yu, K., Anderegg, J., Walter, A., Mascher, F., McDonald, B. A., & Mikaberidze, A. (2018). Ranking quantitative resistance to septoria tritici blotch in elite wheat cultivars using automated image analysis. Phytopathology. 108(5), 568–581.
168. Kaiser, E., Morales, A., Harbinson, J. et al. (2016). Metabolic and diffusional limitations of photosynthesis in fluctuating irradiance in Arabidopsis thaliana. Sci Rep. 6, 31252.
169. Kema, G. H. J., Yu, D., Rijkenberg, F. H. J., Shaw, M. W., & Baayen, R. P. (1996a). Histology of pathogenesis of Mycosphaerella graminicola in wheat. Phytopathology. 86, 777-786.
170. Kema, G., Verstappen, E., Todorova, M. et al. Curr Genet (1996b). Successful crosses and molecular tetrad and progeny analyses demonstrate heterothallism in Mycosphaerella graminicola. Curr Genet. 30, 251.

171. Kema GH, Verstappen EC, Waalwijk C. (2000). Avirulence in the wheat septoria tritici leaf blotch fungus Mycosphaerella graminicola is controlled by a single locus. Mol Plant Microbe Interact. 13(12), 1375-9.

172. Kema, G.H.J., van der Lee, T.A., Mendes, O., Verstappen, E.C., Lankhorst, R.K., Sandbrink, H., van der Burgt, A., Zwiers, L.H., Csukai, M., Waalwijk, C., (2008). Large-scale gene discovery in the septoria tritici blotch fungus Mycosphaerella graminicola with a focus on in planta expression. Mol. Plant Microbe Interact. 21, 1249–1260.

173. Kelm C., S.M. Tabib Ghaffary, H. Bruelheide, M.S. Roder, S. Miersch, W.E. Weber, G.H.J. Kema, B. Saal (2012). The genetic architecture of seedling resistance to Septoria tritici blotch in the winter wheat doubled-haploid population Solitär x Mazurka Mol. Breed. 29, 813-830

174. Keon, J., Antoniw, J., Rudd, J., Skinner, W., Hargreaves, J., & Hammond-Kosack, K. (2005). Analysis of expressed sequence tags from the wheat leaf blotch pathogen Mycosphaerella graminicola (anamorph Septoria tritici). Fungal Genetics and Biology. 42(5), 376–389.

175. Keon, J., Antoniw, J., Carzaniga, R., Deller, S., Ward, J. L., Baker, J. M., … Rudd, J. J. (2007). Transcriptional adaptation of Mycosphaerella graminicola to programmed cell death (PCD) of its susceptible wheat host. Molecular Plant-Microbe Interactions. Mol plant Microbe Interact. 20(2), 178-93.

176. Kildea, S.; Dooley, H.; Phelan, S.; Mehenni-Ciz, J.; Spink, J. (2017). Developing fungicide control programmes for blotch in Irish winter wheat crops. In Modern Fungicides and Antifungal Compounds, Proceedings of the 18th International Reinhardsbrunn Symposium.

177. Kildea, S, Sheppard, L, Cucak, M, Hutton, F. (2021). Detection of virulence to septoria tritici blotch (STB) resistance conferred by the winter wheat cultivar Cougar in the Irish Zymoseptoria tritici population and potential implications for STB control. Plant Pathol. 70, 2137– 2147.

178. Kildea, S., Hellin, P., Heick, T.M. and Hutton, F. (2022). Baseline sensitivity of European Zymoseptoria tritici populations to the complex III respiration inhibitor fenpicoxamid. Pest Manag Sci.78(11), 4488-4496.

179. Kruijt, M., Brandwagt, B. F., & De Wit, P. J. G. M. (2004). Rearrangements in the Cf-9 disease resistance gene cluster of wild tomato have resulted in three genes that mediate Avr9 responsiveness. Genetics. 168(3), 1655–1663.

180. Kondo, T., Kajita, R., Miyazaki, A., Hokoyama, M., Nakamura-Miura, T., Mizuno, S., … Sakagami, Y. (2010). Stomatal density is controlled by a mesophyll-derived signaling molecule. Plant and Cell Physiology. 51(1), 1–8.
181. Kong D, Zhu Y, Wu H, Cheng X, Liang H, Ling HQ. (2008). AtTHIC, a gene involved in thiamine biosynthesis in Arabidopsis thaliana. Cell Res. 18(5), 566-76.
182. Kosambi, D.D. (1944). The Estimation of Map Distances from Recombination Values. Annals of Eugenics. 12, 172-175.
183. Kosellek, C., Pillen, K., Nelson, J.C. et al. (2013). Inheritance of field resistance to Septoria tritici blotch in the wheat doubled-haploid population Solitär × Mazurka. Euphytica. 194, 161–176.
184. Kramer, B., Thines, E., & Foster, A. J. (2009). MAP kinase signalling pathway components and targets conserved between the distantly related plant pathogenic fungi Mycosphaerella graminicola and Magnaporthe grisea. Fungal Genetics and Biology. 46(9), 667–681.
185. Krasuska, E., Cadorniga, C., Tenorio, J., Testa, G., Scordia, D., (2010). Potential land availability for energy crops production in Europe. Modelling and anaylsis. 4(6), 658-673.
186. Kuhlgert, S., Austic, G., Zegarac, R., Osei-Bonsu, I., Hoh, D., Chilvers, M. I., Roth, M. G., Bi, K., TerAvest, D., Weebadde, P., & Kramer, D. M. (2016). MultispeQ Beta: A tool for large-scale plant phenotyping connected to the open photosynQ network. Royal Society Open Science. 3(10).
187. Langlands-Perry, C.; Cuenin, M.; Bergez, C.; Krima, S.B.; Gélisse, S.; Sourdille, P.; Valade, R.; Marcel, T.C. (2022). Resistance of the Wheat Cultivar ‘Renan’ to Septoria Leaf Blotch Explained by a Combination of Strain Specific and Strain Non-Specific QTL Mapped on an Ultra-Dense Genetic Map. Genes. 13, 100.
188. La Camera, S., Balagué, C., Göbel, C., Geoffroy, P., Legrand, M., Feussner, I., … Heitz, T. (2009). The Arabidopsis Patatin-Like Protein 2 (PLP2) Plays an Essential Role in Cell Death Execution and Differentially Affects Biosynthesis of Oxylipins and Resistance to Pathogens. / 469 MPMI. 22(4), 469–481.
189. Le Mire, G.; Siah, A.; Brisset, M.-N.; Gaucher, M.; Deleu, M.; Jijakli, M.H. (2018). Surfactin Protects Wheat against Zymoseptoria tritici and Activates Both Salicylic Acid- and Jasmonic Acid-Dependent Defense Responses. Agriculture, 8, 11.
190. Leath, S., Scharen, A. L., Lund, R. E., & Dietz-Holmes, M. E. (1993). Factors associated with global occurrences of Septoria nodorum blotch and Septoria tritici

blotch of wheat. Plant Dis.Lev-Yadun S, Gopher A, Abbo S. The cradle of agriculture. Science. 288, 1602–1603.

191. Lee, J., Orosa, B., Millyard, L., Edwards, M., Kanyuka, K., Gatehouse, A., … Sadanandom, A. (2015). Functional analysis of a Wheat Homeodomain protein, TaR1, reveals that host chromatin remodelling influences the dynamics of the switch to necrotrophic growth in the phytopathogenic fungus Zymoseptoria tritici. New Phytologist. 206(2), 598–605.

192. Lee, W. S., Devonshire, B. J., Hammond-Kosack, K. E., Rudd, J. J., & Kanyuka, K. (2015). Deregulation of plant cell death through disruption of chloroplast functionality affects asexual sporulation of Zymoseptoria tritici on wheat. Molecular Plant-Microbe Interactions. 28(5), 590–604.

193. Leimkühler, S., Freuer, A., Araujo, J. A. S., Rajagopalan, K. V., & Mendel, R. R. (2003). Mechanistic studies of human molybdopterin synthase reaction and characterization of mutants identified in group B patients of molybdenum cofactor deficiency. Journal of Biological Chemistry. 278(28), 26127–26134.

194. Leo, Â. P. De. (2002). Involvement of the Arabidopsis a -DOX1 fatty acid dioxygenase in protection against oxidative stress and cell death. 29, 61–72.

195. Lev-Yadun, S., Gopher, A., & Abbo, S. (2000). The Cradle of Agriculture. Science, 288, 1602 - 1603.

196. Liaqat Ali, Muhammad Rashid Shaheen, Muhammad Zahid Ihsan, Sajid Masood, Muhammad Zubair, Farrukh Shehzad, Absar-Ul-Haq Khalid, (2022). Growth, photosynthesis and antioxidant enzyme modulations in broccoli (Brassica oleracea L. var. italica) under salinity stress, South African Journal of Botany. 148, 104-111.

197. Li XP, Gilmore AM, Caffarri S, Bassi R, Golan T, Kramer D, Niyogi KK (2004). Regulation of photosynthetic light harvesting involves intrathylakoid lumen pH sensing by the PsbS protein. J Biol Chem 279, 22866–22874.

198. Li, D., Wang, L., Wang, M., Xu, Y. Y., Luo, W., Liu, Y. J., … Chong, K. (2009). Engineering OsBAK1 gene as a molecular tool to improve rice architecture for high yield. Plant Biotechnology Journal. 7(8), 791–806.

199. Li CH, Wang G, Zhao JL, Zhang LQ, Ai LF, Han YF, Sun DY, Zhang SW, Sun Y. (2014). The Receptor-Like Kinase SIT1 Mediates Salt Sensitivity by Activating MAPK3/6 and Regulating Ethylene Homeostasis in Rice. Plant Cell. 26(6) 2538-2553.

200. Li CL, Wang M, Wu XM, Chen DH, Lv HJ, Shen JL, Qiao Z, Zhang W. (2016). THI1, a Thiamine Thiazole Synthase, Interacts with Ca2+-Dependent Protein Kinase CPK33

and Modulates the S-Type Anion Channels and Stomatal Closure in Arabidopsis. Plant Physiol. 170(2), 1090-104.

201. Li Aili, Dengcai Liu, Wuyun Yang, Masahiro Kishii, Long Mao (2018). Synthetic Hexaploid Wheat: Yesterday, Today, and Tomorrow, Engineering. 4(4), 552-558.
202. Liu Z, Zhang Z, Faris JD, Oliver RP, Syme R, et al. (2012) The Cysteine Rich Necrotrophic Effector SnTox1 Produced by Stagonospora nodorum Triggers Susceptibility of Wheat Lines Harboring Snn1. PLOS Pathogens 8(1):
203. Liu, Y.Y., Zhang, L.L., Thompson, I.A., Goodwin, S.B., Ohm, H.W., (2013). Molecular mapping re-locates the Stb2 gene for resistance to Septoria tritici blotch derived from cultivar Veranopolis on wheat chromosome 1BS. Euphytica. 190, 145–156.
204. Liu, L., Tong, H., Xiao, Y., Che, R., Xu, F., Hu, B., … Chu, C. (2015). Activation of Big Grain1 significantly improves grain size by regulating auxin transport in rice. Proceedings of the National Academy of Sciences of the United States of America. 112(35), 11102–11107.
205. Llamas, A., Otte, T., Multhaup, G., Mendel, R. R., & Schwarz, G. (2006). The mechanism of nucleotide-assisted molybdenum insertion into molybdopterin: A novel route toward metal cofactor assembly. Journal of Biological Chemistry. 281(27), 18343–18350.
206. Lokstein, H., Renger, G., & Götze, J. P. (2021). Photosynthetic light-harvesting (antenna) complexes-structures and functions. Molecules. 26(11).
207. Lu, Y. (2016). Identification and roles of photosystem II assembly, stability, and repair factors in Arabidopsis. Frontiers in Plant Science, 7(FEB2016).
208. Mäe Andres, Fillinger Sabine, Sooväli Pille, Heick Thies Marten (2020). Fungicide Sensitivity Shifting of Zymoseptoria tritici in the Finnish-Baltic Region and a Novel Insertion in the MFS1 Promoter, Frontiers in Plant Science. 11.
209. Magboul, A. M., Geng, S., Gilchrist, D. G., & Jackson, L. F. (1992). Environmental Influence on the Infection of Wheat by Mycosphaerella-Graminicola. Ecology and Epidemiology. 82(12), 1407-1413.
210. Mahlein, A.-K., Steiner, U., Hillnhütter, C., Dehne, H.-W., & Oerke, E.-C. (2012). Hyperspectral imaging for small-scale analysis of symptoms caused by different sugar beet diseases. Plant Methods. 8, 3.

211. Mahlein, A. K. (2016). Plant disease detection by imaging sensors – Parallels and specific demands for precision agriculture and plant phenotyping. In Plant Disease. American Phytopathological Society 100(1), 241–254.
212. Mahboubi M., Talebi Reza, Aghaee Sarbarzeh Mostafa, Naji Amir Mohammad, Mehrabi Rahim (2020). Resistance and virulence variability in wheat–Zymoseptoria tritici interactions. Crop and Pasture Science 71, 645-652.
213. Makhdoomi, A., Mehrabi, R., Khodarahmi, M., & Abrinbana, M. (2014). Efficacy of wheat genotypes and Stb resistance genes against Iranian isolates of Zymoseptoria tritici. Journal of General Plant Pathology. 81(1), 5–14.
214. Makhdoomi, A., Mehrabi, R., Khodarahmi, M. et al. (2015). Efficacy of wheat genotypes and Stb resistance genes against Iranian isolates of Zymoseptoria tritici . J Gen Plant Pathol. 81, 5–14.
215. Malnoë, A. (2018). Photoinhibition or photoprotection of photosynthesis? Update on the (newly termed) sustained quenching component qH. Environmental and Experimental Botany. 154, 123–133.
216. Mavroeidi, V. I., & Shaw, M. W. (2006). Effects of fungicide dose and mixtures on selection for triazole resistance in Mycosphaerella graminicola under field conditions. Plant Pathology. 55(6), 715–725.
217. McAndrew, R., Pruitt, R. N., Kamita, S. G., Pereira, J. H., Majumdar, D., Hammock, B. D., … Ronald, P. C. (2014). Structure of the OsSERK2 leucine-rich repeat extracellular domain. Acta Crystallographica Section D: Biological Crystallography. 70(11), 3080–3086.
218. McCartney, C.A., Brûlé-Babel, A.L., Lamari, L., Somers, D.J., (2003). Chromosomal location of a race specific resistance gene to Mycosphaerella graminicola in the spring wheat ST6. Theor. Appl. Genet. 107, 1181–1186.
219. McCartney, C.A., Brûlé-Babel, A.L., Lamari, L., (2002). Inheritance of race-specific resistance to Mycosphaerella graminicola in wheat. Phytopathology. 92, 138–144.
220. McDonald BA, Zhan J, Yarden O, Hogan K, Garton J, Pettway RE. Lucas JA, Bowyer P, Anderson HM. (1999) The population genetics of Mycosphaerella graminicola and Phaeosphaeria nodorum, Septoria on cereals: a study of Pathosystems, 1999Wallingford (UK)CABI (pg. 44-69).
221. McDonald, Bruce & Mundt, Chris. (2016). How Knowledge of Pathogen Population Biology Informs Management of Septoria Tritici Blotch. Phytopathology. 106(9), 948-55.

222. Mehrabi, R., & Kema, G. H. J. (2006). Protein kinase a subunits of the ascomycete pathogen Mycosphaerella graminicola regulate asexual fructification, filamentation, melanization and osmosensing. Molecular Plant Pathology. 7(6), 565–577.

223. Mehrabi, R., Makhdoomi, A. and Jafar-Aghaie, M. (2015). Identification of New Sources of Resistance to Septoria Tritici Blotch Caused by Zymoseptoria tritici. J Phytopathol. 163. 84-90.

224. Mekonnen, T., Haileselassie, T., Kaul, T. et al. (2019). Molecular screening of Zymoseptoria tritici resistance genes in wheat (Triticum aestivum L.) using tightly linked simple sequence repeat markers. Eur J Plant Pathol. 155, 593–614.

225. Merzlyak, M.N., Gitelson, A.A., Chivkunova, O.B. and Rakitin, V.Y. (1999), Non-destructive optical detection of pigment changes during leaf senescence and fruit ripening. Physiologia Plantarum. 106, 135-141.

226. MET OFFICE (2018, 2019) Historical data, Sutton Bonington https://www.metoffice.gov.uk/pub/data/weather/uk/climate/stationdata/suttonboningtondata.txt

227. Meile, L., Croll, D., Brunner, P.C., Plissonneau, C., Hartmann, F.E., McDonald, B.A. and Sánchez-Vallet, A. (2018). A fungal avirulence factor encoded in a highly plastic genomic region triggers partial resistance to septoria tritici blotch. New Phytol. 219, 1048-1061.

228. Mirzadi Gohari A. (2015). Identification and functional characterization of putative (a)virulence factors in the fungal wheat pathogen Zymoseptoria tritici. PhD thesis, Wageningen University, Wageningen, the Netherlands.

229. Morais, D., Laval, V., Sache, I., & Suffert, F. (2015). Comparative pathogenicity of sexual and asexual spores of Zymoseptoria tritici (septoria tritici blotch) on wheat leaves. Plant Pathology. 64(6), 1429–1439.

230. Morton, V. and Staub, T. (2008). A Short History of Fungicides. Online, APSnet Features. doi: 10.1094/APSnetFeature-2008-0308.

231. Motteram, J., Lovegrove, A., Pirie, E., Marsh, J., Devonshire, J., van de Meene, A., … Rudd, J. J. (2011). Aberrant protein N-glycosylation impacts upon infection-related growth transitions of the haploid plant-pathogenic fungus Mycosphaerella graminicola. Molecular Microbiology. 81(2), 415–433.

232. Moustaka, Julietta, Georgia Tanou, Ioannis-Dimosthenis Adamakis, Eleftherios P. Eleftheriou, and Michael Moustakas. (2015). "Leaf Age-Dependent Photoprotective and Antioxidative Response Mechanisms to Paraquat-Induced Oxidative Stress in

Arabidopsis thaliana" International Journal of Molecular Sciences. 16(6), 13989-14006.

233. Müller M, Munné-Bosch S. (2018). Rapid and sensitive hormonal profiling of complex plant samples by liquid chromatography coupled to electrospray ionization tandem mass spectrometry. Plant Methods.18(7),37

234. Müller, P., Li, X. P., & Niyogi, K. K. (2001). Non-photochemical quenching. A response to excess light energy. Plant Physiology. 125(4), 1558–1566.

235. Murchie, E. H., & Ruban, A. V. (2020). Dynamic non-photochemical quenching in plants: from molecular mechanism to productivity. Plant Journal, 101(4), 885–896.

236. Mustafa, G., Zheng, H., Imran, H. K., Long, T., Jia, H., Li, G., . . . Yao, X. (2022). Hyperspectral reflectance proxies to diagnose in-field fusarium head blight in wheat with machine learning. Remote Sensing. 14(12), 2784.

237. Navarro L, Bari R, Achard P, Lison P, Nemri A, Harberd NP, Jones JD (2008). DELLAs control plant immune responses by modulating the balance of jasmonic acid and salicylic acid signaling. Curr Biol. 18, 650–655.

238. Nayak, L., Raval, M. K., Biswal, B., & Biswal, U. C. (2002). Topology and photoprotective role of carotenoids in photosystem II of chloroplast: A hypothesis. Photochemical and Photobiological Sciences. 1(9), 629–631.

239. Nawrocki WJ, Santabarbara S, Mosebach L, Wollman FA, Rappaport F (2016). State transitions redistribute rather than dissipate energy between the two photosystems in Chlamydomonas. Nat Plants 2, 16031.

240. Nehal Samy El-Mougy, Nadia Gamel El-Gamal, Mokhtar Mohamed Abdel-Kader & Mohamed Saied Ali Khalil (2022). Inhibiting septoria leaf blotch disease severity of wheat plants by using foliar spray with two antagonists and growth regulators under natural field conditions, Archives of Phytopathology and Plant Protection. 55(17), 2023-2039.

241. Nelissen, H., Fleury, D., Bruno, L., Robles, P., De Veylder, L., Traas, J., … Lijsebettens, M. Van. (2005). The elongata mutants identify a functional Elongator complex in plants with a role in cell proliferation during organ growth. PNAS. 102 (21), 7754-7759

242. Nes WR, McKean MR. 1977. Biochemistry of steroids and other isoprenoids. University Park Press, Baltimore, MD.

243. Nick V Grishin (1998) The R3H motif: a domain that binds single-stranded nucleic acids. Trends in Biochemical sciences. 23(9). 329-330.

244. Odilbekov, F., He, X., Armoniené, R., Saripella, G. V., Henriksson, T., Singh, P. K., & Chawade, A. (2019). QTL mapping and transcriptome analysis to identify differentially expressed genes induced by Septoria tritici blotch disease of wheat. Agronomy. 9(9).

245. Omrane, S., Sghyer, H., Audéon, C., Lanen, C., Duplaix, C., Walker, A. S., & Fillinger, S. (2015). Fungicide efflux and the MgMFS1 transporter contribute to the multidrug resistance phenotype in Zymoseptoria tritici field isolates. Environmental Microbiology. 17(8), 2805–2823.

246. Orton ES, Rudd JJ, Brown JK. (2017). Early molecular signatures of responses of wheat to Zymoseptoria tritici in compatible and incompatible interactions. Plant Pathol. 66(3), 450-459.

247. O'Driscoll, Steven Kildea, Fiona Doohan, John Spink, Ewen Mullins, (2014). The wheat–Septoria conflict: a new front opening up? Trends in Plant Science. 19(9), 602-610.

248. Palma-Guerrero, J., Torriani, S. F. F., Zala, M., Carter, D., Courbot, M., Rudd, J. J., … Croll, D. (2016). Comparative transcriptomic analyses of Zymoseptoria tritici strains show complex lifestyle transitions and intraspecific variability in transcription profiles. Molecular Plant Pathology. 17(6), 845–859.

249. Park, C. J., & Ronald, P. C. (2012). Cleavage and nuclear localization of the rice XA21 immune receptor. Nature Communications, 3, 1–6.

250. Patel, S., & Dinesh-Kumar, S. P. (2008). Arabidopsis ATG6 is required to limit the pathogen-associated cell death response. Autophagy. 4(1), 20–27.

251. Passari AK, Upadhyaya K, Singh G, Abdel-Azeem AM, Thankappan S, Uthandi S, et al. (2019). Enhancement of disease resistance, growth potential, and photosynthesis in tomato (Solanum lycopersicum) by inoculation with an endophytic actinobacterium, Streptomyces thermocarboxydus strain BPSAC147. PLoS ONE. 14(7)

252. Phillips MA, D'Auria JC, Gershenzon J, Pichersky E. (2008). The Arabidopsis thaliana type I Isopentenyl Diphosphate Isomerases are targeted to multiple subcellular compartments and have overlapping functions in isoprenoid biosynthesis. Plant Cell. 20(3), 677-96.

253. Piaskowska, Dominika, Urszula Piechota, Magdalena Radecka-Janusik, and Paweł Czembor. (2021). "QTL Mapping of Seedling and Adult Plant Resistance to Septoria Tritici Blotch in Winter Wheat cv. Mandub (Triticum aestivum L.)" Agronomy. 11(6), 1108.

254. Pieczul K., I. Świerczyńska, P. Katarzyna, Ś. Ilona (2015). Fungicide sensitivity of Mycosphaerella graminicola (Septoria tritici) isolates Prog. Plant Prot. 55, 316-320.
255. Pietravalle, S., Shaw, M. W., Parker, S. R., & van den Bosch, F. (2003). Modeling of Relationships Between Weather and Septoria tritici Epidemics on Winter Wheat: A Critical Approach. Phytopathology. 93(10), 1329–1339.
256. Ptieczul K., Anna Wąsowska. (2017). The application of next-generation sequencing (NGS) for monitoring of Zymoseptoria tritici QoI resistance, Crop Protection. 92, 143-147.
257. Penuelas, J., Filella, I., Biel, C., Serrano, L., & Save, R. (1993). The reflectance at the 950-970 nm region as an indicator of plant water status. International Journal of Remote Sensing. 14(10), 1887–1905.
258. Penuelas, J., Baret, F. and Filella, I. (1995). Semi-Empirical Indices to Assess Carotenoids/Chlorophyll a Ratio from Leaf Spectral Reflectance. Photosynthetica. 31, 221-230.
259. Prokopová J, Martina Špundová, Michaela Sedlářová, Alexandra Husičková, Radko Novotný, Karel Doležal, Jan Nauš, Aleš Lebeda, (2010). Photosynthetic responses of lettuce to downy mildew infection and cytokinin treatment, Plant Physiology and Biochemistry. 48(8), 716-723.
260. Ponomarenko A., S.B. Goodwin, and G.H.J. Kema. (2011). Septoria tritici blotch (STB) of wheat. Plant Health Instructor.
261. Potuschak, T., Stary, S., Schlo¨gelhofer, P. S., Becker, F., Nejinskaia, V., & Bachmair, A. (1998). PRT1 of Arabidopsis thaliana encodes a component of the plant N-end rule pathway (Vol. 95).
262. Quick, W.P., Stitt, M., (1989). An examination of factors contributing to non-photochemical quenching of chlorophyll fluorescence in barley leaves. Biochim Biophys Acta. 977, 287-296.
263. Rapacz Marcin, Wójcik-Jagła Magdalena, Fiust Anna, Kalaji Hazem M., Kościelniak Janusz (2019). Genome-Wide Associations of Chlorophyll Fluorescence OJIP Transient Parameters Connected With Soil Drought Response in Barley Frontiers in Plant Science. 10
264. Ray S, Anderson JM, Urmeev FI, Goodwin SB, (2003). Rapid induction of a protein disulfide isomerase and defense-related genes in wheat in response to the hemibiotrophic fungal pathogen Mycosphaerella graminicola. Plant Molecular Biology. 53, 741–54.

265. Rehfus, A., Strobel, D., Bryson, R. and Stammler, G. (2018), Mutations in sdh genes in field isolates of Zymoseptoria tritici and impact on the sensitivity to various succinate dehydrogenase inhibitors. Plant Pathol. 67, 175-180.

266. Reynolds M., Scott Chapman, Leonardo Crespo-Herrera, Gemma Molero, Suchismita Mondal, Diego N.L. Pequeno, Francisco Pinto, Francisco J. Pinera-Chavez, Jesse Poland, Carolina Rivera-Amado, Carolina Saint Pierre, Sivakumar Sukumaran, (2019). Breeder friendly phenotyping. Plant Science. 295, 0168-9452.

267. Rgen Ehlting, J. È., Bu È Ttner, D., Wang, Q., Douglas, C. J., Somssich, I. E., & Kombrink, E. (1999). Three 4-coumarate:coenzyme A ligases in Arabidopsis thaliana represent two evolutionarily divergent classes in angiosperms. 19(1), 9-20.

268. Rillo AO, Caldwell RM (1966). Inheritance of resistance to Septoria tritici in Triticum aestivum subsp. vulgare 'Bulgaria 88' (abstract). Phytopathology. 56, 897.

269. Rintamäki, E., Kettunen, R., Tyystjärvi, E. and Aro, E.-M. (1995). Light-dependent phosphorylation of D1 reaction centre protein of photosystem II: hypothesis for the functional role in vivo. Physiologia Plantarum. 93, 191-195.

270. Rohel, E. A., Payne, A. C., Fraaije, B. A., & Hollomon, D. W. (2001). Exploring Infection of Wheat and Carbohydrate Metabolism in Mycosphaerella graminicola Transformants with Differentially Regulated Green Fluorescent Protein Expression. Molecular Plant-Microbe Interactions. 14(2), 156–163.

271. Robert, C. et al., (2008). Coupling a 3D virtual wheat (Triticum aestivum) plant model with a Septoria tritici epidemic model (Septo3D): A new approach to investigate plant-pathogen interactions linked to canopy architecture. Functional Plant Biology. 35(10), 997–1013.

272. Romá-Mateo C, Ríos P, Tabernero L, Attwood TK, Pulido R. (2007). A novel phosphatase family, structurally related to dual-specificity phosphatases, that displays unique amino acid sequence and substrate specificity. J Mol Biol. 374(4), 899-909.

273. Ron M, Avni A. (2004). The receptor for the fungal elicitor ethylene-inducing xylanase is a member of a resistance-like gene family in tomato. Plant Cell. 16(6), 1604-15.

274. Roohparvar, R., De Waard, M. A., Kema, G. H. J., & Zwiers, L. H. (2007). MgMfs1, a major facilitator superfamily transporter from the fungal wheat pathogen Mycosphaerella graminicola, is a strong protectant against natural toxic compounds and fungicides. Fungal Genetics and Biology. 44(5), 378–388.

275. Rossig, C., Reinbothe, C., Gray, J., Valdes, O., Von Wettstein, D., & Reinbothe, S. (2013). Three proteins mediate import of transit sequence-less precursors into the inner

envelope of chloroplasts in arabidopsis thaliana. Proceedings of the National Academy of Sciences of the United States of America. 110(49), 19962.

276. Rouxel T, Balesdent MH. (2005). The stem canker (blackleg) fungus, Leptosphaeria maculans, enters the genomic era. Mol Plant Pathol. 6(3), 225-41.

277. Ryschawy, Julie & Benoit, Marc & Hostiou, Nathalie & Delfosse, C.. (2017). Crop-livestock regions: In-between competition with cash crops and opportunities. Productions Animales. 30, 363-379.

278. A.V. Ruban, D. Phillip, A.J. Young, P. Horton. (1997). Carotenoid-dependent oligomerization of the major chlorophyll a/b light harvesting complex of photosystem II of plants. Biochemistry. 36, 7855-7859.

279. Ruban A.v, Matthew P. Johnson, Christopher D.P. Duffy. (2012). The photoprotective molecular switch in the photosystem II antenna, Biochimica et Biophysica Acta (BBA) – Bioenergetics. 1817(1), 167-181.

280. Rudd, J., Keon, J., Hammond-Kosack, K., (2008). The wheat mitogen-activated protein kinases TaMPK3 and TaMPK6 are differentially regulated at multiple levels during compatible disease interactions with Mycosphaerella graminicola. Plant Physiol. 147, 802–815

281. Rudd, J. J., Kanyuka, K., Hassani-Pak, K., Derbyshire, M., Andongabo, A., Devonshire, J., … Courbot, M. (2015). Transcriptome and Metabolite Profiling of the Infection Cycle of Zymoseptoria tritici on Wheat Reveals a Biphasic Interaction with Plant Immunity Involving Differential Pathogen Chromosomal Contributions and a Variation on the Hemibiotrophic Lifest. Plant Physiology. 167(3), 1158-85.

282. Rudd, J. J. (2015). Previous bottlenecks and future solutions to dissecting the Zymoseptoria tritici-wheat host-pathogen interaction. Fungal Genetics and Biology. 79, 24–28.

283. Saari,E. E R.D. Wilcoxson (1974). Plant disease situation of high-yielding dwarf wheats in Asia and Africa Annu. Rev. Phytopathol. 12, 49-68.

284. Saini, D.K., Chahal, A., Pal, N. et al. (2022). Meta-analysis reveals consensus genomic regions associated with multiple disease resistance in wheat (Triticum aestivum L.). Mol Breeding. 42, 11.

285. Sakuraba, Y., Lee, S. H., Kim, Y. S., Park, O. K., Hörtensteiner, S., & Paek, N. C. (2014). Delayed degradation of chlorophylls and photosynthetic proteins in Arabidopsis autophagy mutants during stress-induced leaf yellowing. Journal of Experimental Botany. 65(14), 3915–3925.

286. Saintenac C, Lee WS, Cambon F, Rudd JJ, King RC, Marande W, Powers SJ, Bergès H, Phillips AL, Uauy C, Hammond-Kosack KE, Langin T, Kanyuka K. (2018). Wheat receptor-kinase-like protein Stb6 controls gene-for-gene resistance to fungal pathogen Zymoseptoria tritici. Nat Genet. 50(3), 368-374.

287. Saintenac, C., Cambon, F., Aouini, L. et al. (2021). A wheat cysteine-rich receptor-like kinase confers broad-spectrum resistance against Septoria tritici blotch. Nat Commun. 12, 433.

288. Saleh, A., Lumbreras, V., Lopez, C., Dominguez-Puigjaner, E., Kizis, D., & Pagès, M. (2006). Maize DBF1-interactor protein 1 containing an R3H domain is a potential regulator of DBF1 activity in stress responses. Plant Journal. 46(5), 747–757.

289. Sanderfoot AA, Assaad FF, Raikhel NV. (2000). The Arabidopsis genome. An abundance of soluble N-ethylmaleimide-sensitive factor adaptor protein receptors. Plant Physiol. 124(4), 1558-69.

290. Sanderson, F. R. (1976). Mycosphaerella graminicola (Fuckel) Sanderson comb. nov., the ascogenous state of Septoria tritici Rob. apud Desm. New Zealand Journal of Botany. 14(4), 359–360.

291. Sánchez-Vallet A., Jeroen R. Mesters, Bart P.H.J. Thomma, (2015). The battle for chitin recognition in plant-microbe interactions, FEMS Microbiology Reviews. 39(2), 171–183.

292. Sánchez-Vallet, A., McDonald, M. C., Solomon, P. S., & McDonald, B. A. (2015). Is Zymoseptoria tritici a hemibiotroph? Fungal Genetics and Biology. 79, 29–32.

293. Savary S, Willocquet L, Pethybridge SJ, Esker P, McRoberts N, Nelson A. (2019). The global burden of pathogens and pests on major food crops. Nat Ecol Evol. 3(3), 430-439.

294. Sasaki-Sekimoto, Y., Taki, N., Obayashi, T., Aono, M., Matsumoto, F., Sakurai, N., … Ohta, H. (2005). Coordinated activation of metabolic pathways for antioxidants and defence compounds by jasmonates and their roles in stress tolerance in Arabidopsis. Plant Journal. 44(4), 653–668.

295. Scalliet, G., Bowler, J., Luksch, T., Kirchhofer-Allan, L., Steinhauer, D., Ward, K., … Fonné-Pfister, R. (2012). Mutagenesis and functional studies with succinate dehydrogenase inhibitors in the wheat pathogen Mycosphaerella graminicola. PLoS ONE. 7(4).

296. Scandalios, J. C. (1994). Differential Accumulation of Manganese-Superoxide Dismutase Transcripts in Maize in Response to Abscisic Acid and High Osmoticum'. Plant Physiol (Vol. 106).
297. Schmeling B, Kulka M (1966). Systemic fungicidal activity of 1,4-oxathiin derivatives. Science. 152, 659.
298. Schuh, W. (1990). Influence of tillage systems on the disease intensity and spatial pattern of Septoria leaf blotch. Phytopathology. 80, 1337-1340.
299. Serrano, I., Audran, C., and Rivas, S. (2016). Chloroplasts at work during plant innate immunity. Journal of Experimental Botany. 67(13), 3845–3854.
300. Shaner G, Buechley G (1989). Inheritance of resistance to Mycosphaerella graminicola in wheat. In: Fried PM (ed) Septoria of cereals proceeding workshop, Zurich. 133–135.
301. Shaw, M. W., and Royle, D. J. (1993). Factors determining the severity of epidemics of Mycosphaerella graminicola (Septoria tritici) on winter wheat in the UK. Plant Pathol. 42, 882-899
302. Shaw, M.W., Bearchell, S.J., Fitt, B.D.L. and Fraaije, B.A. (2008). Long-term relationships between environment and abundance in wheat of Phaeosphaeria nodo-rum and Mycosphaerella graminicola.New Phytol. 177, 229–238.
303. Shen, H., Zhong, X., Zhao, F. et al. (2015). Overexpression of receptor-like kinase ERECTA improves thermotolerance in rice and tomato. Nat Biotechnol 33, 996–1003.
304. Shetty, N. P., Kristensen, B. K., Newmana, M. A., Møller, K., Gregersen, P. L., & Jørgensen, H. J. L. (2003). Association of hydrogen peroxide with restriction of Septoria tritici in resistant wheat. Physiological and Molecular Plant Pathology. 62(6), 333–346.
305. Shetty, N.P., Mehrabi, R., Lütken, H., Haldrup, A., Kema, G.H.J., Collinge, D.B. and Jørgensen, H.J.L. (2007). Role of hydrogen peroxide during the interaction between the hemibiotrophic fungal pathogen Septoria tritici and wheat. New Phytologist. 174, 637-647.
306. Shetty NP, Jensen JD, Knudsen A et al, (2009). Effects of β-1,3-glucan from Septoria tritici on structural defence responses in wheat. Journal of Experimental Botany. 60, 4287–300.
307. Shipton, W.A., Boyd, S.R.J., Rosielle, A.A., Shearer, B.I., (1971). Common Septoria diseases of wheat. Bot. Rev. 37, 231–262.

308. Siah, A., Deweer, C., Duyme, F., Sanssené, J., Durand, R., Halama, P., Reignault, P., (2010). Correlation of in planta endo-beta-1,4-xylanase activity with the necrotrophic phase of the hemibiotrophic fungus Mycosphaerella graminicola. Plant. Pathol. 59, 661–670.
309. M.R. Simón, A.E. Perelló, C.A. Cordo, P.C. Struik (2002). Influence of Septoria tritici on yield, yield components, and test weight of wheat under two nitrogen fertilization conditions. Crop Sci. 42, 1974-1981.
310. Simón, M.R. et al., (2004). Molecular mapping of quantitative trait loci determining resistance to septoria tritici blotch caused by Mycosphaerella graminicola in wheat. Euphytica. 138(1), 41–48.
311. Simón, M.R. et al., (2005). Association between septoria tritici blotch, plant height, and heading date in wheat. Agronomy Journal. 97(4), 1072–1081.
312. Simón, M.R., Ayala, F.M., Cordo, C.A. et al. (2007). The use of wheat/goatgrass introgression lines for the detection of gene(s) determining resistance to septoria tritici blotch (Mycosphaerella graminicola). Euphytica. 154, 249–254.
313. Sims, D. A., & Gamon, J. A. (2002). Relationships between leaf pigment content and spectral reflectance across a wide range of species, leaf structures and developmental stages. Remote Sensing of Environment. 81, 337–354.
314. Skendžić, S.; Zovko, M.; Živković, I.P.; Lešić, V.; Lemić, D. (2021). The Impact of Climate Change on Agricultural Insect Pests. Insects. 12, 440.
315. Skinner, W., Bailey, A., Renwick, A., Keon, J., Gurr, S., & Hargreaves, J. (1998). A single amino-acid substitution in the iron-sulphur protein subunit of succinate dehydrogenase determines resistance to carboxin in Mycosphaerella graminicola. Current Genetics. 34(5), 393–398.
316. Sloat, L.L., Davis, S.J., Gerber, J.S. et al. (2020). Climate adaptation by crop migration. Nat Commun. 11, 1243.
317. Smale, M. (1997). The green revolution and wheat genetic diversity: some unfounded assumptions. World Development. 25(8)
318. Somasco OA, Qualset CO, Gilchrist DG (1996). Single-gene resistance to Septoria tritici blotch in the spring wheat cultivar ‘Tadinia’. Plant Breeding. 115, 261–267.
319. Song MH, Aravind L, Müller-Reichert T, O'Connell KF. (2008). The conserved protein SZY-20 opposes the Plk4-related kinase ZYG-1 to limit centrosome size. Dev Cell. 15(6), 901-12.

320. Song JB, Huang SQ, Dalmay T, Yang ZM. (2012). Regulation of leaf morphology by microRNA394 and its target LEAF CURLING RESPONSIVENESS. Plant Cell Physiol. 53(7), 1283-94.

321. Spyroglou, I., Rybka, K., Czembor, P., Piaskowska, D., Pernisová, M. & Matysik, P. (2022). Higher alterations in leaf fluorescence parameters of wheat cultivars predict more extensive necrosis in response to Zymoseptoria tritici. Plant Pathology. 71, 1454–1466.

322. Srivastava, A., Greppin, G. and Strasser, R.J. (1995). The steady-state chlorophyll a fluorescence exhibits in vivo an optimum as a function of light intensity which reflects the physiological state of the plant. Plant Cell Physiol. 36, 839–848.

323. Staleva, H., Komenda, J., Shukla, M. K., Slouf, V., Kana, R., Polivka, T., et al. (2015). Mechanism of photoprotection in the cyanobacterial ancestor of plant antenna proteins. Nat. Chem. Biol. 11, 287–291.

324. Stammler, G., Brix, H.-D., Glaettli, A., Semar, M., and Schoefl, U. (2007). Biological properties of the carboxamide boscalid including recent studies on its mode of action. Pages 16-21 in: Proc. 16th Int. Congr. Plant Prot. Session 2A, Glasgow, UK.

325. Stammler G, Glattli A, Koch A, Schlehuber S (2010). Mutations in the target protein conferring resistance to SDHI fungicides. In: Dehne HW, Deising HB, Gisi U, Kuck KH, Russell PE, Lyr H (eds) Modern Fungicides and Antifungal Compounds VI. Proceedings 16th International Reinhardsbrunn Symposium 2010. Braunschweig, Germany, pp 195–198.

326. Stammler, G.; Semar, M. (2011). Sensitivity of Mycosphaerella graminicola (anamorph: Septoria tritici) to DMI fungicides across Europe and impact on field performance. EPPO Bull. 41, 149–155.

327. Steinberg, G. (2015). Cell biology of Zymoseptoria tritici: Pathogen cell organization and wheat infection. Fungal Genetics and Biology. 79, 17–23.

328. Stergiopoulos, I., Gielkens, M. M., Goodall, S. D., Venema, K., & De Waard, M. A. (2002). Molecular cloning and characterisation of three new ATP-binding cassette transporter genes from the wheat pathogen Mycosphaerella graminicola. Gene. 289(1–2), 141–149.

329. Stenzel, I., Hause, B., Miersch, O., Kurz, T., Maucher, H., Weichert, H., … Wasternack, C. (2003). Jasmonate biosynthesis and the allene oxide cyclase family of Arabidopsis thaliana. Plant Molecular Biology (Vol. 51).

330. Stephens, C., Ölmez, F., Blyth, H., McDonald, M., Bansal, A., Turgay, E.B., et al (2021). Remarkable recent changes in the genetic diversity of the avirulence gene AvrStb6 in global populations of the wheat pathogen Zymoseptoria tritici. Molecular Plant Pathology. 22, 1121– 1133.
331. Stewart E. L., Hagerty C. H., Mikaberidze A., Mundt C. C., Zhong Z., McDonald B. A. (2016). An improved method for measuring quantitative resistance to the wheat pathogen zymoseptoria tritici using high-throughput automated image analysis. Phytopathology. 106, 782–788.
332. Strasser, R.J. (1985). Dissipative strukturen als thermodynamischer regelkreis des photosyntheseapparates. Berichte Deutsche Botanische Gesellschaft. 98, 53–72.
333. Strasser, Reto & Srivastava, A. & Tsimilli-Michael, Merope. (2000). The fluorescence transient as a tool to characterize and screen photosynthetic samples. Probing photosynthesis: Mechanism, regulation and adaptation.
334. Strasser RJ, Alexandrina D. Stirbet, (2001). Estimation of the energetic connectivity of PS II centres in plants using the fluorescence rise O–J–I–P: Fitting of experimental data to three different PS II models, Mathematics and Computers in Simulation. 56(4–5), 451-462.
335. Strasser, R.J., Tsimilli-Michael, M., Srivastava, A. (2004). Analysis of the Chlorophyll a Fluorescence Transient. In: Papageorgiou, G.C., Govindjee (eds) Chlorophyll a Fluorescence. Advances in Photosynthesis and Respiration, vol 19. Springer, Dordrecht.
336. Strobel, D.; Bryson, R.; Roth, J.; Stammler, G. (2017). Field performance of DMI fungicides against Zymoseptoria tritici across Europe–Compromized by further sensitivity shift? In Modern Fungicides and Antifungal Compounds, Proceedings of the 18th International.
337. Stukenbrock, E. H., Banke, S., Javan-Nikkhah, M., & McDonald, B. A. (2007). Origin and domestication of the fungal wheat pathogen Mycosphaerella graminicola via sympatric speciation. Molecular Biology and Evolution. 24(2), 398–411.
338. Stukenbrock, E. H., Quaedvlieg, W., Javan-Nikhah, M., Zala, M., Crous, P. W., & McDonald, B. A. (2012). Zymoseptoria ardabiliae and Z. pseudotritici , two progenitor species of the septoria tritici leaf blotch fungus Z. tritici (synonym: Mycosphaerella graminicola ). Mycologia. 104(6), 1397–1407.

339. Suffert, F., & Sache, I. (2011). Relative importance of different types of inoculum to the establishment of Mycosphaerella graminicola in wheat crops in north-west Europe. Plant Pathology. 60(5), 878–889.

340. Sundin, D. R., Bockus, W. W., & Eversmeyer, M. G. (1999). Triazole Seed Treatments Suppress Spore Production by Puccinia recondita, Septoria tritici, and Stagonospora nodorum from Wheat Leaves. Plant Disease. 83(4), 328–332.

341. Tabib Ghaffary S. M., O. Robert, V. Laurent, P. Lonnet, E. Margale, T.A.J. van der Lee, R.G.F. Visser, G.H.J. Kema (2011). Genetic analysis of resistance to Septoria tritici blotch in the French winter wheat cultivars Balance and Apache Theor. Appl. Genet. 123, 741-754.

342. Tabib Ghaffary S. M., J.D. Faris, T.L. Friesen, R.G.F. Visser, T.A.J. van der Lee, O. Robert, G.H.J. Kema (2012). New broad-spectrum resistance to Septoria tritici blotch derived from synthetic hexaploid wheat Theor. Appl. Genet. 124, 125-142.

343. Takai, R., Isogai, A., Takayama, S., & Che, F. S. (2008). Analysis of flagellin perception mediated by flg22 receptor OsFLS2 in rice. Molecular Plant-Microbe Interactions. 21(12), 1635–1642.

344. Takahashi, S., Kuzuyama, T., Watanabe, H., and Seto, H. (1998). A 1-deoxy-D-xylulose 5-phosphate reductoisomerase catalyzing the formation of 2-C-methyl-D-erythritol 4-phosphate in an alternative non-mevalonate pathway for terpenoid. 5(17), 9879–9884.

345. Telfer, A., Dhami, S., Bishop, S. M., Phillips, D., & Barber, J. (1994). β-Carotene Quenches Singlet Oxygen Formed by Isolated Photosystem II Reaction Centers. Biochemistry. 33(48), 14469–14474.

346. Thatcher, L. F., Kamphuis, L. G., Hane, J. K., Oñate-Sánchez, L., & Singh, K. B. (2015). The Arabidopsis KH-domain RNA-binding protein ESR1 functions in components of jasmonate signalling, unlinking growth restraint and resistance to stress. PLoS ONE. 10(5).

347. Thies Marten Heick, Annemarie Fejer Justesen, Lise Nistrup Jørgensen (2017). Anti-resistance strategies for fungicides against wheat pathogen Zymoseptoria tritici with focus on DMI fungicides. Crop Protection. 99, 108-117.

348. Thomas, S., Wahabzada, M., Kuska, M. T., Rascher, U., & Mahlein, A. K. (2017). Observation of plant-pathogen interaction by simultaneous hyperspectral imaging reflection and transmission measurements. Functional Plant Biology. 44(1), 23–34.

349. Thompson, A. R., Doelling, J. H., Suttangkakul, A., & Vierstra, R. D. (2005). Autophagic nutrient recycling in Arabidopsis directed by the ATG8 and ATG12 conjugation pathways. Plant Physiology. 138(4), 2097–2110.

350. Tietz, S., Hall, C. C., Cruz, J. A., & Kramer, D. M. (2017). NPQ(T): a chlorophyll fluorescence parameter for rapid estimation and imaging of non-photochemical quenching of excitons in photosystem-II-associated antenna complexes. Plant Cell and Environment. 40(8), 1243–1255.

351. Torriani, S. F. F., Melichar, J. P. E., Mills, C., Pain, N., Sierotzki, H., and Courbot, M. (2015). Zymoseptoria tritici: A major threat to wheat production, integrated approaches to control. Fungal Genet. Biol. 79, 8-12.

352. Tseliou E, Christos Chondrogiannis, Dimitrios Kalachanis, Stavroula Goudoudaki, Yiannis Manoussopoulos, George Grammatikopoulos, (2021). Integration of biophysical photosynthetic parameters into one photochemical index for early detection of Tobacco Mosaic Virus infection in pepper plants, Journal of Plant Physiology. 267.

353. Tucker, C. J. (1979). Red and Photographic Infrared linear Combinations for Monitoring Vegetation. Remote Sensing of Environment (Vol. 8).

354. United Nations, Department of Economic and Social Affairs, Population Division (2022). World Population Prospects 2022.

355. Van Beuningen & Kohli (1990). Deviation from the regression of infection on heading and height as a measure of resistance to septoria tritici blotch in wheat. Plant Dis. 74, 488-493.

356. Van den Bosch, F., Lopez-Ruiz, F., Oliver, R., Paveley, N., Helps, J. and van den Berg, F. (2018). Identifying when it is financially beneficial to increase or decrease fungicide dose as resistance develops. Plant Pathol. 67, 549-560.

357. Van Dijk, M., Morley, T., Rau, M.L. et al. (2021). A meta-analysis of projected global food demand and population at risk of hunger for the period 2010–2050. Nat Food. 2, 494–501.

358. J. W. Van Ooijen and R. E. Voorrips, (2001). “JoinMap 3.0, Software for the Calculation of Genetic Linkage Maps,” Plant Research International, Wageningen.

359. Vergauwen, D., & De Smet, I. (2017). From early farmers to Norman Borlaug — the making of modern wheat. Current Biology. 27(17).

360. Vira M Ubiyvovk, Taras Y Nazarko, Olena G Stasyk, Min Jeong Sohn, Hyun Ah Kang, Andrei A Sibirny, (2002). GSH2, a gene encoding γ-glutamylcysteine synthetase in the methylotrophic yeast Hansenula polymorpha, FEMS Yeast Research. 2(3). 327–332.

361. Viñas-Castells R, Beltran M, Valls G, Gómez I, García JM, Montserrat-Sentís B, Baulida J, Bonilla F, de Herreros AG, Díaz VM. (2010). The hypoxia-controlled FBXL14 ubiquitin ligase targets SNAIL1 for proteasome degradation. J Biol Chem. 285(6), 3794-3805.

362. Waalwijk, C., Mendes, O., Verstappen, E. C. P., de Waard, M. a, & Kema, G. H. J. (2002). Isolation and characterization of the mating-type idiomorphs from the wheat septoria leaf blotch fungus Mycosphaerella graminicola. Fungal Genetics and Biology : FG & B. 35(3), 277–286.

363. Wang D, Qin B, Li X, Tang D, Zhang Y, Cheng Z, Xue Y. (2016). Nucleolar DEAD-Box RNA Helicase TOGR1 Regulates Thermotolerant Growth as a Pre-rRNA Chaperone in Rice. PLoS Genet. 12(2).

364. Wang, H. J., Hsu, Y. W., Guo, C. L., Jane, W. N., Wang, H., Jiang, L., & Jauh, G. Y. (2017). VPS36-dependent multivesicular bodies are critical for plasmamembrane protein turnover and vacuolar biogenesis. Plant Physiology. 173(1), 566–581.

365. Warzecha, T. Skrzypek, E. Adamski, T. Surma, M. Kaczmarek. Z, Sutkowska, A. (2019). Chlorophyll a Fluorescence Parameters of Hulled and Hull-less Barley (Hordeum vulgare L.) DH Lines Inoculated with Fusarium culmorum Plant Pathol J. 35(2), 112-124.

366. Wei Guo, Matthew E. Carroll, Arti Singh, Tyson L. Swetnam, Nirav Merchant, Soumik Sarkar, Asheesh K. Singh, Baskar Ganapathysubramanian, (2021). "UAS-Based Plant Phenotyping for Research and Breeding Applications", Plant Phenomics, Article ID 9840192, 21.

367. White J. W., P. Andrade-Sanchez, M. Gore, K.F. Bronson, T. Coffelt, M.M. Conley, et al. (2012). Field-based phenomics for plant genetics research. Field Crop Res. 133, 101-112.

368. Wilson RE (1985). Inheritance of resistance to Septoria tritici in wheat. In ‘Septoria of cereals – Proceedings of the second international Septoria workshop, 2–4 August 1983, Bozeman, Montana, USA’. (Ed. AL Scharen) pp. 33–35.

369. Winkler, K., Fuchs, R., Rounsevell, M. et al. (2021). Global land use changes are four times greater than previously estimated. Nat Commun. 12, 2501.

370. Wolfe, M. S. (1984). Trying to understand and control powdery mildew. Plant Pathology. 33(4), 451–466.

371. Wu C., Zheng Niu, Quan Tang, Wenjiang Huang, (2008). Estimating chlorophyll content from hyperspectral vegetation indices: Modeling and validation, Agricultural and Forest Meteorology. 148(8–9), 1230-1241.

372. Xavier, AC; Rudorff, BFT, Salomon, MV et al (2006). Hyperspectral field reflectance measurements to estimate wheat grain yield and plant height. Sci. agric. (Piracicaba, Braz.). 63(2).

373. Xie, C., Yang, C., & He, Y. (2017). Hyperspectral imaging for classification of healthy and gray mold diseased tomato leaves with different infection severities. Computers and Electronics in Agriculture. 135, 154–162.

374. Xiong Y, Contento AL, Bassham DC. (2005). AtATG18a is required for the formation of autophagosomes during nutrient stress and senescence in Arabidopsis thaliana. The Plant Journal: for Cell and Molecular Biology. 42(4), 535-546.

375. Xiong J, Cui X, Yuan X, Yu X, Sun J, Gong Q. (2016). The Hippo/STE20 homolog SIK1 interacts with MOB1 to regulate cell proliferation and cell expansion in Arabidopsis. J Exp Bot. 67(5), 1461-75.

376. Xing, Y., Jia, W., & Zhang, J. (2008). AtMKK1 mediates ABA-induced CAT1 expression and H2O2 production via AtMPK6-coupled signaling in Arabidopsis. Plant Journal. 54(3), 440–451.

377. Xinyao He, Gustavo Azzimonti, Mariel del Rosario Sánchez-Vidaña, Silvia A. Pereyra, Carolina Sansaloni, Ana María Hernández-Anguiano, Aakash Chawade, and Pawan K. Singh (2021). Mapping for Adult-Plant Resistance Against Septoria Tritici Blotch in a Common Wheat Line Murga Phytopathology, 111(6), 1001-1007.

378. Xu, F., Xu, S., Wiermer, M., Zhang, Y., & Li, X. (2012). The cyclin L homolog MOS12 and the MOS4-associated complex are required for the proper splicing of plant resistance genes. Plant Journal. 70(6), 916–928.

379. Yamamuro, C., Ihara, Y., Wu, X., Noguchi, T., Fujioka, S., Takatsuto, S., … Matsuoka, M. (2000). Loss of function of a rice brassinosteroid insensitive1 homolog prevents internode elongation and bending of the lamina joint. Plant Cell. 12(9), 1591–1605.

380. Yang F, Li W, Jørgensen HJ. (2013). Transcriptional reprogramming of wheat and the hemibiotrophic pathogen Septoria tritici during two phases of the compatible interaction. PLoS One. 8(11).

381. Yang, N., McDonald, M.C., Solomon, P.S. et al. (2018). Genetic mapping of Stb19, a new resistance gene to Zymoseptoria tritici in wheat. Theor Appl Genet. 131, 2765–2773.

382. Yazdani, M., Zallot, R., Tunc-Ozdemir, M., De Crécy-Lagard, V., Shintani, D. K., & Hanson, A. D. (2013). Identification of the thiamin salvage enzyme thiazole kinase in Arabidopsis and maize. Phytochemistry. 94, 68–73.

383. Yeh, Y. H., Chung, W. C., Liao, J. Y., Chung, C. L., Kuo, Y. F., & Lin, T. te. (2016). Strawberry foliar anthracnose assessment by hyperspectral imaging. Computers and Electronics in Agriculture. 122, 1–9.

384. Yitagesu, T., (2020). Yield Loss Due to Septoria tritici Blotch (Septoria Tritici) of Bread Wheat (Triticum aestivum L.) in the Central Highlands of Ethiopia. Journal of Biology, Agriculture and Healthcare. 10(10)

385. Yu, H.; Wu, J.; Xu, N.; Peng, M. (2007). Roles of f-box proteins in plant hormone responses. Acta Biochim. Biophys. Sin. 39, 915–922.

386. Yuan M., Bruno Pok Man Ngou, Pingtao Ding, Xiu-Fang Xin, (2021). PTI-ETI crosstalk: an integrative view of plant immunity, Current Opinion in Plant Biology, Volume 62.

387. Zandalinas, S.I., Sengupta, S., Fritschi, F.B., Azad, R.K., Nechushtai, R. and Mittler, R. (2021). The impact of multifactorial stress combination on plant growth and survival. New Phytol. 230, 1034-1048.

388. Zarco-Tejada, P. J., Pushnik, J. C., Dobrowski, S., & Ustin, S. L. (2003). Steady-state chlorophyll a fluorescence detection from canopy derivative reflectance and double-peak red-edge effects. Remote Sensing of Environment. 84, 283–294.

389. Zhan, J., Mundt, C. C., & McDonald, B. A. (1998). Measuring immigration and sexual reproduction in field populations of Mycosphaerella graminicola. Phytopathology. 88(12), 1330–1337.

390. Zhan, J., Mundt, C. C., & McDonald, B. a. (2001). Using Restriction Fragment Length Polymorphisms to Assess Temporal Variation and Estimate the Number of Ascospores that Initiate Epidemics in Field Populations of Mycosphaerella graminicola. Phytopathology. 91(10), 1011–1017.

391. Zhan, J., Kema, G. H. J., Waalwijk, C., & McDonald, B. A. (2002). Distribution of mating type alleles in the wheat pathogen Mycosphaerella graminicola over spatial scales from lesions to continents. Fungal Genetics and Biology. 36(2), 128–136.

392. Zhan X, Wang B, Li H, et al. (2012). Arabidopsis proline-rich protein important for development and abiotic stress tolerance is involved in microRNA biogenesis. Proceedings of the National Academy of Sciences of the United States of America. 109(44), 18198-18203.

393. Zhang X, Zhang Q, Xin Q, Yu L, Wang Z, Wu W, Jiang L, Wang G, Tian W, Deng Z, Wang Y, Liu Z, Long J, Gong Z, Chen Z. (2012). Complex structures of the abscisic acid receptor PYL3/RCAR13 reveal a unique regulatory mechanism. Structure. 20(5), 780-90.

394. Zhang Y, Li S, Xue S, Yang S, Huang J, Wang L. (2018). Phylogenetic and CRISPR/Cas9 Studies in Deciphering the Evolutionary Trajectory and Phenotypic Impacts of Rice ERECTA Genes. Front Plant Sci. 10(9), 473.

395. Zhong, Z., Marcel, T. C., Hartmann, F. E., Ma, X., Plissonneau, C., Zala, M., Palma-Guerrero, J. (2017). A small secreted protein in Zymoseptoria tritici is responsible for avirulence on wheat cultivars carrying the Stb6 resistance gene. New Phytologist. 214(2), 619–631.

396. Zhou, R., Yu, X., Ottosen, CO. et al. (2017). Drought stress had a predominant effect over heat stress on three tomato cultivars subjected to combined stress. BMC Plant Biol. 17, 24.

397. Zhou, X., Huang, W., Kong, W., Ye, H., Dong, Y., & Casa, R. (2017). Assessment of leaf carotenoids content with a new carotenoid index: Development and validation on experimental and model data. International Journal of Applied Earth Observation and Geoinformation. 57, 24–35.

398. Zushi K., Naotaka Matsuzoe (2017). Using of chlorophyll a fluorescence OJIP transients for sensing salt stress in the leaves and fruits of tomato, Scientia Horticulturae. 219, 216-221.

399. Zwart R. S., J. Thompson, A. Milgate, U. Bansal, P. Williamson, H. Raman, H.S. Bariana (2010). QTL mapping of multiple foliar disease and root-lesion nematode resistances in wheat Mol. Breed. 26, 107-124.

400. Zwiers, L. H., & De Waard, M. a. (2000). Characterization of the ABC transporter genes MgAtr1 and MgAtr2 from the wheat pathogen Mycosphaerella graminicola. Fungal Genetics and Biology : FG & B. 30(2), 115–125.

401. Zwiers, L. H., Stergiopoulos, I., Gielkens, M. M. C., Goodall, S. D., & De Waard, M. A. (2003). ABC transporters of the wheat pathogen Mycosphaerella graminicola function as protectants against biotic and xenobiotic toxic compounds. Molecular Genetics and Genomics. 269(4), 499–507.